CHAPTER 8

An Environmental Study of USS *Arizona* Bunker C Fuel Oil

Amanda M. Graham

INTRODUCTION

USS *Arizona* was originally commissioned in 1916 as an oil-burning Pennsylvania-class battleship (Lenihan 1990). The ship was a member of Battle Division 8 in Norfolk, VA, where it served through World War I. Because of oil shortages during World War I the ship served as a gunnery training vessel and patrolled the North American Atlantic coast rather than joining other U.S. Navy vessels in Europe (Lenihan 1990). Following World War I and until 1929, USS *Arizona* served in various capacities including acting as a transport vessel and serving in the Pacific Ocean.

In 1929, USS *Arizona* was docked in Norfolk, VA, in order to modernize the vessel. Modernization included an increase in oil capacity from 2,332 to 4,630 tons of oil, adding increased protection from enemy fire, the addition of a modern power plant, and engine upgrades. Blisters were added to the outer hull for additional protection from torpedoes, and armor was added to the upper hull to minimize damage from anti-aircraft fire. The new power plant and engine upgrades allowed the vessel to maintain fleet speed and offset the increased weight load from the addition of more armament (Lenihan 1990). In 1940, post modernization, the ship sailed to the Pacific and was stationed in Pearl Harbor, HI.

On December 7 1941, USS *Arizona* along with other battleships stationed in Pearl Harbor, were attacked. Enemy fire that struck USS *Arizona* penetrated the upper deck armor and exploded near the forward magazine, which sympathetically detonated the magazines. The explosion caused the bow to collapse and the ship to sink while burning for two days following the attack (Lenihan 1990). The ship's bunkers, which hold 4,630 tons oil, had been filled with Bunker C fuel oil prior to the attack, helping to fuel the fire following the explosion. During the days following the attack, USS *Arizona*, USS *West Virginia*, USS *Tennessee*, USS *Maryland*, USS *Oklahoma*, and USS *California* leaked Bunker C fuel oil into the surrounding harbor. Other battleships stationed near USS *Arizona* sustained less damage during the attack and went on to serve during World War II. In comparison, USS *Arizona* was not usable for World War II, but instead the ship was scavenged for parts. *Arizona* remains where it sank, and its significance in the 1941 Pearl Harbor attack is acknowledged physically by a memorial built over the remains of the ship The National Park Service currently manages the memorial.

Although oil was burned off following the Pearl Harbor attack, an unknown amount of oil remains trapped in the ship, and leaks from the ship continuously. The National Park Service Submerged Resources Center collected oil as it leaked from the ship and determined that at least 1 to 2 liters of oil per day leak from the ship into the surrounding harbor (Johnson et al. 2002; Murphy and Russell, personal communication). Little is known about the interior of the ship because of USS *Arizona*'s status as a memorial. Therefore, this study represents a unique opportunity to characterize oil leaking from the ship, determine whether the oil from the ship is present in surrounding sediments, and study the microbial degradation of fuel oil leaking from USS *Arizona*. This information is an important first step in understanding the influence of Bunker C fuel oil leaking from the ship on the surrounding environment, and will also contribute to management strategies for the ship. This study was conducted as part of USS *Arizona* Preservation Project and was designed to address several research domains that are directly concerned with the oil contained within *Arizona*'s hull, understanding its nature and the implications for inferring what is occurring within the hull, and the oil's impact on the environment.

BUNKER C FUEL OIL COMPOSITION AND PROPERTIES

During the crude oil refining process, different distillates are collected based on boiling temperatures (Hunt 1995). Bunker C is from the No. 6 petroleum distillation-boiling fraction, which is the highest distillation-boiling fraction (>400°F), and is sometimes referred to as "No. 6" fuel oil. Bunker C consists of saturates (i.e., *n*-alkanes, branched alkanes, and cycloalkanes), aromatics (i.e., naphthalenes and benzo[*a*]pyrene), heterocycles (i.e., benzothiophenes and naphthobenzothiophenes), asphaltenes, and resins (Irwin et al. 1997). The oil may also contain sulphur and nitrogen, contained in heterocycles, along with vanadium and nickel complexed to asphaltenes (Walker et al. 1976; Irwin et al. 1997; Lunel et al. 2000). Since Bunker C is from the highest petroleum distillation fraction, it contains increased concentrations of high molecular weight carbon molecules in comparison to other lower boiling fraction distillation oils (i.e., diesel) (Irwin et al. 1997). For example, in comparison to other lighter distillate oils, Bunker C contains a large concentration of high molecular weight molecules, especially $C_{12} - C_{34}$ *n*-alkanes and large polycyclic aromatic hydrocarbons (PAHs). Furthermore, approximately 5% of the total PAH concentration consists of four to six ring aromatic hydrocarbons (Irwin et al. 1997; Richmond et al. 2001). The American Petroleum Institute (API) gravity of Bunker C is 12.3° and it has a density of 971 kg/m^3 at 22°C along with a low water soluble fraction (WSF) <10 ppm.

The large concentration of high molecular weight molecules increases the viscosity of Bunker C fuel oil and makes it difficult to use. Therefore, to make the Bunker C more usable it may be blended with a lighter oil (i.e., diesel) (Irwin et al. 1997). Post-distillation additives, such as calcium, cerium, iron, or manganese, may also be added to increase combustion temperatures (Irwin et al. 1997). Thus, the actual composition of Bunker C is variable and dependent upon the distillation process along with any lighter oil blending and post-distillation additives (Irwin et al. 1997).

ENVIRONMENTAL FATE OF BUNKER C FUEL OIL

The original chemical composition of oil greatly influences its susceptibility to weathering processes following release into the environment. Weathering includes biotic (i.e.,

microbial degradation) and abiotic (i.e., evaporation) processes that alter oil composition. Weathering begins immediately following an oil spill and can be temperature and environment dependent (Atlas 1984; NRC 2003). Evaporation and dissolution are the first weathering processes to occur following an oil spill and the extent of both processes is dependent on the type of oil. Heavier oils (i.e., Bunker C fuel oil), which contain an increased concentration of higher molecular weight hydrocarbons are not as susceptible to evaporation and dissolution in comparison to lighter oils (i.e., diesel) containing few high molecular weight hydrocarbons (Atlas 1984; Irwin et al. 1997; NRC 2003). The extent of oil dispersion is also less extensive in heavier oils in comparison to lighter oils. Heavier oils have a much lower water soluble fraction than lighter oils; therefore, following a spill involving heavier oils, fewer hydrocarbons will enter the water column and become associated with suspended sediments or be available to microorganisms for degradation. Heavy fuel oils are less immediately bioavailable to organisms and less degradation or fewer toxic responses may occur (Atlas 1984; NRC 2003). However, heavier oils contain a greater concentration of PAHs, which may absorb into and accumulate in sediments, and remain there for years following an environmental release, making heavier oils a greater long-term environmental threat than lighter oils (Irwin et al. 1997; Bixiam et al. 2001).

Photooxidation is another type of weathering process and occurs when hydrocarbons are oxidized to ketones, aldehydes, alcohols and acids by energy transfer between molecules (Garrett et al. 1998; NRC 2003). Following photooxidation, hydrocarbon products are more water-soluble than their precursors and therefore become more bioavailable (Garrett et al. 1998; NRC 2003). Garrett and colleagues (1998) suggested aromatics were affected by photooxidation more than saturated compounds found in crude oil, indicating that oils with more aromatics have an increased susceptibility to photooxidation.

Emulsification and tarball formation are also important weathering processes. Oil will emulsify when water droplets are formed in oil, and emulsification is dependent on the percentage of resins and asphaltenes in spilled oil (NRC 2003). Heavier oils with higher concentrations of asphaltenes and resins will emulsify before lighter oils (NRC 2003). Tarballs are formed by recalcitrant high molecular weight hydrocarbons, which can sink in the water and deposit in sediments (NRC 2003). Both emulsification and tar ball formation increase the density and viscosity of oil and provide an increased surface area for microbial attachment (NRC

2003). These weathering processes are important in determining the environmental fate of spilled oil.

Following an environmental release, the chemical properties of Bunker C fuel oil make it more difficult to clean up and more likely to persist in the environment in comparison to lighter oils (Irwin et al. 1997; Lunel et al. 2000; Richmond et al. 2001; NRC 2003). Most hydrocarbons in Bunker C have a high molecular weight and therefore are not likely to evaporate (Irwin et al. 1997; Lunel et al. 2000). Following an environmental release of Bunker C, less than 10% of the oil will evaporate, in comparison to lighter oils such as diesel, in which 75% of the oil will evaporate (Irwin et al. 1997; Lunel et al. 2000; Richmond et al. 2001; NRC 2003). The high density, viscosity, and increased concentration of high molecular weight molecules of Bunker C also allow it to sink in freshwater and saltwater and form stable tar balls and emulsify in saltwater (Irwin et al. 1997; Lunel et al 2000; Richmond et al. 2001; NRC 2003). These chemical properties of Bunker C allow it to persist in the environment longer than lighter fuel oils following a spill, and Bunker C has been detected more than 20 years after an environmental spill (Vandermeulen and Singh 1994; Wang et al. 1994; Irwin et al. 1997; NRC 2003). Overall, the original make-up of oil is an important factor in its eventual environmental fate. In addition, utilization of hydrocarbons by microorganisms occurs at the oil-water interface, therefore the amount of oil in the water indicates the amount of oil that will be bioavailable for degradation or toxic response by organisms (Irwin et al. 1997; Barron et al. 1999; Baars 2002).

TOXICITY OF BUNKER C FUEL OIL

The high viscosity and high concentration of PAHs in Bunker C oil composition contributes to its toxicity in the environment (Irwin et al. 1997). However, it is considered to be less toxic than lighter petroleum products, such as diesel, because less Bunker C enters the water column immediately following an oil spill (NOAA 1994; Irwin et al. 1997; Barron et al. 1999; Baars 2002). As a result, the immediate danger to the environment in spills involving Bunker C is the coating of marine organisms as well as ingestion of the fuel oil by marine organisms (Irwin et al. 1997; Richmond et al. 2001; Baars 2002; Hir and Hily 2002). The stability of Bunker C fuel oil in water and its potential persistence in the environment (i.e., sedimentation of PAHs)

results in a long-term environmental persistence and increases the exposure of toxic components to the surrounding environment (Bixian, et al. 2001; Richmond et al. 2001).

Emulsification of Bunker C oil increases the threat of toxicity because it increase, the mobility of toxic compounds including (i.e., PAHs) entering the water column (Irwin et al. 1997; Richmond et al. 2001). Richmond et al. (2001) documented increased toxicity of emulsified Bunker C by using Microtox® assays to detect decreased light emission from bioluminescent bacteria exposed to emulsified Bunker C. The study found a decrease in the toxicity (by Microtox® assays) in microorganisms grown in chitin-amended pre-emulsified Bunker C media in comparison to microorganisms grown in pre-emulsified Bunker C media only. This decrease in toxicity was attributed to PAH adsorption to chitin (Richmond et al. 2001).

Bunker C toxicity to humans is associated with the presence of the 16 PAHs that are listed by the Environmental Protection Agency's (EPA) priority pollutants for remediation (Irwin et al. 1997; Baars 2002). These priority pollutants include naphthalene, acenaphthylene, acenaphthene, fluorene, phenanthrene, anthracene, flouranthene, pyrene, benzo[*a*]anthracene, chrysene, benzo[*b*]fluoranthene, benzo[*k*]fluoranthene, benzo[*a*]pyrene, benzo[*a,h*]anthracene, benzo[*g,h,i*]perylene, and indeno[*c,d*]pyrene (EPA 1984; Baars 2002). PAHs contained in the EPA's priority pollutant list are are 2-ring to 5-ring PAHs and individually suspected carcinogens, (i.e., bezno[*a*]pyrene) (Samanta et al. 2002). While the toxicity of individual PAHs has been demonstrated, PAHs in the environment are encountered as a mixture which may contribute to increased toxicity (Neilson 1994; Samanta et al. 2002). A human toxicity study was performed following a 2.8 million gallon spill of Bunker C by the *Erika* off the coast of Brittany, France in 1999 (Baars 2002; Samanta et al. 2002). Baars (2002) found no toxic effects to humans involved in the spill clean up and tourists in the area following the *Erika* spill. However, individuals that cleaned birds after the spill measured benzo[*a*]pyrene dermal exposure levels of 295 ng/cm^2, far above the human exposure limit value of 2 ng/cm^2 according to the Netherland National Institute of Public Health and the Environment (Baars 2002). Together these studies suggest Bunker C is of toxicologic concern.

BUNKER C FUEL OIL SPILLS IN THE MARINE ENVIRONMENT

Bunker C fuel oil is a major contributor to marine oil spills because of its frequent use and transport in marine vessels. The greatest environmental impact of spills in the open ocean results from the oil washing ashore and contaminating coastal environments. According to the United Kingdom National Environmental Technology Centre, 90-95% of heavy fuel oil spills in the open ocean are washed ashore (Lunel et al. 2000). Following the *Erika* spill in the Atlantic Ocean approximately 65 km south of Britanny, France, much of the oil was washed into coastal waters where it impacted coastal industries such as fishing (Baars 2002).

Bunker C fuel oil causes environmental problems for coastal habitats and has been shown to persist following a spill in coastal areas, including Chedabucto Bay, Nova Scotia, Canada, for over 20 years because of its high concentration of high molecular weight components (Vandermeulen and Singh 1994; Wang et al. 1994). The *Arrow* spilled 528,344 gallons of Bunker C fuel oil near the Chedabucto Bay of Nova Scotia, Canada in 1970. By comparing the oil samples taken in 1990 from beaches considered to have low ecological energy inputs by ocean action to the original *Arrow* oil Vandermuelen and Singh (1994) confirmed that degraded petroleum residues of *Arrow* oil were still present. These authors also demonstrated that *Arrow* oil was still present in samples taken from Jargon Lagoon and Black Duck Cove south of Chedabucto Bay and on the North Atlantic Coast (Vandermeulen and Singh 1994). Furthermore, oil samples taken from Black Duck Cove were in a relatively unweathered form still containing an *n*-alkane profile similar to the original *Arrow* Bunker C oil (Vandermeulen and Singh 1994). PAHs from Black Duck Cove were also similar to the original *Arrow* Bunker C oil and some lower molecular weight aromatics (i.e., naphthalene) were still present (Vandermeulen and Singh 1994). Biomarker profiles, which are used for oil identification, were used to compare oil samples from Jargon Lagoon and Black Duck Cove to original *Arrow* biomarker profiles (Vandermeulen and Singh 1994). Oil samples from both areas had similar biomarker profiles when compared to original *Arrow* Bunker C oil (Vandermeulen and Singh 1994). These biomarker results suggest the unweathered oil present in Black Duck Cove is *Arrow* Bunker C oil that had persisted for over 20 years, from 1970 to 1994. However, not all Bunker C spills exhibit the long-term environmental persistence of the *Arrow* oil spill because of varying coastal conditions.

On December 23 1988, *Nestucca* spilled approximately 230,000 gallons of Bunker C fuel oil in the Pacific Ocean contaminating Washington and Vancouver c oastal areas (Strand et al. 1992). In comparison to the *Arrow* oil, there was little persistence of *Nestucca-* spilled petroleum by the third sampling period in February 1990 (Strand et al. 1992). The contrast in petroleum persistence between the Washington and Vancouver coastline (*Nestucca* spill) and the Nova Scotia coast line (*Arrow* spill) can be explained by the differences in the ocean energy inputs (i.e., wave action, strength of local currents and wind) of the contaminated coastal areas, and in the amount of clean up following the spill (Atlas 1981; Strand et al. 1992; Vandermeulen and Singh 1994). Areas that had extensive Bunker C fuel oil persistence from the *Arrow* were low to medium energy coastal areas. Also, after the 1970 spill, the decision was made to allow these areas to recover naturally rather than clean up the sites (Vandermeulen and Singh 1994). Comparatively, the coastal areas studied from the 1988 *Nestucca* spill were higher energy coastal areas and improvements were made in the clean up of coastal oil spills by use of oil absorbing pads and pom-poms (Strand et al. 1992).

Tracking and monitoring environmental oil spills is difficult because of different weathering parameters, such as biodegradation by microorganisms, that can change components of oil. Therefore, components in oil that are conserved and resistant to biotic and abiotic weathering processes can be used as references to monitor biotic and abiotic weathering (Prince et al. 1994; Frontera-Suau et al. 2002). This is generally accomplished using a conserved suite of compounds found in oil referred to as biomarkers.

OIL BIOMARKERS

Biomarkers (i.e., hopanes) are complex organic molecular fossils that share structural similarity to parent biological precursors, and tend to be resistant to weathering processes (Peters and Moldowan 1993). Biomarker profiles are unique to each oil and can be used to link crude oil to its source (Hunt 1995). Therefore, biomarkers are used extensively for identifying the source of an oil spill along with assessing the extent of oil weathering (Mackenzie 1984; Peters and Moldowan 1993; Kvenvolden et al. 1995; Whittaker and Pollard 1997; Wang et al. 2001b). Biomarkers are derived from environmental inputs during oil formation and closely resemble the parent molecules from which they were formed (Mackenzie 1984; Peters and Moldowan 1993;

Kvenvolden et al. 1995; Whittaker and Pollard 1997; Wang et al. 2001b). For example, pristane and phytane (Figure 8.1) are branched acyclic isoprenoids that are derivatives of phytol, which is associated with chlorophyll (Mackenzie 1984; Peters and Moldowan 1993). Hopane (Figure 8.1) is a pentacyclic triterpane and originates from bacteriohopane, a component of bacterial membranes (Mackenzie 1984; Peters and Moldowan 1993; Prince et al. 1994). Steranes, in comparison, originate from eukaryotic sterols (Peters and Moldowan 1993). Because of their predecessor molecules, pristane, phytane, hopanes and steranes are ubiquitous in oil and therefore are the most commonly used biomarker ratios for oil identification and internal references to determine the extent of weathering (Whittaker and Pollard 1997). Hopanes and steranes are more persistant than pristane and phytane which are prone to microbial degradation and may be degraded within days of a spill (Blumer and Sass 1972; Prince et al. 1994). Therefore, pristane and phytane are only useful for identification and weathering ratios prior to extensive microbial degradation and weathering (Blumer and Sass 1972; Prince et al. 1994; Whittaker and Pollard 1997; Wang et al. 1999; Frontera-Suau et al. 2002). Hopane and sterane ratios have been used as identification and weathering ratios for oil up to 25 years following the original spill (Wang et al. 1998b).
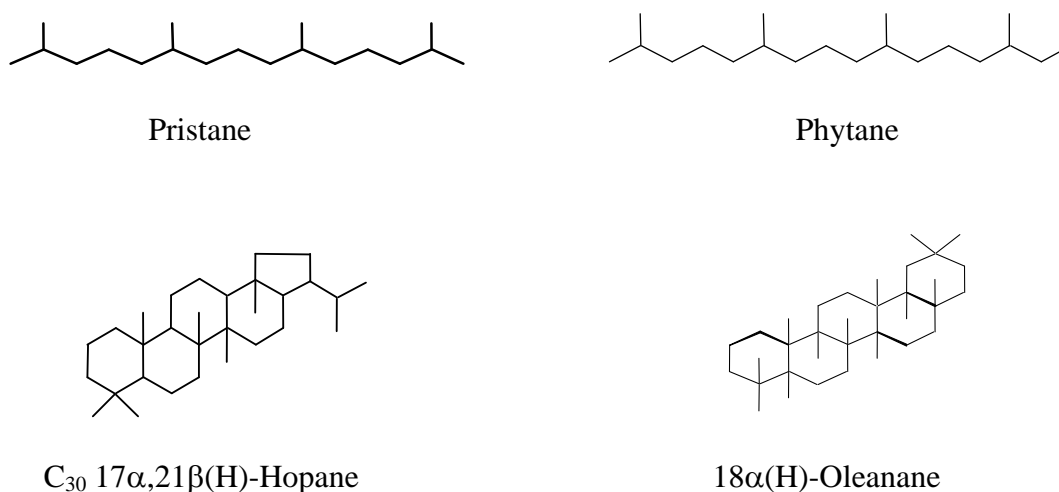

Pristane   Phytane

C$_{30}$ 17α,21β(H)-Hopane   18α(H)-Oleanane

Figure 8.1. Selected biomarker chemical structures.

303

Biomarker ratios are used as a tool for oil identification and also to determine the extent of oil biodegradation (Peters and Moldowan 1993; Prince et al. 1994; Bost et al. 2001; Frontera-Suau et al. 2002). For example, maturity and source correlation ratios indicate the thermal maturity of oil and the original bedrock source. These ratios can be used as identification tools to relate unknown oils to the original source and as a chemical fingerprint for oil to oil relatedness (Peters and Moldowan 1993). For example, Kvenvolden and colleagues (1995) used hopane and sterane ratios to identify an oil source in Prince William Sound, Alaska as input other than the Alaskan North Slope crude oil spilled on March 24 1989 from the *Exxon Valdez*. Furthermore 17α,18α,21β(H)-28,30-bisnorhopane 17α,18α,21β(H)-25,28,30-trisnorhopane, and 18α(H)-oleanane were also detected, and these are three biomarkers compounds not present in Alaskan North Slope crude oil from the *Exxon Valdez*. (Kvenvolden et al. 1995). In addition, other studies have used similar ratios to correlate fresh or weathered oil with its original source (Vandermeulen and Singh 1994; Wang et al. 1994; Wang et al. 1995; Munoz et al. 1997; Wang et al. 1998a; Wang et al. 2001a; Wang et al. 2001b; Zakaria et al. 2001).

Biomarkers can also be used as an internal reference to observe the extent of degradation. Laboratory and field studies have focused on 17α(H),21β(H)-hopane as an internal reference for weathering and degradation studies because it is found in all oils (Peters and Moldowan 1993). In addition, 18α(H)-oleanane (Figure 8.1) is also important for oil weathering and degradation studies, because no laboratory studies have shown it to be degraded although it is found only in oils formed with angiosperm input and therefore is not a ubiquitous biomarker (Peters and Moldowan 1993; Alberdi and Lopez 2000). Prince and colleagues (1994) found 17α(H),21β(H)-hopane to be resistant to microbial degradation, and not produced during oil degradation using Alaskan North Slope crude oil in a laboratory study at 15°C. Pollard et al. (1999) quantified oil degradation in laboratory microcosms containing Fuel oil No. 6 by using biomarker ratios. They found the Σ*n*-alkanes to17α(H),21β(H)-hopane ratio to be the most sensitive to degradation compared to the ratio of Σ*n*-alkanes to branched alkanes pristane and phytane. Aerobic degradation of 17α(H),21β(H)-hopane has been observed in laboratory studies by using a 18α(H)-oleanane to 17α(H),21β(H)-hopane ratio of Bonny Light crude (Frontera-Suau et al. 2002) and Venezuelan crude oils (Bost et al. 2001).

Degradation of 17α(H),21β(H)-hopane has also been observed in field studies. For example degradation of 17α(H),21β(H)-hopane was observed in an oil spill of Arabian Light crude into a tropical ecosystem of Guadeloupe, France in 1986 (Munoz et al. 1997) and also in the Gulf of Quintero Bay, Chile, where the *Metulla* spilled Arabian Light crude and Bunker C fuel oil in 1974 (Wang et al. 2001a). The results of these studies suggest some microorganisms are capable of degrading 17α(H),21β(H)-hopane and therefore a suite of biomarkers should be used to monitor microbial oil degradation.

<div align="center">AEROBIC OIL DEGRADATION</div>

Microorganisms are capable of utilizing many of the compounds in oil as their sole carbon source. Aerobic degradation of oil proceeds by utilizing the saturates in the order of increasing *n*-alkanes, branched alkanes and finally cycloalkanes. Concurrent with *n*-alkane degradation, the aromatics are degraded in order of size, with lower molecular weight aromatic degradation occurring before higher molecular weight aromatics.

Aerobic microbial degradation studies have shown *n*-alkanes are the easiest component of oil to degrade, and degradation of *n*-alkanes has been demonstrated with increasing chain length up to *n*-C_{44} (Haines and Alexander 1974; Atlas 1981). Utilization of *n*-alkanes for growth of microorganisms may proceed by β oxidation (Figure 8.2) with an initial monoterminal attack by monooxygenase forming an alcohol, followed by the formation of an aldehyde. Finally, a monocarboxylic acid is formed (Atlas 1981; Widdel and Rabus 2001). Further utilization of the monocarboxylic acid can be achieved by β-oxidation and the formation of two-carbon unit fatty acids and acetyl coenzyme A, which eventually results in the formation of CO_2 (Schaeffer et al. 1979; Atlas 1981; Salanitro et al. 1997). Branched isoprenoids, such as pristane and phytane, are more difficult for microorganisms to utilize as a carbon source because of methyl branching (Schaeffer et al. 1979; Atlas 1981; Salanitro et al. 1997). Microbial attack of isoprenoids is dependent on the position of methyl branching and strategies other than β oxidation can be utilized if branching occurs in the β-position (Schaeffer et al. 1979). For example, utilization of branched alkanes (i.e., pristane) by an alternate strategy, for example, ω oxidation, forms dicarboxcylic acids and continues until mineralization by β-oxidation (Atlas

1981). Examples of other initial methods of attack by microorganisms are α oxidation or β alkyl group removal (Pirnik 1977).

In contrast to straight and branched alkanes, cycolalkanes are more resistant to microbial attack. Cycloalkanes are found throughout the environment from natural sources (i.e., oil, plants and microbes) along with synthetic sources (Trudgill 1978; Atlas 1981; Perry 1984). Furthermore, cycloalkanes are often used as biomarkers (i.e., hopane) in oil (Peters and Moldowan 1993). Microbial cycloalkane metabolism occurs more readily in cycloalkanes containing a side chain (i.e., methylcyclohexane) than in unsubstituted cycloalkanes (i.e., cyclohexane) (Trudgill 1978; Atlas 1981; Perry 1984).

Utilization of unsubstituted cycloalkanes proceeds by oxidation of the ring forming an intermediate alcohol or ketone. These intermediates can be further utilized by ring cleavage and subsequent β, α, or ω oxidation (Trudgill 1978; Atlas 1981; Perry 1984). Although few microbial cultures have been able to metabolize unsubstituted cycloalkanes, Stirling and colleagues (1977) were able to isolate a *Nocardia* sp. with different cycloalkanes (i.e.,
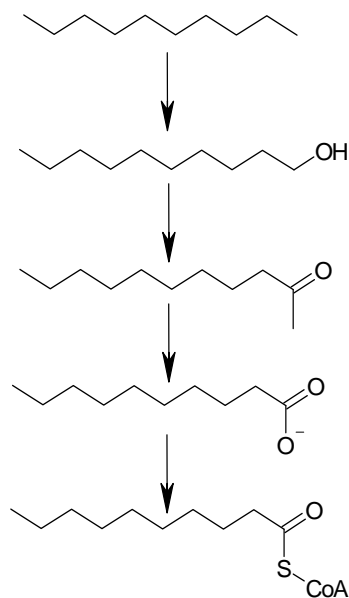

Figure 8.2. β-oxidation pathway for microbial utilization of *n*-alkanes (Adapted from Atlas 1984).

dodecylcyclohexane and heptadecylcyclohexane) as the sole carbon sources. Metabolism of cycloalkanes with a side chain is initiated by β-oxidation of the *n*-alkane, yielding a cyclohexane carboxylic acid (Beam and Perry 1974; Atlas 1981).

Degradation of aromatic hydrocarbons in oil is of special interest because of persistence and carcinogenicity associated with PAHs, which increases with increasing ring size (Cerniglia 1992; Kanaly and Harayama 2000; Dean-Ross et al. 2002). Bunker C fuel oil is made up of 25% aromatics, with approximately 5% of the total PAH concentration consisting of four to six ring aromatic hydrocarbons (Irwin et al. 1997; Richmond et al. 2001). Microbial degradation pathways differ with the amount of substitution and the number of rings present, but are initiated by dioxygenation of an aromatic ring forming *cis*-dihydrodiol (Figure 8.3) (Atlas 1981; Neilson 1994). Pathways for microbial growth with PAHs up to three rings (i.e., naphthalene and phenanthrene) as the sole carbon source have been elucidated in the laboratory (Figure 8.3), indicating that individually these molecules can be readily degraded (Cerniglia 1992). Co-oxidation is an important degradation pathway for high molecular weight PAH molecules with four or more rings (i.e., flouranthene and benzo[*a*]pyrene) (Atlas 1981; Cerniglia 1992; Juhasz and Naidu 2000; Kanaly and Harayama 2000). Few laboratory bacterial cultures have utilized high molecular weight PAHs as a sole carbon source, although there are exceptions for the four ring molecules pyrene, chrysene, and flouranthene. Microorganisms capable of utilizing PAHs with more than four rings (i.e., benzo[*a*]pyrene) as the sole carbon source have not been isolated, although degradation by co-oxidation has been demonstrated in the laboratory and the field (Cerniglia 1992; Juhasz and Naidu 2000; Kanaly and Harayama 2000). Although studies using individual PAHs are important for pathway elucidation, studies observing degradation of mixed PAHs are also important because this is how PAHs occur environmentally. Thus far, studies using PAH mixtures have shown both enhanced (Beckles et al. 1998) and inhibitory (Dean-Ross et al. 2002) degradation effects, which indicates more research is needed to understand microbial degradation of PAH mixtures.

<div align="center">ANAEROBIC OIL DEGRADATION</div>

Anaerobic degradation of oil is important in contaminated sediments, in oil reservoirs and during oil refining and transport. For example, sulfate reducing bacteria are found in oil refining sites where their growth causes corrosion of machinery because of H_2S formation during
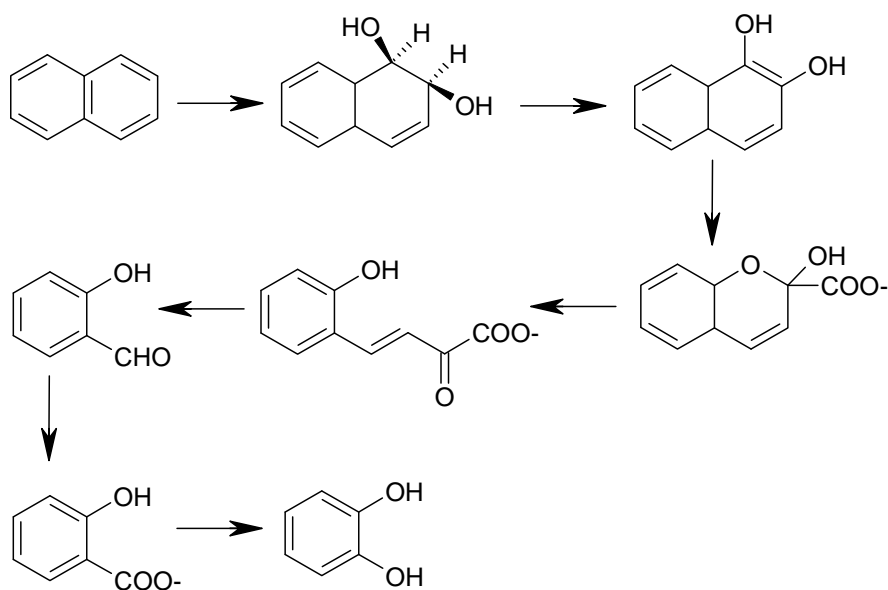
Figure 8.3. Representative pathway for microbial utilization of naphthalene (Adapted from Neilson 1994).

anaerobic metabolism of petroleum (Postgate 1979). Studies since have shown that anaerobic bacteria utilizing different electron acceptors, such as sulfate, nitrate, and ferric iron, are able to degrade hydrocarbons, including aromatics (i.e., toluene) and longer chain *n*-alkanes (i.e., hexadecane) (So and Young 1999; Anderson and Lovely 2000; Elshahed et al. 2001; Boll et al. 2002). Both anaerobic alkane and aromatic degradation are initiated by the same step, the addition of a functional group (i.e., methyl or fumarate) to the respective substrate (Spormann and Widdel 2000). Two sulfate reducing strains, Hxd3 and Pnd3, were found to utilize *n*-alkanes by the addition of a C_1 functional group to the *n*-alkane substrate (Aeckersberg et al. 1998; Rabus et al. 2001; Widdel and Rabus 2001). Anaerobic degradation of toluene, a monoaromatic hydrocarbon, has been widely studied and can be degraded by pure anaerobic cultures utilizing sulfate, nitrate, and ferric iron as an electron acceptor (Spormann and Widdel 2000). The toluene degradation pathway is initiated by fumarate addition to the methyl group by benzylsuccinate synthase which yields benzylsuccinate (Spormann and Widdel 2000; Rabus et al. 2001; Widdel and Rabus 2001; Boll et al. 2002). These studies indicate anaerobic degradation pathways are important to consider in oil degradation.

MICROBIAL INFLUENCE ON SHIPWRECKS

Aerobic and anaerobic microbial metabolism can contribute to the deterioration of a sunken ship by physically influencing the surrounding environment (i.e., pH change) or by degrading materials in or on the ship. For example, studies have shown bacterial communities can physically influence pH and increase deterioration rates of wood, bone and iron (Gregory 1995; McLeod 1995). Other studies have shown that canvas deterioration in a shipwreck was due to microbial degradation (Gregory 1995; Wheeler 2001). This indicates microbial processes can effect shipwrecks chemically (i.e., pH influence) and biologically (i.e., degradation). There is a need to better understand how microbial populations affect the integrity of a shipwreck.

A better understanding of microbial interactions within a shipwreck is specifically important for USS *Arizona* because the ship is made of steel and lies in a temperate saltwater environment, making it very susceptible to corrosion. The ship also contains and is leaking Bunker C oil that can be used as a carbon source for microbial growth, suggesting that microbial metabolic activities may be extensive. Anaerobic degradation of the oil may cause H2S formation, increasing the ship's corrosion rate (Postgate 1979). Future studies can build upon the need to understand how oil degrading microbial communities influence metal corrosion and USS *Arizona* provides an excellent site for this type of scientific research.

SIGNIFICANCE AND OBJECTIVES OF THIS RESEARCH

Since the sinking of USS *Arizona* in 1941, it has been estimated that 1-2 liters of oil are released per day from the ship into the surrounding Pearl Harbor waters (Murphy and Russell, personal communication). The ship rests in a warm saltwater environment, which is conducive to structural corrosion. Further corrosion of the ship may ultimately result in the remaining amount of oil located in the ship to be released into the surrounding Pearl Harbor environment at a faster rate. This study will characterize oil leaking from USS *Arizona* to determine the extent of oil weathering prior to its release into the environment. Furthermore, this study will compare biomarker fingerprints of oil leaking from the ship to biomarkers of oil in sediments. This will determine if oil leaking from the ship is present in surrounding sediments. We will also determine if microorganisms from sediments on and surrounding the ship can degrade oil leaking

from the ship. This study will not only contribute to the overall understanding of the biodegradation and weathering of Bunker C oil in the marine environment, but it will also provide a foundation upon which future management decisions are made by the National Park Service regarding the ship and the surrounding environment. Therefore, the objectives of this study are:

1.   To chemically characterize oil leaking from the ship, including the hopane and sterane biomarkers.

2.   To characterize and fingerprint oil in sediments collected adjacent to and surrounding USS *Arizona*.

3.   To determine if aerobic microorganisms associated with USS *Arizona* sediments are capable of degrading Bunker C fuel oil leaking from the ship and if they influence Bunker C biomarker profiles.

MATERIALS AND METHODS

SEDIMENT AND OIL SAMPLES

Sediment and oil samples were collected from USS *Arizona* located in Pearl Harbor, HI, during 2000 and 2001 by underwater archaeologists from the National Park Service's Submerged Resources Center (Figures 8.4 and 8.5). Sediment samples were collected underwater by divers using 500 ml glass Erlenmeyer flasks. Sediment-filled flasks were brought to the surface, flushed with N_2, capped with black rubber stoppers, and sealed with electrical tape. Flasks were immediately placed in a cooler on ice. Samples of oil leaking from various USS *Arizona* locations (designated A and B) were collected using PVC pipes equipped with 50 ml conical polypropylene tubes attached to the end of the pipe. Conical tubes were brought to the surface, flushed with N_2, capped, and sealed with electrical tape. Samples were shipped on ice from Pearl Harbor to the laboratory in South Carolina and stored at 4°C.

Bow

Port   **Starboard**

Location B

01-029 Starboard Porthole S-43
(second deck, Disbursing Office)

01-018 Starboard Porthole S-38 (second
deck , Captain's Officer Stateroom)

01-026 Starboard Porthole S-34
(Junior Officer Stateroom)

00-004, 00-005, 00-006, 00-007
Starboard Porthole S-31

Location A

00-009 A hatch starboard of
Barbette No. 4

01-032 Midship's Galley

01-015 A hatch starboard of
Barbette No. 4

00-008, 01-019 Starboard Hatch

01-012 Starboard Porthole S-20

00-034 A hatch starboard of
Barbette No. 4

01-027 Starboard Captain's cabin

Barbette No. 4

Port   **Starboard**
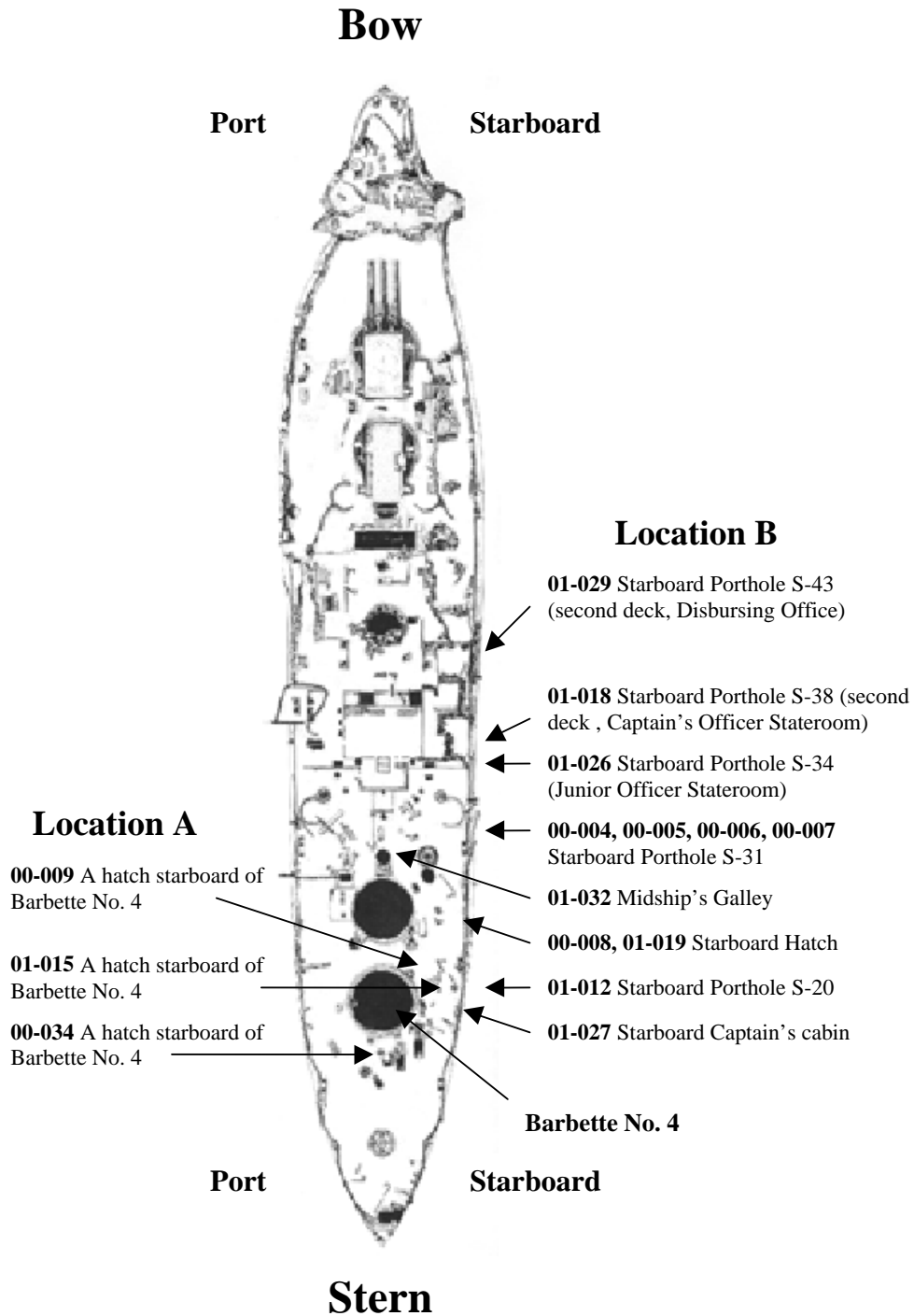
Stern

**Figure 8.4. USS *Arizona* sample locations for oil leaking from the ship. Location A
(stern starboard hatches) and B (stern starboard portholes) represent two different
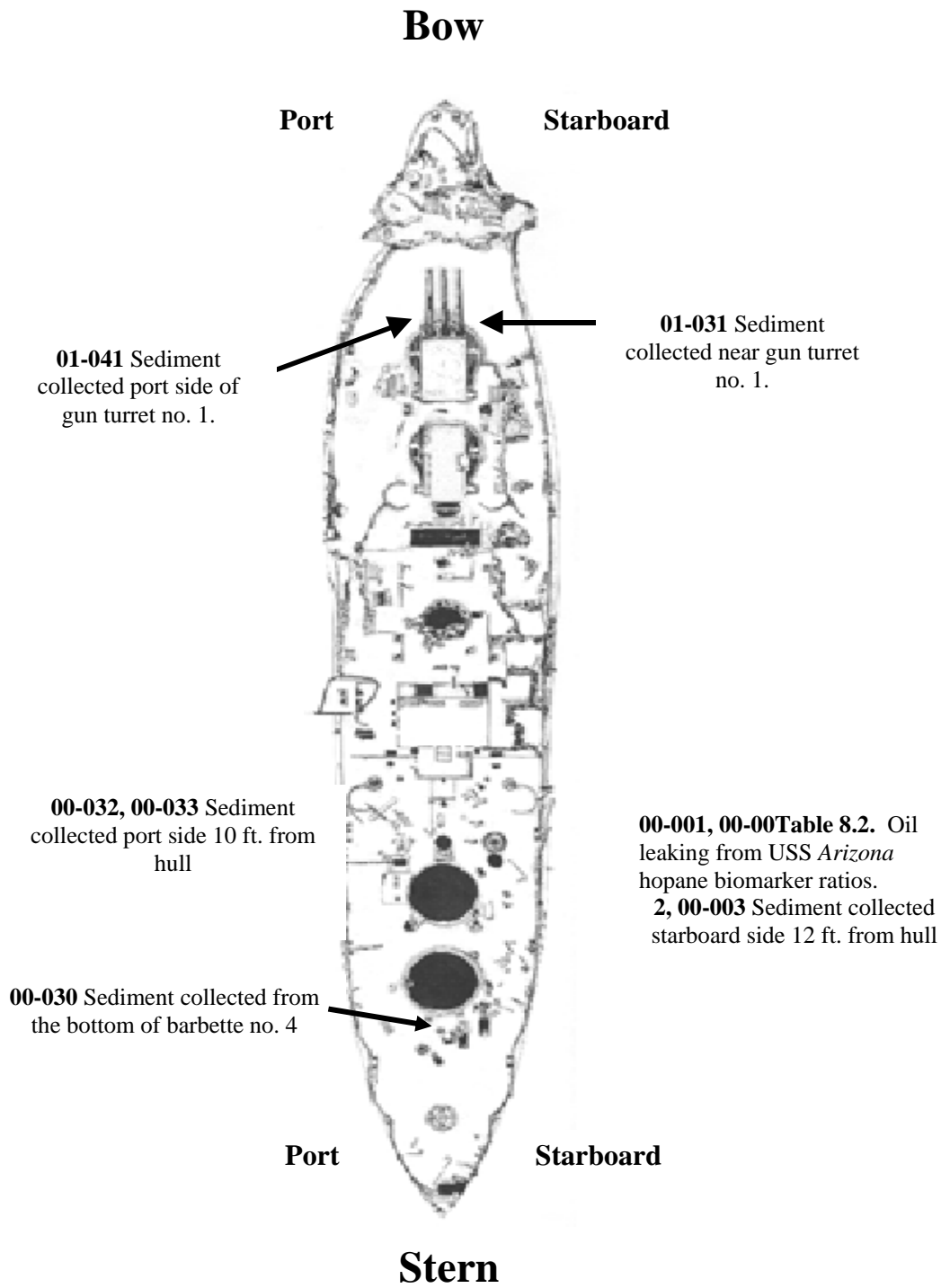general areas of the ship.**

Bow

Port   **Starboard**

01-041 Sediment collected port side of gun turret no. 1.

01-031 Sediment collected near gun turret no. 1.

00-032, 00-033 Sediment collected port side 10 ft. from hull

00-001, 00-00Table 8.2. Oil leaking from USS *Arizona* hopane biomarker ratios.
2, 00-003 Sediment collected starboard side 12 ft. from hull

00-030 Sediment collected from the bottom of barbette no. 4

Port   **Starboard**

Stern

Figure 8.5. USS *Arizona* sediment sample locations.

USS *ARIZONA* OIL EXTRACTIONS

To characterize oil leaking from different areas of the ship, oil samples (that included a mix of oil and seawater) were extracted using dichloromethane (GC Grade, EM Science, Gibbstown, NJ) and NaCl (2% in distilled water). After extracts became clear, five more fractions were collected to ensure good recovery for each sample, and all extracts were combined. Following extraction, samples were evaporated at 50ºC under vacuum to approximately 3 ml. Samples were then transferred to pre-weighed scintillation vials, air-dried, and weighed.

SEDIMENT EXTRACTIONS

To characterize hydrocarbons in sediments collected on the ship and in adjacent sediments, wet sediments were extracted using a Soxhlett apparatus. For each sediment sample, a sub-sample (approximately 2 g) was placed in a cellulose thimble (33 mm x 80 mm, Whatman, Maidstone, England) and extracted with a combination of the following three solvents placed in a round bottom flask: 30 ml acetone (GC Grade, Fisher Scientific, Fair Lawn, NJ), 30 ml hexane (GC Grade, Burdick & Jackson, Muskegon, MI), and 180 ml dichloromethane (GC Grade, EM Science, Gibbstown, NJ). After continuous Soxhlet extraction for 16 h, the extracts were evaporated and weighed.

USS *ARIZONA* ENRICHMENT CULTURES

To enrich for oil degrading microbial communities from USS *Arizona* sediments, Bunker C oil-degrading enrichment cultures were initiated using 1 g of USS *Arizona* wet sediments, 24 ml of GP2 medium, a synthetic saltwater medium supplemented with potassium nitrate (Chang, et al. 2000) that was amended with 2 mg/ml USS *Arizona* 00-034 oil. Oil sample 00-034 was chosen for the enrichment study because it was less weathered in comparison to other samples of USS *Arizona* oil. Enrichments were maintained in the dark at 30°C at 200 rpm and were transferred after 30 days using a 4% inoculum transfer. Samples for oil and microbial community analysis were not taken until after three monthly transfers had occurred. Aliquots (1

ml) were removed from the third monthly transfer at day 30 and stored at –80°C for microbial community structure analysis. The remaining contents of each culture flask were extracted for oil analysis.

USS *ARIZONA* ENRICHMENT CULTURE EXTRACTIONS

To remove oil from USS *Arizona* enrichment cultures, oil was extracted by shaking the entire contents of the culture flasks 5 times with approximately 100 ml of dichloromethane. Extracts were dried with anhydrous sodium sulfate (12-60 mesh, J.T. Baker, Phillisburg, NJ) and evaporated under vacuum to approximately 3 ml at 50ºC. Samples were then transferred to pre-weighed scintillation vials, air-dried and weighed.

OIL ANALYSIS

For all oil analyses, extracted oil (from both oil samples leaking from USS *Arizona* and aerobic enrichment cultures) and sediment solvent-extractable materials were first shaken for 6 h with hexane, and allowed to sit overnight to precipitate the asphaltenes. Deasphaltened samples were analyzed with a Hewlett-Packard Model 5890 Series II *Plus* gas chromatograph using a flame ionization detector and HP-5 column (25 m, 0.32 mm i.d.x 0.17 υm). The initial temperature was 50°C with a 5°C/min rate change to a final temperature of 310°C where it was held for 20 min. The injector temperature was 290°C and the detector temperature was 315°C. Helium was used at the carrier gas at 20.0 psi (Bost et al. 2001). Extractable materials were run at the same time as Bonny Light crude (BLC) oil, an oil that has been thoroughly characterized in the laboratory (Frontera-Suau et al. 2001; Norman et al. 2002), for peak comparisons. An additional peak was further examined in sediment solvent-extractable materials since it was predominant and ubiquitous in all sediment samples. This peak was analyzed collaboratively with Dr. Kevin Crawford (The Citadel, Charleston, SC) using a ThermoQuest gas chromatograph coupled to a Polaris Q mass spectrometer (full scan, EI mode).

PAH AND BIOMARKER ANALYSIS

PAHs and their alkylated homologues, as well as biomarkers (refer to Table 8.1 for a complete list) were analyzed by Dr. Tom McDonald (Texas A&M University, College Station, TX) using a Hewlett-Packard 5890 II gas chromatograph coupled to a Hewlett-Packard mass spectrometer in selected ion monitoring mode (SIM) according to the method of McDonald and Kennicutt (1992). Calibration standards were prepared at five concentrations (from 0.02 – 1 µg/ml) by diluting a commercially available standard (NIST SRM 2266). For each compound of interest, a relative response factor (RRF) was determined for each calibration level, and the 5 RRFs averaged to produce a relative response factor for each compound.

BIOMARKER QUANTITATION

Following analysis, biomarkers concentrations were calculated using peaks from m/z=191 to identify terpanes and m/z=217 to identify steranes (Bost et al. 2001). Peak concentrations were determined by multiplying the area under the peak by the calculated standard. Following concentration calculation, ratios were determined. C_{30} 17α(H),21β(H)-hopane was divided by 18α(H)-oleanane for the hopane to oleanane ratio. This ratio was used to determine if C_{30} 17α(H),21β(H)-hopane was being degraded (Bost et. al. 2001; Frontera-Suau et. al. 2002). C_{27} 17α(H)-22,29,30-trisnorhopane (Tm) and C_{27} 18α(H)-22.29,30-trisnorneohopane (Ts) were used for the Ts/(Ts + Tm) ratio. The concentration of Ts was divided by the sum of Ts and Tm concentrations. This ratio can be used as a maturity and source rock ratio (Peters and Moldowan 1993). The concentrations of C_{31} 17α(H)-homohopane (22*S* and 22*R*) were used for the C_{31} 22*S*/(22*S* + 22*R*) ratio. The concentration of 22*S* was divided by the sum of 22*S* and 22*R* concentrations. This ratio was used to determine if the 22*R* epimer was being degraded in comparison to the 22*S* epimer (Peters and Moldowan 1993). Tricyclic terpane ratios were also calculated from mass chromatograms m/z=191 using the peak areas of C_{28} 13β,21α(H)-tricyclic terpane 22*R* and 22*S* and C_{29} 13β,21α(H)-tricyclic terpane 22*R* and 22*S,* respectively to compare with the peak area of C_{30} 17α,21β(H)-hopane. These ratios were calculated to determine if C_{28}

PAHs and Heterocycles

Compound	Abbreviation	Compound	Abbreviation
Naphthalene	C0N	Fluoranthene	Fl
C1-Naphthalenes	C1N	Pyrene	C0Py
C2-Naphthalenes	C2N	C1-Fluoranthenes/Pyrenes	C1Py
C3-Naphthalenes	C3N	C2-Fluoranthenes/Pyrenes	C2Py
C4-Naphthalenes	C4N	C3-Fluoranthenes/Pyrenes	C3Py
Benzothiophene	C0B	Naphthobenzothiophene	C0Nbf
C1-Benzothiophenes	C1B	C1-Naphthobenzothiophenes	C1Nbf
C2-Benzothiophenes	C2B	C2-Naphthobenzothiophenes	C2Nbf
C3-Benzothiophenes	C3B	C3-Naphthobenzothiophenes	C3Nbf
Biphenyl	Bph	Benz(a)anthracene	BaA
Acenaphthylene	Acl	Chrysene	C0C
Acenaphthene	Ace	C1-Chrysenes	C1C
Dibenzofuran	Dbf	C2-Chrysenes	C2C
Fluorene	C0F	C3-Chrysenes	C3C
C1-Fluorenes	C1F	C4-Chrysenes	C4C
C2-Fluorenes	C2F	Benzo(b)fluoranthene	BbF
C3-Fluorenes	C3F	Benzo(k)fluoranthene	BkF
Anthracene	An	Benzo(e)pyrene	BeP
Phenanthrene	C0P	Benzo(a)pyrene	BaP
C1-Phenanthrene/Anthracenes	C1P	Perylene	Pe
C2-Phenanthrene/Anthracenes	C2P	Indeno(1,2,3-c,d)pyrene	IP
C3-Phenanthrene/Anthracenes	C3P	Dibenzo(a,h)anthracene	DA
C4-Phenanthrene/Anthracenes	C4P	C1-Dibenzo(a,h)anthracenes	C1DA
Dibenzothiophene	C0D	C2-Dibenzo(a,h)anthracenes	C2DA
C1-Dibenzothiophenes	C1D	C3-Dibenzo(a,h)anthracenes	C3DA
C2-Dibenzothiophenes	C2D	Benzo(g,h,i)perylene	BP
C3-Dibenzothiophenes	C3D		

Cycloalkanes

Compound	Abbreviation
C_{30} 17α(H),21β(H)-hopane	C29-Hopane
18α-Oleanane	18α-Oleanane
C_{30} 17α(H),21β(H)-hopane	C30-Hopane

Table 8.1 PAHs, alklyated PAHs and cycloalkanes analyzed by GC-MS.

$13\beta,21\alpha$(H)-tricyclic terpanes or C_{29} $13\beta,21\alpha$(H)-tricyclic terpanes were being degraded in comparison to C_{30} $17\alpha,21\beta$(H)-hopane.

Mass chromatogram peak areas of C_{27} 5α(H),14α(H),17α(H)-sterane (20*S* and 20*R*), C_{27} 5α(H),14β (H),17β (H)-sterane (20*S* and 20*R*) and C_{30} 17α(H),21β(H)-hopane were calculated for the $C_{27}S/C_{30}H$ ratio. This ratio was used to determine if C_{27} -steranes were being degraded in comparison to conserved C_{30} 17α(H),21β(H)-hopane. Mass chromatogram peak areas C_{28} 5α(H),14α(H),17α(H)-sterane (20*S* and 20*R*), C_{28} 5α(H),14β (H),17β (H)-sterane (20*S* and 20*R*) and C_{30} 17α(H),21β(H)-hopane were calculated for the $C_{28}S/C_{30}H$ ratio. This ratio was used to determine if the C_{28}-steranes were being degraded in comparison to conserved C_{30} 17α(H),21β(H)-hopane. Mass chromatogram peak areas of C_{29} 5α(H),14α(H),17α(H)-sterane (20*S* and 20*R*), C_{29} 5α(H),14β (H),17β (H)-sterane (20*S* and 20*R*) and C_{30} 17α(H),21β(H)-hopane were calculated for the $C_{29}S/C_{30}H$ ratio. This ratio was used to determine if the C_{29}-steranes were being degraded in comparison to conserved C_{30} 17α(H),21β(H)-hopane.

DNA EXTRACTION AND ANALYSIS

DNA extractions from aerobic enrichment cultures were performed according to Bost (2001). Aliquots (1 ml) of each enrichment culture were centrifuged for 10 min at 14,000 rpm. The resulting pellet was resuspended in 556 µl of TE buffer (10 mM Tris-HCl, pH 7.5; 1 mM EDTA, pH 8.0) and treated with 11 µl of lysozyme (50 mg/ml, Sigma, St. Louis, MO). After a 30 min incubation at 37°C, proteinase K (3 µl) and SDS (30 µl) were added, and the mixture was incubated for 1 h at 65°C. Following incubation 100 µl of 5 M NaCl and 80 µl hexadecyltrimethylammonium bromide (10% CTAB in O.7 M NaCl, J.T. Baker, Phillipsburg, NJ) were added, and the mixture was incubated for 10 min at 65°C. The mixture was extracted consecutively with chlorform:isoamyl alcohol (24:1), phenol:chloroform:isoamyl alcohol (25:24:1), and chlorform:isoamyl alcohol (24:1) at room temperature, and the supernatant was recovered at each step. Recovered supernatant was resuspended in 450 µl of chilled isopropanol to precipitate DNA and stored at -20°C for at least two hours. The mixture was centrifuged for 10 min at 14,000 rpm and 4°C, then the supernatant was removed. The DNA pellet was washed with 500 µl of chilled 70% ethanol for 30 min. DNA pellet and 70% ethanol were centrifuged for

15 min at 14,000 rpm and 4°C. Supernatant was removed and the DNA pellet was air dried, then resuspended in 50 µl of TE buffer.

DNA AMPLIFICATION

To amplify extracted DNA 16s rDNA was amplified by polymerase chain reaction (PCR), targeting a 323 base pair fragment, using two primers common to the *Bacteria* domain (Ferris et. al. 1996). The forward primer used for amplification was (5570F), *E. coli* positions 1055 to 1070; 5'-ATGGCTGTCGTCAGCT-3', and the reverse primer used for amplification was (9206GCR); *E. coli* positions 1392 to 1406 5'-CGCCCGCCGCGCCCCGCGCCCGGCCCGCCGCCCCCGCCCCACGGGCGTGTGTAC-3'. DNA aliquots of 0.5 ml were added to PCR master mix containing 1x PCR buffer (Promega, Madison, WI), 5 mM $MgCl_2$ (Promega, Madison, WI), 5570F and 9206GCR 10 pM/µl each (Foster City, CA), dNTPs (dGTP, dTTP, dATP, dCTP) 0.2 mM each (Applied Biosystems) 2.5 u/µl Taq Polymerase (Promege, Madison, WI), and 0.1 mg/ml Bovine Serum Albumin (New England Biolabs, Beverly, MA) to a final volume of 50 µl. DNA amplification was performed on the GeneMATE Thermal Cycler (ISC BioExpress, Kaysville, UT). The template DNA was initially denatured for 5 min at 94°C. After the initial denaturation, the PCR cycle was denaturation for 15 s at 94°C, primer extension for 2 min. at 72°C, and annealing for 30 s. The temperature during annealing was decreased by 1ºC from 53ºC to 43ºC, upon reaching 43ºC 20 supplementary annealing cycles were performed. Finally, primer extension was performed at 72°C for 6 min. DNA product was confirmed on an agarose gel in 1xTAE (20mM Tris actate [pH7.4] 10 mM sodium acetate 1mM Na_2-EDTA) and stained with ethidium bromide. DNA was visualized using a UV transilluminator and photographed.

DENATURING GRADIENT GEL ELECTROPHORESIS

Amplified DNA of two 45 µl reactions was combined and purified with the QIAquick PCR purification kit (Qiagen, Chatsworth, CA). Purified DNA in 30 µl aliquots were loaded onto 1X TAE 6% polyacrylamide gels (Fisher Scientific, Fair Lawn, NJ) with a 40% to 60% gradient consisting of 40% (v/v) formamide (Fisher Scientific, Fair Lawn, NJ) and 7 M urea (J.T.

Baker, Phillipsburg, NJ). Denaturing gradient gel electrophoresis (DGGE) was performed using a Dcode Universal Detection System (Bio-Rad, Hercules, CA) for 16 h at 50 volts and 60ºC. Following electrophoresis, gels were stained with 50 ml SYBR Green I (Molecular Bio-Probes, Eugene, OR) for 1 h and visualized using a Bio-Rad VersaDoc system (Bio-Rad, Hercules, CA).

CHARACTERIZATION OF OIL LEAKING FROM USS *ARIZONA*

INTRODUCTION

USS *Arizona* remains in the same place where it sank after the December 7, 1941 attack, and a memorial was built over the site in 1980. The ship's bunkers had been filled with 4,630 tons of Bunker C fuel oil prior to the attack and not all of the oil was burned off during and after the attack. Oil continues to leak from the ship into Pearl Harbor at an estimated rate of 1-2 L per day as determined by collecting oil as it bubbled out of the ship (Lenihan, 1990; Johnson et al., 2002; Murphy and Russell, personal communication). Characterization of the oil leaking from USS *Arizona* can provide an indication of the extent of oil weathering. Oil weathering can occur by abiotic processes (i.e., photodegradation or dissolution into saltwater) or biotic process (i.e., microbial degradation). In addition, examining the compositional changes between oil leaking from different locations may contribute to decisions involving conservation and management of USS *Arizona* by providing indirect information about the environmental conditions in the interior environment of the ship.

GAS CHROMATOGRAPHIC ANALYSIS OF OIL LEAKING FROM USS *ARIZONA*

Samples of oil leaking from 15 locations were collected in 2000 and 2001 from USS *Arizona* (Figure 8.4). The samples contained a mixture of oil and seawater, so they were extracted with dichloromethane and air-dried overnight. Initial gas chromatographic analysis provided a means of monitoring the overall extent of oil weathering, specifically the depletion of *n*-alkanes and the branched alkanes, pristane and phytane. Gas chromatographic traces of oil leaking from the ship differed depending on location (Figures 8.6–8.8). Overall, oil leaking from location A (Figure 8.6) still contained *n*-alkanes and branched alkanes in comparison to oil
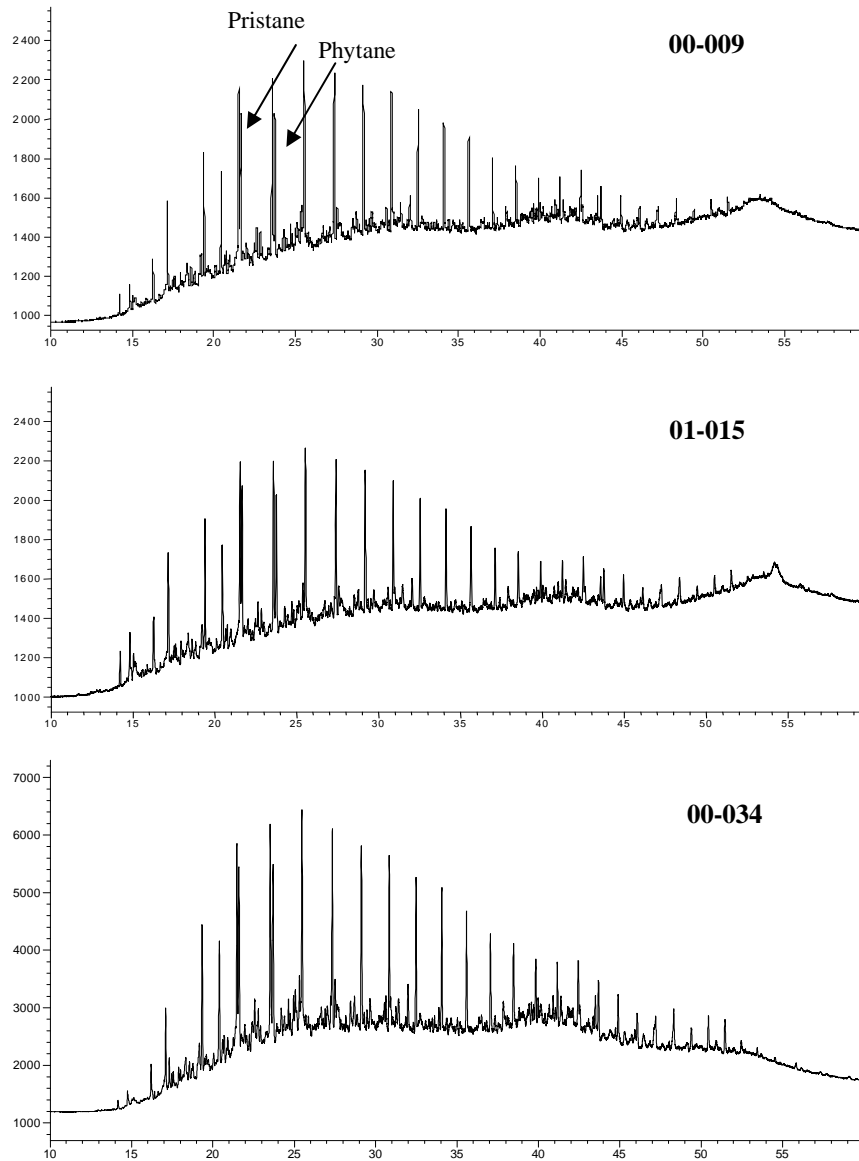
Figure 8.6 GC-FID traces of *USS Arizona* oil samples representative for oil leaking from location A. Oil leaking from location A still contains *n*-alkanes and the branched alkanes, pristane and phytane. In the above chromatograms, the y-axis is the detector response and the x-axis is the retention time in minutes. Detector response for the y-axis is not the same scale for each chromatogram.
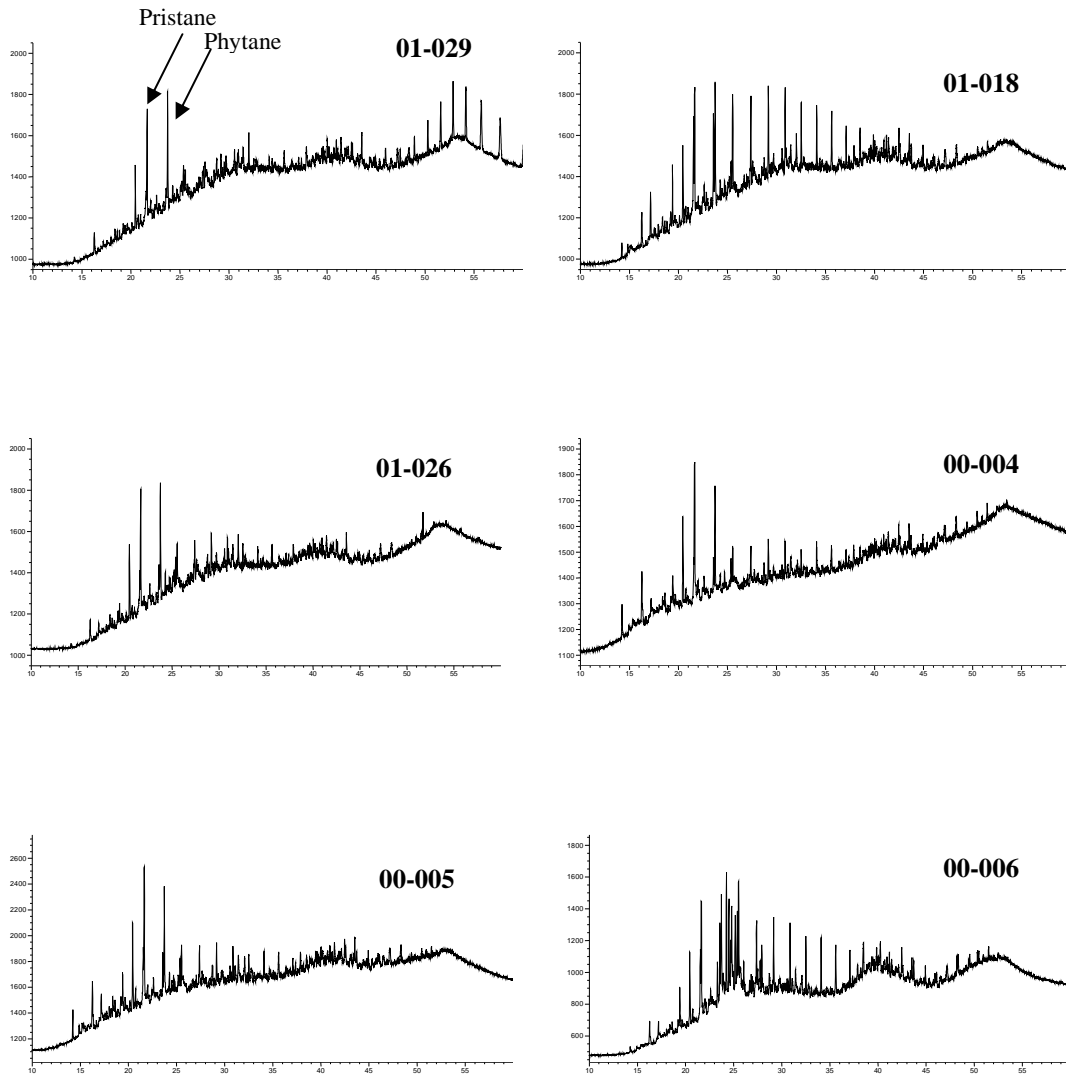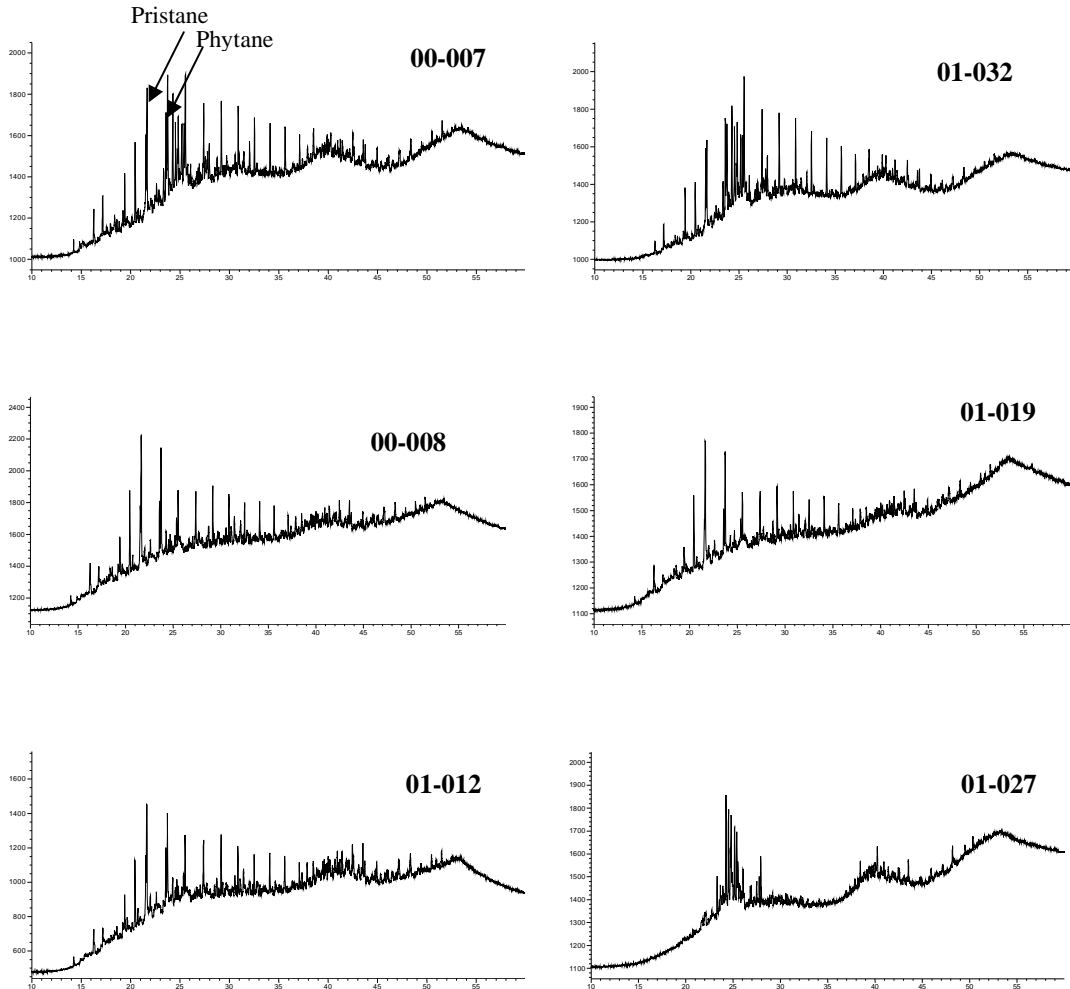
Figure 8.7 GC-FID traces of *USS Arizona* oil samples representative of location B. Oils leaking from location B show significant weathering, most noticeably depletion of *n*-alkanes in comparison to oil leaking from location A. The branched alkanes, pristane and phytane, are still present. In the above chromatograms, the y-axis is the detector response and the x-axis is the retention time in minutes. Detector response for the y-axis is not the same scale for each chromatogram.

Figure 8.8 GC-FID traces of *USS Arizona* oil samples representative of location B. Oils leaking from location B show significant weathering of the oil, most noticeably depletion of *n*-alkanes in comparison to oil leaking from location A. In the above chromatograms, the y-axis is the detector response and the x-axis is the retention time in minutes. Detector response for the y-axis is not the same scale for each chromatogram.

leaking from location B (Figures 8.7 and 8.8). Gas chromatographic traces for 00-009, 01-015 and 00-034 are from location A and contain *n*-alkanes, along with pristane and phytane (Figure 8.6). In comparison, traces for 01-029, 01-018, 01-026, 00-004, 00-005, 00-006, 00-007, 01-032, 00-008, 01-019, 01-012 and 01-027 (Figures 8.7 and 8.8) are from location B and show a depletion of *n*-alkanes but still contain pristane and phytane. Overall, this suggests that oil leaking from location B has undergone more weathering (either biotic or abiotic) than oil leaking from location A.

INDIVIDUAL PAH ANALYSIS OF OIL LEAKING FROM USS *ARIZONA*

Mass spectrometry was utilized to monitor the concentration of 53 target PAHs (including heterocycles) (Table 8.1) in samples of oil leaking from different locations of USS *Arizona*. Triplicates of three oil samples, 01-015 and 00-034 (from location A) and 01-029 (from location B), were chosen for PAH analysis because they showed the least weathering (01-015 and 00-034) or the most weathering (01-029). Overall, mass spectrometry analysis indicated PAHs were still present in all three analyzed samples of oil (Figure 8.9). For oil sample 00-034, one of the three triplicates exhibited a different PAH pattern, causing large standard error bars. Mass spectrometry indicated oil samples 01-029 (location B) and oil sample 00-034 (location A) had fewer low molecular weight PAHs than sample 01-015 (location A) (Figure 8.9). For example, sample 01-029 and 00-034 contained less 2-ring naphthalene, and C_1-C_4 naphthalenes than sample 01-015 leaking from location A. Differences in high molecular weight hydrocarbons from locations A and B were not observed (Figure 8.10).

PAHS COMPARED TO CONSERVED BIOMARKERS

Mass spectrometry also provided data for analysis of the biomarkers $C_{30}17\alpha(H),21\beta(H)$-hopane and $18\alpha(H)$-oleanane present in oil leaking from the ship. The ratio of $C_{30}17\alpha(H),21\beta(H)$-hopane to $18\alpha(H)$-oleanane was calculated for oil extracts to determine if $C_{30}17\alpha(H),21\beta(H)$-hopane was being degraded. Ratios were similar (e.g., 6.17) in all oil samples from USS *Arizona* (Table 8.2), indicating no degradation of $C_{30}17\alpha(H),21\beta(H)$-hopane.
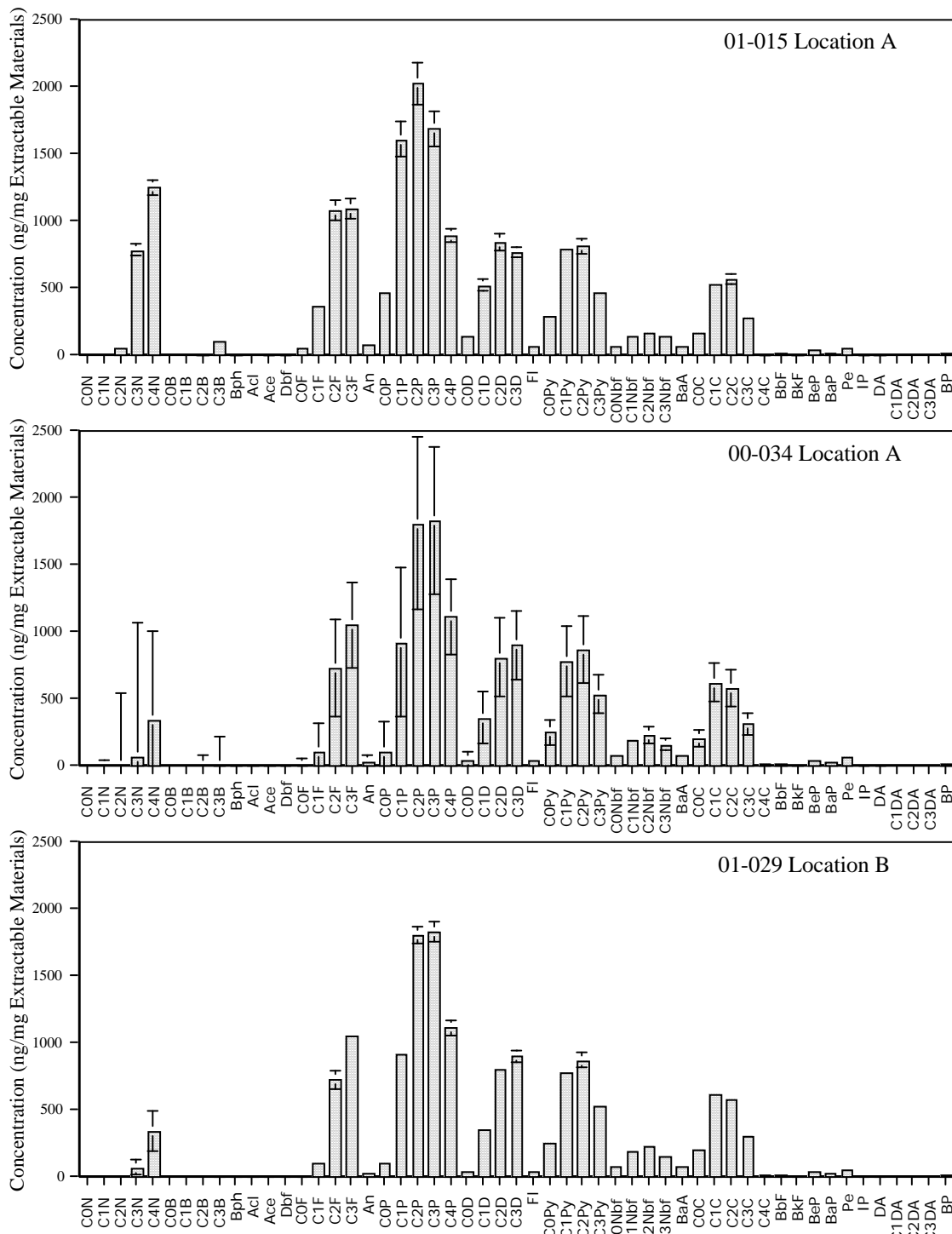
Figure 8.9 Individual PAH analysis for oil leaking from USS *Arizona*. Oil leaking from 00-034 and 01-029 shows a depletion of lower molecular weight PAHs in comparison to oil leaking from 01-015. Abbreviations are defined in Table 8.1 and locations of leaking oil are defined in Figure 8.4.
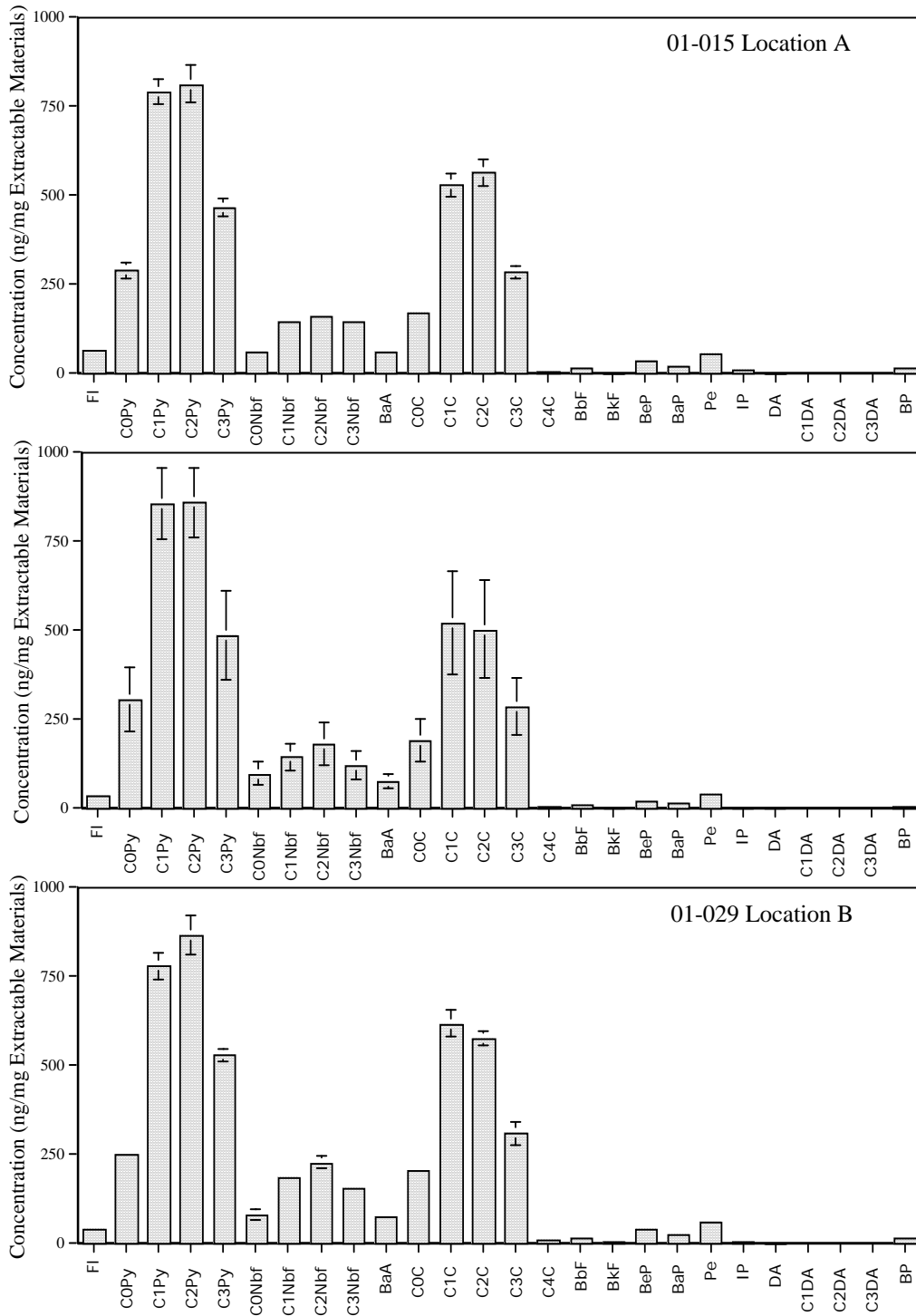
Figure 8.10. Individual PAH analysis of high molecular weight PAHs for oil leaking from USS *Arizona*. Abbreviations are defined in Table 8.1 and locations of leaking oil are defined on Figure 8.4.

Oil	Location	$C_{30}H/18\alpha$ Oleanane [a]	$Ts/(Ts+Tm)$ [b]	$C_{31}S/(C_{31}R + C_{31}S)$ [c]	$C_{28}TT/C_{30}H$ [d]	$C_{29}TT/C_{30}H$ [e]
01-015	A	6.20 ± 0.09	0.53 ± 0.03	0.50 ± 0.01	0.36 ± 0.02	0.36 ± 0.02
00-034	A	5.93 ± 0.25	0.43 ± 0.01	0.50 ± 0.01	0.45 ± 0.01	0.43 ± 0.01
01-029	B	6.25 ± 0.15	0.56 ± 0.01	0.50 ± 0.01	0.31 ± 0.01	0.31 ± 0.01

All values are the means and standard error of triplicate samples.

[a] Calculated from m/z=191 mass chromatogram peak areas of C_{30} $17\alpha(H),21\beta(H)$-hopane and $18\alpha(H)$-oleanane.

[b] Calculated from the m/z=191 mass chromatogram peak areas of C_{27} $17\alpha(H)$-22,29,30-trisnorhopane (Tm) and C_{27} $18\alpha(H)$-22,29,30-trisnorneohopane (Ts).

[c] Calculated from the m/z=191 mass chromatogram peak areas of C_{31} $17\alpha(H)$-homohopane (22S and 22R).

[d] Calculated from the m/z=191 mass chromatogram peak areas of C_{28} $13\beta,21\alpha(H)$-tricyclic terpanes and C_{30} $17\alpha(H)21\beta(H)$-hopane.

Table 8.2. Selected biomarker ratios of oil leaking from USS *Arizona*.

The results indicate that $18\alpha(H)$-oleanane and $C_{30}17\alpha(H),21\beta(H)$-hopane can be used as conserved biomarkers to monitor PAH degradation.

The ratios of total PAHs to the conserved biomarkers were calculated in order to determine relative total PAH ratio changes between oil leaking from different locations of the ship (Table 8.3). Overall, the ratios of total PAHs to conserved biomarkers were greater in oil leaking from location A in comparison to oil leaking from location B (Table 8.3). Total PAHs to conserved $C_{30}17\alpha(H),21\beta(H)$-hopane values were higher in sample 00-034 (from location A) and were lowest in sample 01-029 (from location B) (Table 8.3). Total PAHs to conserved $18\alpha(H)$-oleanane values were also higher in sample 00-034 (from location A) and the lowest ratio was observed in sample 01-029 (from location B) (Table 8.3). For oil sample 00-034, 1 of the 3 triplicates exhibited different PAH concentrations, causing a large standard error for the total PAHs to the conserved biomarkers $C_{30}17\alpha(H),21\beta(H)$-hopane and $18\alpha(H)$-oleanane ratios.

The ratios of low molecular weight total napthalenes to conserved biomarkers $C_{30}17\alpha(H),21\beta(H)$-hopane and $18\alpha(H)$-oleanane were calculated to observe any total naphthalenes ratio changes between oil leaking from different locations of the ship. The ratios of total naphthalenes to conserved biomarkers were greater in oil leaking from location A in comparison to oil leaking from location B (Table 8.3). For example, total naphthalenes to conserved $C_{30}17\alpha(H),21\beta(H)$-hopane values were the greatest in sample 00-034 (from location A) which had a ratio of 18.15 ± 8.24 and were the lowest in sample 01-029 (from location B) which had a ratio of 0.18 ± 0.01 (Table 8.3). The ratio of total naphthalenes to $18\alpha(H)$-oleanane

Oil	Location	Total PAHs:C_{30}-hopane[a]	Total PAHs:18α-oleanane	Total naphthalenes:C_{30}-hopane[a]	Total naphthalenes:18α-oleanane
01-015	A	38.65±0.55	239.65±7.21	4.37±0.29	27.16±2.18
00-034	A	97.70±21.27	590.07±145.05	18.15±8.24	110.60±53.95
01-029	B	25.87±0.99	161.56±6.22	0.18±0.01	4.56±2.46

All values are the means and standard error of triplicate samples.
[a] C_{30}-hopane represents C_{30} 17α(H),21β(H)-hopane.

Table 8.3. USS *Arizona* oil ratios of total PAHs and total naphthalenes to conserved biomarkers.

values were also the greatest in sample 00-034 (from location A) which had a ratio of 110.60±53.95 and decreased to the lowest ratio in sample 01-029 (from location B) which had a ratio of 4.56±2.46 (Table 8.3). One of the oil samples for 00-034 had 1 of the 3 triplicates exhibited a different PAH pattern, causing large standard error for the total naphthalenes to conserved biomarkers C_{30}17α(H),21β(H)-hopane and 18α(H)-oleanane ratios.

BIOMARKER ANALYSIS OF AEROBICALLY DEGRADED BUNKER C CRUDE OIL

Mass spectrometry was used to determine biomarker profiles of oil leaking from USS *Arizona* and determine if weathering processes such as degradation are influencing biomarker profiles. Triplicates of three oil samples 01-015 and 00-034 (from location A) and 01-029 (from location B) were chosen for analysis. Mass chromatograms for *m/z*=191 for hopanes and *m/z* 217 for steranes were analyzed. Mass chromatograms *m/z*=191 for oil leaking from USS *Arizona* showed no discernable differences between oil leaking from different locations 01-015, 00-034 (from location A) and 01-029 (from location B). (Figures 8.11 and 8.12). Mass chromatograms for the *m/z*=217 sterane trace also showed no discernable differences between oil leaking from different locations 01-015, 00-034 (from location A) and 01-029 (from location B). (Figures 8.11 and 8.12).

Biomarker ratios were calculated from mass chromatograms *m/z*=191 as described in section 2 (Table 8.2). Briefly, mass chromatogram peak areas of C_{30} 17α(H),21β(H)-hopane and 18α-oleanane were calculated for the hopane to oleanane ratio. Peak areas of C_{27} 17α(H)-22,29,30-trisnorhopane (Tm) and C_{27} 18α(H)-22,29,30-trisnorneohopane (Ts), were calculated
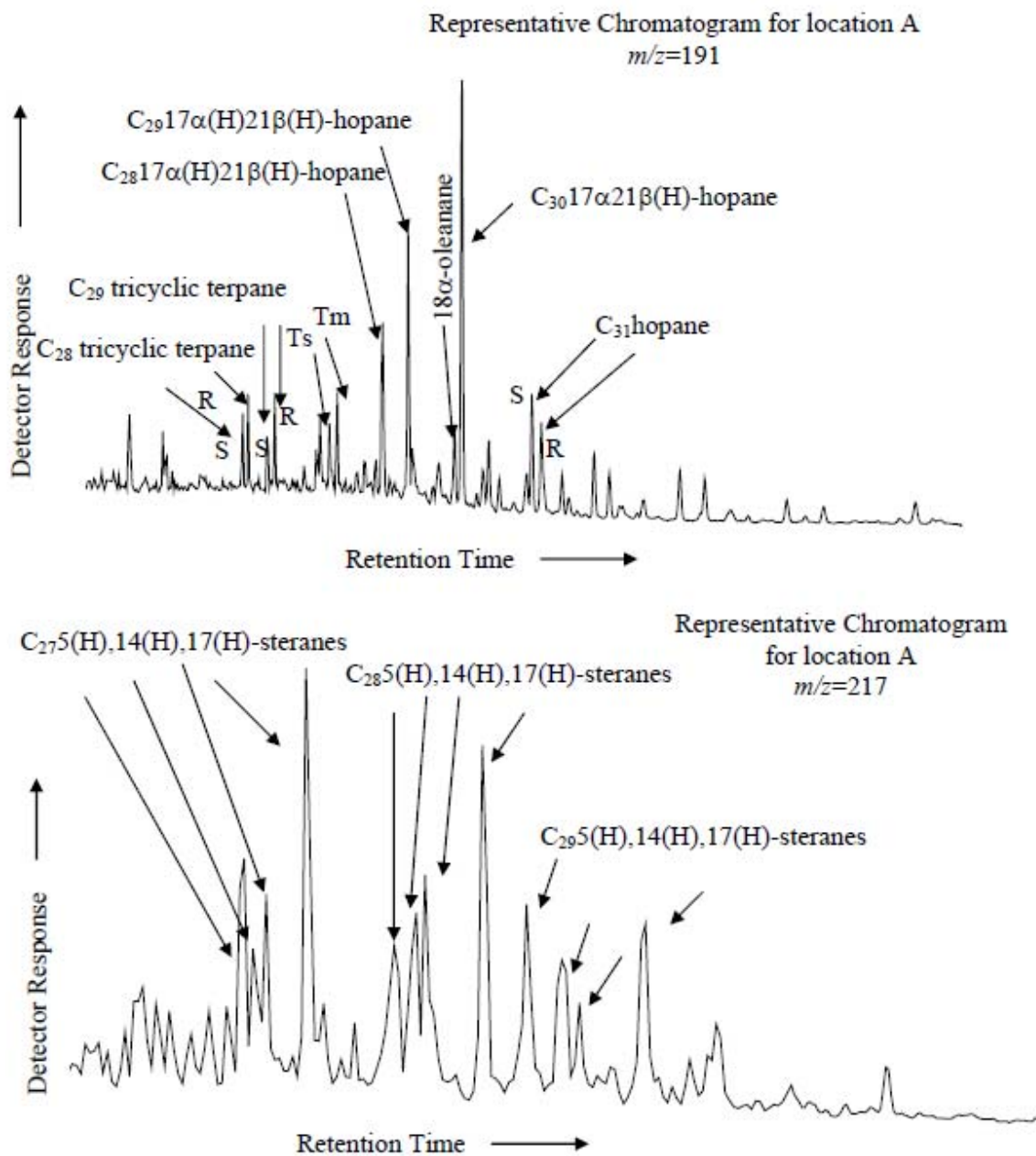
Figure 8.11. Representative mass chromatograms for 01-015 and 00-034 oil leaking from location A of USS *Arizona* for *m/z*=191 (hopanes) and *m/z*=217 (steranes).
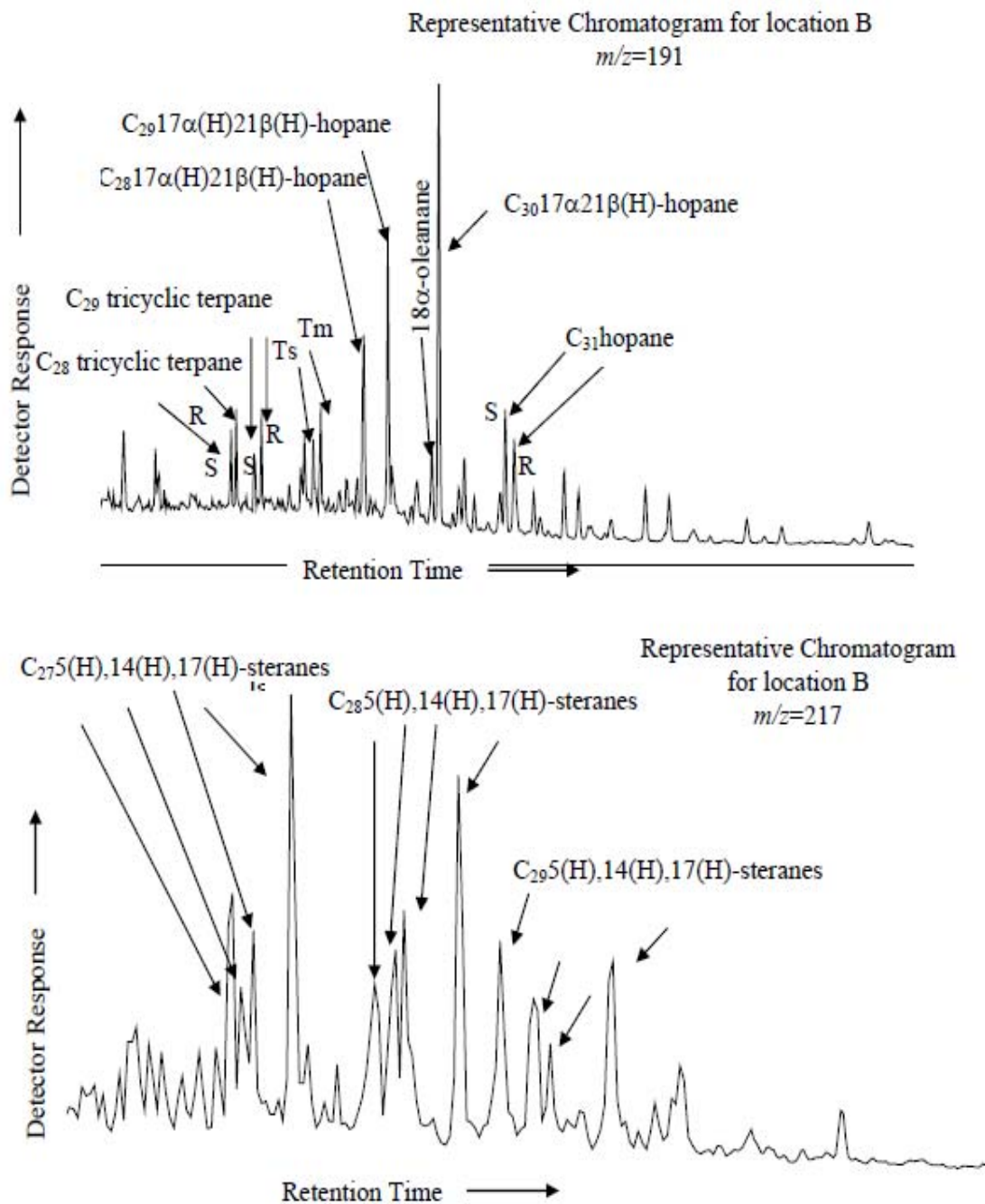
Figure 8.12. Biomarkers mass chromatograms for 01-029 oil leaking from location B of USS *Arizona* for *m/z*=191 (hopanes) and *m/z*=217 (steranes).

for the Ts/(Ts + Tm) ratio. Mass chromatogram peak areas of C_{31} 17α(H)-homohopane (22S and 22R) were calculated for the C_{31} 22S/(22S + 22R) ratio. Tricyclic terpane ratios were also calculated from mass chromatograms m/z=191 using the peak areas of C_{28} $13\beta,21\alpha$(H)-tricyclic terpane 22R and 22S and C_{29} $13\beta,21\alpha$(H)-tricyclic terpane 22R and 22$S,$ respectively to compare with the peak area of C_{30} $17\alpha,21\beta$(H)-hopane (C_{28}TT/C_{30}H and C_{29}TT/C_{30}H, respectively). Ratios calculated from mass chromatograms m/z=191 for oil 01-015, 00-034, and 01-029 had little variability (Table 8.2). For example, ratios for the Ts/(Ts+Tm) ratio ranged from 0.43$\pm$0.01 for oil sample 00-034 (from location A) to 0.56$\pm$0.01 for oil sample 01-029 (from location B) (Table 8.2). In comparison, the ratio of C_{31}S/(C_{31}R + C_{31}S) was 0.50$\pm$0.01 for all oil samples (01-015, 00-034 and 01-029) (Table 8.2). The ratios of C_{28}TT/C_{30}H for samples of oil leaking from the ship ranged from 0.31$\pm$0.01 for sample 01-029 to 0.45$\pm$0.01 for sample 00-034 (Table 8.2). The ratio of C_{29}TT/C_{30}H for oil samples ranged from 0.31$\pm$0.01 for sample 01-029 to 0.43$\pm$0.01 for sample 00-034 (Table 8.2).

Biomarker ratios were also calculated from mass chromatograms m/z=217 (Table 8.4). Details for calculation are in section 2. Briefly, mass chromatogram peak areas of C_{27} 5α(H),14α(H),17α(H)-sterane (20S and 20R), C_{27} 5α(H),14β (H),17β (H)-sterane (20S and 20R) and C_{30} 17α(H),21β(H)-hopane were calculated for the C_{27}S/C_{30}H ratio. Mass chromatogram peak areas C_{28} 5α(H),14α(H),17α(H)-sterane (20S and 20R), C_{28} 5α(H),14β (H),17β (H)-sterane (20S and 20R) and C_{30} 17α(H),21β(H)-hopane were calculated for the C_{28}S/C_{30}H ratio. Mass chromatogram peak areas of C_{29} 5α(H),14α(H),17α(H)-sterane (20S and 20R), C_{29} 5α(H),14β (H),17β (H)-sterane (20S and 20R) and C_{30} 17α(H),21β(H)-hopane were calculated for the C_{29}S/C_{30}H ratio.

Following calculation, sterane biomarker ratios for oil leaking from the ship were compared. Overall oil sample 01-015 and 01-029 ratios were similar to each other and were less than sample 00-034 (Table 8.4). For example, the ratio of C_{27}S/C_{30}H for sample 00-034 was 2.62$\pm$0.11. In comparison, the ratios for samples 01-015 and 01-029 were 1.96$\pm$0.04 and 1.91$\pm$0.06, respectively (Table 8.4). The same ratio pattern is true for C_{28}S/C_{30}H. The ratio for sample 00-034 was 2.13$\pm$0.26 in comparison, the ratios for samples 01-015 and 01-029 were 1.58$\pm$0.01and 1.56$\pm$0.01, respectively (Table 8.4). The same pattern is also present in the

$C_{29}S/C_{30}H$ ratio. The ratio of for sample 00-034 was 1.77 ± 0.07 and, the ratios for samples 01-015 and 01-029 were 1.62 ± 0.09 and 1.58 ± 0.01, respectively (Table 8.4).

CHARACTERIZATION OF HYDROCARBONS IN SEDIMENTS COLLECTED FROM USS *ARIZONA*

INTRODUCTION

USS *California*, USS *Maryland*, USS *Oklahoma*, USS *Tennessee*, USS *West Virginia*, and USS *Arizona* were attacked in Pearl Harbor on December 7, 1941. Every ship was assaulted and released Bunker C fuel oil into the immediate area (Lenihan, 1990). Following the Pearl Harbor attack, USS *Arizona* sank and unlike the other ships it was not recovered for use during World War II (Lenihan, 1990). Instead, USS *Arizona* remains in the same place it sank, continually leaking Bunker C fuel oil into the environment (Lenihan, 1990). During 1961, a memorial was built over the ship to commemorate the lives lost during the Pearl Harbor attack (Lenihan, 1990; Pearl Harbor Natural Resources Trustees, 1999). The ship and memorial are both managed by the National Park Service. Because the ship is considered a memorial, oil remaining inside cannot be physically removed, therefore oil continues to leak into Pearl Harbor.

Oil	Location	$C_{27}S/C_{30}H$ [a]	$C_{28}S/C_{30}H$ [b]	$C_{29}/C_{30}H$ [c]
01-015	A	1.96 ± 0.04	1.58 ± 0.01	1.62 ± 0.09
00-034	A	2.62 ± 0.11	2.13 ± 0.26	1.77 ± 0.07
01-029	B	1.91 ± 0.06	1.56 ± 0.01	1.58 ± 0.01

All values are the means and standard error of triplicate samples.
[a] Calculated from m/z=217 mass chromatogram peak areas of $C_{27}5\alpha(H),14\alpha(H),17\alpha(H)$-sterane (20S and 20R), $C_{27}5\alpha(H),14\beta(H),17\beta(H)$-sterane (20S and 20R) and $C_{30} 17\alpha(H),21\beta(H)$-hopane.
[b] Calculated from m/z=217 mass chromatogram peak areas of $C_{28}5\alpha(H),14\alpha(H),17\alpha(H)$-sterane (20S and 20R), $C_{28}5\alpha(H),14\beta(H),17\beta(H)$-sterane (20S and 20R) and $C_{30}17\alpha(H),21\beta(H)$-hopane.
[c] Calculated from m/z=217 mass chromatogram peak areas of of $C_{29}5\alpha(H),14\alpha(H),17\alpha(H)$-sterane (20S and 20R) $C_{29}5\alpha(H),14\beta(H),17\beta(H)$-sterane and $C_{30} 17\alpha(H),21\beta(H)$-hopane.

Table 8.4. Oil leaking from USS *Arizona* sterane biomarker ratios.

USS *Arizona* is not the only source of contamination in Pearl Harbor. Another source is the nearby U.S. Navy facility, which contributes anthropogenic compounds (i.e., PAHs, PCBs, and metals) to the sediments (Ashwood and Olsen, 1988; U.S.Navy, 1998). In addition, Chevron released 41,244 gallons of Bunker C oil into Pearl Harbor during a refinery oil spill on May 4, 1996 (Pearl Harbor Natural Resource Trustees, 1999).

The objective of this study was to characterize hydrocarbons in the sediments adjacent to and surrounding USS *Arizona*. Sediment extracts were examined by GC-FID (for *n*-alkane and branched alkanes) and GC-MS for PAHs and their alkylate homologues as well as biomarkers (m/z-191 and m/z=217). The biomarker profiles of oil extracted from sediments can be compared to biomarker profiles of oil leaking from USS *Arizona*. Therefore, a comparison of patterns can be used to determine if oil leaking from the ship is present in Pearl Harbor sediments.

GAS CHROMATOGRAPHIC ANALYSIS OF SEDIMENT SOLVENT-EXTRACTABLE MATERIALS

Sediment samples from 8 locations were collected from Pearl Harbor during the summers of 2000 and 2001 (Figure 8.5). Solvent-extractable materials obtained from sediments by continuous soxhlet extraction averaged 1.79±0.35 mg extractable material/g of dry sediment (Table 8.5). Following gravimetric measurement, GC-FID analysis of sediment extracts

Sediment	Location	Solvent-Extractable Material (mg/g)[a]
00-001	Stern section, starboard side, 12 ft. from hull	2.15±0.58
00-002	Stern section, starboard side, 12 ft. from hull	0.99±0.57
00-003	Stern section, starboard side, 12 ft. from hull	1.00±0.11
00-032	Stern section, port side, 10 ft. from hull	1.23±0.17
00-033	Stern section, port side, 10 ft. from hull	1.04±0.29
00-030	Stern section, bottom of barbette No. 4	2.59±0.11
00-031	Bow section, gun turret No. 1	0.99±0.61
01-041	Bow section, port side of gun turret No. 1	1.37±0.38

All values are the average of triplicate samples with the standard errors of those values.
[a]mg extractable material per gram of dry sediment.

Table 8.5. USS Arizona sediment solvent-extractable material

indicated the presence of *n*-alkanes along with the presence of several ubiquitous peaks (Figures 8.13–8.16). Bonny Light crude (BLC) oil was analyzed by gas chromatography during the same run as the sediment extracts, demonstrating peaks in sediment extracts that co-eluted with *n*-alkanes in BLC suggesting *n*-alkanes are present in the sediments (Figures 8.13–8.16).

The large ubiquitous peak (observed at a retention time of 26.821) found in all solvent-extractable materials was identified as butylated hydroxytoluene (BHT) (*m/z*=205) by GC-MS (Figure 8.17). In order to elucidate the source of the BHT, soxhlet extraction was conducted without sediments, containing only solvent, boiling chips, and a cotton thimble. BHT was detected in these extracts by GC-MS (Figure 8.18). However, BHT was also detected by GC-MS in oil sample 00-034 of oil leaking from USS *Arizona* that was not extracted using a soxhlet apparatus (Figure 8.19)*.* A soxhlet extraction control with just solvents was not conducted.

PAH ANALYSIS OF SEDIMENT SOLVENT-EXTRACTABLE MATERIALS

Further analysis of sediment solvent-extractable material by GC-MS for 53 PAHs and their alklyated homologues (and heterocycles) was conducted. The higher standard error for PAHs detected in sediment extracts (as compared to GC-MS analysis of PAHs in oil leaking from the ship) may be due to inherent variability in the sediments sampled. Using mass spectrometry, low molecular weight PAHs, naphthalene and fluorene or their alkylated homologues, were not detected. However, a number of high molecular weight PAHs (i.e., pyrene, chrysene) were detected (Figures 8.20–8.22).

PAHS COMPARED TO CONSERVED BIOMARKERS

GC-MS analysis of the biomarkers $C_{30}17\alpha(H),21\beta(H)$-hopane and $18\alpha(H)$-oleanane present in USS *Arizona* sediments (Table 8.6) was also conducted. The total amount of PAHs was variable in sediments, ranging from 426.97 ± 236.71 to 16278.60 ± 10105.12 ng PAH/mg dry sediment. The ratios of total PAHs to conserved biomarkers $C_{30}17\alpha(H),21\beta(H)$-hopane ranged from 0.44 ± 0.09 to 10.43 ± 4.86. Total PAHs to $18\alpha(H)$-oleanane ranged from 1.38 ± 0.30 to 37.14 ± 20.14 (Table 8.7).
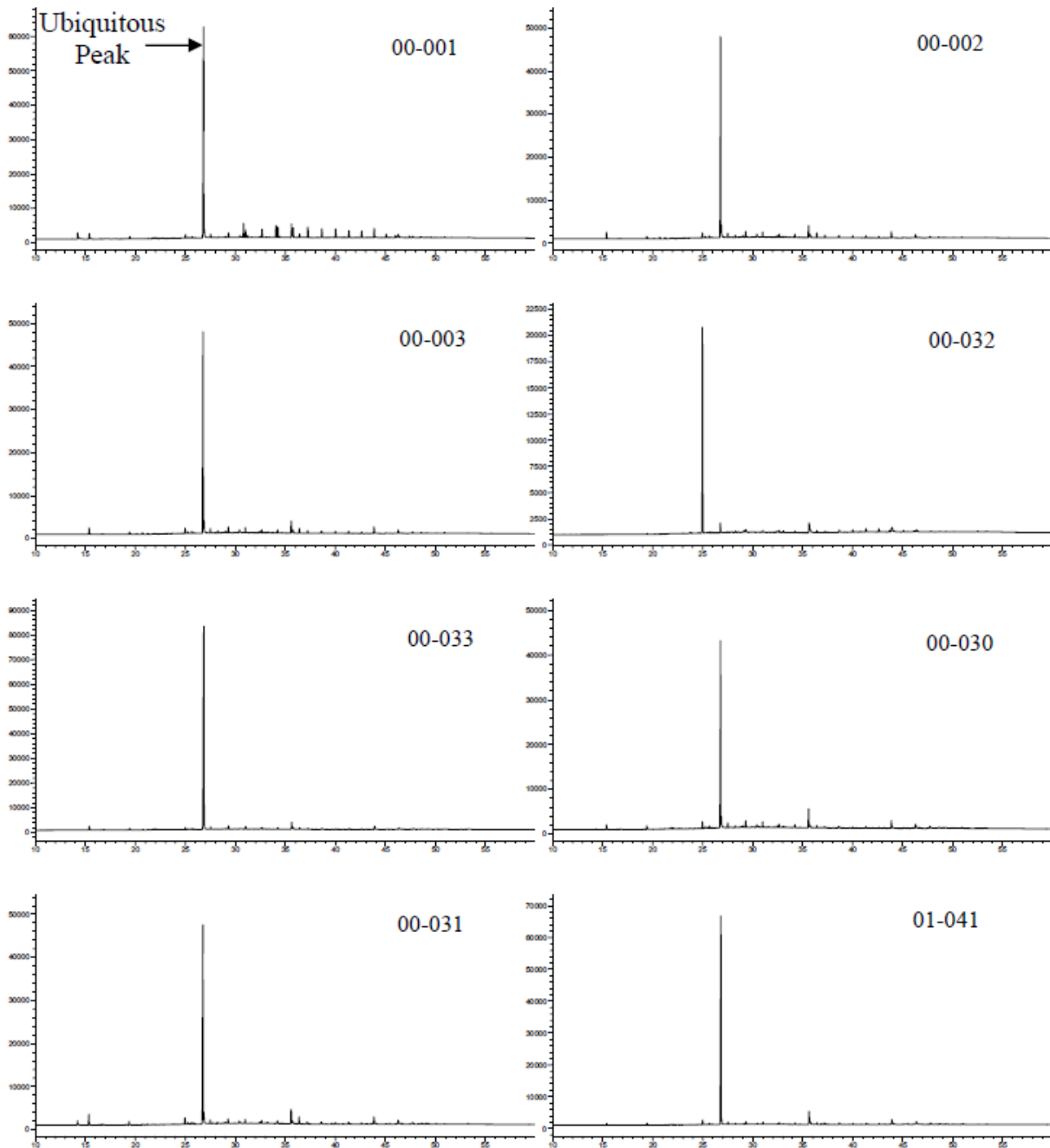
Figure 8.13. Gas chromatograms of solvent-extractable materials removed from sediments. There was a ubiquitous peak found in all sediments extracts. In the above chromatograms, the y-axis is the detector response and the x-axis is the retention time in minutes.
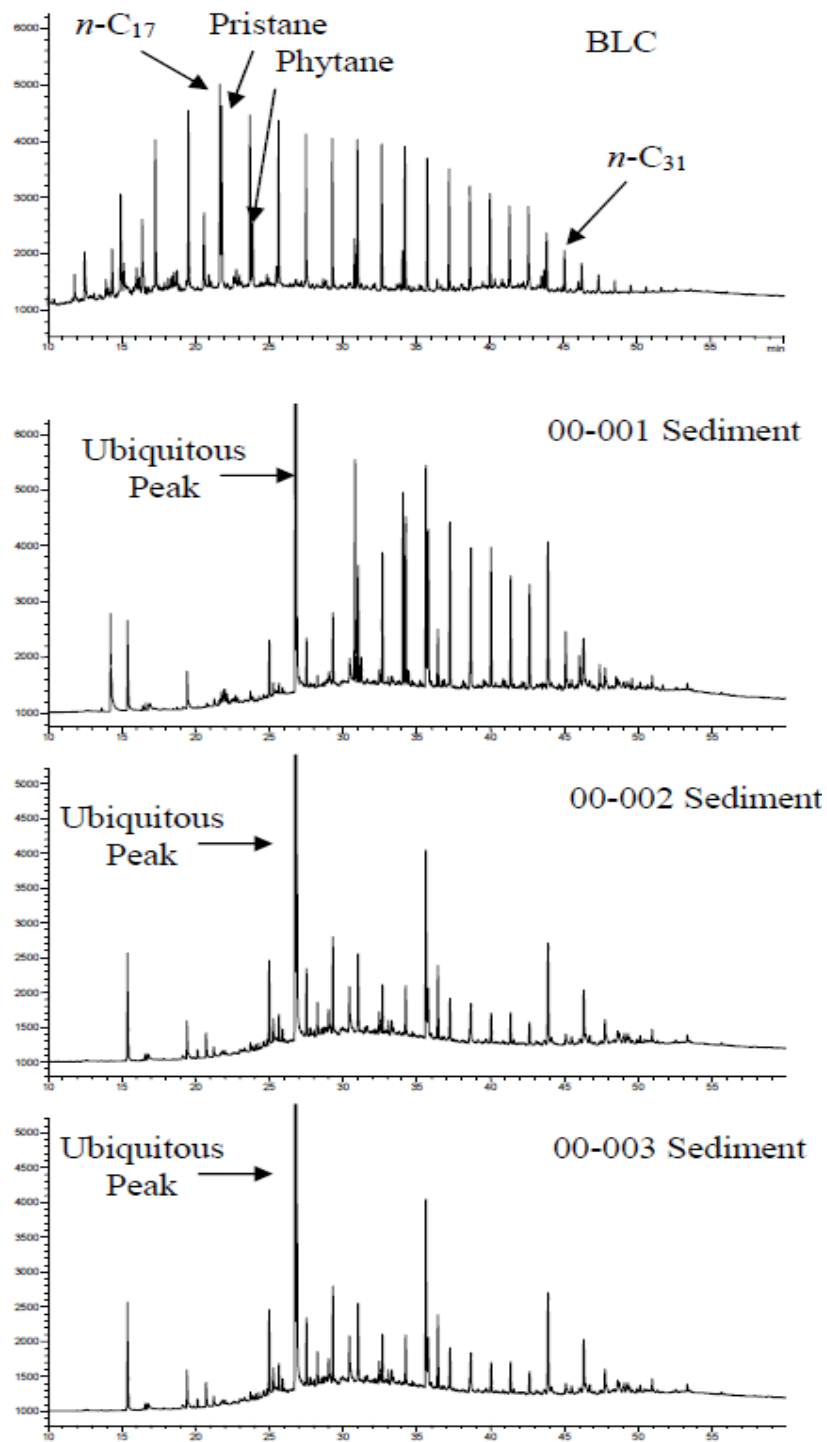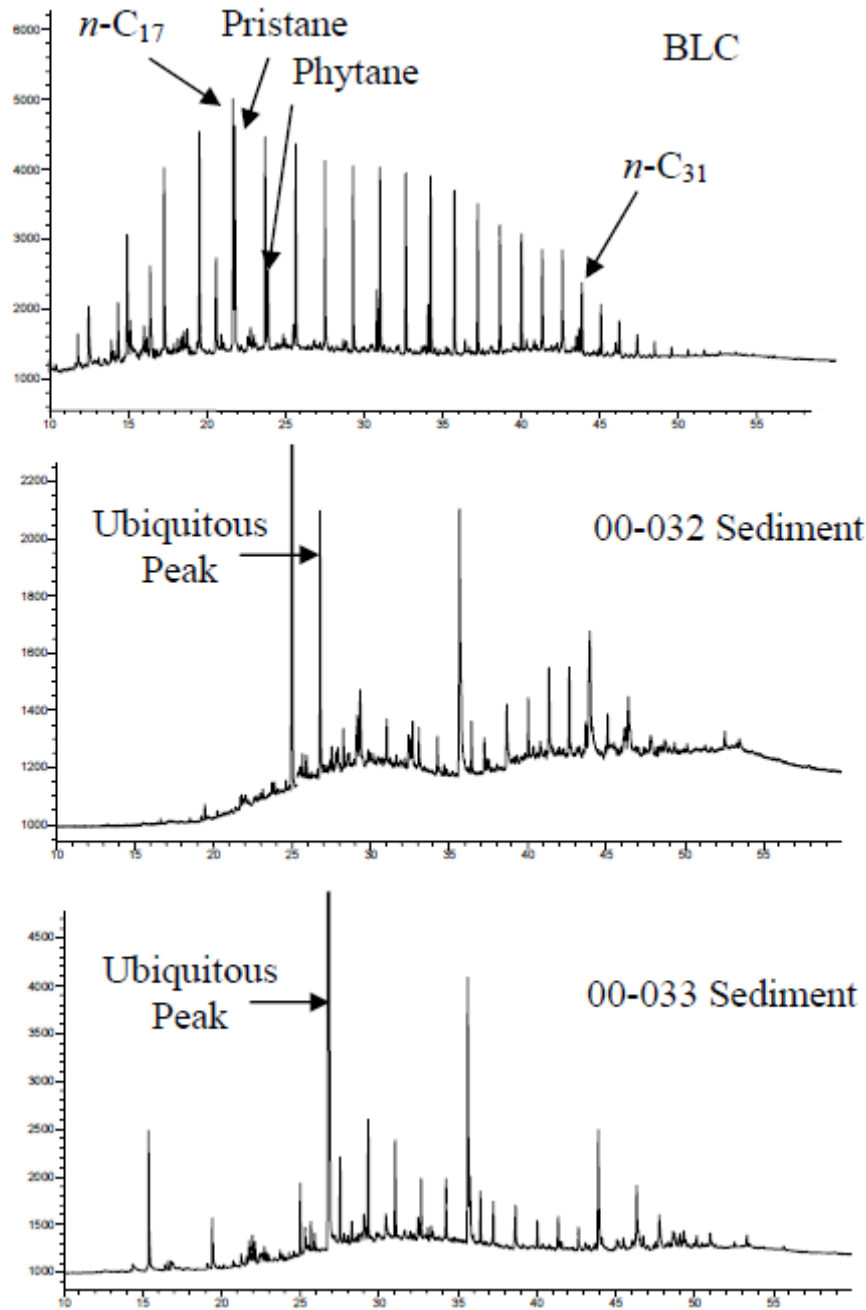
Figure 8.14. Gas chromatograms of solvent-extractable materials removed from sediments collected 12 ft. from the stern starboard hull. A GC trace for BLC (top trace) was conducted to compare retention times. Extracts contained *n*-alkanes and a ubiquitous peak found in all sediments. In the above chromatograms, the y-axis is detector response and x-axis is the retention time in minutes. The chromatograms have been scaled to a lower detector response than the highest peak to observe smaller peaks in the trace. The y-axis is not the same scale for each chromatogram.
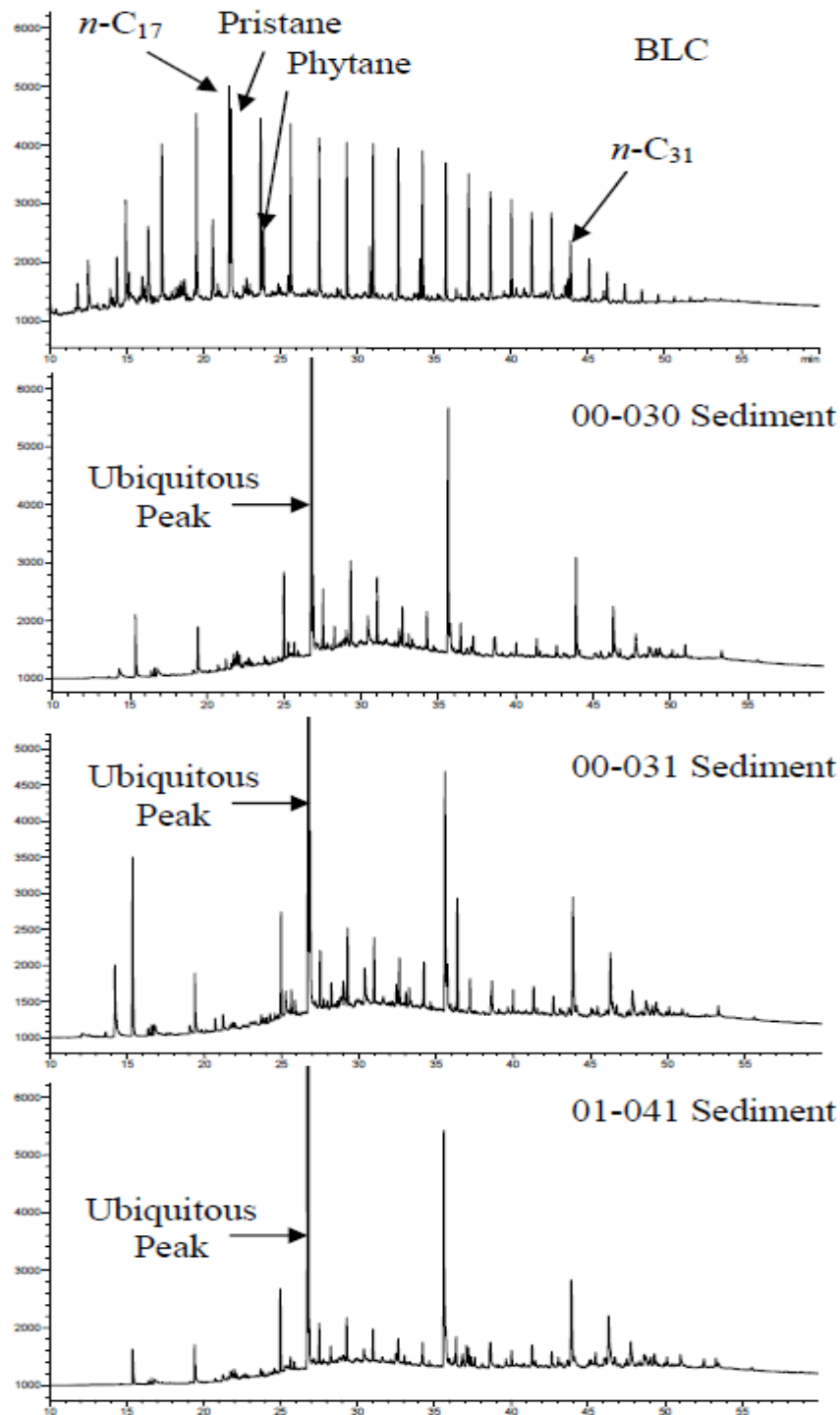
Figure 8.15. Gas chromatograms of solvent-extractable materials removed from sediments collected 12 ft. from the port starboard hull. A GC trace for BLC (top trace) was conducted to compare retention times. Extracts contained *n*-alkanes and a ubiquitous peak found in all sediments. In the above chromatograms, the y-axis is detector response and x-axis is the retention time in minutes. The chromatograms have been scaled to a lower detector response than the highest peak to observe smaller peaks in the trace. The y-axis is not the same scale for each chromatogram.

Figure 8.16. Gas chromatograms of solvent-extractable materials removed from sediments collected on top of the ship. A GC trace for BLC (top trace) was conducted to compare retention times. Extracts contained *n*-alkanes and a ubiquitous peak found in all sediments. In the above chromatograms, the y-axis is detector response and x-axis is the retention time in minutes. The chromatograms have been scaled to a lower detector response than the highest peak to observe smaller peaks in the trace. The y-axis is not the same scale for each chromatogram.
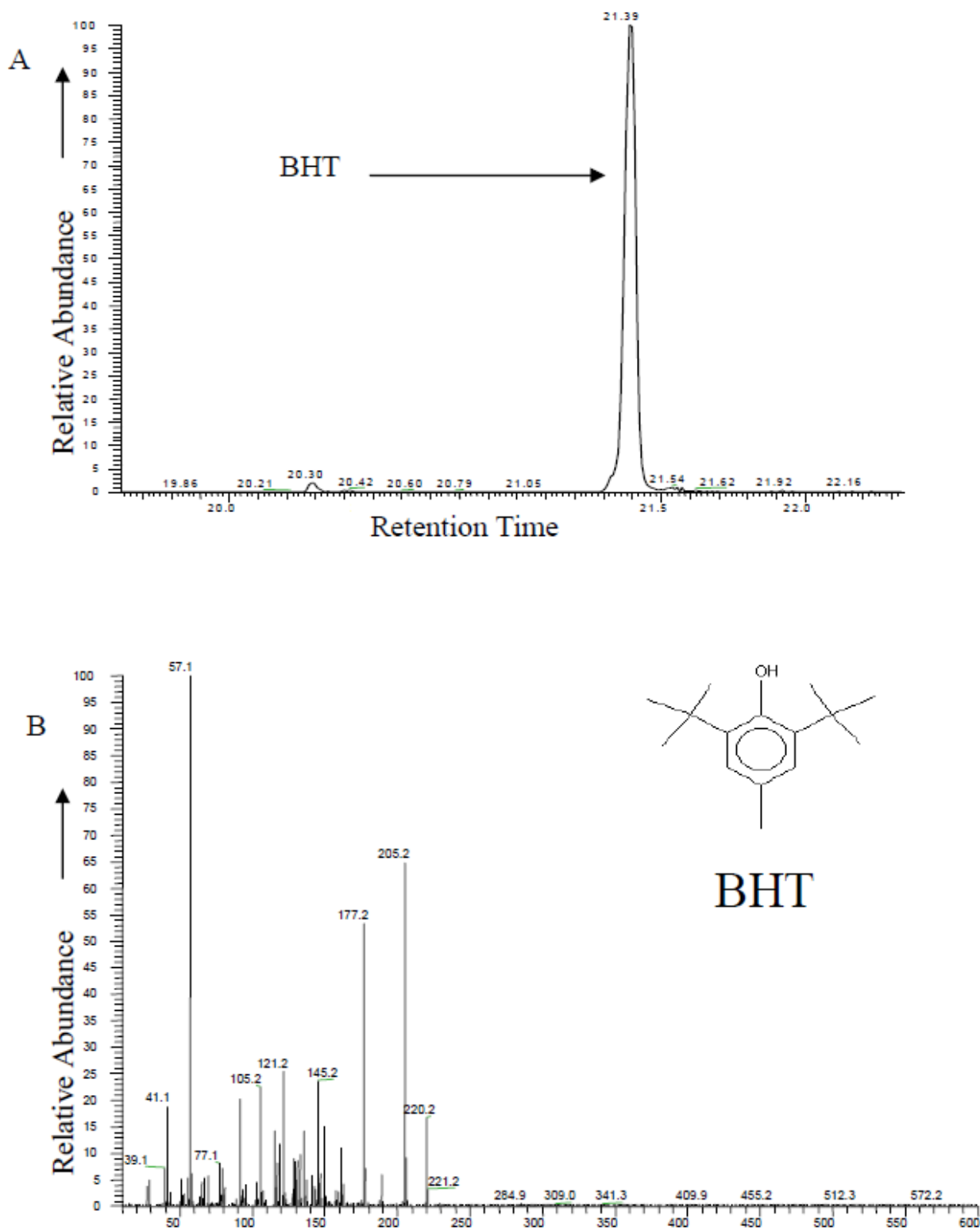
Figure 8.17. Total ion chromatogram (TIC) trace of the ubiquitous peak found in all sediment extracts (A). The mass spectra monitored at *m/z*=205 was identified as butylated hydroxytoluene (BHT) (B)
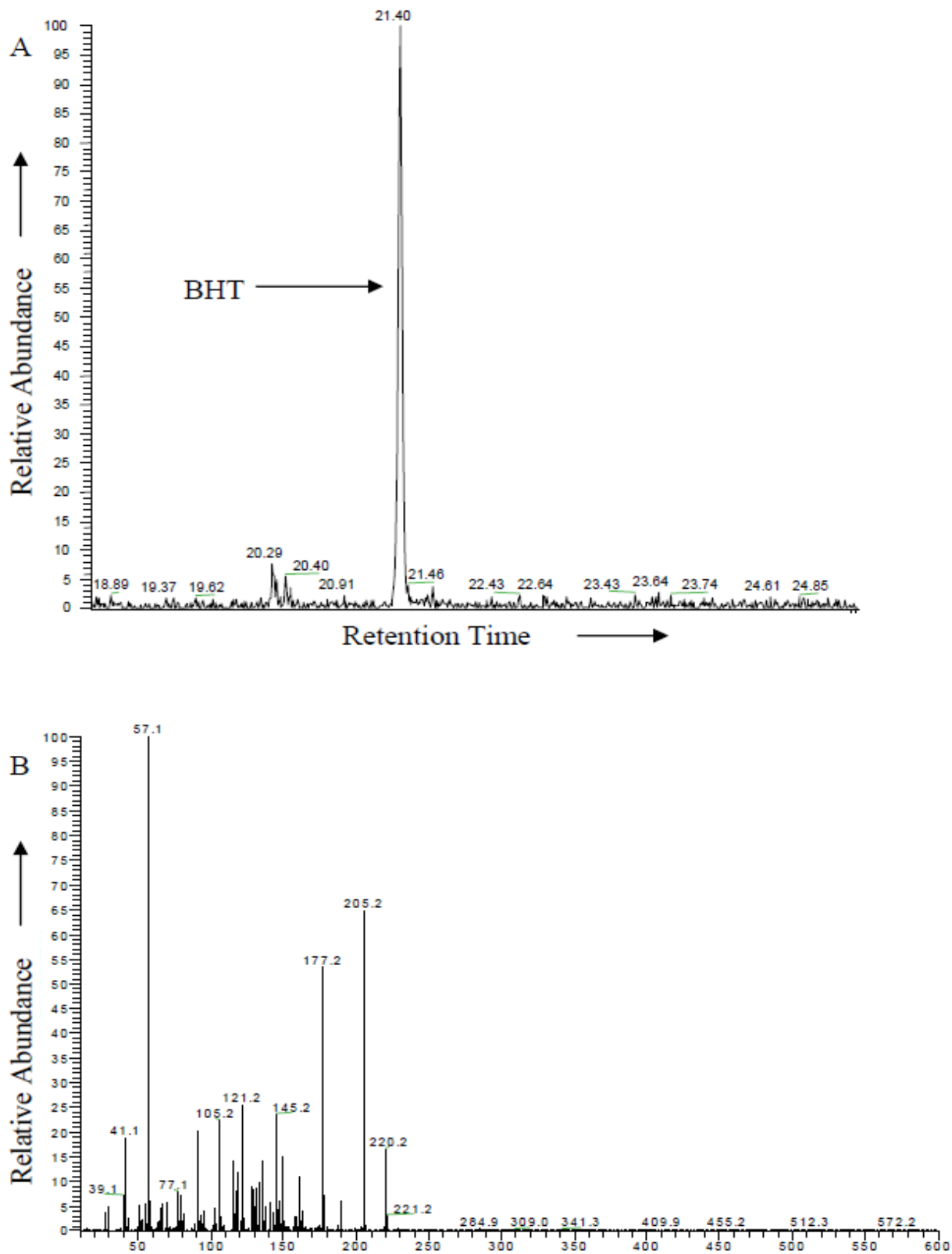
Figure 8.18. Total ion chromatogram (TIC) trace of BHT found in boiling chip and thimble extracts (A). The mass spectra monitored at *m/z*=205 was identified as BHT (B).
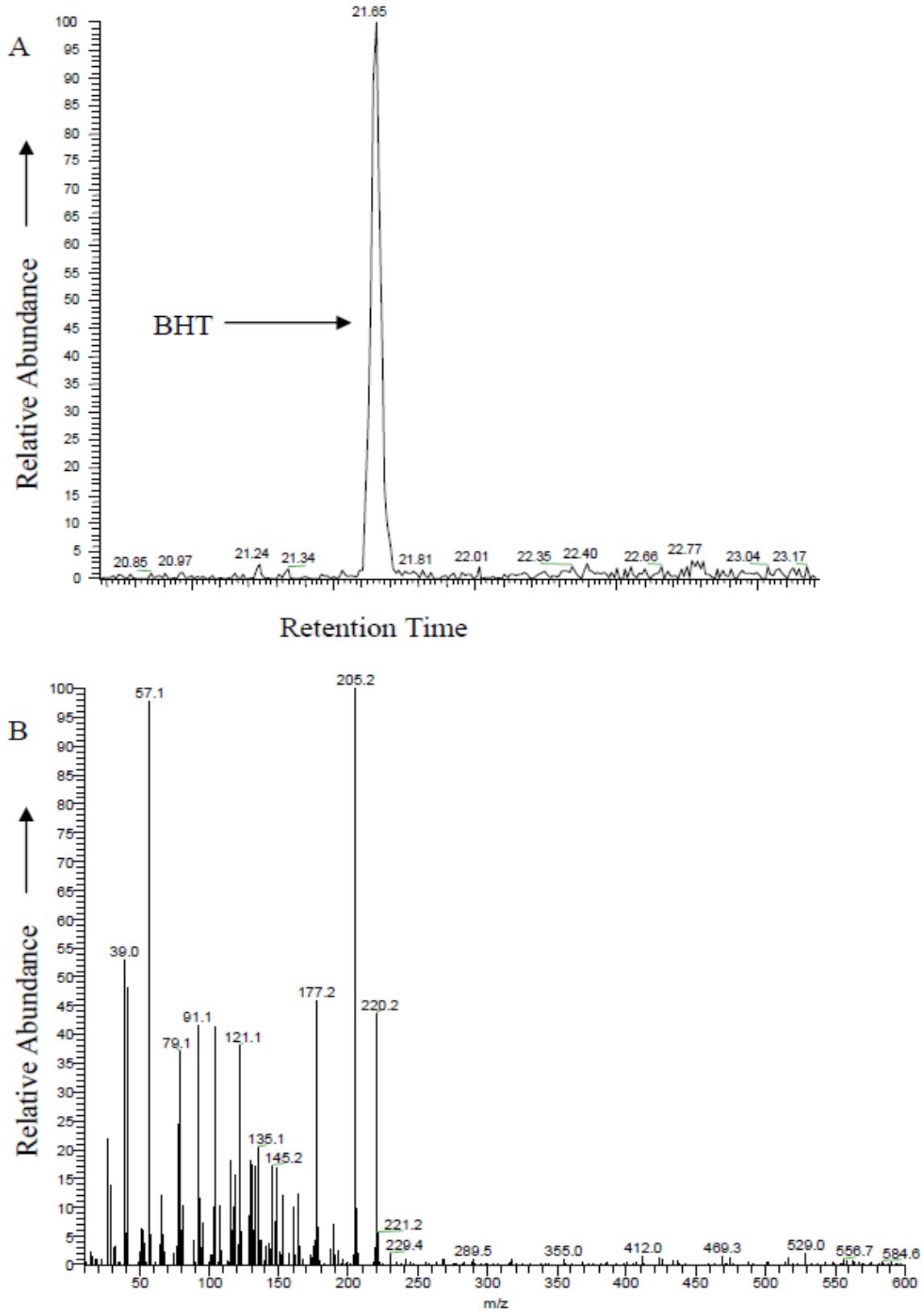
Figure 8.19. Total ion chromatogram trace of BHT found in oil sample 00-034 leaking from USS *Arizona* (A). The mass spectra monitored at *m/z*=205 was identified as BHT (B).
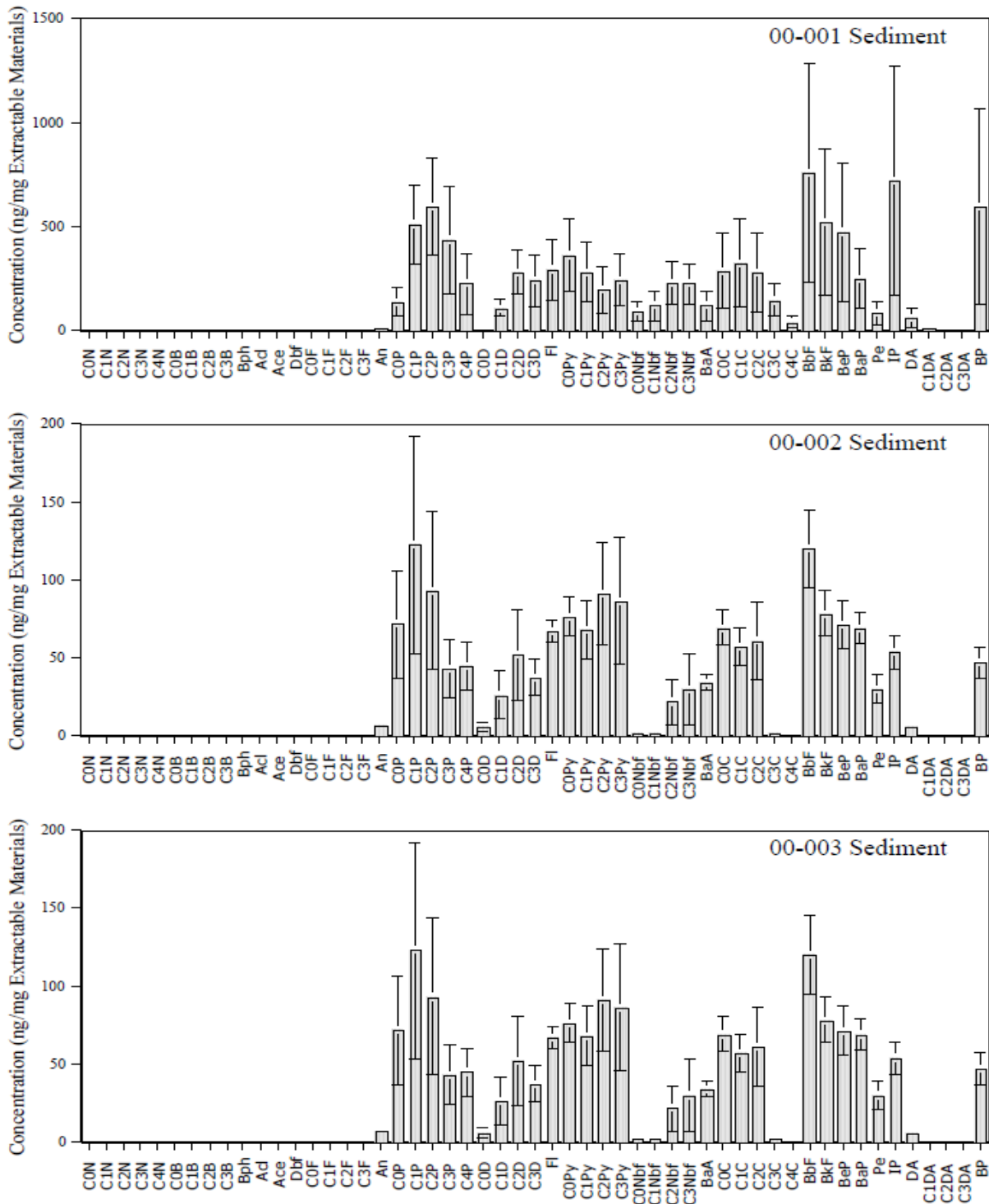
Figure 8.20. Individual PAH analysis for solvent-extractable materials from sediments collected 12 ft. off the stern starboard side of USS *Arizona*. There are no detectable amounts of low molecular weight PAHs (i.e., naphthalene), but high molecular weight PAHs (i.e., pyrene) were detected. Concentration (y-axis) is not the same scale for each histogram. Abbreviations are defined in Table 8.1 and locations of sediments are defined in Figure 8.5.
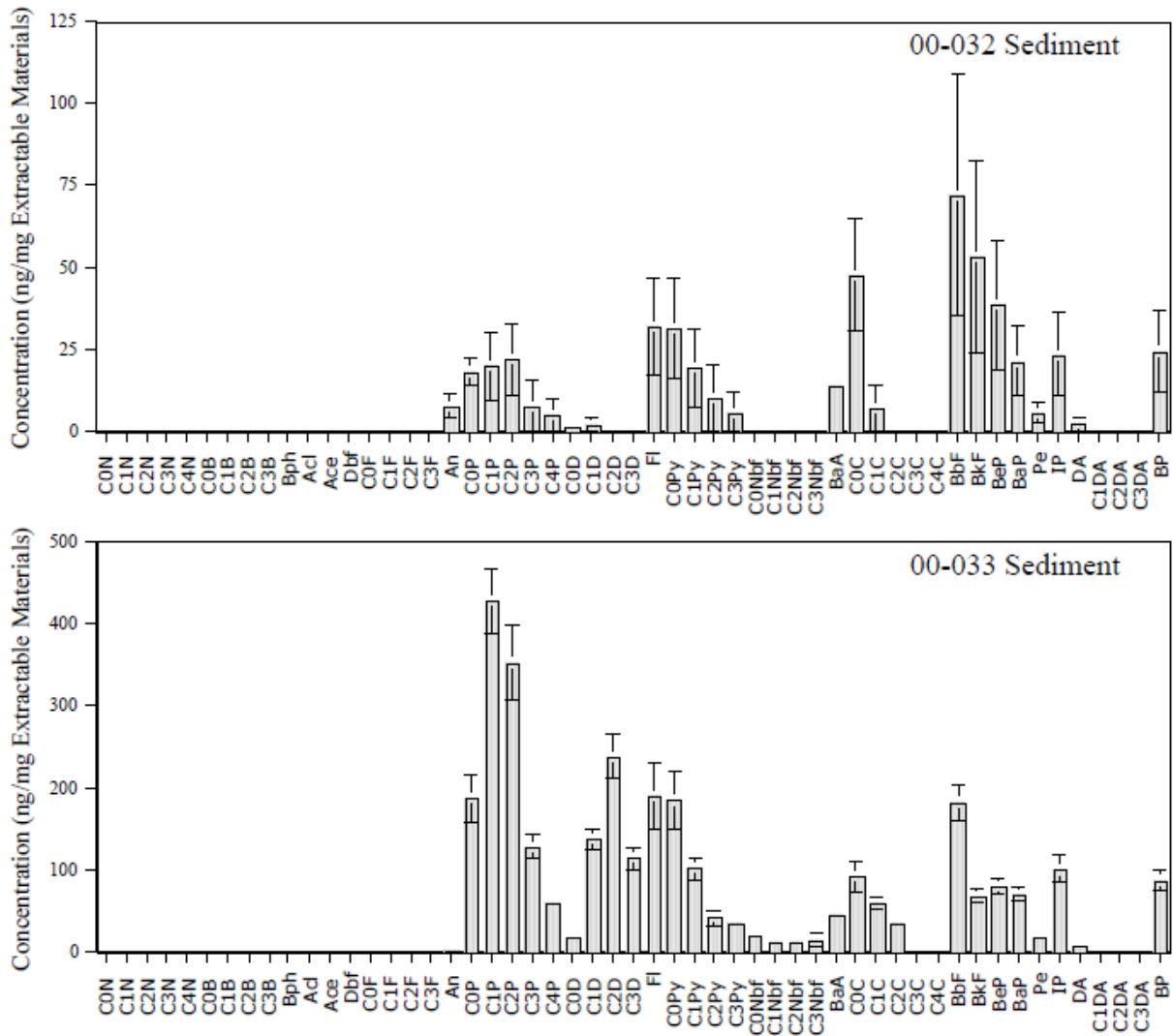
Figure 8.21. Individual PAH analysis for solvent-extractable materials from sediments collected 10 ft. off the port side of USS *Arizona*. There are no detectable amounts of low molecular weight PAHs (i.e., naphthalene), but high molecular weight PAHs (i.e., pyrene) were detected. Concentration for the y-axis is not the same scale for each histogram. Abbreviations are defined in Table 8.1 and locations of sediments are defined in Figure 8.5.
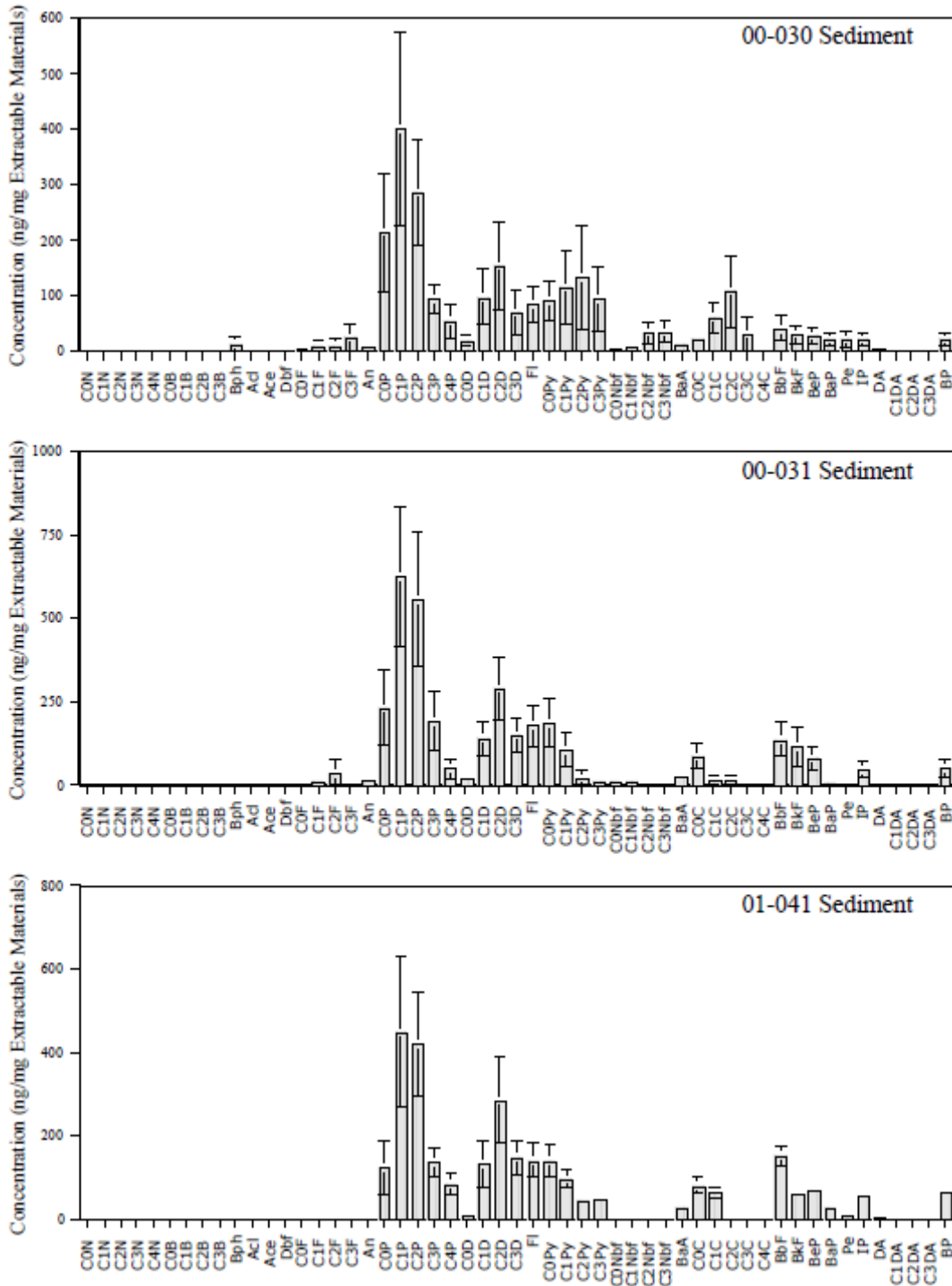
Figure 8.22. Individual PAH analysis for solvent-extractable materials from sediments collected on top of USS *Arizona*. There are no detectable amounts of low molecular weight PAHs (i.e., naphthalene), but high molecular weight PAHs (i.e., phenanthrene) were detected. Concentration for the y-axis is not the same scale for each histogram. Abbreviations are defined in Table 8.1 and locations of sediments are defined in Figure 8.5.

Sediment	$C_{30}H/18\alpha$ Oleanane[a]	$Ts/(Ts+Tm)$[b]	$C_{28}TT/C_{30}H$[c]	$C_{29}TT/C_{30}H$[d]
00-001	3.16±0.29	0.37±0.04	0.20±0.08	0.19±0.08
00-002	9.21±5.30	0.37±0.01	0.63±0.46	1.16±0.98
00-003	2.80±1.03	0.86±0.37	0.38±0.12	0.42±0.11
00-032	4.11±0.68	0.45±0.04	0.17±0.08	0.22±0.12
00-033	3.38±0.40	0.45±0.07	0.20±0.08	0.19±0.08
00-030	2.82±0.96	0.52±0.09	0.98±0.32	0.77±0.30
00-031	2.19±0.68	0.44±0.03	0.61±0.34	0.65±0.32
01-041	2.95±0.43	0.43±0.14	0.20±0.08	0.20±0.08

All values are means and standard error of triplicate samples.

[a]Calculated from m/z=191 mass chromatogram peak areas of $C_{30}17\alpha(H),21\beta(H)$-hopane and $18\alpha(H)$-oleanane.

[b]Calculated from the m/z=191 mass chromatogram peak areas of $C_{27}17\alpha(H)$-22,29,30-trisnorhopane (Tm) and $C_{27}18\alpha(H)$-22,29,30-trisnorneohopane (Ts).

[c]Calculated from the m/z=191 mass chromatogram peak areas of $C_{28}13\beta,21\alpha(H)$-trycyclic terpanes and $C_{30}17\alpha(H),21\beta(H)$-hopane.

[d]Calculated from the m/z=191 mass chromatogram peak areas of $C_{29}13\beta,21\alpha(H)$-trycyclic terpanes and $C_{30}17\alpha(H),21\beta(H)$-hopane

Table 8.6. Hopane biomarker ratios calculated for sediment solvent-extractable materials collected from different locations on and near USS *Arizona*.

Sediment	Total PAHs[a]	Total PAHs:$C_{30}H$[b]	Total PAHs:18α-oleanane
00-001	9286.36±5164.92	10.43±4.86	37.14±20.14
00-002	16278.60±10105.12	9.36±7.56	19.85±9.64
00-003	1661.33±369.16	9.51±7.44	21.68±9.22
00-032	426.97±236.71	1.57±1.38	3.67±6.35
00-033	3160.40±402.41	0.44±0.09	1.38±0.30
00-030	2484.10±1171.70	9.79±9.20	19.47±10.58
00-031	3476.83±1428.96	7.14±6.66	20.47±18.96
01-041	2915.63±823.17	9.04±5.32	22.70±10.36

All values are the means and standard error of triplicate samples.

[a]The ng amount of PAHs per mg of dry sediments.

[b]$C_{30}H$ represents $C_{30}17\alpha(H),21\beta(H)$-hopane.

Table 8.7. Ratio of total PAHs to biomarkers of USS *Arizona* sediment solvent-extractable material.

BIOMARKER ANALYSIS OF SEDIMENT SOLVENT-EXTRACTABLE MATERIALS

GC-MS was used to examine USS *Arizona* sediment biomarker profiles, focusing on mass chromatograms m/z=191 peak areas (for terpanes / hopanes) and m/z=217 (for steranes) (Figures 8.23–8.28). In m/z 191 mass chromatograms, C_{28-31} hopanes, Ts and Tm, as well as C_{28-29} tricyclics were detected. Biomarker ratios were then calculated from m/z=191 peak areas (Table 8.7). Peak areas of $C_{30}17\alpha(H),21\beta(H)$-hopane and 18α-oleanane were used to determine if $C_{30}17\alpha(H),21\beta(H)$-hopane was being degraded relative to the stable 18α-oleanane. Peak areas of $C_{27}17\alpha(H)$-22,29,30-trisnorhopane (Tm) and $C_{27}18\alpha(H)$-22,29,30-trisnorneohopane (Ts) were calculated for the Ts/(Ts + Tm) ratio.

Tricyclic terpane ratios were also calculated from mass chromatograms m/z=191 using the peak areas of $C_{28}13\beta,21\alpha(H)$-tricyclic terpane (22*R* and 22*S*) and $C_{29}13\beta,21\alpha(H)$-tricyclic terpane (22*R* and 22*S*) to compare with the peak area of $C_{30}17\alpha(H),21\beta(H)$-hopane. These ratios were calculated to determine if C_{28} and C_{29} tricyclic terpanes were being degraded in comparison to $C_{30}17\alpha,21\beta(H)$-hopane. Ratios calculated from mass chromatograms m/z=191 for solvent-extractable materials from sediments were variable and had no discernable differences between different sampling areas (Table 8.6). For example, the Ts/(Ts+Tm) ratio ranged from 0.37 ± 0.04 to 0.86 ± 0.37 (Table 8.6).

In sediment extracts, the C_{27}, C_{28}, and C_{29} steranes were detected by GC-MS (m/z=217). Biomarker ratios were also calculated from peak areas of mass chromatograms m/z=217 as decribed in section 2. Briefly, mass chromatogram peak areas of C_{27} - $C_{29}5\alpha(H),14\alpha(H),17\alpha(H)$-sterane (20S and 20R), C_{27} - $C_{29}5\alpha(H),14\beta(H),17\beta(H)$-sterane (20S and 20R), and $C_{30}17\alpha(H),21\beta(H)$-hopane were calculated for the $C_{27}S/C_{30}H$, $C_{28}S/C_{30}H$, and $C_{29}S/C_{30}H$ ratios. Sterane biomarker ratios for solvent-extractable materials from sediments had no discernable differences between different sampling areas because of large standard errors in the calculated ratios (Table 8.8).
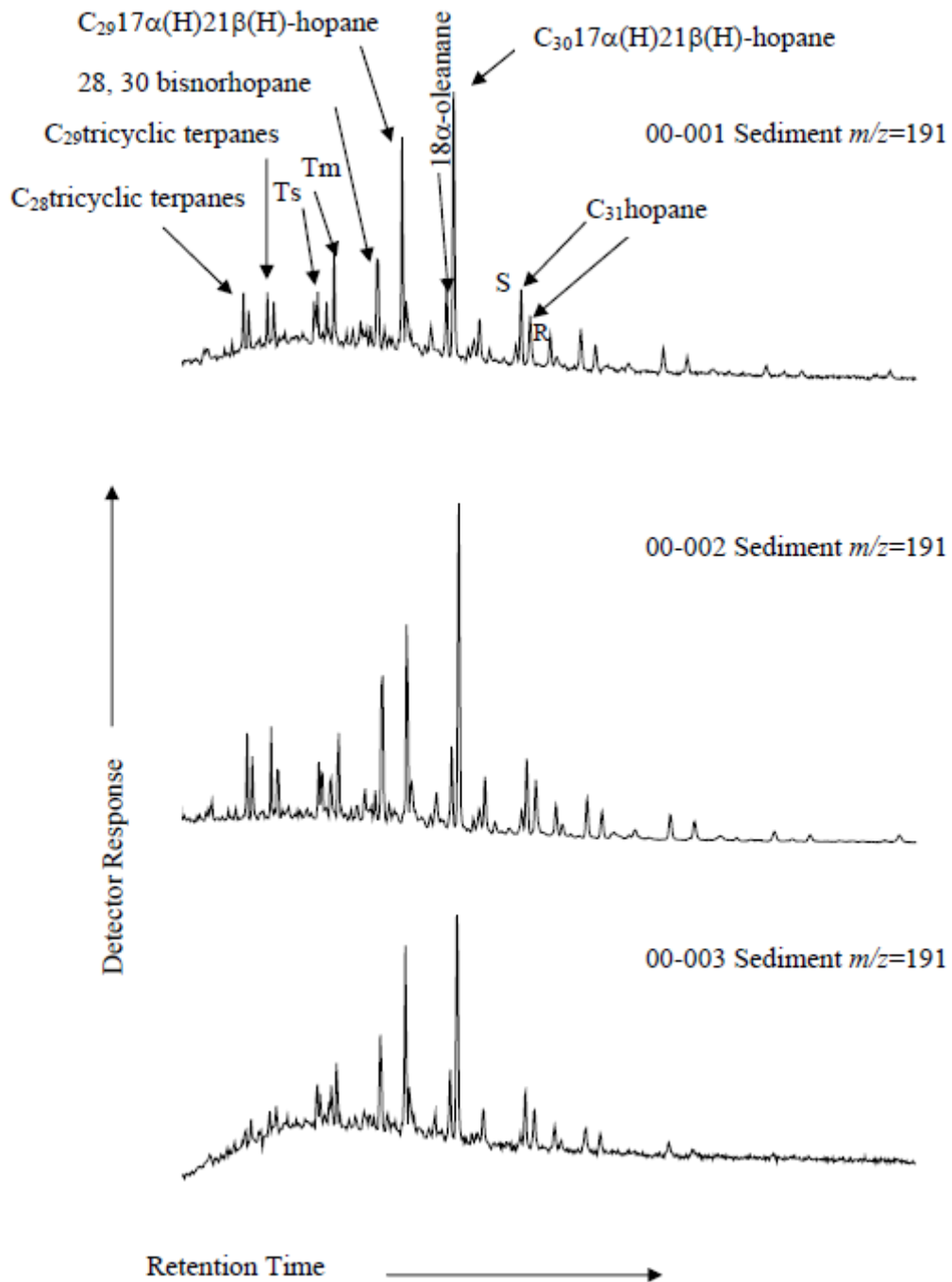
Figure 8.23. GC-MS chromatograms (*m/z*=191) of solvent-extractable material from sediments collected from the stern section, starboard side, 12 ft. from hull. Chromatograms are representative of triplicate samples.

Figure 8.24. GC-MS chromatograms (*m/z*=191) of solvent-extractable material from sediments collected from the stern section, port side, 10 ft. from hull. Chromatograms are representative of triplicate samples.

Figure 8.25. GC-MS chromatograms (*m/z*=191) of solvent-extractable material from sediments collected on top of the ship. Chromatograms are representative of triplicate samples.
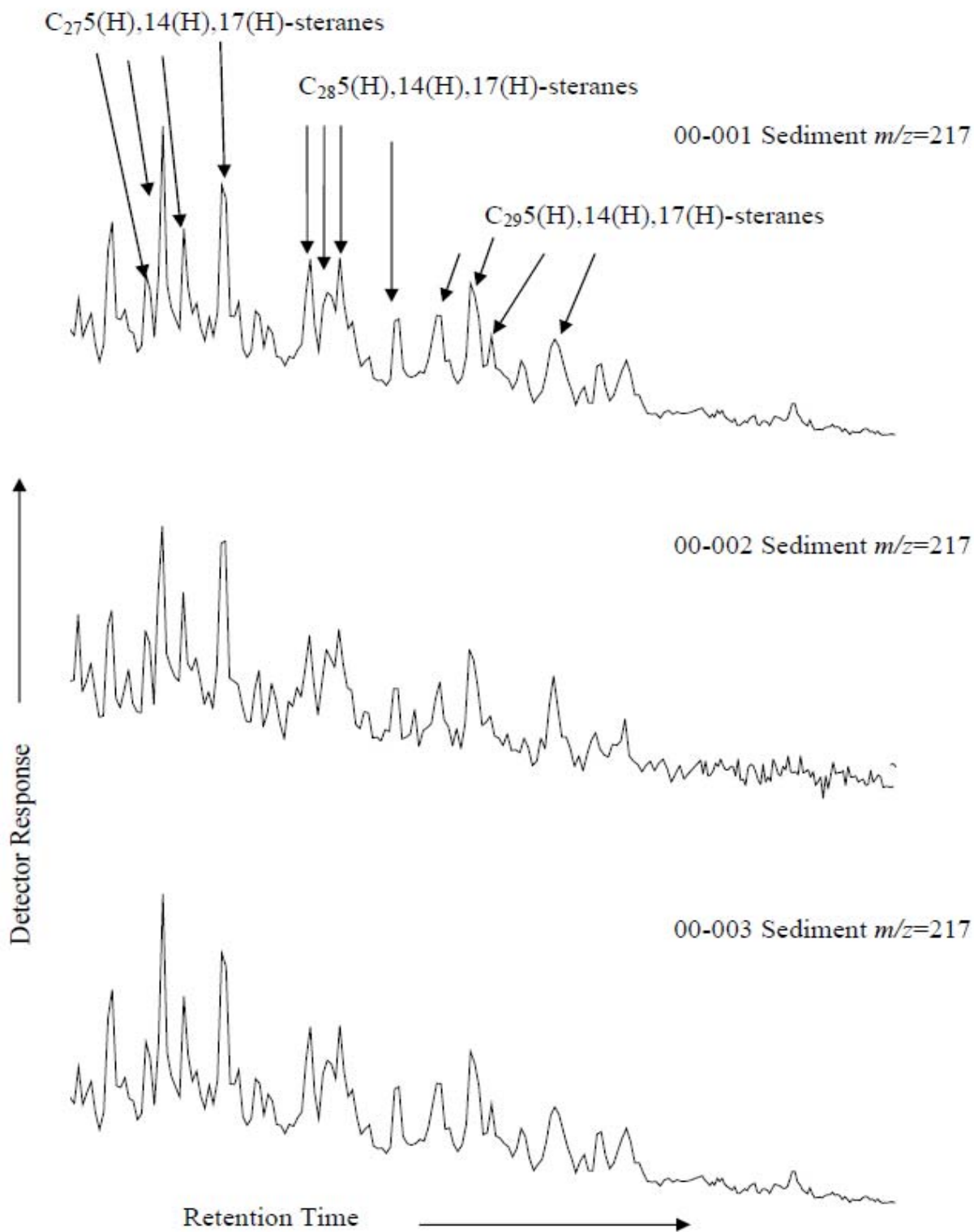
Figure 8.26. GC-MS chromatograms (*m/z*=217) of solvent-extractable material from sediments collected from the stern section, starboard side, 12 ft. from hull. Chromatograms are representative of triplicate samples.
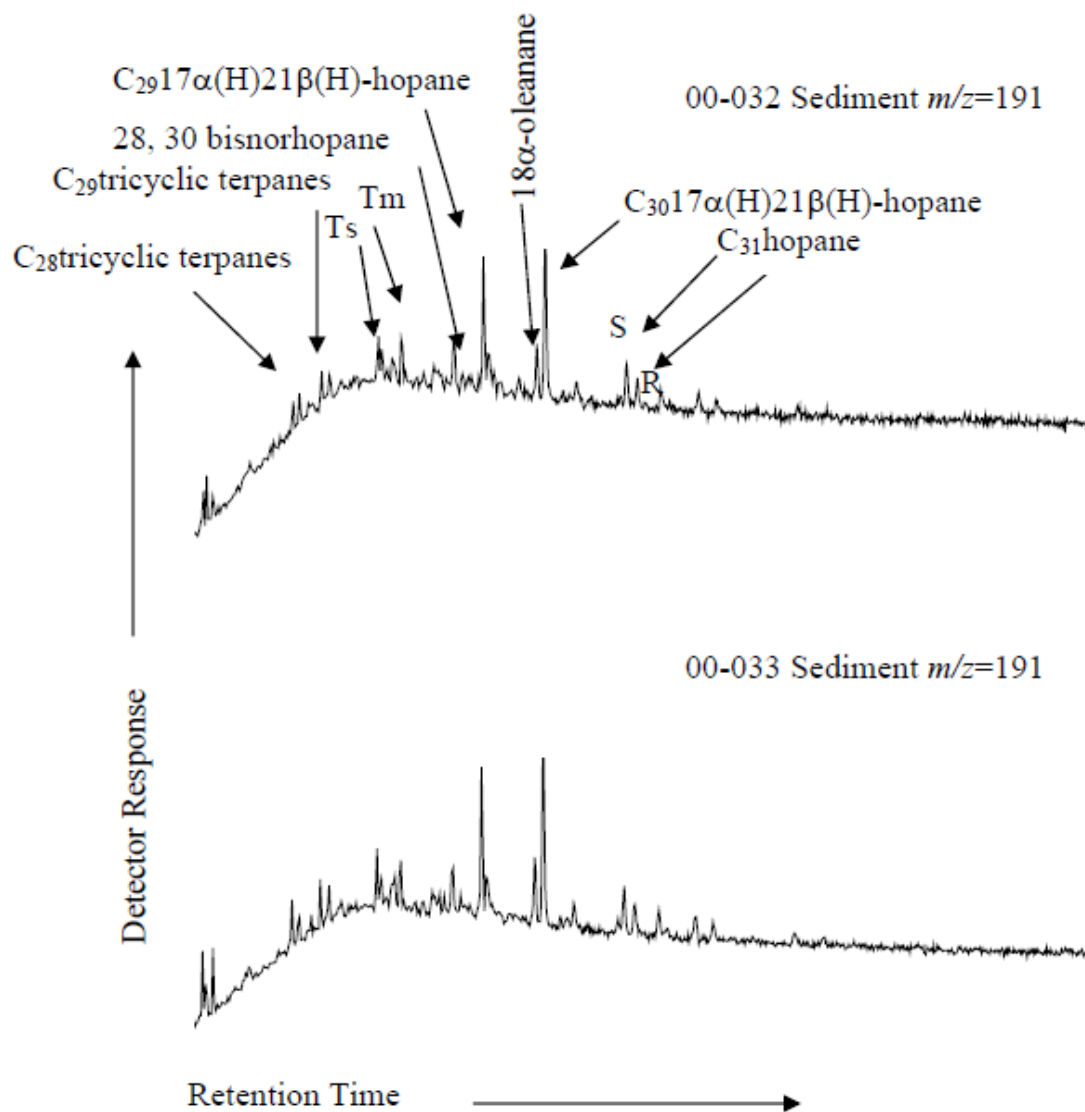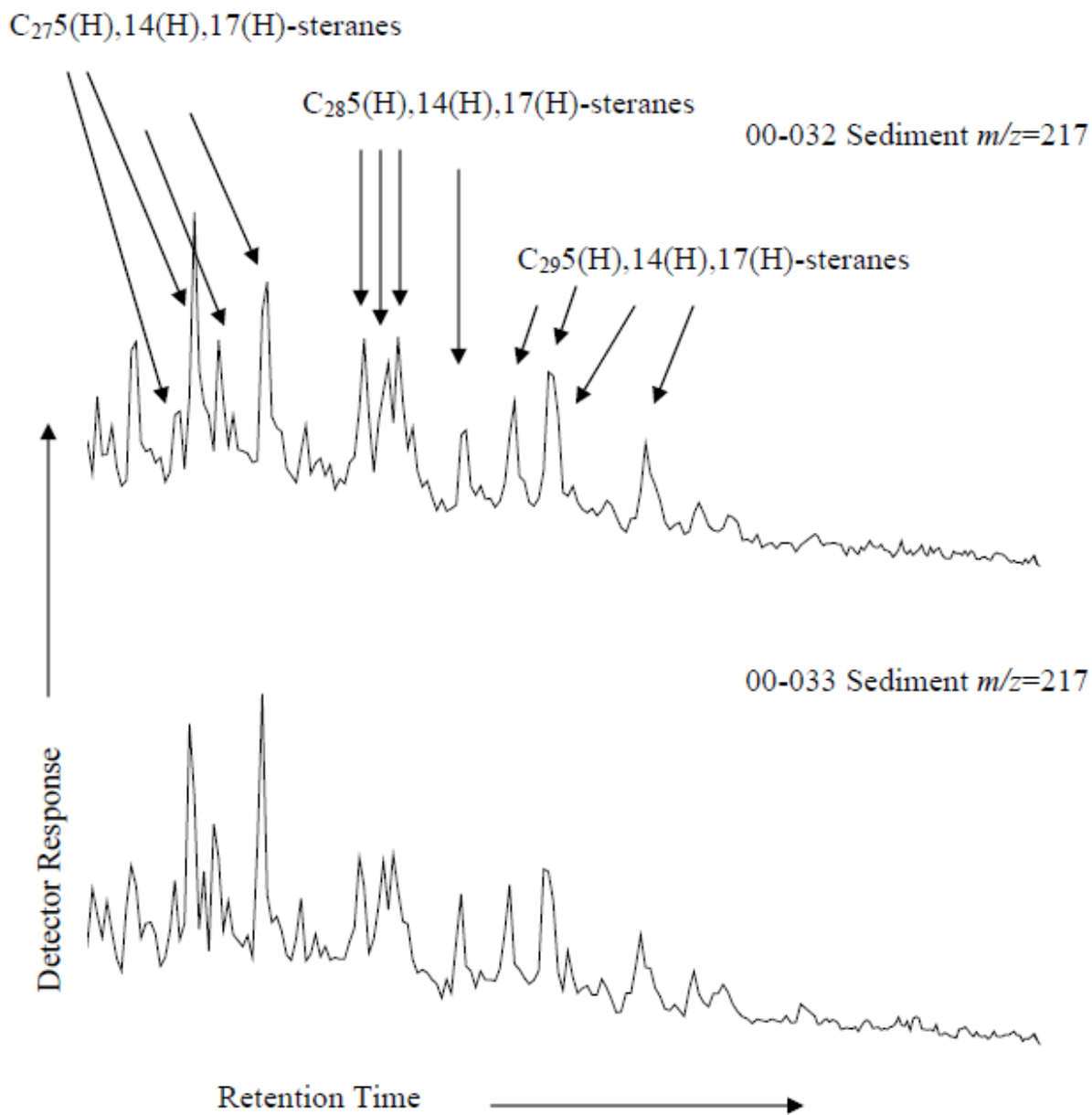
Figure 8.27. GC-MS chromatograms (*m/z*=217) of solvent-extractable material from sediments collected from the stern section, port side, 10 ft. from hull. Chromatograms are representative of triplicate samples.
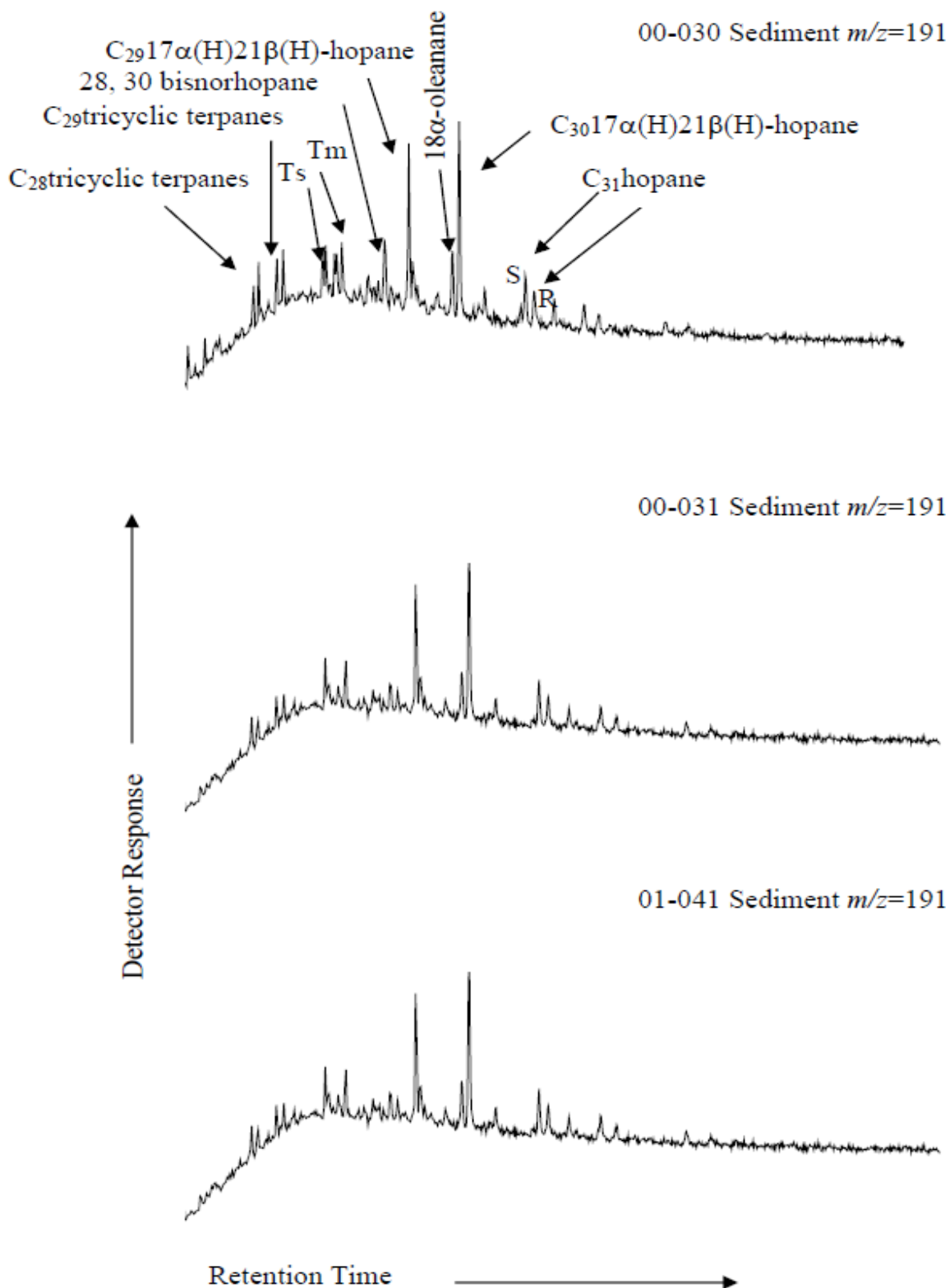
Figure 8.28. GC-MS chromatograms (*m/z=217*) of solvent-extractable material from sediments collected on top of the ship. Chromatograms are representative of triplicate samples.
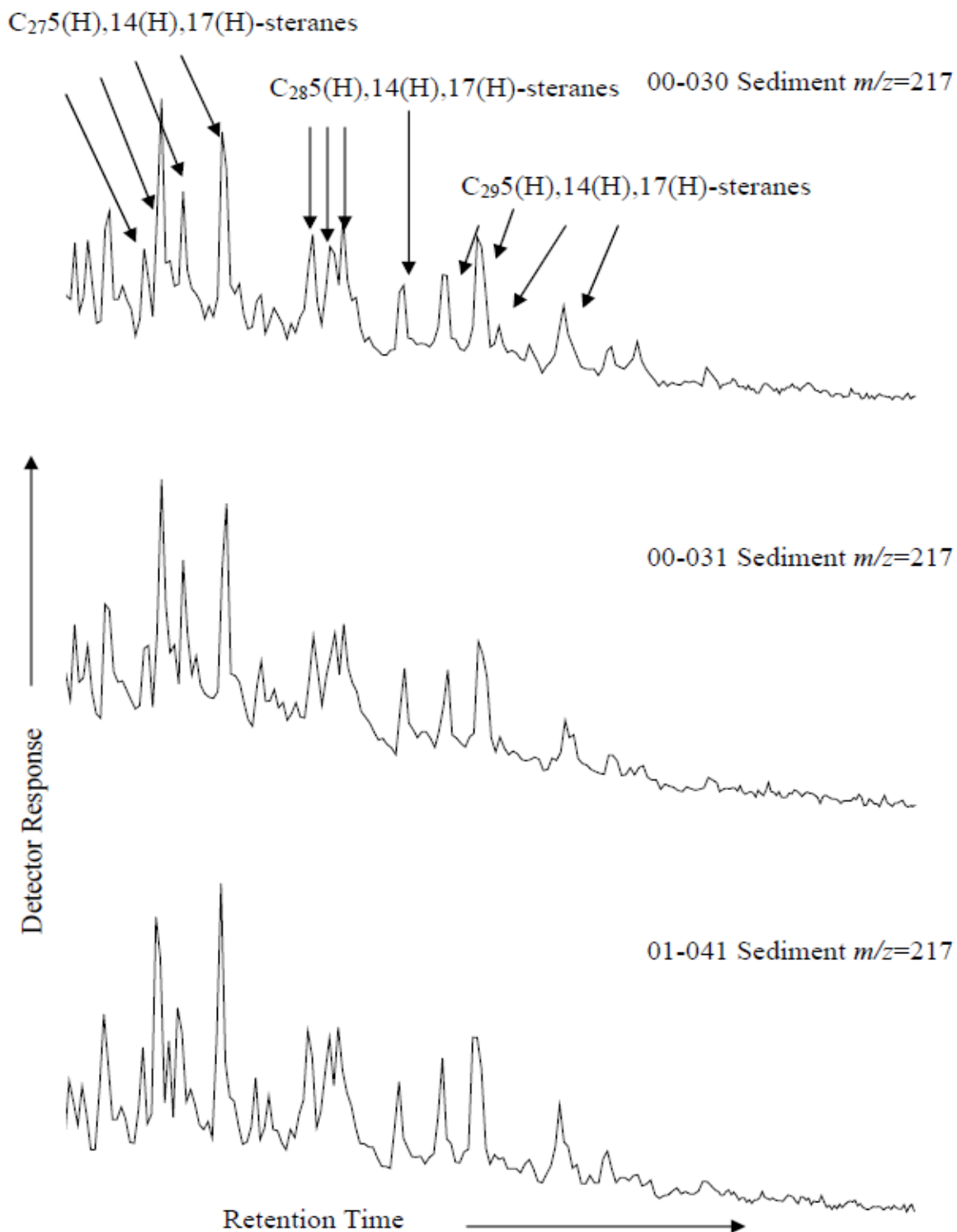
Sediment	$C_{27}S/C_{30}H^a$	$C_{28}S/C_{30}H^b$	$C_{29}/C_{30}H^c$
00-001	0.98±0.01	0.68±0.06	0.74±0.05
00-002	1.15±0.66	1.84±1.44	1.58±1.10
00-003	1.27±0.15	0.75±0.13	0.83±0.14
00-032	1.24±0.35	0.79±0.20	0.66±0.07
00-033	1.17±0.10	0.57±0.01	0.70±0.04
00-030	1.59±0.19	1.09±0.34	1.07±0.18
00-031	1.95±0.19	1.60±0.56	1.19±0.32
01-041	1.28±0.05	0.58±0.01	0.65±0.01

All values are the means and standard error of triplicate samples.
[a]Calculated from m/z=217 mass chromatogram peak areas of $C_{27}5\alpha(H),14\alpha(H),17\alpha(H)$-sterane (20$S$ and 20R), $C_{27}\alpha(H),14\beta(H),17\beta(H)$-sterane (20$S$ and 20R) and $C_{30}17\alpha(H),21\beta(H)$-hopane.
[b]Calculated from m/z=217 mass chromatogram peak areas of $C_{28}5\alpha(H),14\alpha(H),17\alpha(H)$-sterane (20$S$ and 20R), $C_{28}5\alpha(H),14\beta(H),17\beta(H)$-sterane (20$S$ and 20R) and $C_{30}17\alpha(H),21\beta(H)$-hopane.
[c]Calculated from m/z=217 mass chromatogram peak areas of $C_{29}5\alpha(H),14\alpha(H),17\alpha(H)$-sterane (20$S$ and 20R), $C_{29}5\alpha(H),14\beta(H),17\beta(H)$-sterane and $C_{30}17\alpha(H),21\beta(H)$-hopane.

Table 8.8. Sterane biomarker ratios calculated for sediment solvent-extractable materials collected from different locations on and near USS *Arizona*.

DEVELOPMENT OF BUNKER C FUEL OIL DEGRADING AEROBIC ENRICHMENT CULTURES

INTRODUCTION

Bunker C fuel oil is one of the most commonly spilled oils in the marine environment, and studies have shown the oil can persist in the environment for years (Strand et al., 1992; Irwin et al., 1997; Lunel et al., 2000). Bunker C was found in sediments examined twenty years after the *Arrow* spill in Chedabucto Bay, Novia Scotia, Canada (Vandermeulen and Singh, 1994). Studies have shown Bunker C fuel oil is degradable by microorganisms in laboratory enrichments, despite the increased concentrations of high molecular weight hydrocarbons (Mulkins-Phillips and Stewart, 1974; Minas and Gunkel, 1995; Wang et al., 1998a). In a laboratory study involving microbial degradation of Bunker C, gravimetric measurements showed enrichment cultures were able to degrade 30% to 85% of the non-asphaltenic components of the oil (Mulkins-Phillips and Stewart, 1974).

USS *Arizona* offers a unique opportunity to study the microbial degradation of Bunker C fuel oil. The sediments adjacent to the ship have been chronically exposed for over 60 years to

the oil leaking from the ship. In addition, hydrocarbon contaminants from other sources in Pearl Harbor, (i.e., US Navy facility and Chevron) may be present. Therefore, it would be expected that environmental conditions found in Pearl Harbor sediments may have enriched for microbial communities capable of degrading hydrocarbons (Floodgate, 1984; Frontera-Suau et al., 2002). In addition, structural differences in microbial communities from different sediment sampling locations may influence the extent of degradation.

In order to monitor petroleum degradation, internal components of oil that are resistant to biotic and abiotic weathering processes can be used as an internal reference to monitor the progression of degradation (Peters and Moldowan, 1993; Prince et al., 1994; Bost et al., 2001; Frontera-Suau et al., 2002). These compounds, referred to as internal markers or biomarkers, are more resistant to biotic and abiotic weathering than other components of oil. However, laboratory and field studies have shown that microbial communities are capable of influencing biomarker profiles by aerobically degrading various biomarkers that are generally considered to be conserved (Munoz et al., 1987; Moldowan et al., 1995; Bost et al., 2001; Wang et al., 2001a; Frontera-Suau et al., 2002). Possible degradation of biomarkers is an important consideration when using them as an internal reference to determine the extent of oil degradation.

The results presented in this section focus on determining if aerobic bacteria in sediments adjacent to and on top of USS *Arizona* can degrade the Bunker C fuel oil leaking from the ship. In addition, a molecular approach to examining microbial community structure, DGGE was used to determine if microbial enrichment cultures enriched from sediments were similar. Finally, analysis of biomarkers, specifically m/z=191 (for hopanes) and m/z=217 (for steranes), were examined to see if enrichment cultures were capable of degrading biomarkers found in oil leaking from the ship.

AEROBIC ENRICHMENT CULTURE DEGRADATION OF OIL LEAKING FROM USS *ARIZONA*

Eight different enrichment cultures (in triplicate) were initiated from sediments collected from USS *Arizona* sampling locations (Figure 8.4). For each aerobic enrichment culture initiated, triplicate Erlenmeyer flasks were inoculated with sediment from the different locations. Therefore, each of the triplicates is an independent (separate) culture. Following the third

monthly transfer, gravimetric measurements of oil extracted from the 8 enrichment cultures grown in triplicate and uninoculated controls, were determined after a 30 day incubation. The gravimetric measurements indicate the amount of oil lost during the 30 days of microbial growth and also includes abiotic losses of oil occurring during the incubation period. The uninoculated control showed a 6.13%±0.65% average decrease in the weight of recovered oil. In comparison, inoculated aerobic enrichment cultures averaged a 31.03%±4.58% decrease in the weight of recovered oil (Table 8.9). For enrichments 00-001, 00-030, and 00-033, 1 of the 3 triplicate cultures exhibited less degradation of oil. Therefore, these enrichments did not show as much oil loss and had larger standard errors than other enrichments throughout these experiments. For example, enrichment 00-001 had triplicates with gravimetric weights 14.71 mg, 5.24 mg, and 4.08 mg.

GAS CHROMATOGRAPHIC ANALYSIS OF OIL FROM ENRICHMENT CULTURES

Following gravimetric measurements, oil extracted from aerobic enrichment cultures following 30 days of growth were analyzed by gas chromatography utilizing flame ionization detection to determine the extent of *n*-alkane and branched alkane degradation in comparison to oil extracted from uninoculated controls. Gas chromatographic traces of oil extracted from the enrichment cultures demonstrated degradation of *n*-alkanes and branched alkanes along with a decrease in the unresolved complex mixture (UCM) in comparison to uninoculated control samples (Figure 8.29). The decrease in the UCM, which consists of unresolvable PAHs as well as heterocycles, indicates PAHs may be degraded also, although PAHs must be further resolved by GC-MS analysis.

PAH ANALYSIS OF OIL FROM AEROBIC ENRICHMENT CULTURES.

Mass spectrometry was conducted to determine concentrations of individual PAHs present in oil extracted from the aerobic enrichment cultures and uninoculated controls. Overall, mass spectrometry indicated a decrease of low molecular weight hydrocarbons (i.e., naphthalene, alkylated naphthalenes, flourene, and alkylated flourenes) in the enrichment cultures compared

Aerobic Enrichment	Inoculum Source	Percent Loss
Control	Uninoculated Control	6.13±0.65
00-001	Stern section, starboard side, 12 ft. from hull	28.99±9.92
00-002	Stern section, starboard side, 12 ft. from hull	39.37±1.50
00-003	Stern section, starboard side, 12 ft. from hull	32.36±1.37
00-032	Stern section, port side, 10 ft. from the hull	36.89±0.01
00-033	Stern section, port side, 10 ft. from the hull	22.22±2.44
00-030	Stern section bottom of barbette No. 4	32.53±10.52
00-031	Bow section, gun turret no. 1	36.48±1.53
01-041	Bow section, port side of gun turret no. 1	34.14±6.42

All values are the averages of triplicate samples with the standard errors of those values. The uninoculated control was maintained under the same conditions as aerobic enrichments for 30 days without microbial inoculum.

Table 8.9. Gravimetric analysis of oil extracted from USS *Arizona* aerobic enrichments.
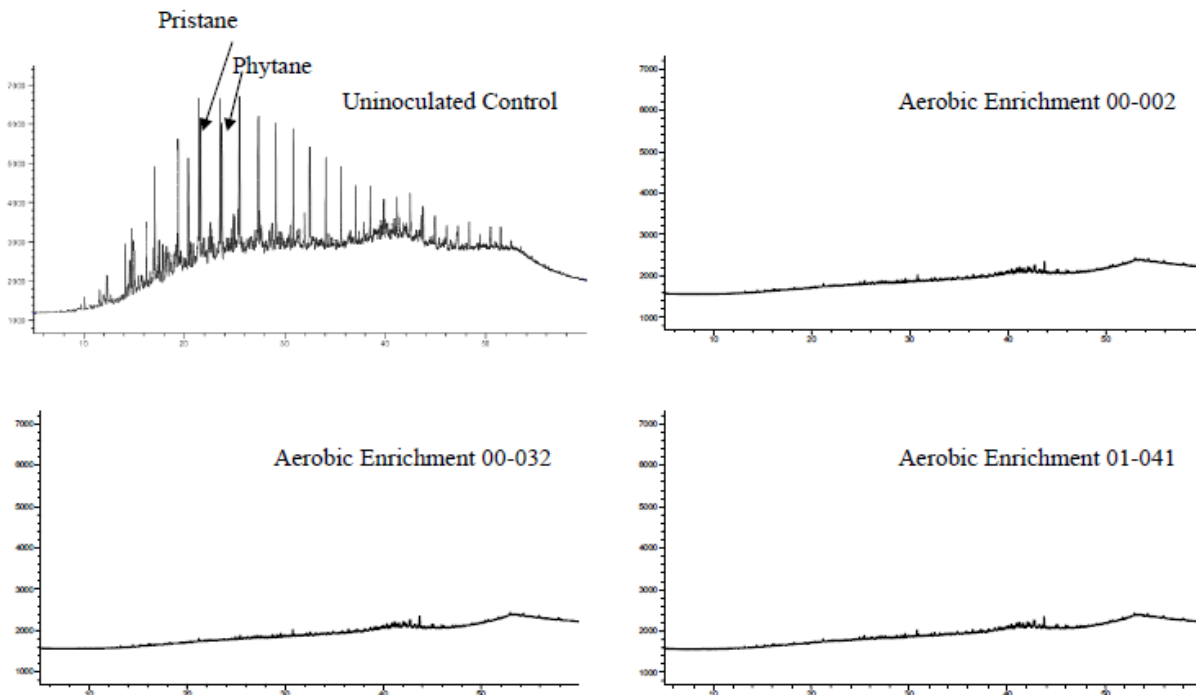
Figure 8.29. Gas chromatographic traces of oil extracted from USS *Arizona* aerobic enrichment cultures. The uninoculated control after 30 days still contains *n*-alkanes and branched alkanes. In comparison, following 30 days of microbial growth with Bunker C fuel oil as the only carbon source, loss of *n*-alkanes and the branched alkanes, pristane, and phytane, were observed. The y-axis is the detector response and x-axis is the retention time in minutes.

to the uninoculated controls (Figures 8.30 and 8.31). The concentration of higher molecular weight PAHs (i.e., perylene) were persistent relative to other PAHs when compared to the uninoculated control (Figures 8.32 and 8.33). It is important to note that during oil degradation, compounds that are not degraded will increase in concentration relative to the total amount of remaining oil. This occurrence does not indicate an increase in the absolute quantity of these compounds.

Enrichments 00-002, 00-003, and 01-041 had increased concentrations of C1-dibenzo(a,h)anthracene (C1DA) relative to other PAHs and the uninoculated control indicating no degradation of C1DA (Figures 8.34 and 8.35). Furthermore, enrichment 01-041 also did not demonstrate degradation of C2-phenanthrene/anthracene (C2Nbf) or C3-phenanthrene/anthracene (C3Nbf) relative to other USS *Arizona* aerobic enrichment cultures (Figures 8.34 and 8.35). Enrichment 01-041 also exhibited less pyrene degradation relative to other USS *Arizona* aerobic enrichment cultures (Figures 8.34 and 8.35).

PAHS COMPARED TO CONSERVED BIOMARKERS.

Gas chromatography coupled to mass spectrometry also provided $18\alpha(H)$-oleanane and C_{30} $17\alpha(H),21\beta(H)$-hopane concentrations in oil extracted from USS *Arizona* aerobic enrichment cultures and uninoculated controls after a 30 day incubation. Ratios for C_{30} $17\alpha(H),21\beta(H)$-hopane to $18\alpha(H)$-oleanane were calculated to determine if C_{30} $17\alpha(H),21\beta(H)$-hopane was being degraded relative to $18\alpha(H)$-oleanane. To date, no laboratory or field studies have shown degradation of $18\alpha(H)$-oleanane (Peters and Moldowan, 1993). Ratios of C_{30} $17\alpha,21\beta(H)$-hopane to $18\alpha(H)$-oleanane varied little between oil extracted from aerobic enrichments and uninoculated controls after 30 days of incubation, indicating no degradation of $C_{30}17\alpha(H),21\beta(H)$-hopane (Table 8.10).

The ratios of total PAHs to conserved biomarkers $18\alpha(H)$-oleanane and $C_{30}17\alpha(H),21\beta(H)$-hopane from aerobic enrichments with 30 days microbial growth in comparison to the uninoculated control decreased, indicating a loss of PAHs (Table 8.11). For example, the total PAH to $C_{30}17\alpha(H),21\beta(H)$-hopane ratio for the uninoculated control was

Figure 8.30. Individual PAH analysis for oil extracted from USS *Arizona* aerobic enrichments initiated from sediments surrounding the ship following 30 days growth indicates a substantial loss of PAHs in comparison to the uninoculated control. Abbreviations for PAH compounds are defined in Table 8.1 and locations for sediments used for aerobic enrichment inoculum are defined in Figure 8.5.

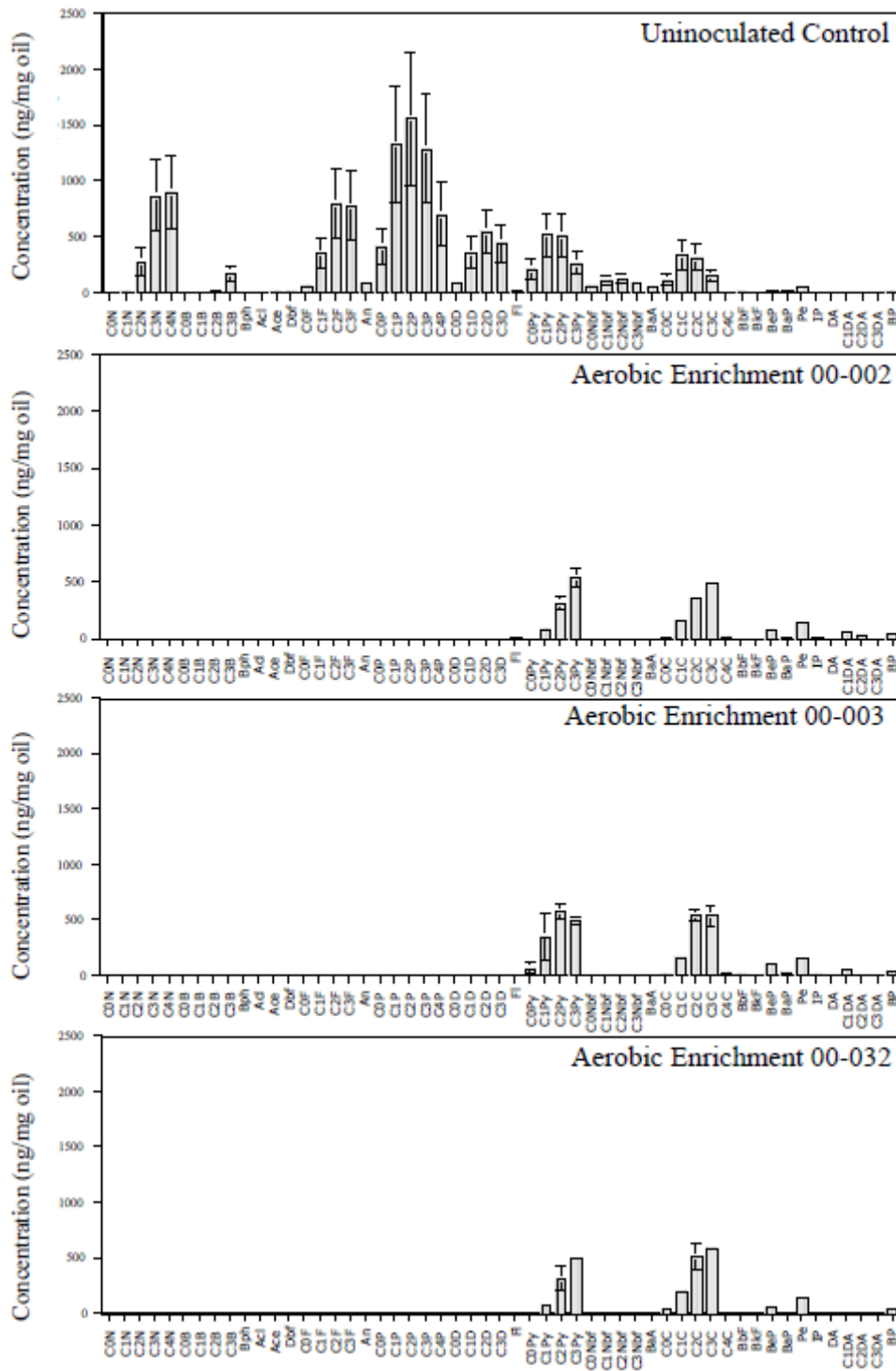**Figure 8.31. Individual PAH analysis for oil extracted from USS *Arizona* aerobic enrichments initiated from sediments on top of the ship following 30 days incubation indicates a substantial loss of PAHs in comparison to the uninoculated control. Abbreviations for PAH compounds are defined in Table 8.1 and locations for sediments used for aerobic enrichment inoculum are defined in Figure 8.5.**
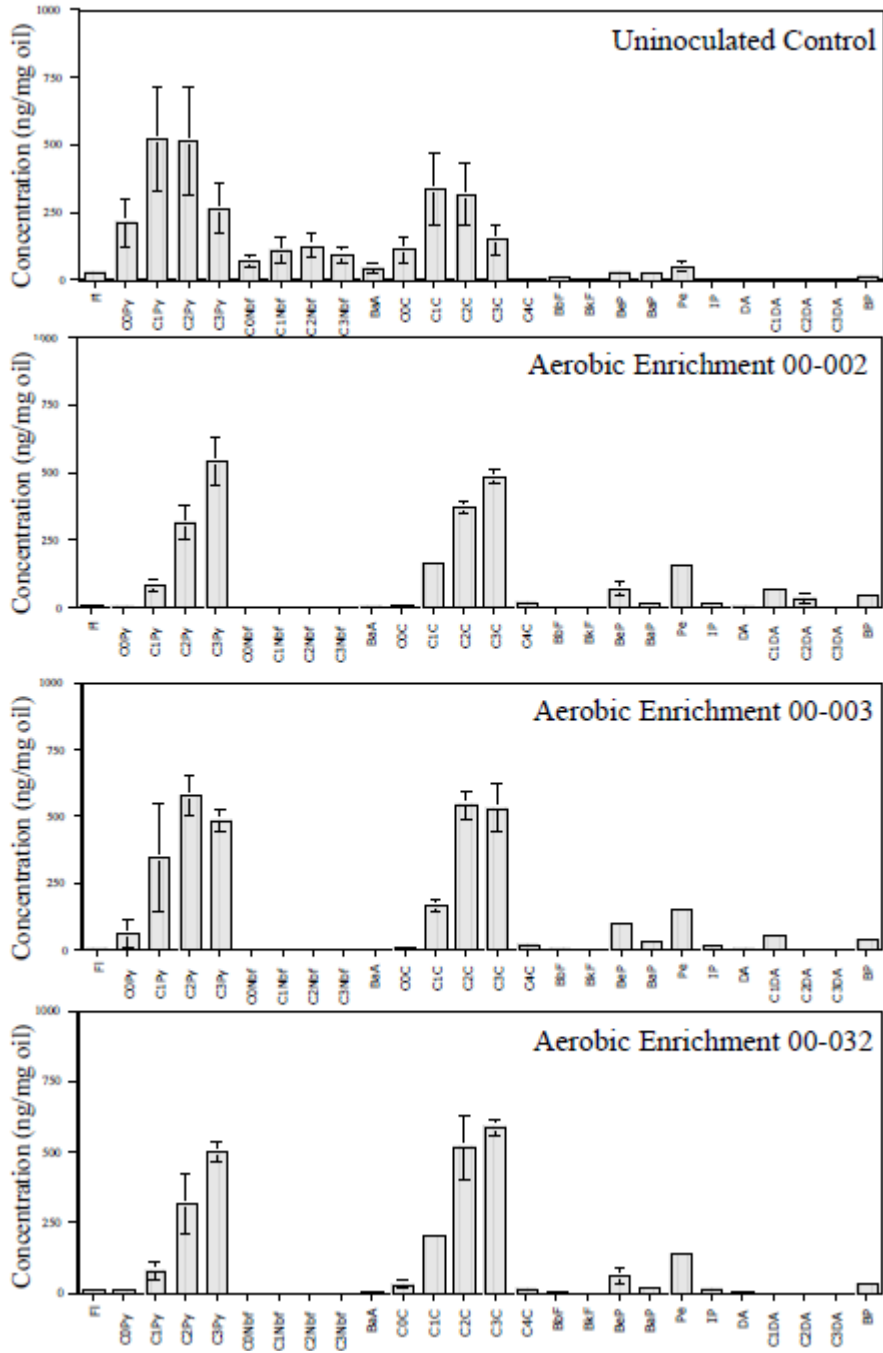
Figure 8.32. Individual PAH analysis of high molecular weight PAHs for oil extracted from USS *Arizona* aerobic enrichments initiated from sediments surrounding the ship following 30 days growth. Abbreviations for PAH compounds are defined in Table 8.1 and locations for sediments used for aerobic enrichment inoculum are defined in Figure 8.5.
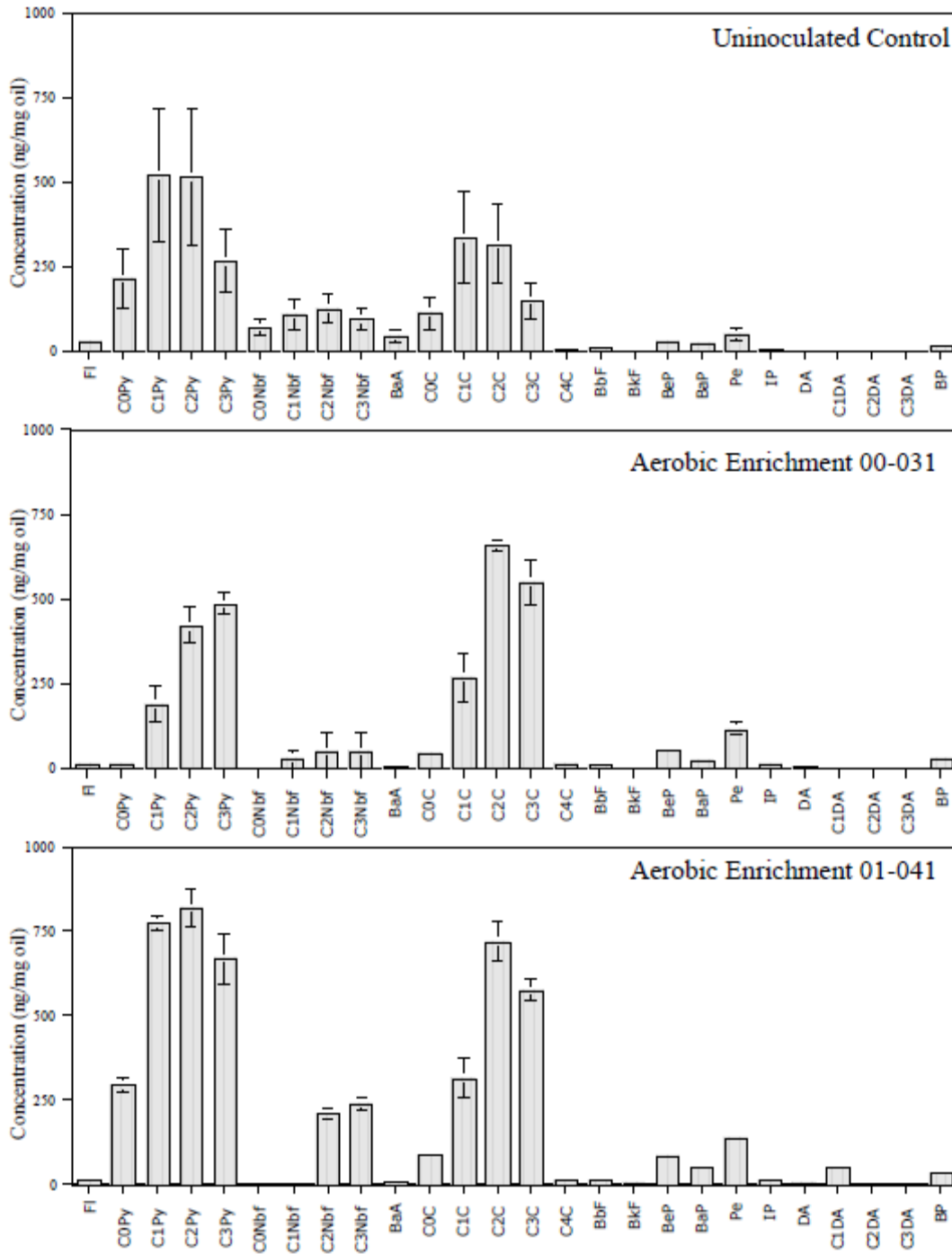
Figure 8.33. Individual PAH analysis of high molecular weight PAHs for oil extracted from USS *Arizona* aerobic enrichments initiated from sediments on top of the ship following 30 days growth. Abbreviations for PAH compounds are defined in Table 8.1 and locations for sediments used for aerobic enrichment inoculum are defined in Figure 8.5.
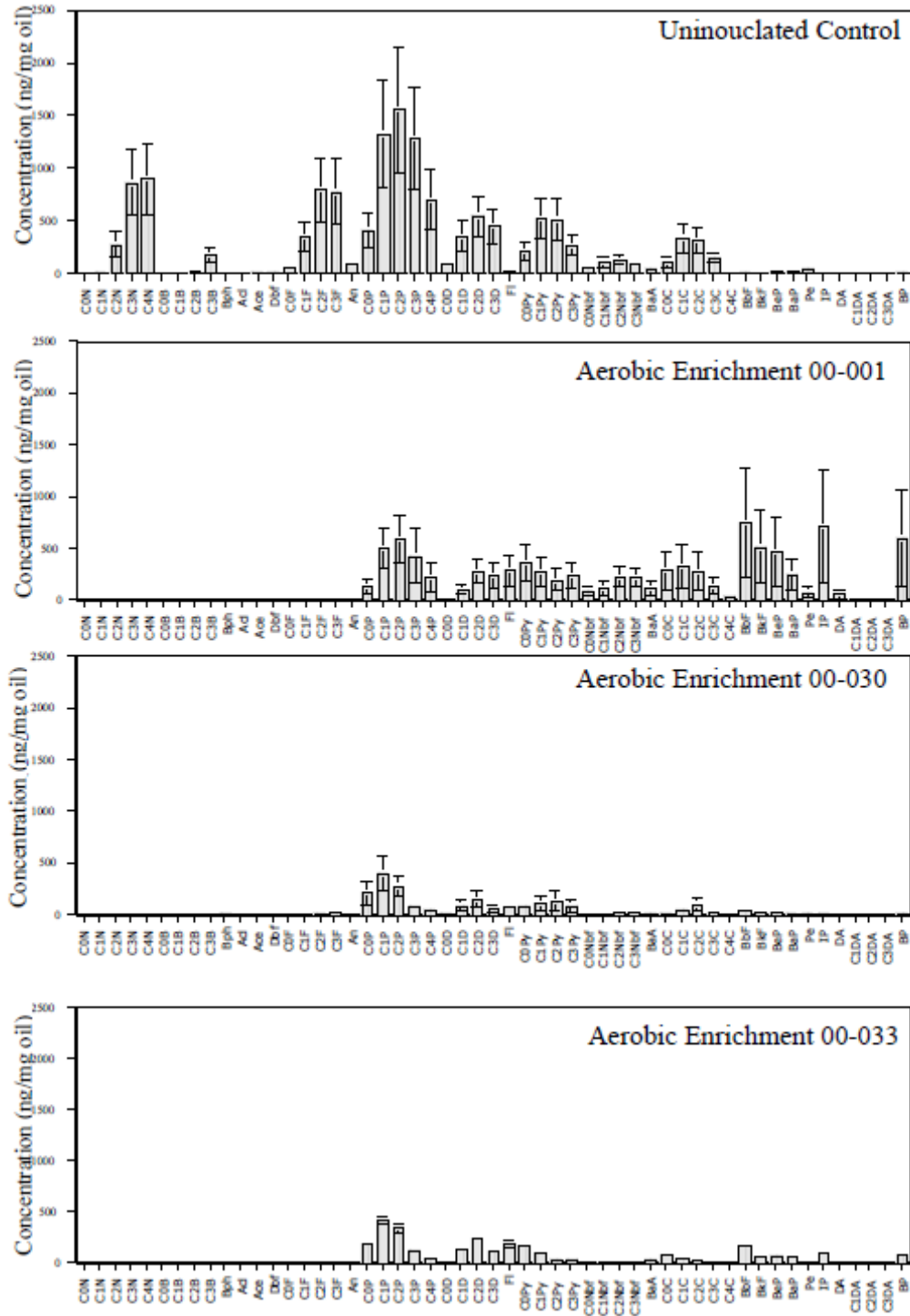
Figure 8.34. Individual PAH analysis for oil extracted from USS *Arizona* aerobic enrichments following 30 days incubation. These enrichments had one of the three triplicates that did not show oil degradation. Abbreviations for PAH compounds are defined in Table 8.1 and locations for sediments used for aerobic enrichment inoculum are defined in Figure 8.5.
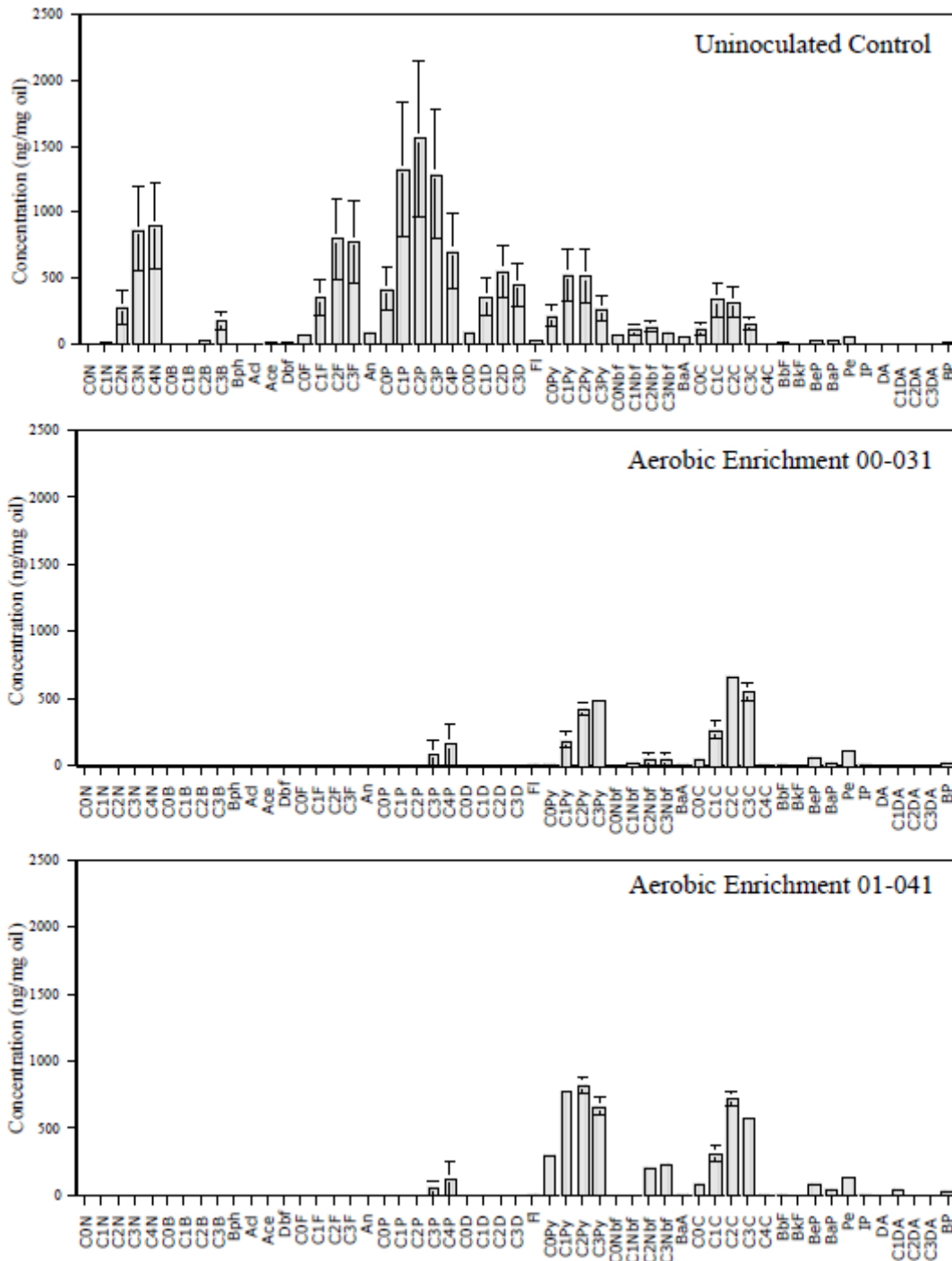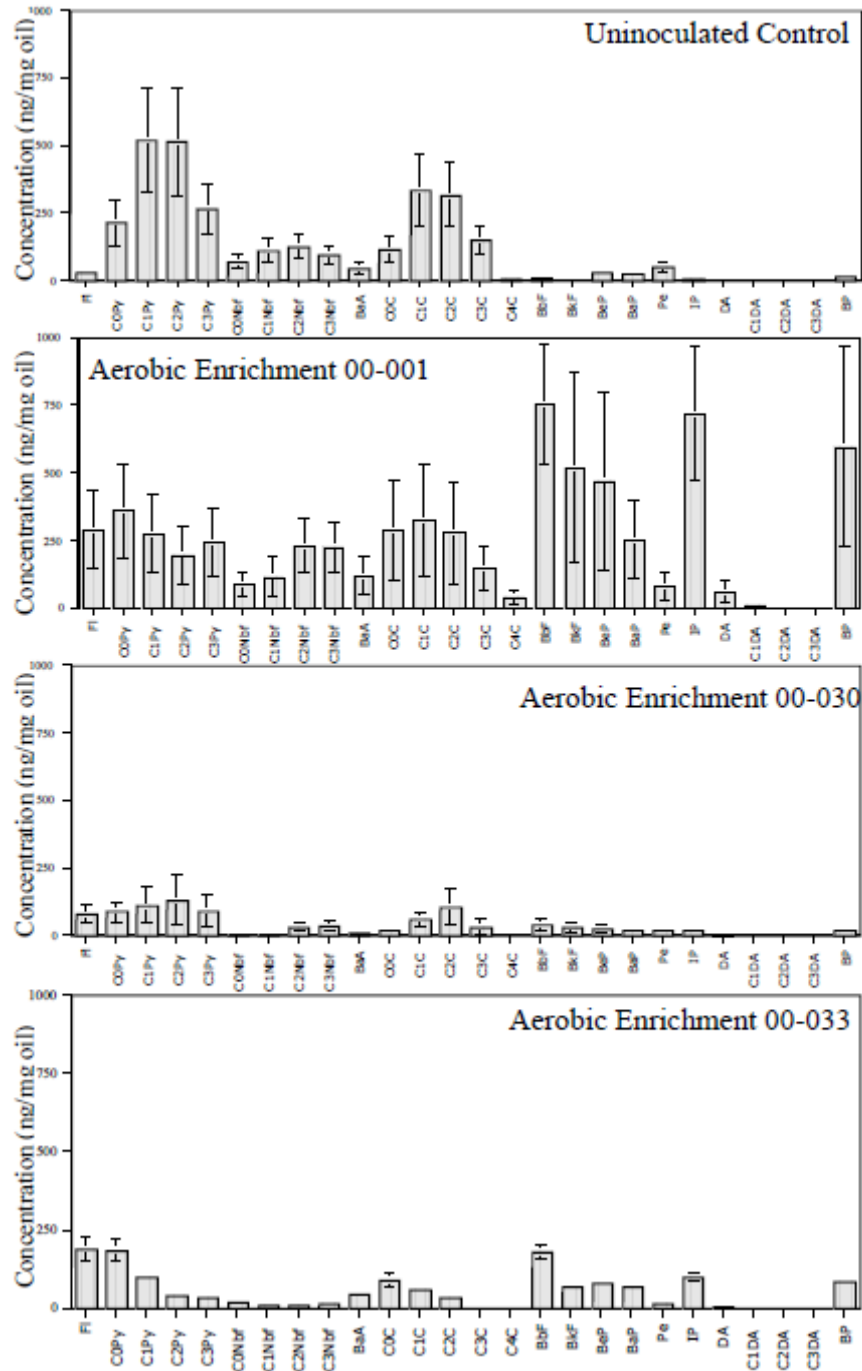
Figure 8.35. Individual PAH analysis of high molecular weight PAHs for oil extracted from USS *Arizona* aerobic enrichments following 30 days incubation. These enrichments had one of the three triplicates that did not show oil degradation. Abbreviations for PAH compounds are defined in Table 8.1 and locations for sediments used for aerobic enrichment inoculum are defined in Figure 8.5.

Aerobic Enrichment	$C_{30}H/18\alpha$ oleanane[a]	$Ts/(Ts+Tm)$[b]	$C_{31}S/(C_{31}R + C_{31}S)$[c]
Uninoculated Control	4.95±0.16	0.36±0.02	0.52±0.03
00-001	5.14±0.03	0.27±0.04	0.57±0.01
00-002	5.09±0.05	0.39±0.05	0.57±0.01
00-003	5.08±0.05	0.31±0.01	0.56±0.01
00-032	5.11±0.04	0.26±0.07	0.58±0.01
00-033	4.55±0.43	0.37±0.45	0.52±0.02
00-030	5.06±0.06	0.37±0.03	0.55±0.02
00-031	5.07±0.09	0.41±0.05	0.56±0.01
01-041	5.09±0.03	0.39±0.11	0.58±0.01

All values are the means and standard error of triplicate samples. The uninoculated control was maintained under the same conditions as aerobic enrichments for 30 days without microbial inoculum.
[a]Calculated from m/z=191 mass chromatogram peak areas of $C_{30}17\alpha(H),21\beta(H)$-hopane and $18\alpha(H)$-oleanane.
[b]Calculated from the m/z=191 mass chromatogram peak areas of $C_{27}17\alpha(H)$-22,29,30-trisnorhopane (Tm) and $C_{27}18\alpha(H)$-22,29,30-trisnorneohopane (Ts).
[c]Calculated from the m/z=191 mass chromatogram peak areas of $C_{31}17\alpha(H)$-homohopane (22*S* and 22*R*).

Table 8.10. Hopane biomarker ratios calculated for aerobic microbial enrichment cultures initiated from Pearl Harbor sediments after 30 days of biodegradation.

Aerobic Enrichment	$C_{30}H/18\alpha$ oleanane[a]	$Ts/(Ts+Tm)$[b]	$C_{31}S/(C_{31}R + C_{31}S)$[c]
Uninoculated Control	4.95±0.16	0.36±0.02	0.52±0.03
00-001	5.14±0.03	0.27±0.04	0.57±0.01
00-002	5.09±0.05	0.39±0.05	0.57±0.01
00-003	5.08±0.05	0.31±0.01	0.56±0.01
00-032	5.11±0.04	0.26±0.07	0.58±0.01
00-033	4.55±0.43	0.37±0.45	0.52±0.02
00-030	5.06±0.06	0.37±0.03	0.55±0.02
00-031	5.07±0.09	0.41±0.05	0.56±0.01
01-041	5.09±0.03	0.39±0.11	0.58±0.01

All values are the averages of triplicate samples with the standard errors of those values. The uninoculated control was maintained under the same conditions as aerobic enrichments for 30 days without microbial inoculum.
[a]$C_{30}H$ represents $C_{30}17\alpha(H),21\beta(H)$-hopane.

Table 8.11. USS *Arizona* aerobic enrichment ratios of total PAHs to biomarkers.

15.32$\pm$4.30 and the same ratio for USS *Arizona* aerobic enrichment cultures ranged from
1.66$\pm$0.14 for enrichment 00-002 to 15.32$\pm$12.89 for enrichment 00-001.

DGGE ANALYSIS OF AEROBIC ENRICHMENT CULTURE MICROBIAL COMMUNITIES.

DGGE analysis was performed to determine differences in the microbial community
structure of the aerobic enrichment cultures. For each aerobic enrichment culture initiated,
triplicate Erlenmeyer flasks were inoculated with sediments from the different locations.
Therefore, each of the triplicates (designated A, B, and C) is an independent (separate) culture.
Following 30 days of incubation, the microbial community DNA was extracted from each of the
triplicates for each enrichment culture, and then amplified using a 323 bp region of the V9 region
of the 16s rDNA. This is a region conserved in the domain *Bacteria*. Following DNA
amplification, DNA was run on DGGE. DGGE separates DNA based on the sequence,
therefore, each band has the potential to represent a single micoorganism. All DNA extracts
were run on the same DGGE gel for band comparison. DGGE revealed multiple banding
patterns with an average of 10 bands per enrichment lane (Figure 8.36). There was variability
between banding patterns of enrichment culture triplicates and since each of the triplicates was
incubated in a separate flask, some variability might be expected. Enrichments 00-001, 00-030,
and 00-033, each had 1 of the 3 triplicate cultures that exhibited less degradation of oil, and these
enrichments had fewer DGGE bands. For example, triplicate A in enrichment culture 00-001
contained 8 bands and less degradation of oil was observed than triplicates B and C (Figure
8.36). Triplicates B and C had 10 and 11 bands, respectively (Figure 8.36).

BIOMARKER ANALYSIS OF AEROBICALLY DEGRADED BUNKER C CRUDE OIL.

Analysis of oil from USS *Arizona* aerobic enrichments by GC-MS was used to determine
if aerobic microbial degradation was influencing crude oil biomarker profiles, and to determine if
biomarker profiles from aerobic enrichments were similar to biomarker profiles in sediments and
oil leaking from the ship. Mass chromatograms for hopanes (m/z=191) and steranes (m/z 217)
were examined. Chromatograms for (m/z=191) hopanes showed few changes in the key
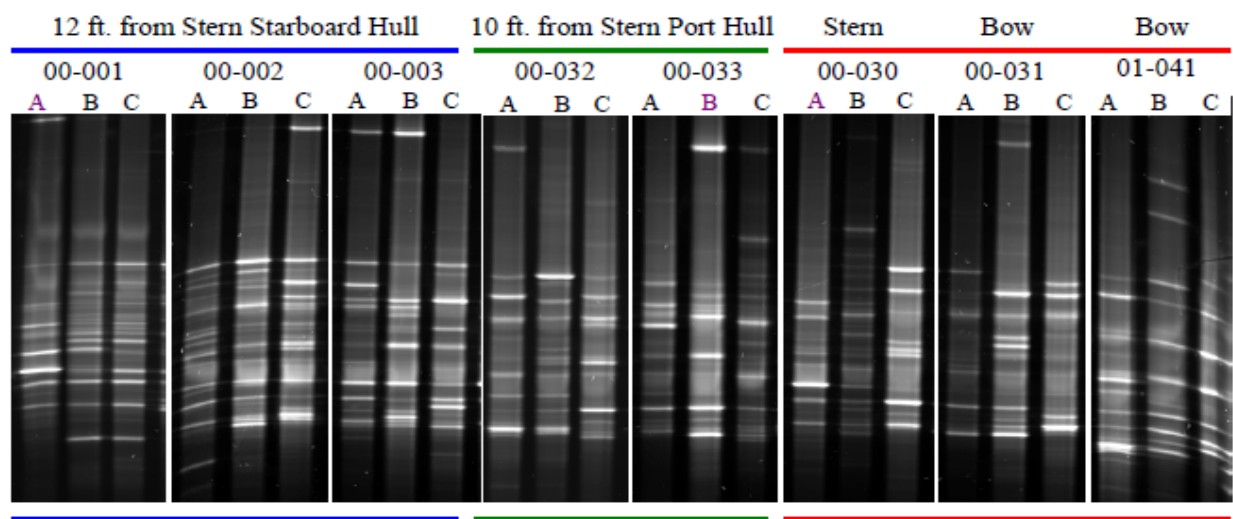
Figure 8.36. DGGE analysis of USS *Arizona* aerobic enrichment cultures. Triplicate cultures are designated by A, B and C. The blue bar denotes enrichment cultures that were inoculated with sediments collected from the stern section, starboard side, 12 ft. from the hull. The green bar denotes enrichment cultures that were inoculated with sediments collected from the stern section, port side, 10 ft. from the hull. The red bar denotes enrichment cultures that were inoculated with sediments collected from the top of the ship, and title above indicates the section they were collected from (bow or stern). The purple letters denotes enrichments that not did show degradation (00-001 A, 00-033 B and 00-030 A).

biomarkers (i.e., $C_{30}17\alpha(H),21\beta(H)$-hopane) compared to the uninoculated control (Figure 8.37).

However, there was a decrease in the C_{28} - $C_{29}13\beta,21\alpha(H)$-tricyclic terpane 22R and 22S

epimers in oil extracted from aerobic enrichment cultures in comparison to the uninoculated

control (Figure 8.37).

Mass chromatograms for (*m/z*=217) sterane trace showed a decrease in C_{27} steranes in oil

extracted from aerobic enrichment cultures in comparison to the uninoculated control (Figure

8.38). There was no decrease in C_{28} steranes and C_{29} steranes in aerobic enrichment cultures

(Figure 8.38).

Biomarker ratios were calculated from mass chromatograms *m/z*=191 as detailed in

section 2 to examine whether changes were occurring to biomarker profiles. Briefly, mass

chromatogram peak areas of $C_{30}17\alpha(H),21\beta(H)$-hopane and 18α-oleanane were calculated for

the hopane to oleanane ratio (Table 8.10). Peak areas of $C_{27}17\alpha(H)$-22,29,30-trisnorhopane

(Tm) and $C_{27}18\alpha(H)$-22,29,30-trisnorneohopane (Ts), were calculated for the Ts/(Ts + Tm) ratio.

Figure 8.37. GC-MS chromatograms (*m/z*=191) of hopanes extracted from USS *Arizona* aerobic enrichments and uninoculated controls following 30 days of microbial incubation. Chromatograms are representative of triplicate samples.
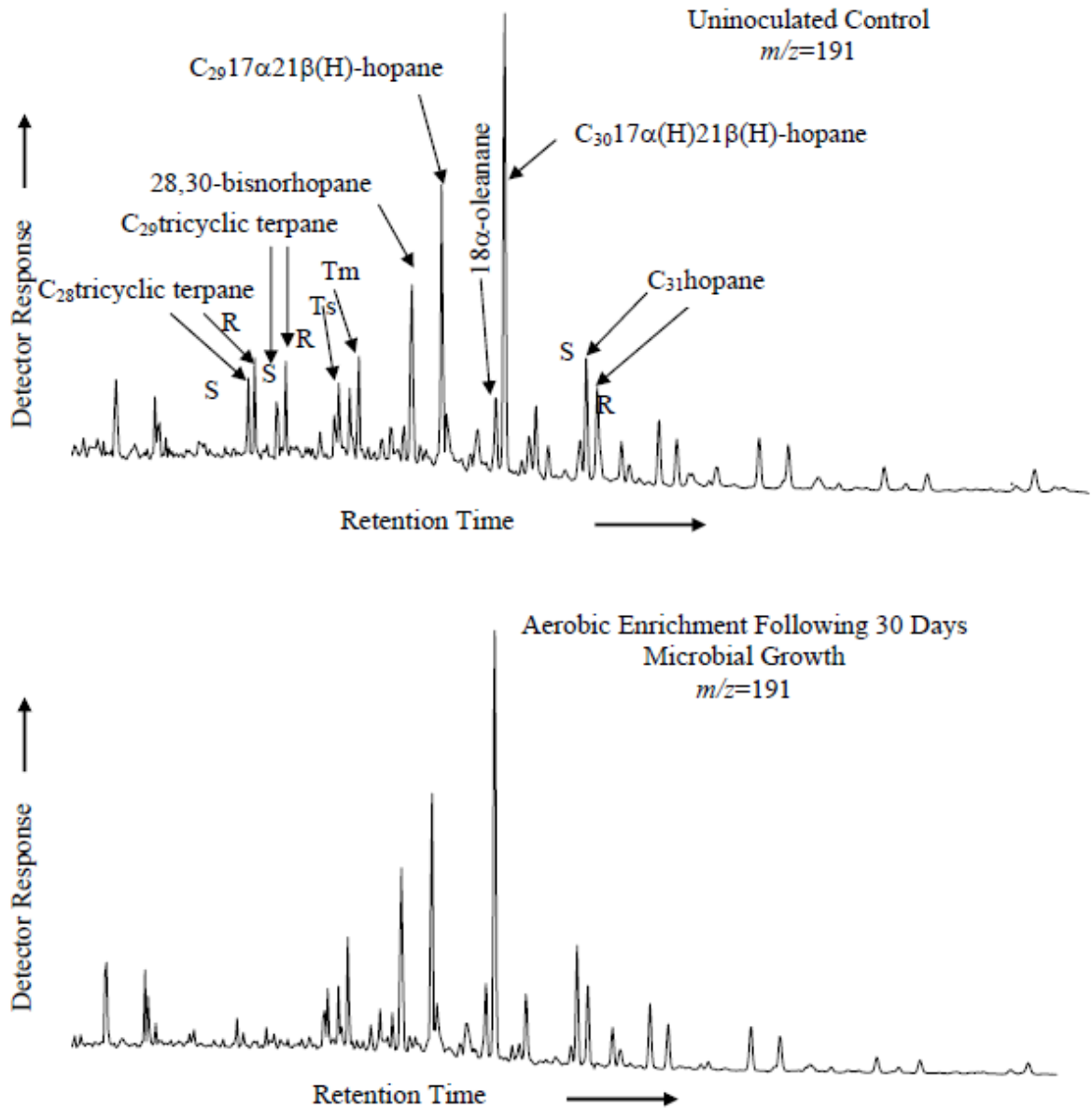
366

Figure 8.38. GC-MS chromatograms (*m/z*=217) of steranes extracted from USS *Arizona* aerobic enrichments and uninoculated controls following 30 days of microbial incubation. Chromatograms are representative of triplicate samples.
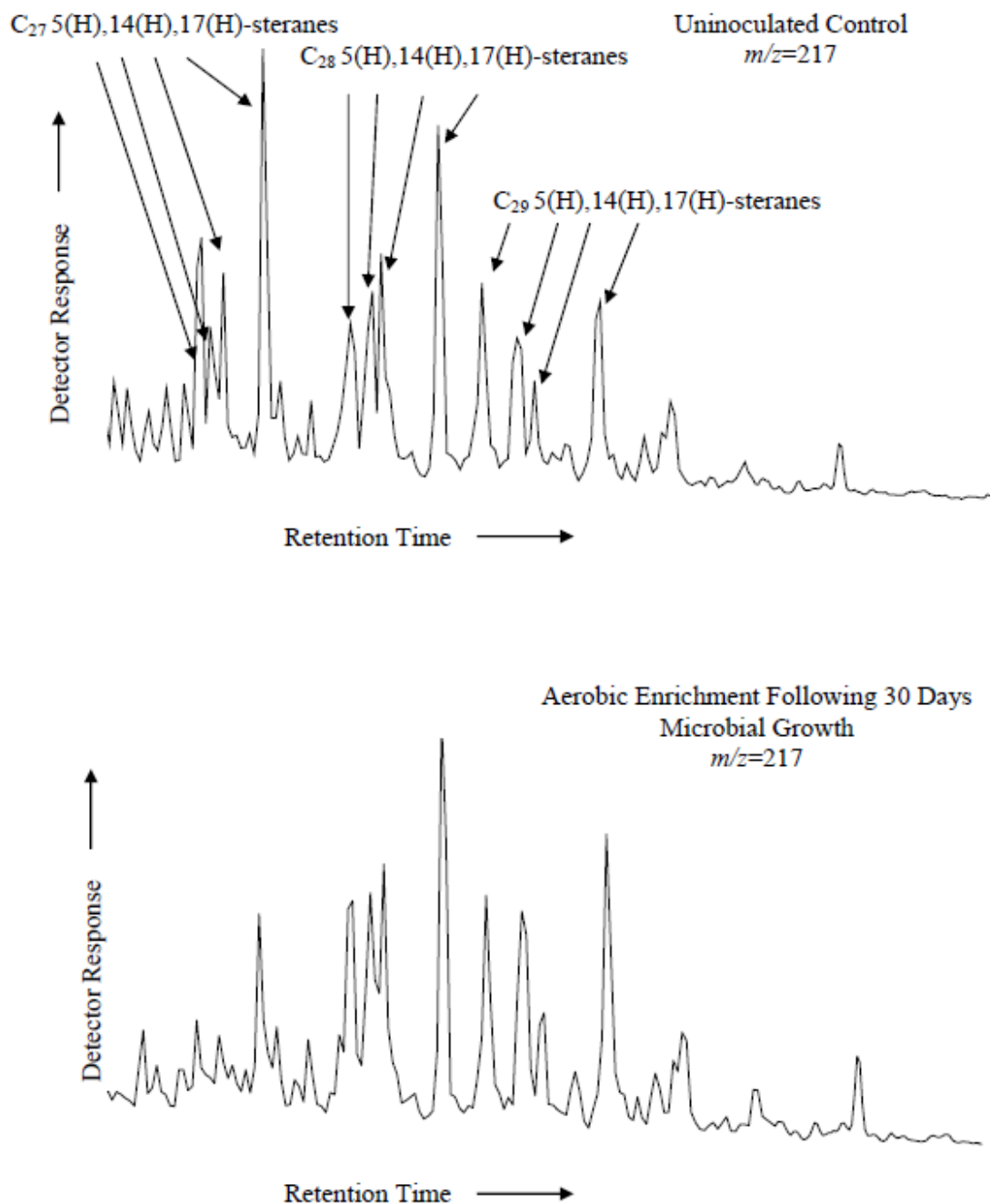
Aerobic Enrichment	$C_{27}S/C_{30}H$[a]	$C_{28}S/C_{30}H$[b]	$C_{29}S/C_{30}H$[c]
Uninoculated Control	1.46 ± 0.67	1.17 ± 0.41	0.97 ± 0.39
00-001	1.06 ± 0.60	1.42 ± 0.15	1.51 ± 0.07
00-002	0.51 ± 0.01	1.35 ± 0.04	1.48 ± 0.04
00-003	0.55 ± 0.03	1.45 ± 0.07	1.45 ± 0.01
00-032	0.52 ± 0.01	1.35 ± 0.03	1.49 ± 0.03
00-033	1.34 ± 0.57	1.75 ± 0.19	1.44 ± 0.05
00-030	1.05 ± 0.59	1.32 ± 0.13	1.49 ± 0.06
00-031	0.83 ± 0.32	1.44 ± 0.13	1.47 ± 0.06
01-041	0.52 ± 0.06	1.61 ± 0.07	2.63 ± 1.01

All values are the means and standard error of triplicate samples. The uninoculated control was maintained under the same conditions as aerobic enrichments for 30 days without microbial inoculum.
[a]Calculated from *m/z*=217 mass chromatogram peak areas of $C_{27}5\alpha(H),14\alpha(H),17\alpha(H)$-sterane (20*S* and 20*R*), $C_{27}5\alpha(H),14\beta(H),17\beta (H)$-sterane (20*S* and 20*R*) and $C_{30}7\alpha(H),21\beta(H)$-hopane.
[b]Calculated from *m/z*=217 mass chromatogram peak areas of $C_{28}5\alpha(H),14\alpha(H),17\alpha(H)$-sterane (20S and 20R), $C_{28}5\alpha(H),14\beta(H),17\beta (H)$-sterane (20*S* and 20*R*) and $C_{30}17\alpha(H),21\beta(H)$-hopane.
[c]Calculated from *m/z*=217 mass chromatogram peak areas of $C_{29}5\alpha(H),14\alpha(H),17\alpha(H)$-sterane (20*S* and 20*R*) $C_{29}5\alpha(H),14\beta(H),17\beta (H)$-sterane and $C_{30} 7\alpha(H),21\beta(H)$-hopane.

Table 8.12. Sterane biomarker ratios calculated for aerobic microbial enrichment cultures initiated from Pearl Harbor sediments after 30 days of biodegradation.

Mass chromatogram peak areas of $C_{31}17\alpha(H)$-homohopane (22*S* and 22*R*) were calculated for the $C_{31}22S/(22S + 22R)$ ratio. Overall, these ratios did not change in USS *Arizona* aerobic enrichment cultures in comparison to the uninoculated control (Table 8.10).

Tricyclic terpane ratios were calculated from mass chromatograms (*m/z*=191) peak areas of C_{28} - $C_{29}13\beta,21\alpha(H)$-tricyclic terpane (22*R* and 22*S*) to compare with the peak area of $C_{30}17\alpha,21\beta(H)$-hopane. These ratios were calculated to determine if the C_{28} and C_{29} tricyclic terpanes were being degraded in comparison to $C_{30}17\alpha,21\beta(H)$-hopane. For the uninoculated control, the ratio for C_{28} and $C_{29}13\beta,21\alpha(H)$-tricyclic terpane 22*R* and 22*S* to $C_{30}17\alpha,21\beta(H)$-hopane was 0.20 ± 0.08 and 0.19 ± 0.08, respectively. For the enrichment cultures, this ratio could not be calculated because the tricyclic terpanes were below the detection limit.

Biomarker ratios were also calculated from mass chromatograms *m/z*=217 (Table 8.10). Details for calculation are in section 2. Briefly, mass chromatogram peak areas of $C_{27}5\alpha(H),14\alpha(H),17\alpha(H)$-sterane (20*S* and 20*R*), $C_{27}5\alpha(H),14\beta (H),17\beta (H)$-sterane (20*S* and 20*R*) and $C_{30}17\alpha(H),21\beta(H)$-hopane were calculated for the $C_{27}S/C_{30}H$ ratio. Mass chromatogram peak areas $C_{28}5\alpha(H),14\alpha(H),17\alpha(H)$-sterane (20*S* and 20*R*), $C_{28}5\alpha(H),14\beta$

(H),17β (H)-sterane (20*S* and 20*R*) and $C_{30}17\alpha(H),21\beta(H)$-hopane were calculated for the $C_{28}S/C_{30}H$ ratio. Mass chromatogram peak areas of $C_{29}5\alpha(H),14\alpha(H),17\alpha(H)$-sterane (20S and 20R), $C_{29}5\alpha(H),14\beta(H),17\beta$ (H)-sterane (20*S* and 20*R*) and $C_{30}17\alpha(H),21\beta(H)$-hopane were calculated for the $C_{29}S/C_{30}H$ ratio (Table 8.10)

Ratios for C_{27} steranes were lower in USS *Arizona* aerobic enrichment cultures in comparison to the uninoculated control. For example, the uninoculated control ratio for $C_{27}S/C_{30}H$ was 1.46±0.67 (Table 8.10). In comparison, the $C_{27}S/C_{30}H$ ratio ranged from 0.51±0.01 for enrichment 00-002 to 1.34±0.57 for enrichment 00-033 (Table 8.12). Enrichments 00-001, 00-030, and 00-033, had 1 of the 3 triplicate cultures with less degradation of oil, and these enrichments high higher $C_{27}S/C_{30}H$ ratios in comparison to the uninoculated control and had larger standard errors than other enrichments. For example, enrichment 00-033 had triplicates with $C_{27}S/C_{30}H$ ratios of 1.29, 2.36, and 0.39.

DISCUSSION

The National Park Service estimates that 2,200 tons of Bunker C fuel oil remain aboard USS *Arizona*, and it has been estimated that 1-2 L of the oil leaks each day from the ship to the surface seawater (Johnson et al., 2002; Murphy and Russell, personal communication). Oil leaking from the ship and in surrounding Pearl Harbor sediments has never been fully characterized. The objectives of this study were to obtain fundamental information on the oil leaking out of the ship, to compare oil from the ship to oil in surrounding sediments, and to determine the biodegradability of the oil leaking from the ship by microorganisms enriched from Pearl Harbor sediments. In addition, characterization of the biomarker profiles in these studies provided a foundation for additional comparisons. A better understanding of the abiotic and biotic weathering processes influencing the oil may contribute to USS *Arizona* management and conservation decisions in the future.

OIL LEAKING OUT OF USS *ARIZONA*

First, chemical characterization of the oil was conducted to determine the extent of abiotic and biotic weathering processes. Previous studies have shown that *n*-alkanes are the first

oil component to be lost by both biotic weathering processes (i.e., biodegradation) and abiotic weathering processes (i.e., evaporation) following an environmental spill (Wang et al., 1994; Whittaker and Pollard, 1997; Wang et al., 1998a; Prince, et al., 2002; NRC, 2003). Following loss of *n*-alkanes, a decrease in the branched alkanes (pristane and phytane) is generally observed (Blumer and Sass, 1972; Wang et al., 1994; Whittaker and Pollard, 1997; Wang, et al., 1998a; NRC, 2003). Characterization of oil leaking from USS *Arizona* by chromatography indicated *n*-alkanes were still present in oil leaking from the hatches near barbette no. 4 (location A). In comparison, oil leaking from the stern starboard portholes (location B) had a decrease in *n*-alkanes, suggesting that oil leaking from location B is more weathered than oil leaking from location A.

Further GC-MS characterization of the oil leaking from the ship was conducted to quantitatively characterize the PAHs present. High molecular weight PAHs (i.e., chrysene and pyrene) tend to be more resistant to microbial degradation in comparison to lower molecular weight PAHs (i.e., naphthalenes and flourenes) (Cerniglia, 1992; Dean-Ross et al., 2002; Wang et. al, 1998; NRC, 2003). Lower molecular weight PAHs are more readily degraded by microorganisms and are more susceptible to abiotic weathering processes such as dissolution and evaporation than high molecular weight PAHs (Wang et al., 1994; Wang et. al, 1998a; Michel and Hayes, 1999; NRC, 2003). PAHs were detected in all samples of oil leaking from USS *Arizona*. For example, sample 01-015 (from location A) contained low molecular weight naphthalenes and flourenes along with similar amounts of high molecular weight PAHs. The presence of higher concentrations of naphthalenes in sample 01-015 in comparison to lower concentrations of naphthalenes in sample 01-029 suggests sample 01-015 is less weathered. Naphthalene and its alkylated homologues are often the first PAHs to be lost by weathering following release of oil into the environment (Wang et al., 1994).

The similarity between the high molecular weight PAH histograms for all three samples of oil leaking from the ship suggests either no weathering of high molecular weight PAHs or the same extent of weathering for all three samples. Since there is no original sample of oil from USS *Arizona* available, we cannot definitively say that no weathering of the high molecular weight PAHs has occurred. Also, we cannot compare our PAH data directly to another Bunker C fuel oil sample because the oil is a complex mixture that may undergo post-distillation processes, including the addition of additives, therefore modifying its composition (Irwin et al.,

1997). Since some low molecular weigh PAHs are still present in all three samples and high

molecular weight PAHs are weathered more slowly than low molecular weight PAHs, it is

probable that little or no weathering of high molecular weight PAHs has occurred.

The ratios for total PAHs to conserved biomarkers indicated that oil leaking from

location B had fewer total PAHs than oil leaking from location A, although these results are not

definitive. Sample 00-15 from location A had a ratio value closer to sample 01-029 that may

suggest that 00-015 is more weathered than 00-034 oil leaking from location A. PAH data for oil

leaking from the ship does not support this observation. A more probable explanation for large

ratio differences between sample 00-015 and 00-034 can be attributed to the large variation

between replicates that resulted in a larger standard error in 00-034. By disregarding this

triplicate, the ratio for total PAHs to $C_{30}17\alpha,21\beta(H)$ hopane for sample 00-034 became

118.97 ± 2.73 (compared to 97.70 ± 21.27 when all three triplicates are considered) which indicates

more PAHs are present in 00-034 than 01-015.

The PAH results for oil leaking from USS *Arizona* in comparison to the GC-FID results

suggests oil leaking from the ship differs primarily in *n*-alkanes. GC-FID results showed

differences in *n*-alkanes from different locations, but branched alkanes pristane and phytane were

present in samples from all locations. Furthermore, data for PAH analysis indicated that except

for naphthalene, PAH concentrations were similar. Overall, this indicates that *n*-alkanes and

naphthalenes are the only compounds decreasing in oil from location B in comparison to location

A. This is consistent with oil weathering patterns, since *n*-alkanes and low molecular weight

PAHs are the first to decrease after an environmental release of oil (Blumer and Sass, 1972;

Wang et al., 1994; Wang et. al, 1998a; Michel and Hayes, 1999; NRC, 2003).

Overall, oil leaking from location A was less weathered than oil leaking from location B,

indicating that perhaps oil leaking from location B has been exposed to an environment more

favorable for weathering before it leaves the ship than oil leaking from location A. Another

possibility is that conditions are more conducive to degradation in the reservoir (original ship

location of oil that is leaking from location B). The ship has a total of four decks, with oil

bunkers on the bottom of the ship and the sides of decks four (the lowest deck) and three (above

deck four) (Lenihan, 1990; Murphy and Russell, personal communication). Oil leaking from

location A may take a more direct path out of the ship to the surface or pool on the third deck of

the ship (Murphy and Russell, personal communication). The third deck of the ship may have

less seawater exchange and dissolved oxygen, therefore the environment may be less conducive for oil weathering processes, especially microbial degradation (Murphy and Russell, personal communication). In comparison, it is possible that oil leaking from location B is taking more time to travel from the original bunker to the surface of the ship, allowing more time for chemical changes in the oil before leaking to the surface. Furthermore, oil leaking from location B could be leaking from the bunker to the second deck, which has seawater exchange, introducing nutrients and dissolved oxygen required for microbial degradation processes.

Components of oil that are resistant to abiotic and biotic forms of weathering, known as biomarkers, are useful internal indicators of degradation. Biomarkers can also be used as a fingerprint to identify oil (Peters and Moldowan, 1993). In this study, hopanes and steranes were analyzed in three samples of oil leaking from USS *Arizona*. Analysis of 01-015, 00-034, and 01-029 indicated that there were no statistical differences in biomarker profiles in oil leaking from different locations of the ship (ANOVA, p=0.054). The similarity between biomarker profiles and calculated biomarker ratios also suggested that biomarkers were not degraded in the samples of oil leaking from the ship. Furthermore, ratios for selected biomarkers were similar, suggesting that oil leaking from USS *Arizona* is from the same (or very similar) source.

OIL EXTRACTED FROM USS *ARIZONA* SEDIMENTS.

Crude oil can persist in sediments and is often identified years after its initial deposition (Wang et al., 1994; Vandermeulen and Singh, 1994; Wang et al., 1998b). To obtain information about the presence of petroleum hydrocarbons in sediments on or adjacent to USS *Arizona*, hydrocarbons were extracted by a continuous soxhlet extraction technique. In general, the amount of solvent extractable material per gram of sediment was low (1.79 mg extractable material/ g dry sediment) in comparison to other hydrocarbon-contaminated sediments studies in our laboratory (ranged from 1.91 – 84.08 mg extractable material/ g dry sediment) (Frontera-Suau et al., 2002).

Gas chromatographic traces of USS *Arizona* sediment solvent-extractable materials showed a common peak in all sediment extracts. This peak was identified using GC-MS as BHT, an antioxidant that is present in some foods, cosmetics, plastics, and rubber products (Fries and Puttman, 2002). Studies have detected BHT in rainwater, ground water, and sediments

across the world (Jungclaus et. al, 1978; Fries and Puttman, 2002), although degradation studies have shown that BHT is quickly broken down in the environment (Mikami et al., 1979; Inui et al., 1979). The source of BHT in Pearl Harbor sediments is unknown, and it is possible that some of the BHT observed in our samples was due to the thimble or boiling chips during the soxhlet extraction process. However, we did detect BHT in samples of the oil leaking from the ship. The concentration observed in extracts of sediments samples was high (as observed by relative detector response) suggesting that BHT was (or had been) deposited in USS *Arizona* sediments. Fries and Puttman (2002) attributed the concentrations of BHT observed in water and sediment samples, despite the ability of microorganisms to easily degrade BHT, to the fact that BHT is used in large quantities in many countries (i.e., USA, Germany, England).

In USS *Arizona* sediments, high molecular weight *n*-alkanes, ranging from approximately $C_{20} – C_{32}$, were observed on gas chromatographic traces. Shorter chain length *n*-alkanes, as well as pristane and phytane, were not readily observed. GC-MS analysis demonstrated that low molecular weight PAHs were below the detection limit in USS *Arizona* sediments, but high molecular weight PAHs were present. The low concentration of low molecular PAHs could be due to weathering, since these compounds are generally lost to biotic and abiotic weathering processes prior to high molecular weight PAHs.

The detection of hopane and sterane biomarkers in sediment solvent-extractable materials further suggests oil is present in the sediment samples collected from USS *Arizona.* Biomarker compounds from the *m/z*=191 trace were identified that are not ubiquitous in all oils. The biomarkers 28, 30 bisnorhopane (often referred to as C_{28}hopane) and 18α(H)-oleanane are not found in all oils, and together are characteristic of oil from Miocene Monterey Formation source rock in California (Peters and Moldowan, 1993; Kvenvolden et al., 1993; Kvenvolden et al., 2002). Both 28, 30 bisnorhopane and 18α(H)-oleanane were detected in oil leaking from the ship and in sediment solvent-extractable materials. This suggests that oil leaking from the ship may be depositing into surrounding sediments, although it is possible that an oil other than USS *Arizona* is contributing to the 28, 30 bisnorhopane and 18α(H)-oleanane biomarker profiles.

Since biomarker profiles and calculated biomarker ratios are often diagnostic for different oils, a comparison of key biomarker ratios between the oil leaking from the ship and the sediments can be made. The $C_{30}H/18α$ oleanane ratio ranged from 5.93 ± 0.25 to 6.25 ± 0.15 for samples of oil leaking from the ship, compared to 2.19 ± 0.68 to 9.21 ± 5.30 for the sediment

samples. In general, this ratio was lower for sediment samples, suggesting that either hopane was being degraded relative to oleanane, or that other hydrocarbon inputs were influencing the ratio.

USS *ARIZONA* AEROBIC ENRICHMENT CULTURES.

It is well documented that microorganisms can degrade petroleum (Haines and Alexander, 1974; Mulkins-Phillips and Stewart, 1974; Atlas, 1981; Atlas, 1984). In addition, studies have shown that Bunker C fuel oil is degradable, although less degradable than other lighter crude oils (i.e., Louisiana crude oil) (Walker, et al., 1976). The pattern of microbial degradation of different components of crude oil follows a predictable pattern. Degradation of the saturate fraction occurs first, with degradation of *n*-alkanes then branched alkanes. Concurrently and following saturate degradation, PAHs are degraded, depending on ring size and alkylation.   PAH degradation proceeds from non-alkylated to increasing alkylation ($C_0 > C_1 > C_2 > C_3 > C_4 >$) (Fedorak and Westlake, 1984; Wang et al., 1998a). Low molecular weight PAHs are degraded before high molecular weight PAHs (>3-rings) (Cerniglia, 1992; Dean-Ross et al., 2002; Wang et. al, 1998a).

To determine the degradability of oil leaking from the ship, aerobic enrichment cultures were initiated from sediments collected from different locations as the microbial inoculum source. Oil leaking from the ship was used as the sole carbon source for aerobic enrichment cultures. Following a 30-day growth period, oil was extracted from enrichments and gravimetric measurement showed an average oil loss of $31.03 \pm 4.58\%$. This was greater than the losses observed in uninoculated controls ($6.13 \pm 0.65\%$), suggesting that degradation of USS *Arizona* Bunker C crude oil was occurring. Gas chromatographic traces of the oil extracted from the aerobic enrichment cultures showed depletion of the *n*-alkanes and branched alkanes (pristane, phytane). Further analysis by GC-MS demonstrated degradation of low molecular weight PAHs (i.e., naphthalenes and fluorenes) and some high molecular weight PAHs (i.e., pyrene) in the aerobic enrichment cultures. It is important to note that high molecular weight PAHs (i.e., chrysene and pyrene) persisted. Chrysene and pyrene, along with other high molecular weight PAHs are thought to be mutagenic and carcinogenic (Samanta et al., 2002).

Our laboratory studies, using defined conditions, show oil leaking from the ship is

degradable by microbial communities enriched from sediments collected on and near the ship. Furthermore, degradation was not dependent on microbial communities from specific sediment collection locations around the ship. These results correlate with other studies that have examined microbial degradation of Bunker C crude oil. Minas and Gunkel (1995) determined that 25.6% of Bunker C was degraded in soil microcosms grown at 18˚C. Wang and colleagues (1998a) observed a 23% loss of Bunker C in freshwater enrichments inoculated with 8 well-characterized petroleum-degrading bacteria. In the latter study, pristane and phytane were still present in oil extracted from enrichments. Comparatively, our study did show degradation of pristane and phytane.

The microbial community analysis of USS *Arizona* aerobic enrichment cultures was performed by DGGE. DGGE provide a fingerprint of the microbial community based on the specific amplification of a 323 bp fragment of the 16S rRNA of microorganisms contained in the domain *Bacteria* (Ferris et. al, 1996). DNA extracts from aerobic enrichments (in triplicate) were run on the same gel to allow comparisons between different enrichments. DGGE profiles of the aerobic enrichment cultures suggested some banding pattern differences between different enrichment cultures and for some triplicates of the same enrichment cultures. Differences in banding patterns may be due to different microorganisms present in the original sediment inoculum (since the sediments were from different locations), and by flask-to-flask variability between triplicate enrichment cultures. There were some similar bands observed between sediment inoculum location, but overall there was not a consistent pattern or microbial community fingerprint based on location. Future studies, collaborative with corrosion biologists, will focus on the characterization of the facultative bacteria in these enrichment cultures, and their ability to accelerate biocorrosion of the ship during hydrocarbon degradation.

Biomarkers are compounds that are more resistant to microbial degradation than other components of oil, and can be used as an internal reference to monitor weathering in oil (Peters and Moldowan, 1993; Prince et al., 1994; Whittaker and Pollard, 1997). Although these compounds are considered resistant to degradation, both laboratory (Bost et al., 2001; Frontera-Suau et. al, 2002) and field studies (Moldowan, et al., 1995; Munoz et al., 1997; Wang et al., 2001a) have demonstrated biomarker degradation.

Oil extracted from USS *Arizona* aerobic enrichment cultures was analyzed by GC-MS to monitor *m/z*=191 (hopanes/terpanes) and *m/z*=217 (steranes) biomarkers to determine if there

were any differences in the biomarker profile following 30 days of microbial growth. Results showed a depletion of C_{28}-C_{29} 13β,21α(H)-tricyclic terpanes (22*R* and 22*S*) and a decrease in the C_{27} steranes. These results are of interest because previous biomarker degradation studies in our laboratory have shown C_{30} 17α(H),21β (H)-hopane degradation but no tricyclic terpane or sterane degradation (Bost et al., 2001; Frontera-Suau et. al, 2002). Furthermore, tricyclic terpanes are thought to be degraded following C_{30} 17α(H),21β (H)-hopane degradation, which we did not observe (Reed, 1977; Siefert and Moldowan, 1979; Peters and Moldowan, 1993). In the laboratory, Chosson et al. (1991) demonstrated degradation of the C_{27} steranes preferentially over the C_{28} and C_{29} steranes by seven Gram-positive bacterial strains; no Gram-negative bacterial strains were found capable of degrading these compounds.

A field study by Wang and colleagues (2001a) observed alteration of biomarkers 24 years following a spill of Arabian crude and Bunker C fuel oil in Banco Satelite, Chile in 1974. In the study, biomarkers from samples collected in 2000 were compared to fresh Arabian crude. The study showed biomarker alteration of oil still present in sediments proceeded by weathering of diasteranes>C_{27} steranes>tricyclic terpanes>hopanes>norhopanes and C_{29}-αββ-steranes. This procession of biomarker alteration is similar to the procession observed in this study. Oil leaking from USS *Arizona* and used for the aerobic enrichment cultures did not contain diasteranes, but we did observe C_{27} steranes and C_{28}-C_{29} tricyclic terpane degradation. However, we did not observe hopane degradation, the next biomarker group to be degraded in the Wang (2001b) study.

CONCLUSIONS

The objectives of this study included characterizing oil leaking from USS *Arizona*, characterizing petroleum hydrocarbons in the sediments and determining if oil leaking from the ship was degradable by microorganisms enriched from surrounding sediments. Oil characterized from USS *Arizona* suggests that oil leaking from different ship locations are exposed to different environments, based on the extent of *n*-alkane weathering for oil leaking from the stern starboard hatches compared to oil leaking near barbette no. 4. Biomarkers in oil leaking from the ship were also identified in sediments collected near and on top of the ship. Biomarkers 28, 30 bisnorhopane and 18α(H)-oleanane were of special interest because they are not found in all oils

and were detected in oil leaking from the ship and in surrounding sediments. It is probable that oil leaking from the ship is present in surrounding sediments, but it is also possible that hydrocarbons, including biomarkers, from other sources are present in the sediments as well. Aerobic enrichment cultures initiated from USS *Arizona* sediments were capable of degrading different components (i.e., *n*-alkanes, branched alkanes, and PAHs) of Bunker C leaking from the ship. Certain high molecular weight PAHs (i.e. perylene) remained in oil extracted from enrichment cultures and did not decrease in concentration. These enrichments were capable of degrading the biomarkers C_{28}-C_{29} tricyclic terpanes and C_{27} steranes. C_{28}-C_{29} tricyclic terpanes and C_{27} steranes were also present in sediments, although in varying concentrations. This is interesting because C_{28}-C_{29} tricyclic terpanes and C_{27} steranes were degraded by USS *Arizona* enrichment cultures in the laboratory. C_{28}-C_{29} tricyclic terpanes and C_{27} steranes

In summary, these studies have contributed to our fundamental understanding of the oil that is leaking from USS *Arizona*, and the potential of microorganisms indigenous to Pearl Harbor sediments in degrading this oil. In addition, we have conducted the first comprehensive hydrocarbon fingerprint of Pearl Harbor sediments adjacent to and surrounding the ship. The results of these studies will be shared with the National Park Service Submerged Resources Center, and contribute to future management decisions regarding the conservation and preservation of USS *Arizona.*

REFERENCES

Aeckersberg, F., F. A. Rainey, and F. Widdel
1998 Growth, Natural Relationships, Cellular Fatty Acids and Metabolic Adaption of Sulfate-Reducing Bacteria that Utilize Long Chain Alkanes Under Anoxic Conditions. *Archives Microbiology* 170: 361-369.

Alberdi, M., and L. Lopes
2000 Biomarker 18α(H)-oleanane: Ageochemical Tool to Assess Venezuelan Petroleum Systems. *Journal of South American Earth Sciences* 13:751-759.

Anderson, R. T., and D. R. Lovely
2000 Hexadecane Decay by Methanogenesis. *Nature* 404:722.

Ashwood, T. L., and C. R. Olsen
1988 Pearl Harbor Bombing Attack: A Contamination Legacy Revealed in the Sedimentary Record. *Marine Pollution Bulletin* 19:68-71.

Atlas, R. M.
1981 Microbial Degradation of Petroleum Hydrocarbons: An Environmental Perspective. *Microbiological Reviews* 45:180-209.

1984. *Petroleum Microbiology*. 1st ed. Macmillan Publishing Company. New York.

Baars, B. J.
2002 The Wreckage of the Oil Tanker *Erika* Human Health Risk Assessment of Beach Cleaning, Sunbathing and Swimming. *Toxicology Letters* 128:55-68.

Barron, M. G., T. Podrabsky, S. Ogle, and R. W. Ricker
1999 Are Aromatic Hydrocarbons the Primary Determinant of Petroleum Toxicity to Aquatic Organisms? *Aquatic Toxicology* 46:253-268.

Beam, H. W., and J. J. Perry
1974 Microbial Degradation and Assimilation of n-alkyl-Substituted Cycloparaffins. *Journal of Bacteriology* 118:394-399.

Beckles, D. M., C. H. Ward, and J. B. Hughes
1998 Effect of Mixtures of Polycyclic Aromatic Hydrocarbons and Sediments on Flouranthene Biodegradation Patterns. *Environmental Toxicology and Chemistry* 17:1246-1251.

Bixian, M., F. Jiamo, Z. Gan, L. Zheng, M. Yushun, S. Guoying, and W. Xingmin
2001 Polycyclic Aromatic Hydrocarbons in Sediments from Pearl River and Estuary, China: Sapatial and Temporal Distribution and Sources. *Applied Geochemistry* 16:1429-1445.

Blumer, M. and J. Sass
      1972 Oil Pollution: Persistence and Degradation of Spilled Fuel Oil. *Science* 176:1120-
      1122.

Boll, M., G. Fuchs, and J. Heider
      2002 Anaerobic Oxidation of Aromatic Compounds and Hydrocarbons. *Current Opinion
      in Chemical Biology* 6:604-611.

Bost, F. D., R. Frontera-Suau, T. J. McDonald, K. E. Peters, and P. J. Morris
      2001 Aerobic Biodegradation of Hopanes and Norhopanes in Venezuelan Crude Oils.
      Organic Geochemistry 32:105-114.

Cerniglia, C. E.
      1992 Biodegradation of Polycyclic Aromatic Hydrocarbons. *Biodegradation* 3:351-368.

Chang, Y. J., J. R. Stephen, A. P. Richter, A. D. Venosa, J. Bruggemann, S. J Macnaughton, G.
      A. Kowlachuk, J. R. Haines, E. Kline, and D. C. White
      2000 Phylogenetic Analysis of Aerobic Freshwater and Marine Enrichment Cultures
      Efficient in Hydrocarbon Degradation: Effect of Profiling Method. *Journal of Microbial
      Methods* 40:19-31.

Chosson, P., C. Lanau, J. Connan, and D. Dessort
      1991 Biodegradation of Refractory Hydrogen Biomarkers from Petroleum Under
      Laboratory Conditions. *Nature* 351(6328):640-642.

Dean-Ross, D., J. Moody, and C. E.Cerniglia
      2002 Utilization of Mixtures of Polycyclic Aromatic Hydrocarbons by Bacteria Isolated
      from Contaminated Sediment. FEMS *Microbiology Ecology* 41:1-7.

Elshahed, M. S., L. M. Gieg, M. J. Mcinerney, and J. M. Suflita
      2001 Signature Metabolites Attesting to the *in situ* Attenuation of Alkylbenzenes in
      Anaerobic Environments. *Environmental Science and Technology* 35:682-689.

Environmental Protection Agency [EPA]
      1984 *List of the Sixteen PAHs with Highest Carcinogenic Effect*. IEA Coal Research,
      London.

Ferris, M. J., G. Muyzer, and D. M. Ward
      1996 Denaturing Gradient Gel Electrophoresis Profiles of 16S rRNA-Defined
      Populations Inhabiting a Hot Spring Microbial Mat Community. *Applied and
      Environmental Microbiology* 62:340-346.

Floodgate, G. D.
      1984 The Fate of Petrolum in Marine Ecosystems. In *Petroleum Microbiology* (R. M.
      Atlas, Ed.), pp. 61-98. McMillan Publishing Co., New York, NY.

Fries, E. and W. Puttman
>   2002 Analysis of the Antioxidant Butylated Hydroxytoluene (BHT) in Water by Means
>   of Solid Phase Extraction Combined with GC-MS. *Water Research* 36:2319-2327.

Frontera-Suau, R., F. D. Bost, T. J. McDonald, and P. J. Morris
>   2002 Aerobic Biodegradation of Hopanes and Other Biomarkers by Crude Oil-Degrading
>   Enrichment Cultures. *Environmental Science and Technology* 36:4585-4592.

Garrett, R. M., I. J. Pickering, C. E. Haith, and R. C. Prince
>   1998 Photooxidation of Crude Oils. *Environmental Science and Technology* 32:3719-
>   3723.

Gregory, D.
>   1999 Monitoring the Effect of Sacrificial Anodes on the Large Iron Artifacts on the Duart
>   Point Wreck, 1997. *International Journal of Nautical Archaeology* 28(2):164-173.

>   1995 Experiments into the Deterioration Characteristics of Materials on the Duart Point
>   Wreck Site: An Interim Report. *The International Journal of Nautical Archaeology*
>   24:61-65.

Haines, J. R., and M. Alexander
>   1974 Microbial Degradation of High Molecular Weight Alkanes. *Applied Microbiology*
>   28:1084-1085.

Hir, M. L., and C. Hily
>   2002 First Observations in a High Rocky-Shore Community After the *Erika* Oil Spill
>   (December 1999, Brittany France). *Marine Pollution Bulletin* 44:1243-1252.

Ho, K., Patton, J. S., Latimer., R. J. Pruell, M., Pelletier, R. McKinney, and S. Jayaraman
>   1999 The Chemistry and Toxicity of Sediment Affected by Oil from the *North Cape*
>   Spilled into Rhode Island Sound. *Marine Pollution Bulletin* 38:314-323.

Hughes, J. B.
>   1999 Cytological-Cytogentic Analyses of Winter Flounder Embryos Collected from the
>   Benthos at the Barge *North Cape* Oil Spill. *Marine Pollution Bulletin* 38:30-35.

Hunt, J. M.
>   1995 *Petroleum Geochemistry and Geology*. 2nd ed. W.H. Freeman and Company, New
>   York.

Inui, H., K. Itoh, M. Matsuo, and J. Miyamoto
>   1979 Studies on Degradation of 2,6-di-*tert*-butyl-4-methylphenol (BHT) in the
>   Environment. Part-II: Biodegradability of BHT with Activated Sludge. *Chemosphere*
>   6:383-91.

Irwin, R. J., M. VanMouwerik, L. Stevens, M. D. Seese, and W. Basham
      1997 National Park Service, Water Resources Division Environmental Contaminants
      Encyclopedia, Fuel Oil No. 6 Entry.

Johnson, D. L., W. N. Weins, J. D. Makinson, L. E. Murphy, L. E. Conlin, M. A. Russell, and P.
      J. Morris
      2002 In situ *Corrosion Studies on the Battleship USS* Arizona *Part I. Corrosion*.

Juhasz, A. L. and R. Naidu
      2000 Bioremediation of High Molecular Weight Polycyclic Aromatic Hydrocarbons: A
      Review of the Microbial Degradation of benzo[*a*]pyrene. *International Biodeterioration
      and Biodegradation* 45:57-88.

Jungclaus, G. A., V. Lopez-Avila and R. A. Hites
      1978 Organic Compounds in Industrial Waste Water: A Case Study of Their
      Environmental Impact. *Environmental Science and Technology* 12:88-96.

Kanaly, R. A. and S. Harayama
      2000 Biodegradation of High-Molecular-Weight Polycyclic Aromatic Hydrocarbons by
      Bacteria. *Journal of Bacteriology* 182:2059-2067.

Kvenvolden, K. A., F.D. Hostettler, J. B. Rapp, and P. R. Carlson
      1993 Hydrocarbons in Oil Residues on beaches of Islands of Prince William Sound,
      Alaska. *Marine Pollution Bulletin* 26:24-29.

Kvenvolden, K. A., F. D. Hostettler, P. R. Carlson, J. B. Rapp, C. N. Threlkeld. and A. Warden
      1995 Ubiquitous Tar Balls with a California-Source Signature on the Shorelines of Prince
      William Sound, Alaska. *Environmental Science and Technology* 29:2684-2694.

Kvenvolden, K .A., F. D. Hostettler, R. W. Rosenbauer, T. D. Lorensen, W. T. Castle and S.
      Sugarman
      2002 Hydrocarbons in Recent Sediment of the Monterey Bay National Marine Sanctuary.
      Marine Geology 181:101-113.

Lenihan, D. J.
      1990 *USS Arizona Memorial and Pearl Harbor National Historic Landmark*. 2 ed. Vol.
      No. 23. Submerged cultural resources study. Santa Fe, NM: Southwest Cultural
      Resources Center Professional Papers.

Lunel, T., A. Crosbie, L. Davies, and R. P. J. Swannell
      2000 The Potential for Dispersing Bunker C (IFO-380) Fuel Oils: Initial Results.
      Prepared by: National Environmental Technology Centre, Culham, Abingdon
      Oxfordshire, United Kingdom. 12 pp.

Mackenzie, A. S.
    1984 Applications of Biological Markers in Petroleum Geochemistry. In *Advances in Petroleum Geochemistry* (J. Brooks, and D. Weite, Eds.), Vol. 1, pp. 115-213. Academic Press, London.

McDonald, T. J. and M. C. Kennicutt
    1992 Fractionation of Crude Oils by HPLC and Quantitative Determination of Aliphatic and Aromatice Biological Markers by GC-MS with Selected Ion Monitoring. *LC-GC* 10:935-938.

McLeod, I. D.
    1995 *In Situ* Corrosion Studies on the Duart Point Wreck, 1994. *International Journal of Nautical Archaeology* 24(1):53-59.

Mills, M. A., T. J. McDonald, J. S. Bonner, M. A. Simon, and R. L. Autenrieth
    1999 Method for Quantifying the Fate of Petroleum in the Environment. *Chemosphere* 39:2563-2582.

Michael, J. and M. O. Hayes
    1999 Weathering Patterns of Oil Residues Eight Years After the *Exxon Valdez* Oil Spill. *Marine Pollution Bulletin* 38:855-863.

Mikami, N., H. Gomi, and J. Miyamoto
    1979 Studies on Degradation of 2,6-di-*tert*-butyl-4-methylphenol (BHT) in the Environment. Part-I: Degradation of ^{14}C-BHT in soil. *Chemosphere* 5:305-310.

Minas, W. and W. Gunkel
    1995 Oil Pollution in the North Sea- A Microbiological Point of View. *Helgolander Meeresunters* 49:14-158

Moldowan, J. M., J. Dahl, M. A. Mcaffrey, W. J. Smith and J. C. Fetzer
    1995 Application of Biological Marker Technology to Bioremediation of Refinery By-products. *Energy and Fuels* 9:155-162.

Mulkins-Phillips, G. J., and J. E. Stewart
    1974 Effect of Environmental Parameters on Bacterial Degradation of Bunker C Oil, Crude Oils, and Hydrocarbons. *Applied Microbiology* 28:915-922.

Munoz, D., M. Guiliano, P. Doumenq, F. Jacquot, P. Scherrer, and G. Mille
    1997 Long Term Evolution of Petroleum Biomarkers in Mangrove Soil (Guadeloupe). *Marine Pollution Bulletin* 34:868-874.

National Oceanic and Atmospheric Administration [NOAA]
    1994 NOAA/ Hazardous Materials Response and Assessment Division Fact sheet: No. 6 fuel oil (Bunker C) spills.

National Research Council [NRC]
    2003. Oil in the sea III: Inputs, Fates, and Effects.

Neilson, A. J.
    1994 Organic Chemicals in the Aquatic Environment: Distribution, Persistence, and Toxicity. CRC Press, Boca Raton, FL.

Nishigima, F. N., R. R. Weber, and M. C. Bicego
    2001 Aliphatic and Aromatic Hydrocarbons in Sediments of Santos and Cananeia, SP, Brazil. *Marine Pollution Bulletin* 42:1064-1072.

Norman, R. S., R. Frontera-Suau, and P. J. Morris
    2002 Variability in *Psuedomonas aeruginosa* lipopolysaccharide Expression During Crude Oil Degradation. *Applied and Environmental Microbiology* 10:5096-5103.
.
Pearl Harbor Natural Resource Trustees.
    1999 Restoration Plan and Environmental Assessment for the May 14, 1996 Chevron Pipeline Oil Spill into Waiau Stream and Pearl Harbor, Oahu, Hawaii. Prepared by: U.S. Department of Defense, U.S. Department of the Interior, National Oceanic and Atmospheric Administration, and State of Hawaii. 122 pp.

Perry, J. J.
    1977 Microbial Metabolism of Cyclic Hydrocarbons and Related Compounds. *CRC Critical Reviews in Microbiology* 5:387-412.

    1984 Microbial metabolism of cyclic alkanes. *In* "Petroleum Microbiology" (R. M. Atlas, Ed.), pp. 61-98. McMillan Publishing Co., New York, NY.

Peters, K. E., and J. M. Moldowan
    1993 *The Biomarker Guide: Interpreting Molecular Fossils in Petroleum.* Prentice-Hall Inc., Englewood Cliffs, NJ.

Pirnik, M. P.
    1977 Microbial Oxidation of Methyl Branched Alkanes. *Critical Reviews in Microbiology* 5:413-422.

Pollard, J. T., M. Whittaker, and G. C. Risden
    1999 The Fate of Heavy Oil Wastes in Soil Microcosms I: A Performance Assessment of Biotransformation Indices. *The Science of the Total Environment* 226:1-22.

Postgate, J. R.
    1979 *The Sulphate-Reducing Bacteria*. Cambridge University Press, Cambridge, Great Britain.

Prince, R. C., D. L. Elmendorf, J. R. Lute, C. S. Hsu, C. E. Halth, J. D. Senius, G. J. Dechert, G. S. Douglas, and E. L. Butler
    1994 17α(H),21β(H)-Hopane as a Conserved Internal Marker for Estimating the Biodegradation of Crude Oil. *Environmental Science and Technology* 28:142-145.

Prince, R. C., R. T. Stibrany, J. Hardestine, G. S. Douglas, and E. H. Owens
    2002 Aqueous Vapor Extraction: A Previously Unrecognized Weathering Process Affecting Oil Spills in Vigorously Aerated Water. *Environmental Science and Technology* 36:2822-2825.

Rabus, R., H. Wilkes, A. Behrends, A. Armstroff, T. Fischer, A. J. Pierik, and F. Widdel 2001 Anaerobic Initial Reaction of *n*-alkanes in a Denitrifying Bacterium: Evidence for (1-methylpentyl) Succinate as Initial Product and for Involvement of an Organic Radical in *n*-hexane Metabolism. *Journal of Bacteriology* 183:1707-1715.

Reed, W. E.
    1977 Molecular Compositions of Weathered Petroleum and Comparison with its Possible Source. *Geochimica et Cosmochimica Acta* 41:237-247.

Richmond, S. A., J. E. Lindstrom, and J. F. Braddock
    2001 Effects of Chitin on Microbial Emulsification, Mineralization Potential, and Toxicity of Bunker C Fuel Oil. *Marine Pollution Bulletin* 42:773-779.

Salanitro, J. P., P. B Dorn, M. H. Huesemann, K. O. Moore, I. A. Rhodes, L. M. R. Jackson, T. E. Vipond, M. M. Western, and H. L. Wisniewski
    1997 Crude Oil Hydrocarbon Bioremediation and Soil Ecotoxicity Assessment. *Environmental Science and Technology* 31:1769-1776.

Samanta, S. K., O. V. Singh, and R. K. Jain
    2002 Polycyclic Aromatic Hydrocarbons: Environmental Pollution and Bioremediation. *Trends in Biotechnology* 20:243-248.

Schaeffer, T. L., S. G. Cantwell, J. L. Brown, D. S. Watt, and R. R. Fall
    1979 Microbial Growth on Hydrocarbons: Terminal Branching Inhibits Biodegradation. *Applied and Environmental Microbiology* 38:742-746.

Sierfert W. K. and J. K. Moldowan
    1979 The Effect of Biodegradation on Steranes and Terpanes in Crude Oil. *Geochimica et Cosmochimica Acta* 43:111-126.

So, C. M., and L. Y.Young
    1999 Isolation and Characterization of a Sulfate-Reducing Bacterium that Anaerobically Degrades Alkanes. *Applied and Environmental Microbiology* 65:2969-2976.

Spormann, A. M., and F. Widdel
       2000 Metabolism of Alkylbenzenes, Alkanes, and Other Hydrocarbons in Anaerobic
       Bacteria. *Biodegradation* 11:85-105.

Stirling, L. A., R. J. Watkinson, and I. J. Higgins
       1977 Microbial Metabolism of Alicyclic Hydrocarbons: Isolation and Properties of a
       Cyclohexane Degrading Bacterium. *Journal of General Microbiology* 99:119-125.
.
Strand, J. A., V. I. Cullinan, E. A. Crecelium, T. J. Fortman, R. J. Citterman, and M. L.
       Fleischmann
       1992 Fate of Bunker C Fuel Oil in Washington Coastal Habitats Following the December
       1988 *NESTUCCA* Oil Spill. *Northwest Science* 66:1-14.

Trudgill, P. W.
       1978 Microbial Degradation of Alicyclic Hydrocarbons. *In Developments in
       Biodegradation of Hydrocarbons* (J. R. Watkinson, Ed.), pp. 47-84. Marcel Dekker, Inc.,
       New York.

U.S. Navy
       1998 Fact Sheet No. 2: Pearl Harbor Sediment Remedial Investigation/Feasibility Study.

Vandermeulen, J. H., and J. G. Singh
       1994 *Arrow* Oil Spill, 1970-90: Persistence of 20-yr Weathered Bunker C Fuel Oil.
       Canadian Journal of Fisheries Aquatic Science 51:845-855.

Volkman, J. K., D.G. Holdsworth, G. P. Neill and H. J. Bavor, Jr.
       1992 Identitfication of Natural, Anthropogenic and Petroleum Hydrocarbons in Aquatic
       Sediments. *The Science of the Total Environment* 112:203-219.

Walker, J. D., L. Petrakis, and R. R. Colwell
       1976 Comparison of the Biodegradability of Crude and Fuel Oils. *Canadian Journal of
       Microbiology* 22:598-602.

Wang, Z., M. Fingas, S. Blenkinsopp, G. Sergy, M. Landriault, L. Sigouin, J. Foght, K. Semple,
       and D. W. S. Westlake
       1998a Comparison of Oil Compositional Changes Due to Biodegradation and Physical
       Weathering in Different Oils. *Journal of Chromatography* 809:89-107.

Wang, Z., M. Fingas, S. Blenkinsopp, G. Sergy, M. Landriault, L. Sigouin, and P. Lambert.
       1998b. Study of the 25-year-old *Nipisi* Oil Spill: Persistence of Oil Residues and
       Comparisons Between Surface and Subsurface Sediments. *Environmental Science and
       Technology* 32:2222-2232.

Wang, Z., M. Fingas, E. H. Owens, L. Sigouin, and C. E. Brown
    2001 Long-Term Fate and Persistence of Spilled *Metula* Oil in a Marine Salt Marsh
    Environment: Degradation of Petroleum Biomarkers. *Journal of Chromatography*
    926:275-290.

Wang, Z., M. Fingas, and S. P. Page
    1999 Oil Spill Identification. *Journal of Chromatography A.* 843:369-411.

Wang, Z., M. Fingas, and G. Sergy
    1994 Study of 22-Year Old *Arrow* Oil Samples Using Biomarker Compounds by
    GC/MS. *Environmental Science and Technology* 28:1733-1746.

Wang, Z., M. Fingas, and G. Sergy
    1995 Chemical Characterization of Crude Oil Residues from an Arctic Beach by GC/MS
    and GC/FID. *Environmental Science and Technology* 29:2622-2631.

Wang, Z., M. Fingas, and L. Sigouin
    2001 Characterization and Identification of a "Mystery" Oil Ppill from Quebec (1999).
    Journal of Chromatography A 909:155-169.

Wheeler, A. J.
    2002 Environmental Controls on Shipwreck Preservation: the Irish Context. *Journal of
    Archaeological Science* 29:1149-1159.

Whittaker, M., and J. T. Pollard
    1997 A Performance Assessment of Source Correlation and Weathering Indices for
    Petroleum Hydrocarbons in the Environment. *Environmental Toxicology and Chemistry*
    16:1149-1158.

Widdel, F., and R. Rabus
    2001 Anaerobic Biodegradation of Saturated and Aromatic Hydrocarbons. *Current
    Opinion in Biotechnology* 12:259-276.

Witt, G.
    1995 Polycyclic Aromatic Hydrocarbons in Water and Sediment of the Baltic Sea.
    Marine Pollution Bulletin 31:237-248.

Zakaria, M. P., T. Okuda, and H. Takada
    2001 Polycyclic Aromatic Hydrocarbons (PAHs) and Hopanes in Stranded Tar-balls on
    the Coasts of Peninsular Malaysia: Applications of Biomarkers for Identifying Sources of
    Oil Pollution. *Marine Pollution Bulletin* 42:1327-1366.

CHAPTER 9

Long-Term Monitoring Program: Structure, Oil, Artifacts and Environment

Matthew A. Russell and Larry E. Murphy

INTRODUCTION

The National Park Service's (NPS) Submerged Resources Center (SRC) developed monitoring protocols and began systematically monitoring changes to USS *Arizona*'s accessible external areas in 1986 (Henderson 1989) as part of the USS *Arizona* Documentation Project conducted from 1983–1989 (Lenihan 1989). This was among the first such efforts on sunken metal hulls, along with the Western Australian Maritime Museum's investigation of SS *Xantho* which began about the same time (McCarthy 2000). The 1986 *Arizona* project established 61 photo-monitoring stations affixed to the hull to mount a camera to document the growth and change of concretion and biological communities covering *Arizona*'s external hull. In addition, 55 stations were marked with short PVC pipes attached to weights to monitor changes in sediment accumulation on horizontal surfaces across the hull. Each pipe marked a location where depth of sediment was taken for each observation period. This early monitoring effort was conducted sporadically by the USS *Arizona* dive team from 1986 until 1990. The program ceased when personnel changes reduced the dive team, and the park was no longer able to collect

the monitoring information. The earlier monitoring program has been superseded by the present program.

While the earlier studies attempted to monitor visible changes on the hull and deck, the present study, The USS *Arizona* Preservation Project, is directed at characterizing processes affecting the hull and determining their rate. This data contributes to a predictive model whose attributes and variables can be altered to reflect changing conditions and incorporation of new data as they are developed. In addition to the structural changes and oil release measurements, artifact and environmental variables are included and measured as part of the monitoring plan. Most aspects of the current monitoring project are quantitative; however, some, like comparative biological-based environmental observations, are qualitative. This chapter presents the monitoring program and its rationale.

The current long-term monitoring program was developed primarily to directly measure changes in *Arizona*'s structural integrity and quantify the rate of change to revise and provide controls for the predictive Finite Element Model (FEM, see Chapter 6). The present monitoring program takes several different forms, but each is designed to allow researchers and managers to quantify physical changes to *Arizona*'s hull fabric and project a long-term deterioration curve.

The present research and monitoring program began in 1998 when an oil catchment device was fabricated to measure oil release. Previously, only the leak points for oil were recorded. Additional monitoring techniques have been developed and applied during the USS *Arizona* Preservation Project based on the research domains and investigations conducted during the project. The NPS, through a cooperative effort between the USS *Arizona* Memorial and the SRC and their collaborators, has committed to continuing the monitoring program into the future to provide the most accurate depiction of *Arizona*'s hull status. Continuation of the program and inclusion of additional monitoring methods will provide an important cumulative data base useful to determining threshold levels of hull structural changes and to revise the predictive model and evaluate its accuracy. To be most effective and to facilitate comparative analyses, these cumulative measurements are being incorporated into a Geographical Information System (GIS). This chapter reports on the methodology and results through 2006 for primary monitoring methods used for long-term structural and environmental impact evaluation: Global Positioning System (GPS) hull movement monitoring, galley-specific crack monitoring, oil-release rate monitoring, environmental monitoring of water quality and sediment contamination attributable

to *Arizona,* general environmental observations and the GIS program developed to incorporate cumulative data.

STRUCTURAL INVESTIGATIONS AND MONITORING

Monitoring for significant structural alterations over time depends on an understanding of the hull structure and the sediments that support it. There are two primary concerns addressed by structural monitoring: collapse of the hull, which alters its nature as a National Historic Landmark (NHL), naval memorial and war grave; and increasing concern for potential catastrophic oil release of the approximately half-million gallons of Bunker C fuel oil remaining aboard in the intact aft portion of the hull. Because the vessel's superstructure was completely removed during salvage operations (see Chapter 3), only the hull will be addressed. Removal of the superstructure has the effect of appreciably reducing the weight supported by hull structural elements, which extends their predicted time to structural alteration and collapse.

In this discussion, hull structure change over time is subsumed beneath the issue of oil release. Predictive modeling of hull changes in general is addressed in depth in Chapter 6. Knowledge of *Arizona*'s hull is also useful for understanding the difficulty and implications of the often suggested "Why don't you just pump the oil out of the hull?" question often posed to park employees and others.

Characterization of *Arizona*'s hull structure began with collection, digitization, indexing and collating more than 250 original hull construction blueprints and those of the 1929–1931 refit. The next steps were to describe the hull's constituent metal and establish a corrosion rate that incorporated both the corrosion that has taken place to date and the present corrosion rate for incorporation into the FEM. Corrosion characterization and measurements are presented in Chapter 5. A necessary component to full characterization of the hull in its present condition is a model of the blast damage from the forward magazine explosion and other bomb damage to be incorporated into the FEM. Funding has been insufficient to accommodate the development of the blast impact for incorporation into the FEM to date.

Focusing on oil release potential requires an understanding of where in the vessel oil was contained. Historical records indicate that *Arizona* was nearly fueled to emergency capacity immediately before the December 7, 1941 attack—emergency capacity was approximately 6,100

tons of fuel (see Chapter 3). Assuming that 40% of the stern hull remains intact, one can derive
a general estimate that there could be as much as 600,000 gallons remaining aboard, less that lost
during and since the attack (Figure 9.1).

There is very limited access to interior spaces, as determined through extensive
exploration of the stern with a VideoRay Remote Operated Vehicle (ROV) during fieldwork
conducted as part of this project. At the time of the attack, most of the hatches were secured,
particularly in the lower deck areas, which normally maintained Material Condition "X-Ray"
with doors and fittings closed. Some areas, shaft alleys, engine rooms, and fire rooms, were in
Condition "Zed," the highest level of security, where doors were secured and locked to maximize
watertight conditions in battle; some were in Condition Y, intermediate between the two. Upon
the sounding of "General Quarters" at the outset of the attack, *Arizona*'s crew began moving all
areas to Condition Zed. This level was only partially achieved due to the suddenness of the
attack and *Arizona*'s early demise (see Chapter 3). The historical assessment of *Arizona*'s
material condition has been found to be accurate for the accessible areas, particularly the third
deck, which has very limited access. Closed and secured doors and hatches contribute to the
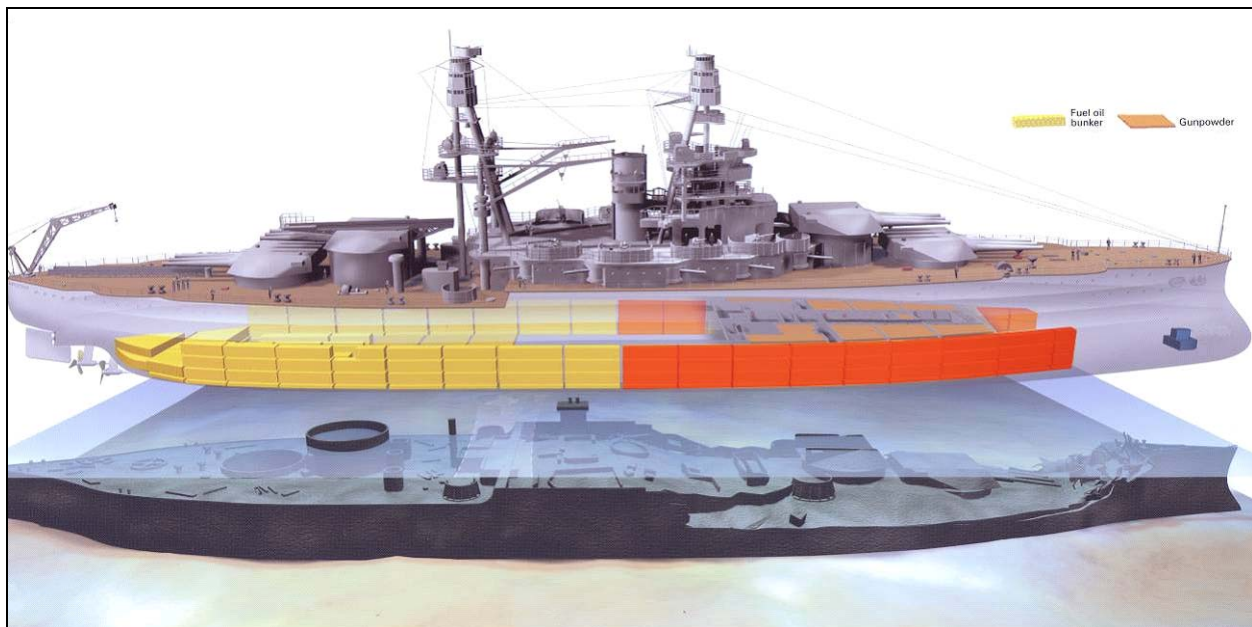hull's integrity.

Figure 9.1. Graphic of oil bunker locations relative to hull damage. The yellow bunkers in the aft section (left) are presumed intact. This graphic depicts 50% of the hull remaining, rather than the more accurate 40% (Graphic by National Geographic Society).

Currently, only a small portion of the third deck is accessible, and a smaller yet portion of the first platform, which is the deck level above the topmost oil bunker. There is no direct access to any oil bunker in the hull. Access would have to be gained by cutting through many structural elements. At the amidships section, most of the bunkers are near the hull sides, again not directly accessible because of armor and the torpedo blister. The hull is buried to the level above its normal waterline (Figure 9.2). There is no present estimate of the amount of sediment that may be within the hull at the second platform level and below. Direct ROV observations in the second and third deck levels, which are accessible and have been explored, reveal they contain significant sediment, which decreases the deeper into the hull one goes. In undamaged areas or areas with few penetrations, there may be little sediment due to lack of access to suspended sediment transport and few open doorways. Any access to oil bunkers would require excavation, certainly on the exterior, cutting bulkheads, deck and hull structures, including splinter deck and side armor plate, which would compromise the integrity of the hull and weaken the whole structure, even with significant shoring of passages.

Another complicating factor in *Arizona* oil removal, unlike the several successful oil removals (such as USS *Mississinewa,* a World War II oiler sunk in Ulithi Harbor, Yap State, Federated States of Micronesia) is that large oil bunkers are not connected by a simple piping system. In the case of *Mississinewa*, which was not armored, the hull was inverted allowing easy
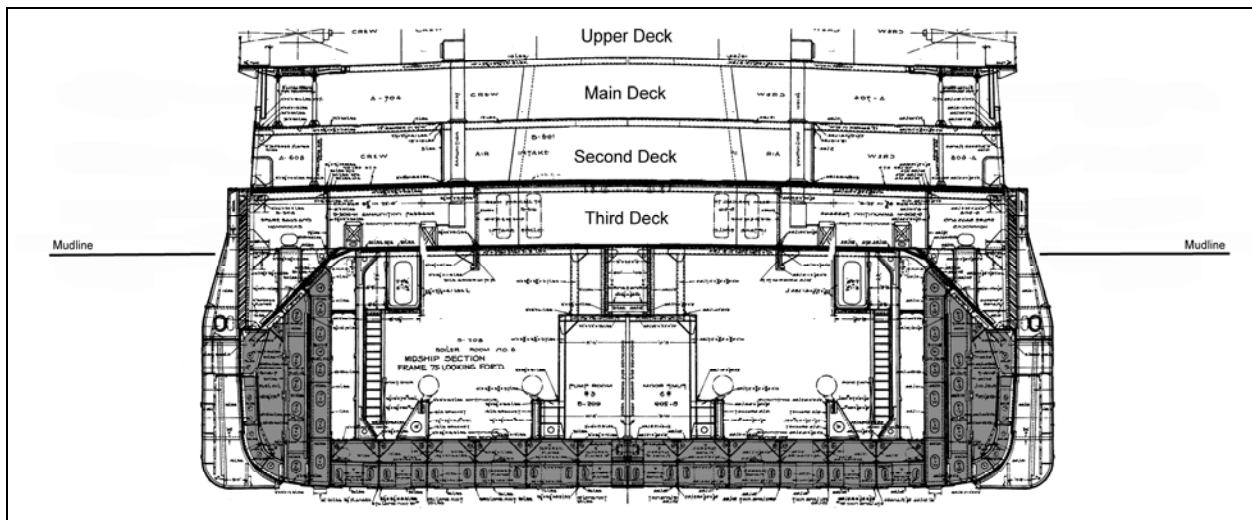

Figure 9. 2. *Arizona* **hull cross-section at frame 75. Dark areas are oil bunkers and the line indicates the current seabed level relative to the hull (Graphic by NPS-SRC).**

access to the single hull bottom greatly facilitating oil removal through a "hot tap process." In *Arizona*, bunkers are of varying size and are found throughout the ship: on the first platform, there are 30 bunkers; on the second platform, 34 bunkers; in the hold, 28 bunkers; and in the double bottom, 36 bunkers. The rationale for the large number of separate oil bunkers is that it is part of the defensive strategy of battleships. With more separated bunkers, the less likely a vessel could be put out of commission by sustaining damage to its fuel supply. Half or so of these bunkers remain and must be assumed to still contain oil. Approximately 50 to 60% of the oil bunkers in the forward hull were destroyed by the explosion that sank the ship. Each oil bunker is independently piped, suggesting that any oil removal plan could likely require accessing each bunker individually.

STRUCTURAL MONITORING

As internal and external structures of *Arizona*'s hull corrode and weaken, various parts of the vessel will differentially-experience shifting, settling and ultimately, collapse. All indications are that significant structural change is not imminent, and this is supported by the Finite Element Analysis (FEA, see Chapter 6). Since NPS presence on *Arizona* began in 1982, qualitative assessment by researchers observed that upper deck areas in and around the ship's galley (located amidships on the upper deck, just forward of the Memorial) show signs of change—widening cracks and some deck sagging and collapse were first observed by SRC researchers in 2000. This observation and the need to test and refine the FEM led to development of quantitative hull structural monitoring.

External GPS Monitoring

In order to determine whether internal collapse occurs in the hull, SRC researchers devised a monitoring protocol to quantitatively measure long-term stability across *Arizona*'s hull. The tool selected to monitor hull stability was high-resolution, survey grade, dual-frequency Global Positioning System (GPS). The SRC has been incorporating GPS and GIS into hydrographic survey since 1993, and adapted this nascent technology to underwater archeology (Murphy and Smith 1995, 1996; Shope et al. 1995). In recent years, this technology has reached

the point that extremely accurate, reliable instruments are available to the civilian survey market. Dual-frequency GPS receivers make it possible to collect positional data accurate to within a few millimeter Circle-of-Error Probable (CEP) at a 95% confidence level in three dimensions. This highly accurate GPS technology has been used to monitor movement of everything from historic buildings to mountain tops, and it is the most appropriate technology available for use on *Arizona*. At the same time, traditional "low-tech" methods for monitoring structural movement, such as simple, plastic crack monitors, were also used in specific locations.

The primary method used to monitor overall physical changes to USS *Arizona*'s hull is a network of discrete, real-world positions physically affixed to the ship whose three-dimensional coordinates are derived using very high-resolution GPS instruments. The GPS points were initially established on the vessel in June 2001. Eight datum points were selected to provide a network of monitoring points distributed longitudinally and transversly on the upper portions of *Arizona*'s hull on exposed horizontal structures (Figure 9.3). These points, when measured to high accuracy, provide information on internal hull structure changes. By plotting changes over time, both the quantity and direction (vector) of change in hull structure will be observable. Originally, the points were established by shooting hardened, pointed threaded bolts into the deck steel with a velocity tool adapted for underwater use. To limit corrosion of the stainless steel threaded bolts, a cone of pH-neutral epoxy was placed around each bolt with only the top of the bolt exposed (Figure 9.4). This technique was wholly unsuccessful; by 2003 the bolts had all but completely disappeared. In 2003, PVC pipe and fittings were used to replace the stainless steel bolts (Figures 9.5 and 9.6). The PVC was secured to the deck with epoxy at each of the eight monitoring points across *Arizona*'s exposed decks.
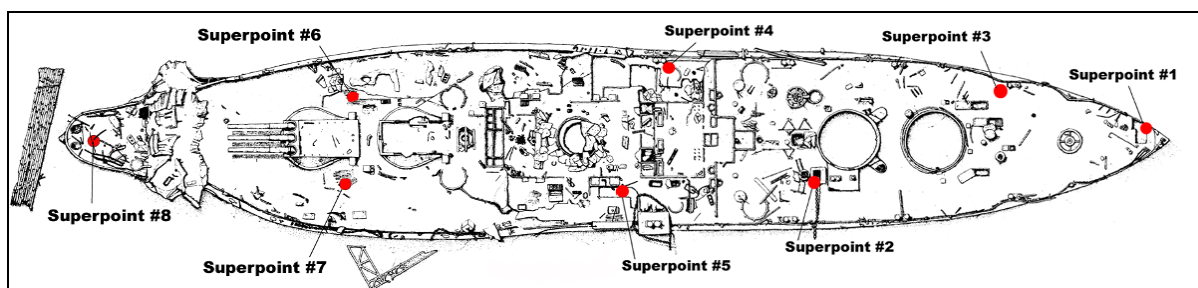
Figure 9.3. GPS monitoring points ("superpoints") on *Arizona* main and upper decks (Drawing by NPS-SRC).

Figure 9.4. Surveying GPS monitoring points on *Arizona*, here using original velocity tool-set, stainless steel bolt surrounded by epoxy (NPS Photo by Brett Seymour).

Figure 9.5. Comparison of the original, left, and current GPS monitoring points. Note: 2001 epoxy covered by pioneering organisms (NPS Photo by Brett Seymour).
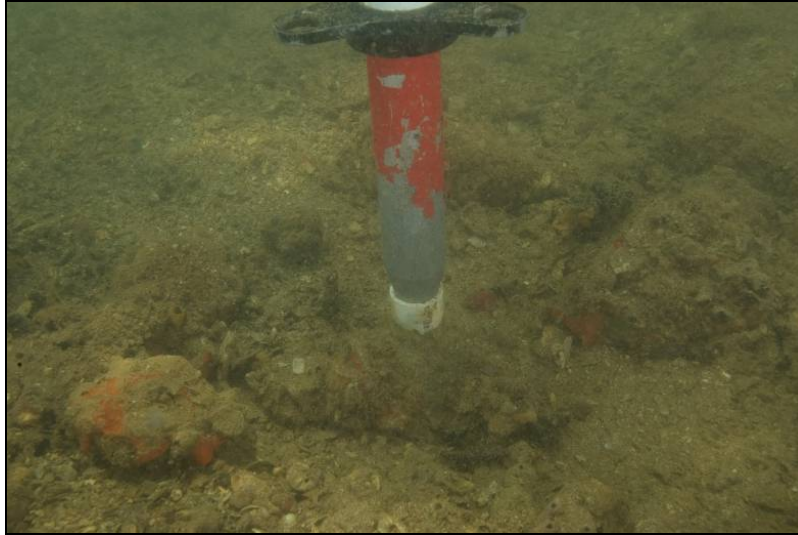
Figure 9.6. Surveying GPS monitoring points on *Arizona*, here using replacement PVC epoxyed to metal. This accommodates the point and facilitates set up. Note epoxy has been covered with pioneering organisms (NPS Photo by Brett Seymour).

Because GPS signals do not penetrate water, the GPS antenna had to be secured above the surface precisely above the survey datum point. SRC had earlier designed an underwater tripod, really a quadrapod, to accomplish this task. The tripod has three hollow aluminum legs that fill with water for stability when submerged and a fourth central leg filled with lead shot that is placed precisely on the point to be located. The underwater tripod has easily adjustable legs so that the center pole can be precisely positioned vertically above the datum point using a set of bull's eye levels attached (Figure 9.7). Divers add 5-ft. aluminum extension poles until they extend above the surface where a GPS antenna can be attached. Just as in terrestrial survey, the GPS receiver is programmed to account for the offset or Height of Instrument (HI) of the tripod and extension poles, which is exact because both the tripod's center leg and extension length have been manufactured to close tolerances and measured.

At each datum point, in-water NPS surveyors leveled the underwater tripod over the point using bull's eye levels affixed to the center pole (Figures 9.7–9.9). Once leveled, the GPS antenna is attached with a quick release to take the position reading.   Using advanced survey data acquisition and post-processing techniques and software, data for each point were collected with sub-centimeter accuracy in three dimensions, or about the area of a pencil eraser. The structural monitoring points (nicknamed "superpoints") were scheduled to be re-surveyed every two years to determine if, and in what direction, the ship is moving, shifting, or settling.
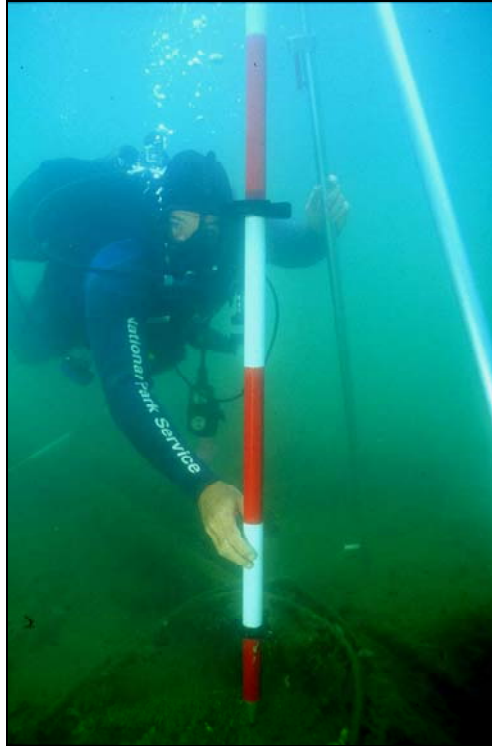
Figure 9.7. Surveying GPS monitoring points on *Arizona*. Black object above diver's' mask on the survey pole is a set of bull's eye levels used to level the quadrapod (NPS Photo by Brett Seymour).
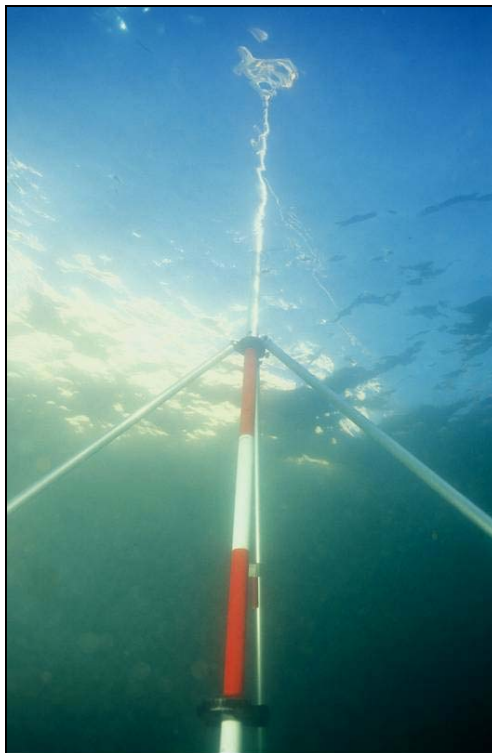

Figure 9.8. Surveying GPS monitoring points on *Arizona* using purpose-built quadrapod to support high-resolution GPS antenna above datum point (NPS Photo by Brett Seymour).

Figure 9.9. GPS surveying "Superpoint #2," forward of barbette no. 3 (NPS Photo by Brett Seymour).

During the 2001 field season when the initial occupation of the monitoring points took place, the NPS partnered with the U.S. Army's 29th Engineer Battalion Survey Platoon, who provided state-of-the-art, Trimble Navigation, Ltd. (Sunnyvale, CA) 4700 SSE survey grade, dual-frequency GPS receivers, and a survey team. At that time, NPS owned no survey grade GPS receivers. The occupation time of each point for the 4700 receivers is two minutes. Several points were positioned several times to verify accuracy and reproducibility. Results are presented in Table 9.1.

In the intervening two-year period, NPS acquired the necessary carrier-phase survey grade instruments to complete the survey in-house. Tim Smith, NPS GPS coordinator from the NPS Resources Inventory and Monitoring Division (RIMD) and Mark Duffy, GIS specialist from Assateague Island National Seashore, provided instruments and expertise to conduct the high-resolution underwater monitoring point reoccupation in 2003.

The 2003 reoccupation used a Trimble R8 Global Navigation Satellite System (GNSS) using 5700 Total Station Receivers. The Trimble R8 GPS system consists of a wireless base station, which is set up daily on an established survey monument near the park visitor center, and a field receiver, which mounted on the underwater tripod on site. The base station monitors its

Name	Description	Northing	Easting	Elevation (m)	Hori. Diff 2001-2003 (m)	Vert. Diff 2001-2003 (m)
USARSP001_01	June 2001 point	2362935.105	608919.734	-2.297		
USARSP001A_03	Nov. 2003 re-survey	2362935.115	608919.765	-2.254	0.032	0.043
USARSP001_03	New Nov. 2003 point	2362934.233	608918.321	-2.268		
USARSP001_06	June 2006 re-survey	2362934.259	608918.319	-2.271	0.027	0.003
USARSP002_01	June 2001 point	2362896.933	608879.359	-1.361		
USARSP002A_03	Nov. 2003 re-survey	2362896.939	608879.371	-1.385	0.014	0.024
USARSP002_03	New Nov. 2003 point	2362904.018	608897.789	-3.094		
USARSP002_06	June 2006 re-survey	2362904.02	608897.809	-3.051	0.021	-0.043
USARSP003_01	June 2001 point	2362925.038	608894.502	-2.36		
USARSP003A_03	Nov. 2003 re-survey	2362925.055	608894.522	-2.316	0.027	0.043
USARSP003_03	New Nov. 2003 point	2362926.047	608895.48	-2.208		
USARSP003_06	New June 2006 point	2362920.822	608890.76	-2.378		
USARSP004_01	June 2001 point	2362898.324	608848.58	-0.431		
USARSP004A_03	Nov. 2003 re-survey	2362898.341	608848.592	-0.433	0.021	0.002
USARSP004_03	New Nov. 2003 point	2362898.455	608848.344	-0.406		
USARSP004_06	June 2006 re-survey	2362898.452	608848.333	-0.372	0.012	-0.034
USARSP005_01	June 2001 point	2362878.249	608854.245	-2.077		
USARSP005A_03	Nov. 2003 re-survey	2362878.287	608854.237	-2.081	0.039	0.004
USARSP005_03	New Nov. 2003 point	2362878.116	608854.349	-2.015		
USARSP005_06	June 2006 re-survey	2362878.105	608854.356	-2.051	0.013	0.036
USARSP006_01	June 2001 point	2362864.903	608808.081	-6.52		
USARSP006A_03	Nov. 2003 re-survey	2362864.996	608808.115	-6.264	0.1	0.256
USARSP006_03	New Nov. 2003 point	2362865.352	608807.89	-6.46		
USARSP006_06	June 2006 re-survey	2362865.402	608807.799	-6.466	0.103	0.006
USARSP007_01	June 2001 point	2362850.831	608817.579	-7.842		
USARSP007A_03	Nov. 2003 re-survey	2362850.707	608817.458	-7.64	0.173	0.202
USARSP007_03	New Nov. 2003 point	2362850.872	608816.92	-7.671		
USARSP007_06	June 2006 re-survey	2362850.904	608816.948	-7.665	0.042	-0.006
USARSP008_01	June 2001 point	2362833.694	608779.754	-1.551		
USARSP008_03	New Nov. 2003 point	2362836.838	608780.678	-1.529		
USARSP008_06	June 2006 re-survey	2362836.839	608780.682	-1.529	0.004	0.000

Table 9.1. GPS survey data for USS *Arizona*.

reported monument position from various satellites in the GPS constellation—when satellites gave inaccurate locations for the base station, the base station generates a corrected position for those satellites and broadcasts the corrected differential signal to the field receiver via a radio operating at 450 mHz, thus eliminating the need for post-processing and greatly accelerating data acquisition. Shorter occupation time, in the case of dynamic environments like underwater precision surveying, reduces CEP. The 5700s only require a five-second occupation. Several readings can be taken in a short time, which minimizes any tripod movement from current or waves.

Collection software used was Trimble's TerraSync™. This software was selected because it is the first mobile GIS software to integrate GIS data collection capabilities with survey-grade GPS mapping. This software expedited the field data collection and increased overall accuracy. The dive team used the software to carry USS *Arizona* GIS Project location and map data with them from point to point using a Trimble Recon, an ultra-rugged, waterproof handheld computer or Personal Data Assistant (PDA) designed for field data collection. This expedited on site point location and reduced field time for the reoccupation.

During the 2003 reoccupation, the first problem encountered was that most of the epoxy encased stainless steel bolts had corroded away. The epoxy did not prevent electrolytic corrosion of the stainless steel embedded in the mild steel of the deck plates. Each point was reoccupied as best as possible, but new points not subject to corrosion had to be established. PVC was used, and each new point was established adjacent to the original point (see Figure 9.5). The diameter of the PVC datum point was selected to accommodate the point of the underwater tripod to both provide a solid support and facilitate deployment (see Figure 9.6). Each of these new points was then surveyed and became the permanent monitoring points or "superpoints" (see Table 9.1).

The second reoccupation of the GPS monitoring points occurred in June 2006. Tim Smith from RIMD again collected survey data, this time using dual-frequency GPS receivers supplied by Gateway National Recreation Area. The 2003 methodology was again used in 2006. One of the PVC points established in 2003 was dislodged during the survey because the wood to which it had been affixed had deteriorated, and it had to be re-established, this time on deck steel. This occupation of all eight superpoints was successful (see Table 9.1).

Although accuracy of each point was mathematically calculated to about 0.5 cm (CEP), it is necessary to apply a more conservative threshold of change to evaluation of future monitoring re-occupations as directly reflective of hull structural changes. We have determined the significant structural change threshold to be 10 cm because of environmental conditions and differences in equipment and stadia variations. Instrument error, set-up error, or most likely, nearly imperceptible antenna movement caused by water movement, which is generally averaged out during the longer occupation times than used on land surveys, can create cumulative errors of perhaps 5 cm or more. Consequently, we cannot reliably attribute any observed change that is less than 10 cm to vessel movement; however, corroborative evidence would be sought for any level of change observed. Because the GPS points exist as a network of positions, aggregate changes in the positions of more than one point, even if less than 10 cm, could potentially indicate net movement of hull structure. Horizontal and vertical differences recorded between 2003 and 2006 are consistently below the 5 cm circle of error (see Table 9.1). From this dataset, it can be concluded that no measurable movement occurred during the 2½ year period.

For this structural monitoring program to be valid there must be an important assumption made: that the sediments beneath *Arizona*'s hull are fully compressed and stable so that changes measured in survey point positions are the result of changes to the hull interior and not the result of support sediments beneath the hull compressing. To provide a control for geological conditions, an intensive investigation of the sediments around the hull was conducted in partnership with the U.S. Geological Survey. The conclusions of this investigation are that the sediments beneath USS *Arizona* are nearly fully compressed and stable (see Chapter 10).

External Crack Monitoring

Researchers in the 1980s observed the deck sagging forward of the galley area while mapping the hull. At the start of the USS *Arizona* Preservation Project, this midships-area was sagging and beginning to collapse. It represents the aft-most damage from the forward magazine detonation, and does not contribute to the battleship's overall structural integrity, especially oil-containing spaces. These upper deck areas were expected to be the first to show signs of weakening because they are most affected by the blast.

The galley-area on the second deck and those decks below have been damaged by the enormous explosion that sank the vessel, and they constitute the aft edge of the blast crater (Figures 9.10–9.12). The forward magazine blast force undercut the lower hull structure and the decks forward sufficiently for turret nos. 1 and 2 to have dropped more than 20 ft. The deck forward of the stack slopes down into the lower hull. The main deck and portions of the upper deck now are nearly even with the top of the 13-in. armor belt on the starboard side, and lower than it on the port side. Other deck areas were blown upward, and hull sides above the armor belt were blown outward nearly horizontal with the hull. The shell plate blown outward above the armor belt was removed during salvage of the superstructure in the 1940s. An indication of the extent and location of damage in this area can be derived from salvage reports (see Chapter 3). These salvage reports indicate divers were able to move forward within the hull during damage assessment dives to frame 76 on the main and second decks and not forward of frame 78 below the third deck. However, on the third deck in ammunition passageways A-504-M and A-505-M, access was possible as far forward as frame 66 (Paine 1943:5). This midships-area is the most damaged of the aft portion of the vessel, and it is here that most oil leaking occurs (see below). In addition to GPS, from 2001 to 2006 structural changes in the upper deck crew's galley (frames 80–88) were monitored using a series of plastic crack monitors normally used to measure crack movement in historic buildings (Figure 9.13). In June 2001, six plastic monitors were affixed over cracks in the upper deck galley where *Arizona*'s deck collapse had been qualitatively observed. These crack monitors were checked periodically to see if the cracks widened or shifted. After several years of monitoring, most of the gauges showed little movement, although at least one (#4) had fallen into an expanding hole on the starboard side of the galley floor as part of a limited upper deck collapse. The research team decided that the limited data they provided did not justify replacing the gauges as they broke or became dislodged, which happened frequently. Active monitoring of crack gauges ended in 2006, but they will be periodically checked as part of the ongoing monitoring project.

Internal Monitoring

Internal structural monitoring of USS *Arizona* has been a qualitative process primarily using the VideoRay ROV to visually examine and photographically document interior areas and
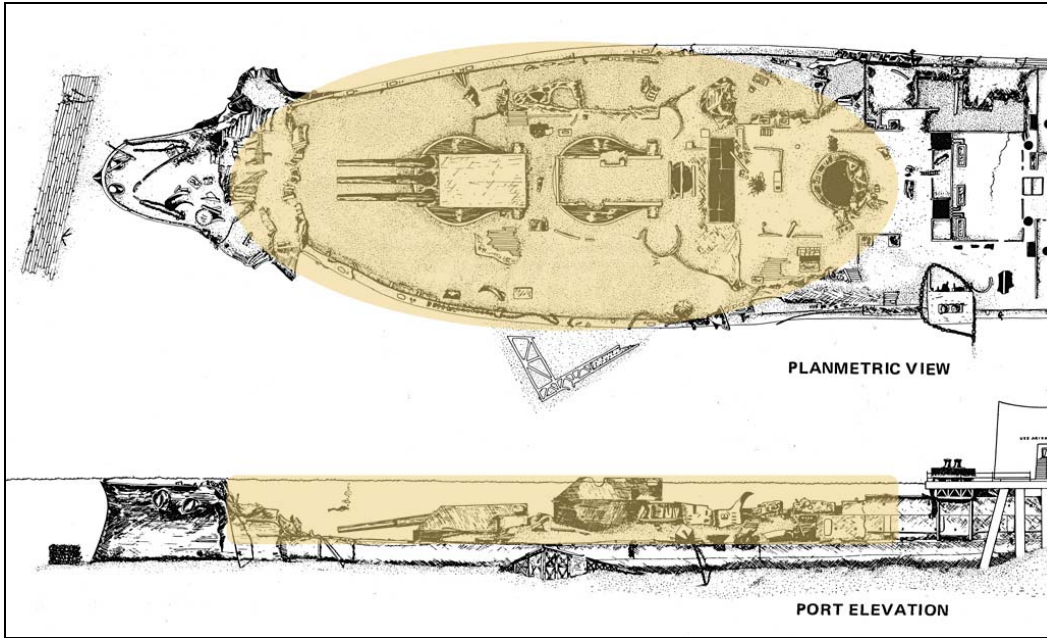
Figure 9.10. *Arizona* **bow showing blast crater (highlighted) and weakened upper deck area from frame 10 to 78, or about 270 ft. of hull (Drawing by NPS-SRC).**

Figure 9.11. Plan view of USS *Arizona* with upper deck galley-area highlighted (Drawing by NPS-SRC).

Figure 9.12. Plan view of *Arizona* galley area showing cracks and collapsed areas. ***Arizona*'s bow is to the bottom of the drawing, port side to the right. Crack monitors are identified by numbers (Drawing by NPS-SRC).**

Figure 9.13. Crack monitor in *Arizona* galley-area (NPS Photo by Brett Seymour).

note observable changes over time. Interior investigation took place from 2001–2005 in all accessible areas for measuring and monitoring interior envi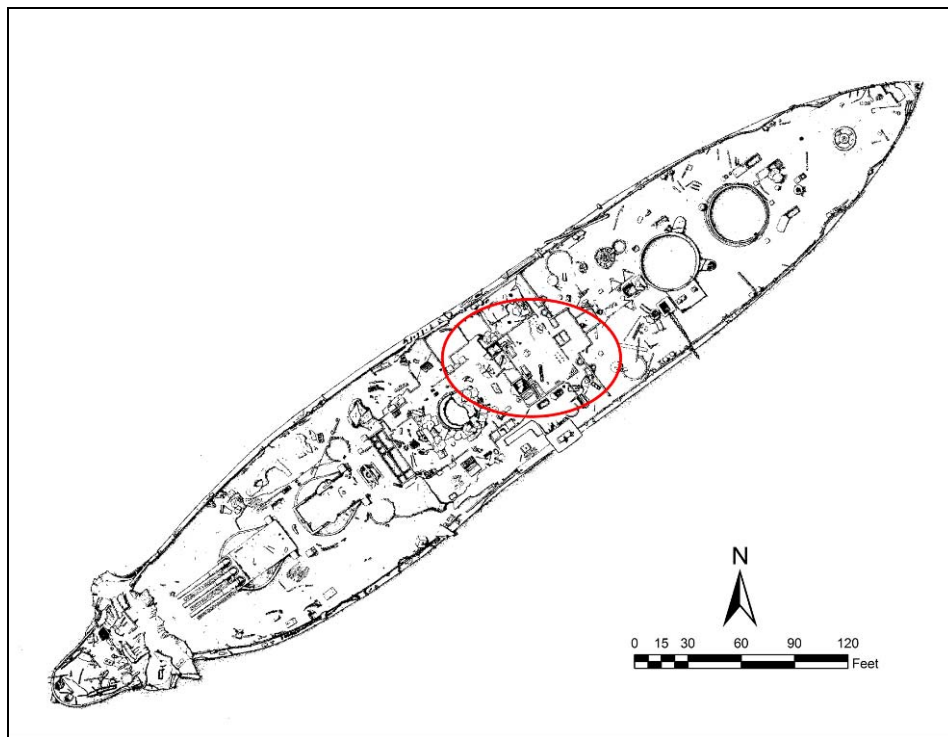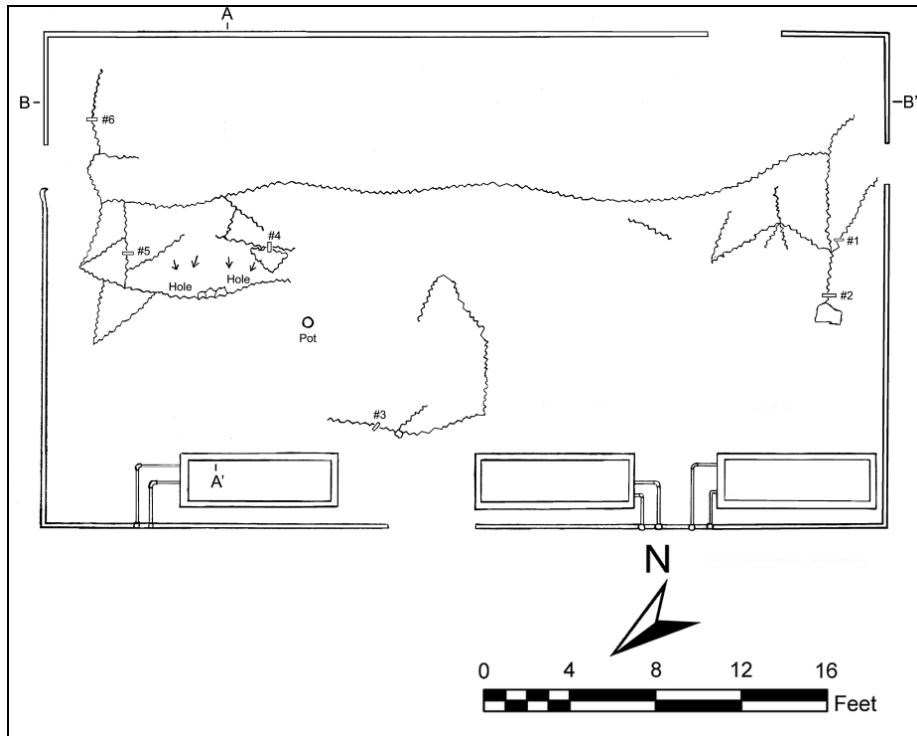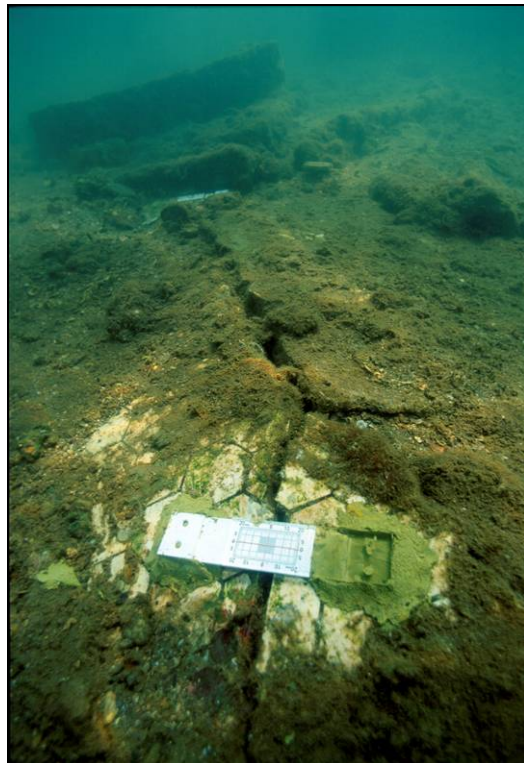ronmental factors and corrosion parameters. During this process, overall internal structural condition was observed and noted, and no observable changes to internal spaces were noted during this period. Areas investigated were identified using blueprints and, like all data and imagery, incorporated into the USS *Arizona* (USAR) GIS Project (Figures 9.14–9.16). All areas accessible to the 9 in. x 9 in. x 14 in. ROV were explored, which means that for additional areas to be accessed by either ROV or divers, structural alteration of the interior must occur.

OIL MONITORING

A considerable amount of analytical attention has been directed toward the oil in and around USS *Arizona*. Oil samples have been collected and analyzed, primarily with a gas chromatograph connected to mass spectrometer in selected ion monitoring mode (SIM) and with a flame ionization detector and HP-5 column (see Chapter 8). Primary oil samples are from the hull's interior, from open water release as an oil drop slowly floats to the surface, and from the
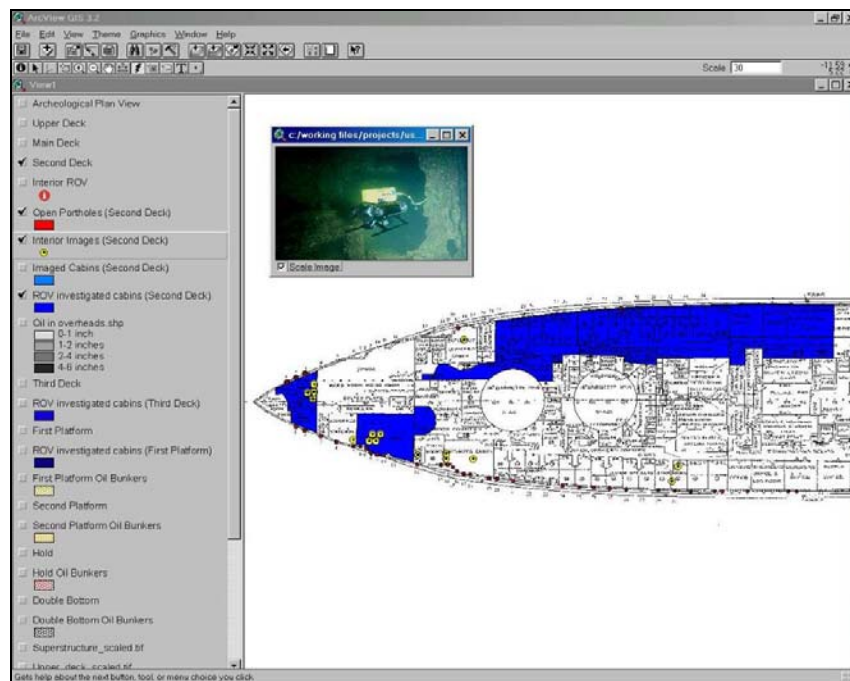

Figure 9.14. Second deck areas investigated with the VideoRay ROV (Image from USAR GIS Project).
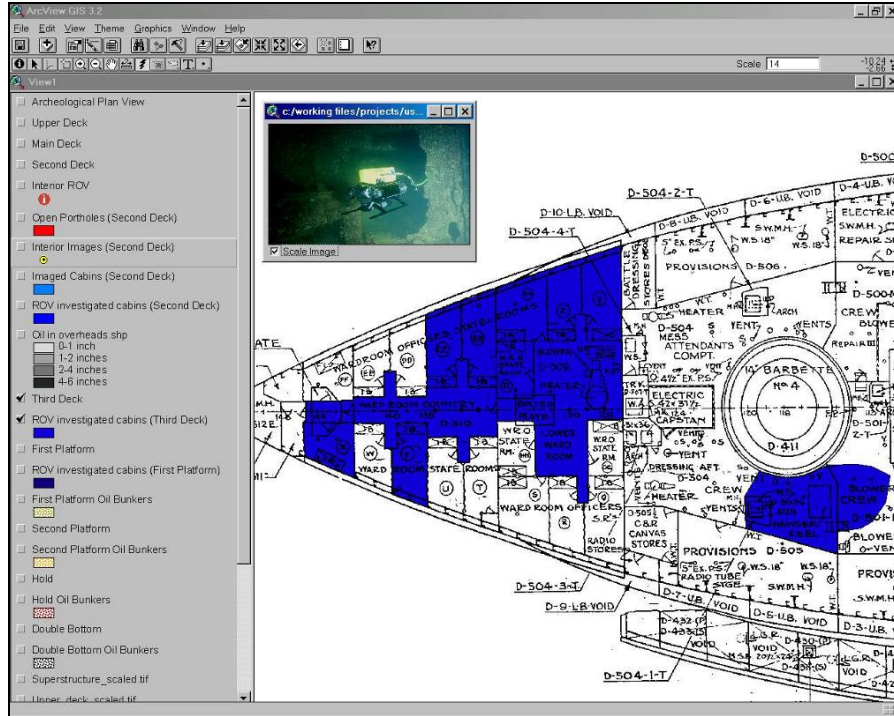
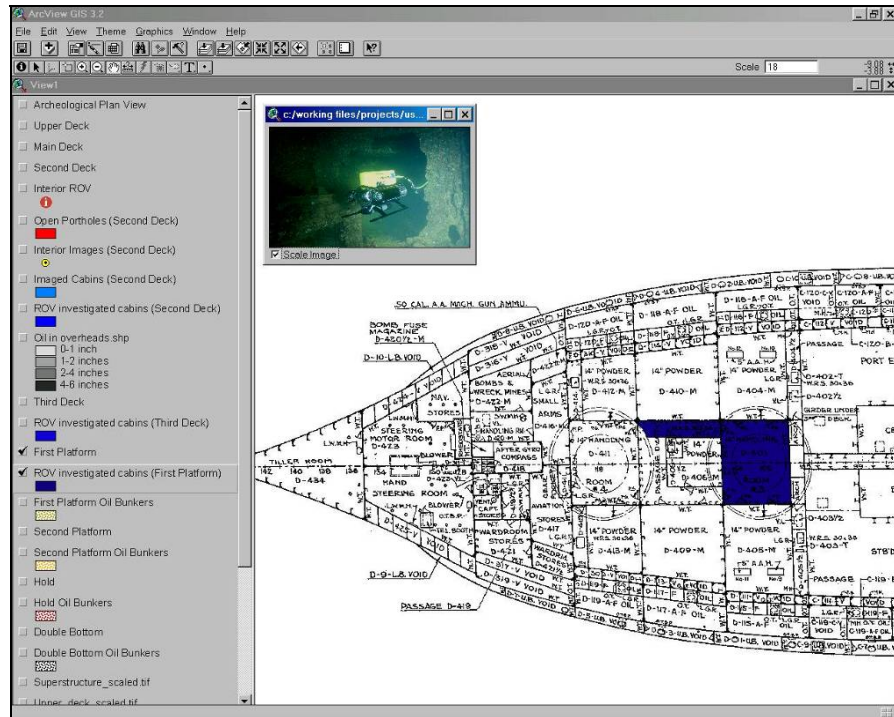**Figure 9.15. Third Deck areas investigated with the VideoRay ROV (Image from USAR GIS Project).**

Figure 9.16. First platform areas investigated with the VideoRay ROV (Image from USAR GIS Project).

sediments on and near the ship. Laboratory analysis and experimentation indicate most samples had reduced *n*-alkanes present, which is the result of microbiological degradation and occurs after approximately 30 days of exposure to sea water or sediment-borne microbes. These results allow each oil leak location to be designated "degraded" or "undegraded." Undegraded oil indicates that the oil has been in contact with open sea water (an environment that exists in second and main deck spaces with openings to the outside) for fewer than 30 days. This undegraded oil potentially indicates an interior structural failure of primary oil containment spaces. Only a single source, a hatch on the starboard side of barbette no. 4 at frame 119, produces undegraded oil (see Chapter 8).

INTERNAL OIL MONITORING

Internal oil observations and samples were collected with the VideoRay ROV (Figure 9.17), although most internal oil samples were collected from cabin overheads by reaching through an open second deck port hole on *Arizona*'s starboard side with a PVC pipe. No oil was observed in the port overhead spaces, likely due to the ship's 2–3° port list, which funnels the buoyant oil to the higher, starboard side. Oil has collected in most observable, starboard-side second deck cabin overheads, and the depth of oil in each cabin overhead was measured to give an idea of where internal oil releases are concentrated. A PVC pipe was pushed vertically up to the cabin overhead to obtain a depth (thickness) measurement of the oil layer, and samples were collected when the pipe was extracted (Figure 9.18). The results of oil depth measurements in overhead compartments on the second deck (Figure 9.19) indicate that oil concentrations increase moving forward from the stern, with the highest concentrations between frames 88–98. This is consistent with increased oil release observations in the upper deck, midships area (forward of frame 92). However, it also reinforces the observation that oil release in the midships and galley area is primarily "degraded" oil coming from secondary oil concentrations in second and main deck cabin overheads, not "undegraded" oil coming from primary oil containment spaces. The main deck (aft of frame 92) above oil-containing cabin overheads is apparently sound; there is no oil leakage above these second deck spaces. The closest oil leaks to this area are two open hatches on the main deck that continually release oil drops (see Figure 9.19). The oil coming from the aft-most hatch is different than the oil in cabin overheads, in that

Figure 9.17. VideoRay ROV rigged for interior oil collection (NPS Photo by Brett Seymour).

Figure 9.18. Internal oil measurement and oil sample collected by reaching PVC pipe in porthole and pushing vertically to the overhead. Overhead oil depth is indicated by oil on pipe (NPS Photo by Brett Seymour).
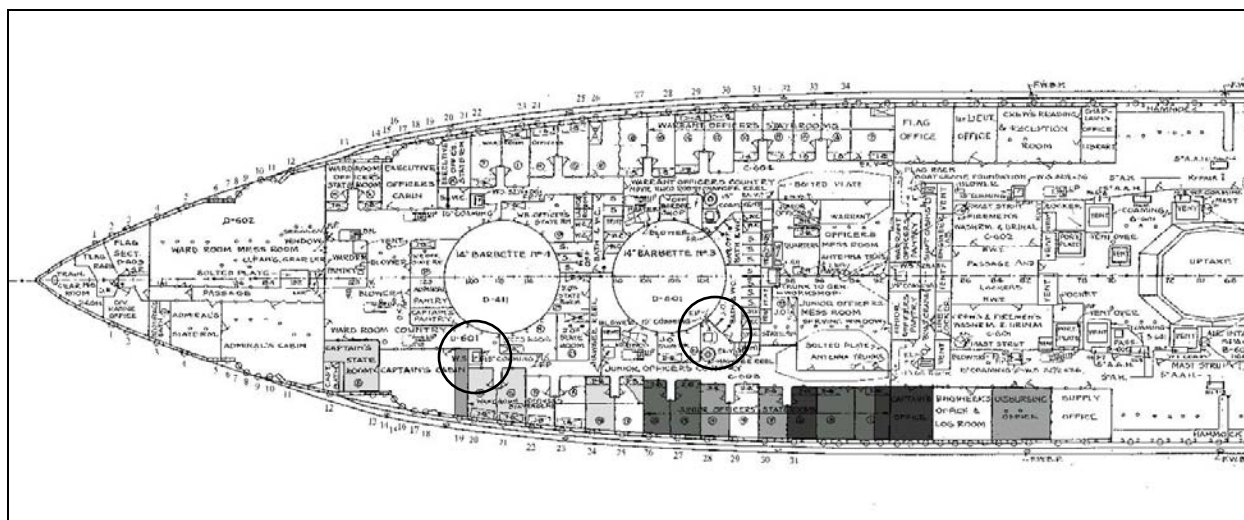
Figure 9.19. Illustration of thickness of overhead oil on *Arizona*'s starboard second deck (stern to the left). Relative darkness represents thickness of oil in each cabin overhead, and hatches releasing oil are circled (Graphic by NPS-SRC).

it is the only location producing undegraded oil. In addition, ROV observations have indicated the source of undegraded oil from the aft-most main deck hatch is below the third deck. All the other released oil tested has reduced *n*-alkanes (and other constituents), matching oil from the cabin overheads, which indicates microbial degradation has occurred through the oil's exposure to seawater (and microbial communities) of more than 30 days (see Chapter 8 and below). Most likely, oil leaking from the forward-most main deck hatch, and all other oil release points, is coming from reservoirs pooled beneath the main and upper decks where it is degraded for some time before being released.

Oil samples will continue to be collected as part of the *Arizona* monitoring program. Differences in oil sample constituents reflect differences in the environment the oil has been subjected to in containment and time of exposure to seawater. Additional and more detailed analysis of various oil leak locations can potentially inform about changes that are occurring within the vessel. At this point, undegraded oil is believed to indicate oil freshly released from primary containment spaces within the ship. An increase in release, either steady or episodic, of undegraded oil implies structural changes may have taken place in oil bunkers.

EXTERNAL OIL RELEASE MONITORING

Since 1998, the SRC and USS *Arizona* Memorial (USAR) have monitored oil release rates from *Arizona*'s hull. Oil release observed during the 1980s *Arizona* documentation project originated from a hatch on the starboard side of barbette no. 3, at frame 103, and later from a hatch on the starboard side of barbette no. 4, near frame 119 (see Figure 9.19).

Open water column samples for analysis are collected by simply catching a drop of oil as it rises to the surface (Figure 9.20). For measuring release rates in the current USS *Arizona* Preservation Project, we used a custom-designed, purpose-built catchment tent that funnels oil droplets into hole in the top fitted for a 32-oz. collection jar (Figure 9.21 and 9.22). The first tent was constructed in 1998 by USIA Corporation (St. Helens, Oregon), followed by a revised version in 2002. The tent is set up above an oil release point and left in place for a specific time period, after which the volume of oil collected is measured, and an average 24-hour release rate calculated. Systematic oil release monitoring began in 1998, focused on the two starboard hatches that had been identified in the 1980s, and continued in 2003, 2004, and 2006, with each including more oil release locations.

Figure 9.20. USS *Arizona* open water oil sampling (NPS Photo by Brett Seymour).

Figure 9.21. Oil catchment tent deployed on *Arizona* (NPS Photo by Brett Seymour).

Figure 9.22. Oil catchment tent deployment on *Arizona* (NPS Photo by Brett Seymour).

During fieldwork from 1998 to the present, gradually increasing quantities of oil have been qualitatively reported from the area forward of the Memorial; however, comprehensive measurement of oil release forward of the Memorial in the upper deck galley was not completed until June 2006. At this point, it is unclear if there has been cumulative increase in the oil being released from the hull. The 2006 oil release monitoring was the first cumulative oil leak collection conducted that collected oil from every observable oil release location on the hull. The 2006 release rates comprise the baseline for comparing all future oil release measurements. Prior to 2006, only selected oil release points were measured; there was no attempt to measure the cumulative quantity from all observable release points.

In June 2006, the catchment tent was set up over eight separate locations on *Arizona*'s deck that actively leak oil. At some locations the tent was left in place for a full 24-hr. period, while others were collected for 3 or 4 hr. and a 24-hr. equivalent release volume calculated. A cumulative total of 9.5 qt. (9.0 l) was measured from the eight leak locations (Figure 9.23). Locations measured in June 2006 represent those leaking more or less continuously and did not include locations that may have sporadic or periodic leaking.
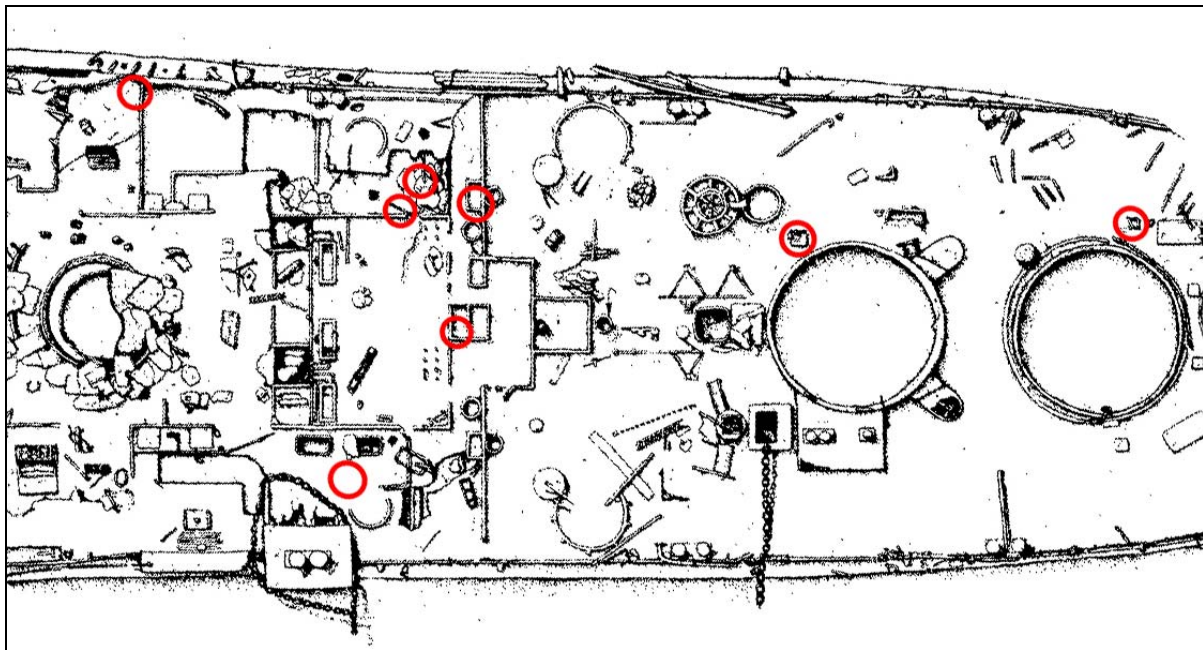

Figure 9.23. Oil release points measured on *Arizona*'s hull, June 2006 (bow is to left) (Graphic by NPS-SRC).

Measured 24-hr release rates have gradually increased each year in direct proportion to the number of locations monitored: in 1998, 1.0 qt. (0.95 l) was measured from one location; in 2003, 2.1 qt. (2.0 l) were measured from two locations; in 2004, 2.3 qt. (2.2 l) were measured from two locations; in 2006, 9.5 qt. (9.0 l) were measured from eight locations (Tables 9.2 and 9.3). June 2006 oil release measurements are the most comprehensive completed to date— increase in oil release over previous years is in part explained by more release locations being systematically measured than previously. Only future monitoring of release points can establish whether there is a cumulative increase or not.

There is no indication of increase in of oil volume released from the primary oil containment spaces in the ship's lower decks. The increase in oil observed appears to be most likely from redistribution of secondary oil contained in overhead spaces on the main and upper decks caused by gradual collapse of upper decks forward of the Memorial, which have the highest corrosion rates and were also affected by the 1941 explosion (see Chapter 5). Primary oil containment spaces (oil bunkers), located on *Arizona*'s lower decks, are well below the harbor bottom and likely have lower corrosion rates than any measured on the outside of the hull. Measured corrosion rates below the harbor bottom are the lowest rates observed on the hull, about 25% of the 4.5 mils per year (mpy) predicted from the laboratory derived corrosion rates of mild steel in seawater (see Chapter 5). This is because corrosion is primarily driven by the presence of dissolved oxygen, and the environment below the mud of the harbor bottom, as well as water in the interior spaces is anaerobic. Periodic measurements of internal water quality, however, should be part of the ongoing monitoring process.

Undegraded oil release measured from the aft-most main deck hatch on the starboard side of barbette no. 4 in June 2006 is lower than in previous years. These data suggest that oil release directly from primary oil containment spaces may have decreased over the last several years,

Year	Number of Locations Measured	Average Total Amount Measured Per 24 Hours (quarts)	Average Total Amount Measured Per 24 Hours (liters)
1998	1	1	0.95
2003	2	2.1	2
2004	2	2.3	2.2
2006	8	9.5	9

Table 9.2. Number of oil locations measured and quantities recovered, by year.

Year	Location	Date	Amount	Time	Total per 24 hr. (qt.)	Total per 24 hr. (l)
1998	Oil hatch starboard of No.3 barbette	8/29/98	800 ml	22 hrs. 39 min.	0.9	0.85
1998	Oil hatch starboard of No.3 barbette	8/31/98	700 ml	27 hrs. 35 min.	0.64	0.61
1998	Oil hatch starboard of No.3 barbette	9/06/98	175 ml	3 hrs.	1.5	1.4
2003	Oil hatch starboard of No.4 barbette	11/18/03	42.5 oz.	24 hrs.	1.33	1.25
2003	Oil hatch starboard of No.4 barbette	11/19/03	42.5 oz.	24 hrs.	1.33	1.25
2003	Oil hatch starboard of No.3 barbette	11/20/03	16-24 oz.	24 hrs.	0.5-0.75	0.47-0.7
2004	Oil hatch starboard of No.4 barbette	11/09/04	14 oz.	6 hrs.	1.75	1.66
2004	Oil hatch starboard of No.3 barbette	11/11/04	16 oz.	24 hrs.	0.5	0.47
2006	Oil hatch starboard of No.4 barbette	06/20/06	5 oz.	4 hrs.	0.94	0.89
2006	Oil hatch starboard of No.4 barbette	06/21/06	5.2 oz.	4 hrs.	0.97	0.92
2006	Oil hatch starboard of No.3 barbette	06/23/06	10 oz.	24 hrs.	0.31	0.3
2006	Starboard of galley, on deck	06/24/06	5 oz.	24 hrs.	0.16	0.15
2006	Starboard of galley starboard bulkhead, forward of doorway	06/26/06	<1 oz.	48 hrs.	<0.016	<0.015
2006	Starboard gunwale, frame 68	06/28/06	8 oz.	24 hrs.	0.25	0.24
2006	Port, forward corner of vegetable locker	06/28/06	9.4 oz.	4 hrs.	1.8	1.7
2006	Port side of galley, on deck	06/29/06	5 oz.	3 hrs.	1	0.95
2006	Starboard side of galley, at transverse bulkhead between upper deck and main deck.	06/29/06	20 oz.	3 hrs.	5	4.7

Table. 9.3. Oil release quantities by year.

supporting the supposition that increased oil release is from secondary oil containment in cabin overheads below the main and upper deck spaces forward of the Memorial, in the area of the observed deck collapse.

Oil release rates can vary considerably with differing wind, tide and harbor conditions. More oil is clearly released during choppy harbor conditions and when tour boat and other ship's wakes pass near *Arizona*'s hull, which further supports the oil source as shallow overhead spaces rather than from primary oil containment spaces. Wake pressure waves can dislodge oil residing in overhead spaces. Large vessel wakes within Pearl Harbor are significant; divers working on the hull are occasionally displaced as large vessels pass. This impact to the hull is somewhat

exacerbated because ships tend to pass close by the USS *Arizona* Memorial in tribute. The June 2006 measurements not only included many more source locations (all that could be located), it is likely that these measurements represent near maximum release rates. The June 2006 oil release measurements were conducted during RIMPAC naval exercises, which is a period when the number of reported ship moves in Pearl Harbor is generally 10 times the normal number. Consequently, June 2006 oil release measurements represent conditions under which maximum release from wake disturbance is expected.

Periodic monitoring of all oil release locations on *Arizona* should be continued and USAR personnel on the Memorial should continue daily recording of oil release observations. To quantify effects of differing weather and harbor conditions on oil release rates, more frequent in-water monitoring under diverse conditions should be considered in the future to produce data that can be correlated with episodic release increases and lead to a prediction as to when wave driven episodic releases may occur. The most comprehensive oil release monitoring can be accomplished by capturing surface oil downstream from *Arizona*'s hull. An oil capturing and monitoring system should be investigated collaboratively with the U.S. Navy and U.S. Coast Guard. This would likely involve a boom erected between *Arizona*'s bow and *Missouri*, with regular oil removal and measurement by Navy or Coast Guard oil response personnel. Ideally, a remote sensing device measuring surface oil could be deployed and alarmed to warn of significant oil increase that requires mobilization of the Pearl Harbor Oil Response capability.

OIL RELEASE IN CREW'S GALLEY AREA

As discussed previously, the upper deck, midships galley-area (frames 80–88), just forward of the Memorial, is presently the principal oil release area on *Arizona*'s hull. This area is heavily damaged from the forward magazine blast that sank the vessel, representing the stern reach of the blast crater (see Figure 9.10 and Chapter 3). The decks are sagging, and there has been limited collapse observed, which is why this area was chosen for deploying the crack monitors (see Figures 9.11 and 9.12). During 1941 salvage investigations, divers noted that there was only access forward to frames 76 and 78. Forward of this location, the main, second, third, first platform, second platform and hold decks collapsed on top of one another to the level of the top of the 13-in. armor belt, as the blast undercut deck support structures. Turret nos. 1 and 2

both collapsed downward more than 20 ft. (Figure 9.24). The lower decks area beneath the galley area were certainly damaged as evidenced by both the forward multiple deck collapse, but also by the original film of *Arizona*'s explosion, which shows the magazine explosion clearly vented upward through the stack area, which is just forward of the galley area (Lott 1978:40). This indicates the blast most certainly affected adjacent spaces aft, including the galley.

The oil escaping from the hull in the galley area comes through the sediments, which appear to be fully saturated with oil in several locations. Oil release has increased in this area based on comparisons with the 1980s fieldwork. Additional oil leaking from lower decks floats to the area beneath these sediments, and dislodges trapped oil that rises to the surface (Figure 9.25). It is a reasonable question to ask "where does the oil leaking through the galley area sediments likely originate?" A partial answer is revealed by an examination of the ship's blueprints on this area, specifically focusing on ship's plans in the area between frames 70–90. The crew's galley was on the upper deck. Directly beneath this area, below the third deck were engine, boiler, distribution and pump spaces (Figures 9.26–9.32). Oil bunkers are on the first platform and below. There is no record of damage to these spaces, only the main and third decks are mentioned as being accessed by divers during the salvage work, but it is very likely there is damage to the engine and boiler spaces in this area. Oil could be coming from associated piping, machinery, cracked or damaged bunkers, and trapped in overhead spaces. Episodic releases may be caused by further collapse of lower decks, much like that observed on the upper deck area. More likely, the oil in the galley area is resulting from original battle damage, and weakened decks collapsing and releasing trapped oil that rises up from engine, boiler and pump spaces, than from deteriorating oil bunkers. The rising oil is directed by collapsed decks to cracked areas surrounding the upper deck galley that contain sediment, where the oil saturates the sediment and is released.
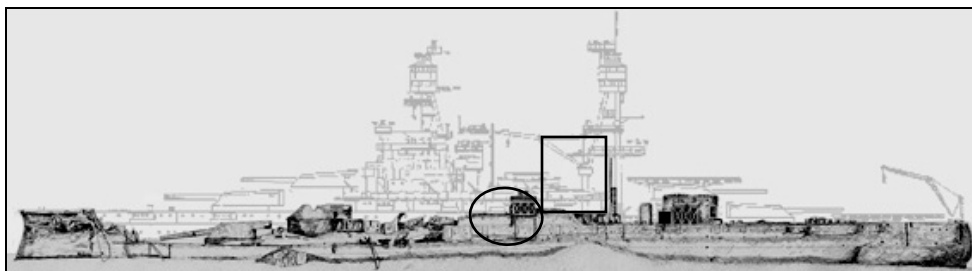
Figure 9.24. USS *Arizona* wreck overlay on intact vessel plans. Oval indicates galley area oil release area and rectangle is Memorial location (Graphic by NPS-SRC).

Figure 9.25. Sediments in crew's galley area forward of Memorial. Dark areas are oil saturated sediments. White oval circles a drop of released oil moving toward the surface (NPS Photo by Brett Seymour).
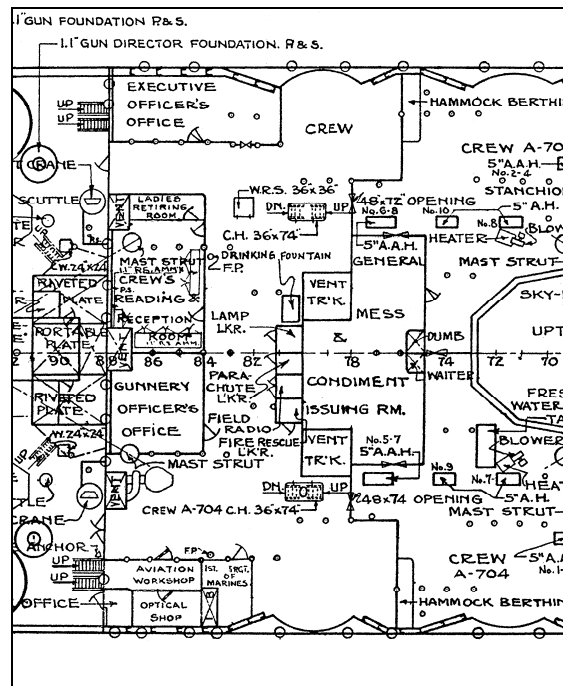
Figure 9.26 *Arizona* main deck blueprint, frames 70-90. Stack is on right, towards the bow. Reportedly, divers were able to reach frame 76 on this deck, which is the condiment issuing room just aft of the stack (USS *Arizona* Memorial Archives).

416
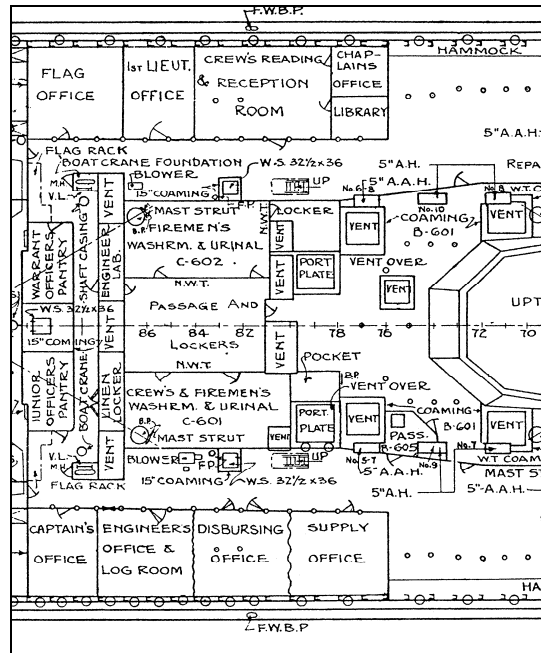
Figure 9.27. Second deck, frames 70-90 (USS *Arizona* Memorial Archives).
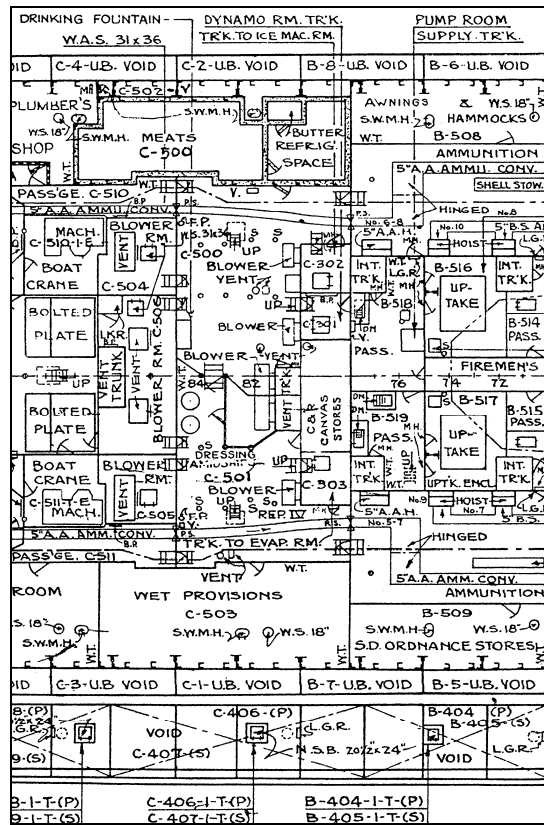
Figure 9.28. Third and splinter deck, frames 70-90. Divers were able to reach frame 78, likely through the centerline fireman's passage. Frame 78 is a watertight bulkhead (USS *Arizona* Memorial Archives).

417
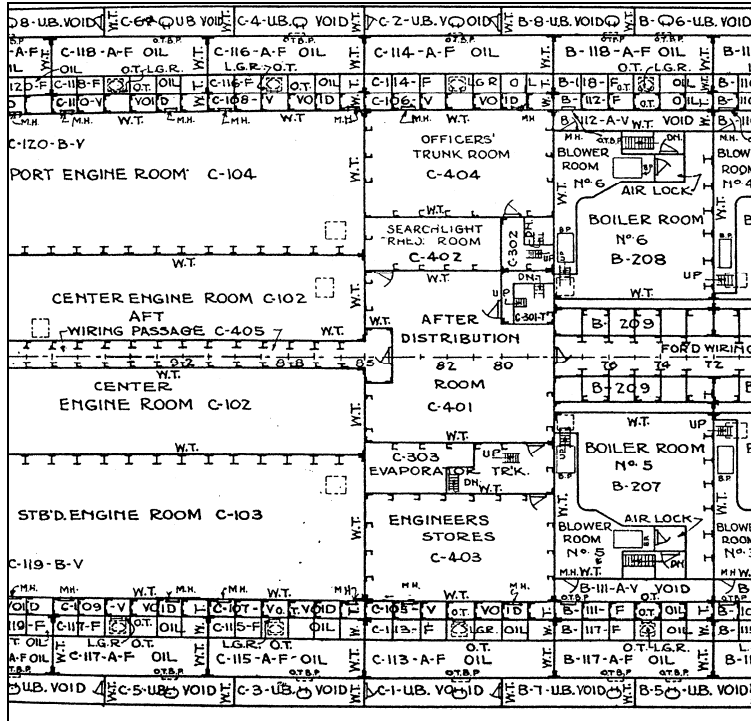
Figure 9.29. First platform, frames 70-98. This area is between the three engine rooms and boiler spaces, and contains the after distribution room.   It is the highest level in the ship that contains oil bunkers (USS *Arizona* Memorial Archives).
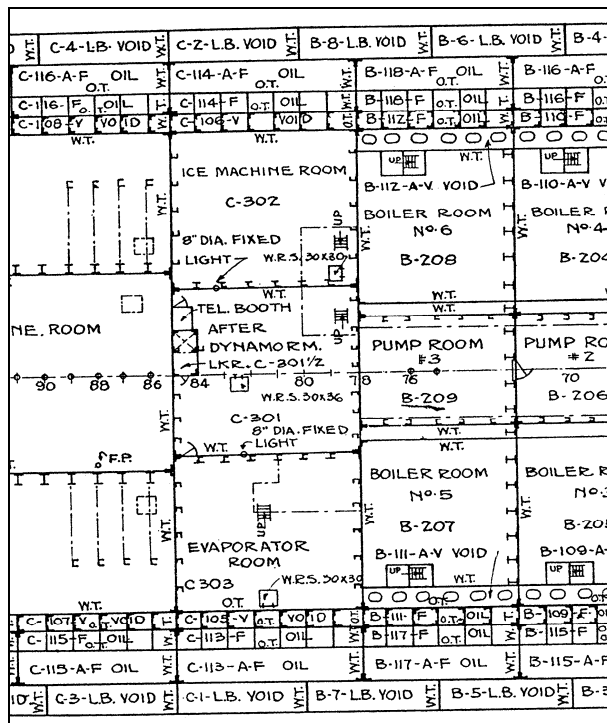
Figure 9.30. Second platform, frames 70-90, contains engine and boiler spaces as well as pump rooms (USS *Arizona* Memorial Archives).
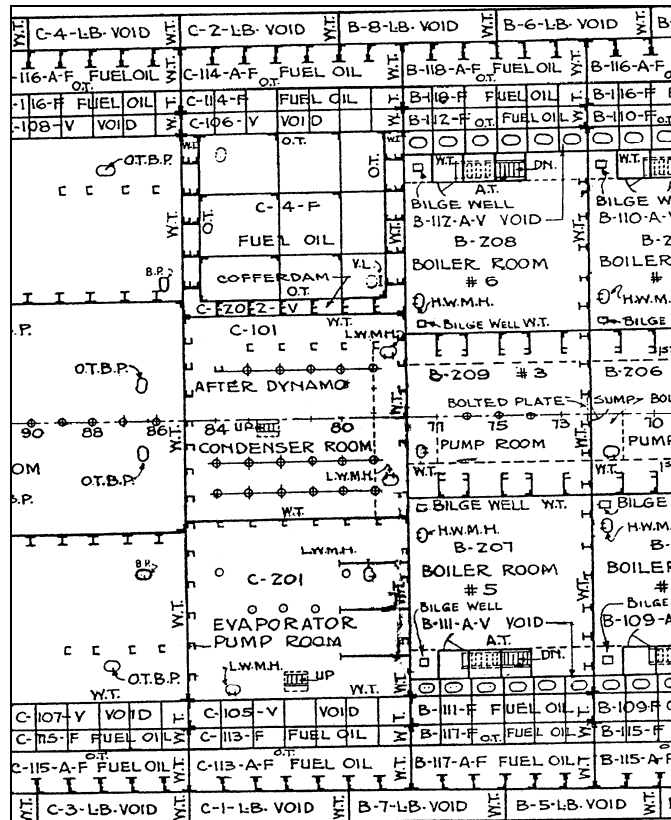
Figure 9.31. Hold, frames 70-90, including engine, boiler spaces, and pump rooms (USS *Arizona* Memorial Archives).
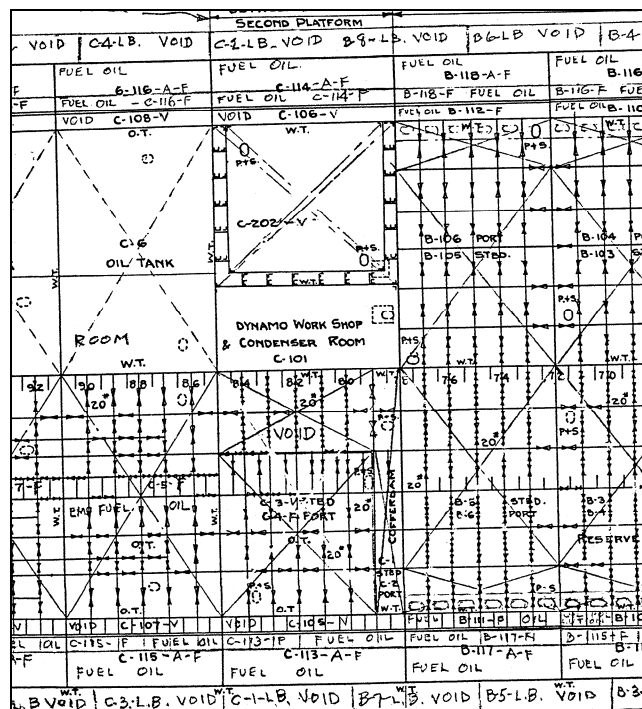
Figure 9.32. Double bottom, frames 70-90. It is unlikely that this area suffered significant damage from the magazine blast (USS *Arizona* Memorial Archives).

419

ARTIFACT MONITORING PROGRAM

Growing concern by USS *Arizona* management prompted by evidence of increased unauthorized diving led to the development of an artifact monitoring program. SRC archeologists conducted an intensive survey of the accessible open deck areas, primarily main and upper decks for visible artifacts. Artifacts were mapped in place through a combination of baseline trilateration, trilateration from mapped features, and a combination of GPS and total station survey. Each artifact received a unique numbered tag with its inventory number on one side and "US Government Property – Do Not Remove," on the other (Figure 9.33). A spreadsheet with the artifact number, general location, description, dates relocated, UTM coordinates and survey data, and photograph and video imagery identifier fields, was created. More than 450 artifacts have been inventoried and are being monitored. The artifact monitoring program is ongoing, and it will become increasingly important as development of Ford Island progresses.

Figure 9.33. USS *Arizona* artifact with monitoring tag affixed (NPS photo by Brett Seymour).

QUALITATIVE ENVIRONMENTAL MONITORING

Submerged Resources Center personnel have been conducting research on USS *Arizona* since 1983. During the course of this research, scientists and archeologists working on *Arizona* have noted a general improvement in overall environmental conditions. This improvement manifests in increased visibility and increased coral growth, and fauna presence and diversity on the hull (Figure 9.34). In 1986, researchers conducted a biological inventory of growth attached to the hull and deck. There were about 25 common taxa of organisms living on the hull and about 25 species of fish observed. Most of the encrusting organisms were filter feeding organisms such as vermetid mollusks, oysters, bryozoans, tube worms, sponges, tunicates and algae. Resurveys were conducted in 1987 and 1988, and monitoring station photographs were taken and analyzed (Henderson 1989). The monitoring program could not be sustained and was discontinued afterwards. In addition, lack of funding prevented a repeat inventory for quantitative inventory comparison as a part of the current research project, which is needed. However, presence of seahorses (identified by USS *Arizona* Memorial personnel as *Hippocampus kuda*, or yellow seahorse, Figure 9.35), first observed in 2005, indicates improving water quality in Pearl Harbor. Qualitative comparisons can also be made through photographic evidence taken of features during the 1980s documentation project and more recent photographs of the same objects (Figures 9.36–9.39). This 20-year observation period of biological indicators on USS *Arizona* show that both the environment in and around *Arizona* is relatively benign, and the general conditions of Pearl Harbor have markedly improved in the last two decades.

Continued biological observations and documentation will be part of a future monitoring program. A full biological inventory of *Arizona*'s hull and proximity is needed, and comparisons with the 1986 inventory and implications should be made. Biological inventories should be conducted periodically, ideally at 3–5-year intervals. In addition, a complete ecotoxicological study is needed of the sediments on and near *Arizona*, and down current along the Ford Island beach zone. Biomarker analysis has provided a signature of *Arizona*'s oil (see Chapter 8). This analysis has also identified constituents, such as butylated hydroxytoluene (BHT), which is not a component of Bunker C fuel, but is found in jet fuel, from a sediment sample just 10 ft. from *Arizona*'s hull. A full analysis of the degradation of *Arizona*'s oil and a quantification of its environmental impact, particularly in the context of Pearl Harbor where there are other point

Figure 9.34. Live coral on *Arizona*'s deck (2006), which requires good water quality to grow. There was no hard coral observed in 1986 (NPS Photo by Brett Seymour).
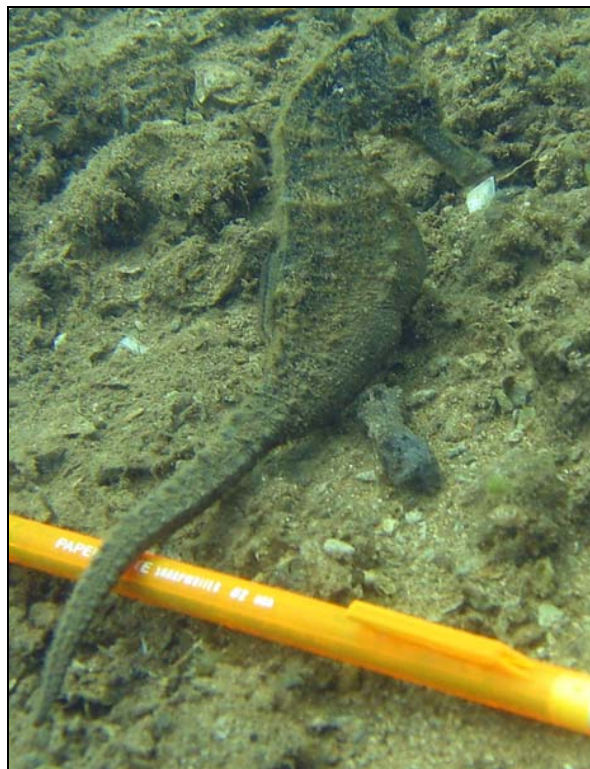
Figure 9. 35. Sea horse (*Hippocampus kuda*) on *Arizona*'s deck, first observed in 2005 (NPS photo by Jennifer Burbank).

Figure 9.36. Gas cylinder *Arizona*'s deck in 1983 (NPS photo by Larry E. Murphy).

Figure 9.37. Gas cylinder *Arizona*'s deck in 2005, with hard coral (NPS photo by Brett Seymour).

Figure 9.38. Inverted ventilator, on *Arizona*'s aft deck in 1983 (NPS photo by Larry E. Murphy).

Figure 9.39. Inverted ventilator, on *Arizona*'s aft deck in 2005 (NPS photo by Brett Seymour).

sources of petroleum, is needed to inform management decisions that address the actual environmental impact of the *Arizona* oil release. It is easy in today's climate of growing concern about the environment to intuitively attribute severe environmental impact from the quite visible *Arizona* oil slick (actually only several microns thick) that could prompt ill considered and inappropriate intervention to remove the oil. As should be clear from data presented in this report and incorporated into the predictive FEM in Chapter 6, *Arizona*'s hull does not appear to be in any danger of imminent collapse, and consequently there is no urgency to remove the oil to preserve the environment or prevent "environmental catastrophe." There is certainly sufficient time to collect additional data and refine the predictive model while actively monitoring the environment to determine precisely the impact of the oil leaking from the ship. What is needed is scientific data that describes and quantifies the actual environmental impact of Bunker C fuel oil from *Arizona* and develops a predictive model of environmental impact for various levels of release. Insufficient funding has prevented this important environmental analysis from being accomplished to date. We consider these data critical in future management consideration of the balance between natural environment-impact and the historic and cultural importance of USS *Arizona* and its long-term preservation.

USS *ARIZONA* GEOGRAPHIC INFORMATION SYSTEM (GIS)

GIS technology provides a solution for maintaining a spatially related, cumulative record of information on USS *Arizona* that allows analysis and manipulation to produce additional data sets and relationships not otherwise available. One of the first steps in developing this database was the location, collation, and examination of nearly 8,000 scanned *Arizona* blueprints and technical drawings, which are stored on 75 DVDs. More than 250 original ships plans and blueprints were selected from the blueprint set for incorporation into both the FEM and the GIS. These digital plans were provided to the National Institute of Standards and Technology (NIST) and the NPS-RIMD, who contracted with Northrop Grumman Mission System (Lakewood, CO, a division of defense contractor Northrop Grumman, Los Angeles, CA) to develop a GIS appropriate for long-term management of *Arizona* data that incorporated current and historical data. Currently, the GIS is stored on RIMD servers and available to scientists and researchers.

Upon completion of the USS *Arizona* Preservation Project GIS, it will be made accessible to the general public. The software used for this project is ESRI's (Redlands, CA) ArcIMS software.

The first step in developing the GIS was to vectorize the raster format scanned blueprints and create a geodatabase of USS *Arizona* that includes all information for each cabin and space available on the plans—each object, space or cabin is a digitally separate entity with all attributes linked to it through the geodatabase (Figure 9.40–9.42).

For the GIS to progress all spatial data had to be georectified. This georectification was begun by collecting more than 35 survey grade kinematic points on the ship's hull. These points served as rectification points for the *Arizona* maps created in the 1980s, blueprints and other spatially related data, and as datum points for detailed mapping areas for the artifact inventory and monitoring program. Points were selected on the ship that were easily recognized and collated with the digitized *Arizona* drawings. A combination of underwater tripod and stadia rod survey was used (see above). The "superpoints" discussed earlier were also incorporated into this georectification project as additional rectification points.

Figure 9.40. Georectified blueprints of USS *Arizona* (Image from USAR GIS Project).
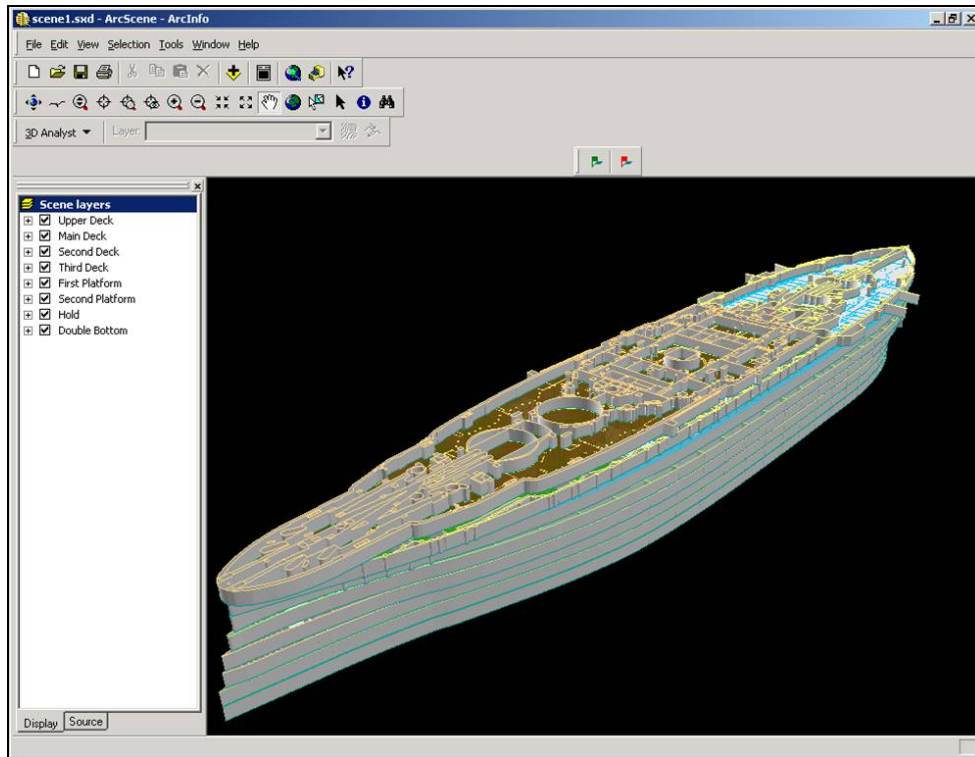
Figure 9.41. *Arizona* **deck layers, georectified, vectorized and set for queries (Image from USAR GIS Project).**
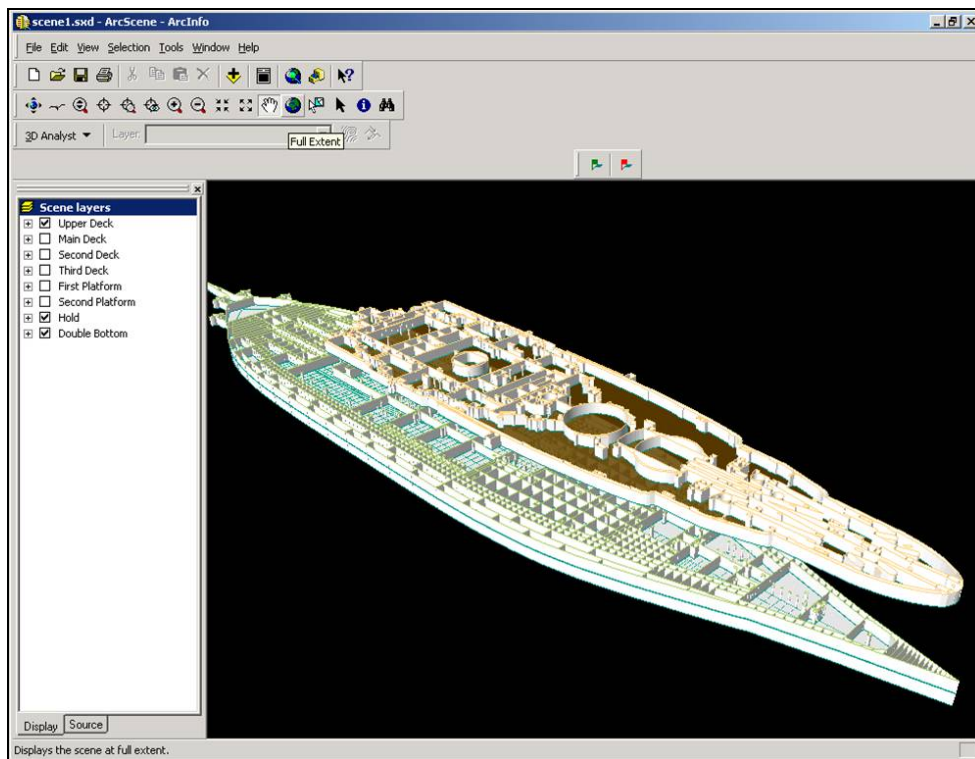
Figure 9.42. *Arizona* **interior deck spaces, each of which can be queried for associated data (Image from USAR GIS Project).**

Observations made by researchers, for instance, portable items found on the decks or bulkhead conditions observed in ship compartments by the ROV, have been recorded in the GIS. Eventually, more than 2,000 engineering drawings of individual rooms and features will be vectorized and added to the geodatabase along with more than 3,000 historical and current photographs, images and documents. All will be searchable either by name or location.

Using these base maps and geodatabase, scanned ship's plans can be "linked" to their appropriate object or location on the ship. Next, a webpage and ArcIMS website was developed that incorporated annotated vector polygon layers of the USS *Arizona* that logically track associations to a database of digital reference imagery. The web map is currently a prototype, and plans are made for its revision and updating of new scientific data and historical and current photographs and video.

The web site currently provides functionality to view all eight layers of USS *Arizona*, query for specific features in each layer, identify features in each layer (name and description fields are most useful), and includes standard interactive map tools such as pan and zoom. Each layer is rendered with 30% transparency so that deck features below the current deck may be seen "through" the top most deck that is displayed. The decks are accurately ordered in the table of contents from top to bottom and georectified. All standard web map functions are included in this HTML map service.

The prototype website has two custom functions that allow scanned engineering drawings to be viewed through the web interface. These tools are located on the left frame under the title "Access Images" and are named: *by Feature* and *by Query*. The first tool enables the user to select a feature on a deck of the ship and query the geodatabase for images and data associated to that feature (Figure 9.43). If multiple images are related to one feature (ammunition passage or gun turret for example), a list of images is returned with their description for selection. The user selects one of the images and it opens a new browser window to view the image. The prototype utilizes Lizard Tech's loss-less image compression format for image storage and viewing. A Lizard Tech browser plug-in is required for viewing the images in a standard web browser and can be downloaded as necessary.

The second custom tool (*Access Images by Query*) queries the database directly to produce a unique list of image themes (Figure 9.44). The user chooses a theme and is returned a list of all the images and their descriptions that fall under that theme. As the user selects an
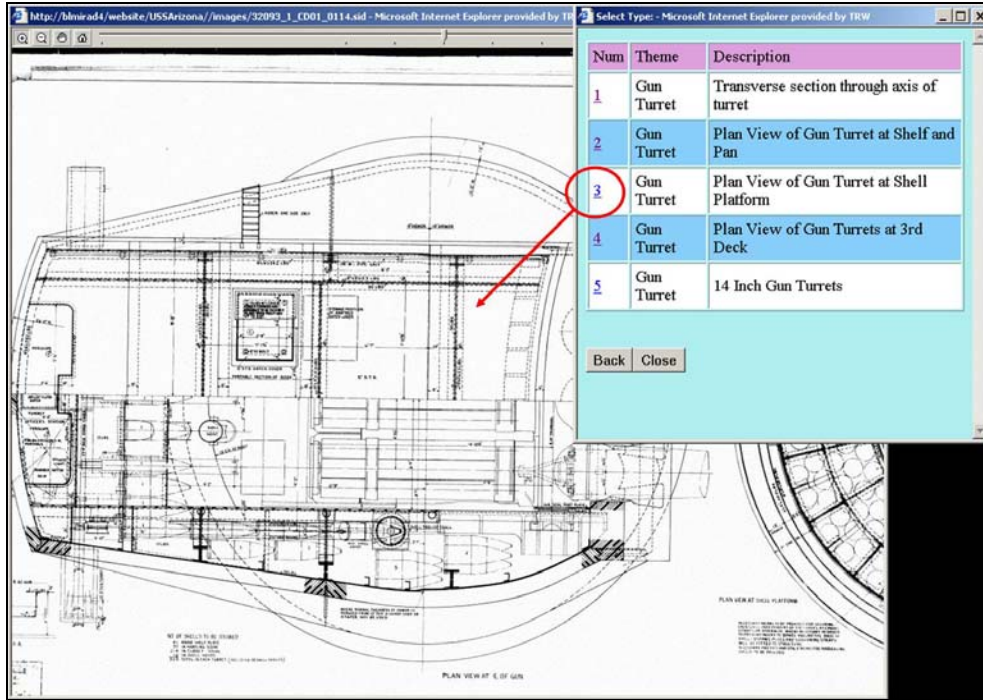
Figure 9.43. Selection by feature from blueprints. Each space is a separate entity and has associated features to access geodatabase. Clicking on a space brings up all additional data (Image from USAR GIS Project).
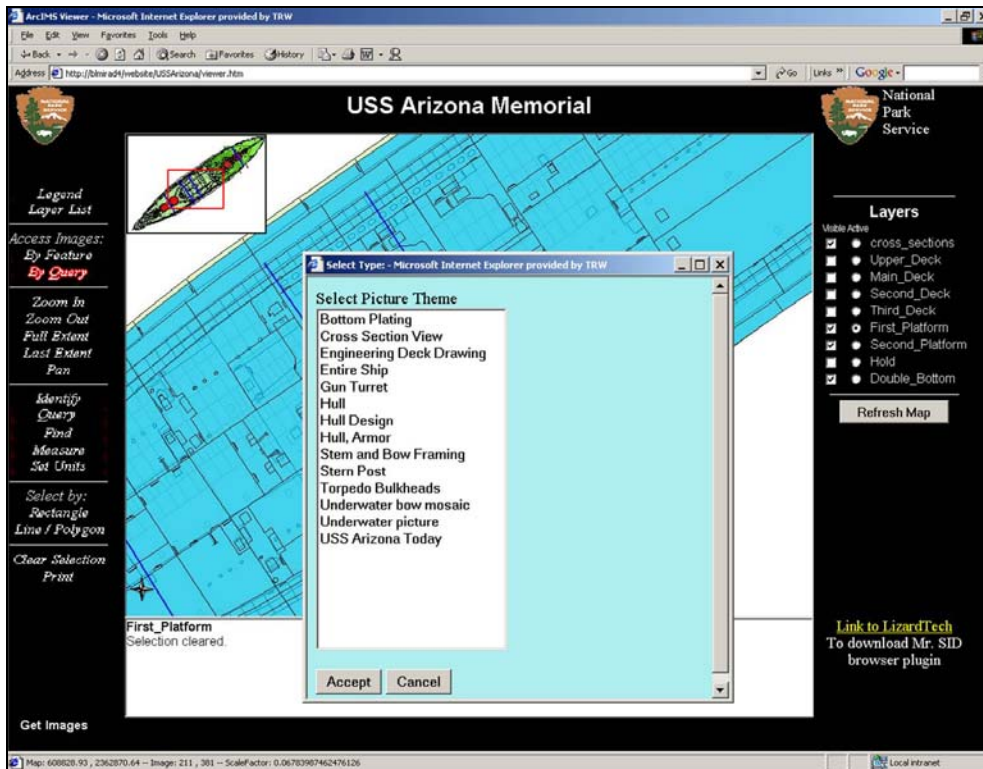
Figure 9.44. Example of accessing images and geodatabase by query (Image from USAR GIS Project).

image, a new browser window is opened to display the image. Each database image must have metadata, whose generation can be time consuming. Metadata enables the document management process to work. Each image is described and given a subject or "theme", much like a keyword, that links to specific features in the eight levels of the geodatabase by a unique feature-id (key field).

The final step in the process is to refine the project and database, eventually incorporating all scanned plans from *Arizona*, and porting the project to an NPS network, which would allow mobile and remote access to the plans and related data in the geodatabase by various researchers and, ultimately, the public.

REFERENCES

Henderson, S.
> 1989 Biofouling and Corrosion Study. In *Submerged Cultural Resources Study: USS Arizona Memorial and Pearl Harbor National Historic Landmark*, edited by D. J. Lenihan, pp. 117-156. Submerged Resources Center Professional Papers No. 9. National Park Service, Santa Fe.

Lenihan, D. J. Editor
> 1989 *Submerged Cultural Resources Study: USS* Arizona *Memorial and Pearl Harbor National Historic Landmark*. Submerged Resources Center Professional Papers No. 9. National Park Service, Santa Fe.

Lott, A.S. Editor
> 1978 *USS* Arizona *Ship's Data: A Photographic History*. Fleet Reserve Association, Honolulu.

McCarthy, M.
> 2000 *Iron and Steamship Archaeology: Success and Failure on the S.S. Xantho.* The Plenum Series in Underwater Archaeology, New York.

Murphy, L.E. and T.G. Smith
> 1995 Submerged in the Past: Mapping the Beguiling Waters of Florida's Biscayne and Dry Tortugas National Parks. *Geoinfo Systems* 5(10):26-33.

> 1996 Global Positioning System (GPS). In Encyclopedia of Underwater Archaeology, edited by James P. Delgado, pp. 171 -172. British Museum Press, London.

Paine R.W.
> October 7, 1943 Memo from Commandant Navy Yard , Pearl Harbor to Chief, Bureau of Ships. Subject: U.S.S. *Arizona* (BB-39) War Damage Report. On file, USS *Arizona* Memorial Archives, Honolulu.

Shope S.M., L.E. Murphy and T. G. Smith
> 1995 Found at Sea: Charting Florida's Sunken Treasures *GPS World* 6(5):22-34.

CHAPTER 10

A Geotechnical Investigation of the Stress History and Settlement Potential of Sediment Supporting USS *Arizona*

Robert E. Kayen, Brad Carkin, and Homa J. Lee

INTRODUCTION

In November 2003, the National Park Service contracted a private drilling company, Ernest K. Hirata & Associates, Inc., to sample sediment at three borehole sites surrounding the USS *Arizona* Memorial. During a one week drilling effort, from November 13–20, 52 m of sediment were sampled.

The three boreholes are located as follows: B1A is located midship between the USS *Arizona* and Ford Island (E608813, N2362945) in 8.5 m of water at the time of drilling; B2 is located directly northeast of the vessel (E608943, N23662957) in 11.9 m of water at the time of drilling; B3 is located directly southwest of the vessel (E608749, N23662811) in 11.3 m of water at the time of drilling (Figure 10.1). The boreholes B1A, B2, and B3 have sub-bottom drill depths of 15.2, 21,3, and 15.2 m. USS *Arizona* is currently resting on the floor of Pearl Harbor, submerged and tilting away from Ford Island. Immediately following the attack, on December 7, 1941, portions of the deck and railing were sub-aerially exposed, along with the superstructure and guns removed during salvage operations (Figure 10.2). The superstructure and guns were removed in 1942. Photos taken in the winter and spring of 1942 clearly show much of the vessel

Figure 10.1. Boreholes B1a, B2 and B3 located around the hull of USS *Arizona*, west of Ford Island.
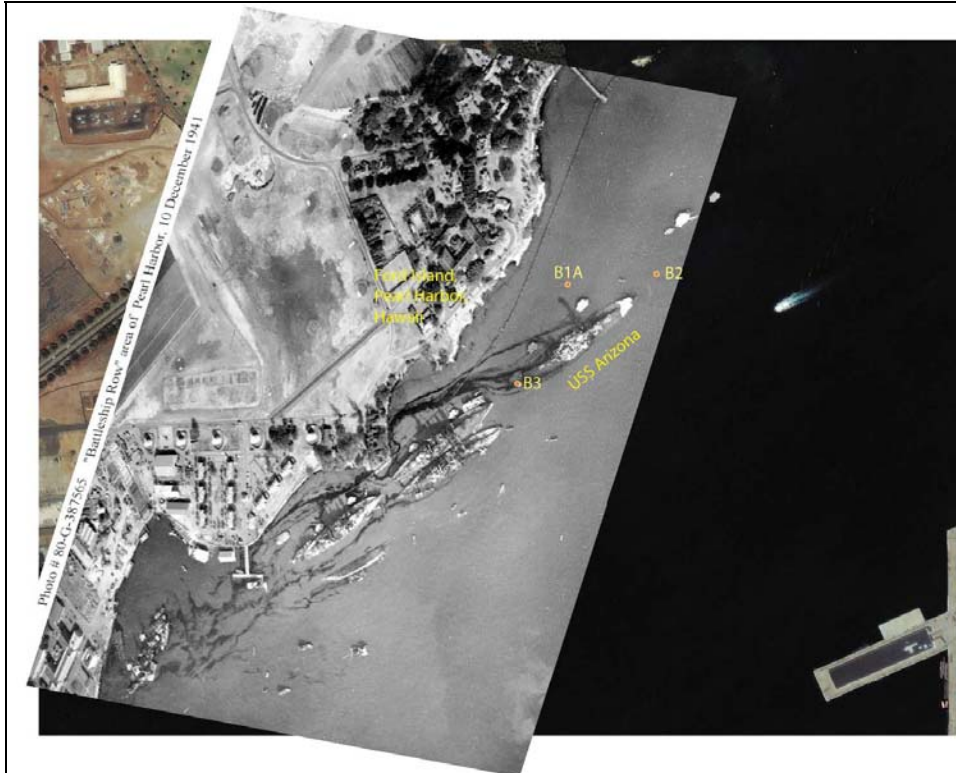
Figure 10.2. An overlay of DOD photo 80-G-387565, taken December 10, 1941, on Figure 10.1, showing the location of the vessel and boreholes. Most of the vessel was still sub-aerially exposed after the attack.

deck at, or above, water level (Figures 10.3–10.5). Today, 63 years later, the deck of the vessel is submerged in up to approximately 2 m of water.

This chapter investigates the settlement and tilt of the vessel through a geotechnical analysis of sediment drilled around the stern, shoreward mid-ship, and bow of the vessel. We characterize the state of stress within the sediment, the relation between that stress state and the effective overburden load placed on the sediment due to the existing sediment load, and the added stress of the submerged USS *Arizona*.

CORING OPERATIONS

Field sampling operations, taken from a small drill barge, were focused on collecting soil samples with several coring devices. In general, the drillers sampled sediment with either 100 mm Shelby tubes or 75 mm steel pipe (Figure 10.6). The Shelby tubes are enameled, non-reactive, sample tubes designed for acquiring sediment with saline pore water. The recovered samples are encased in whole-round steel liner tube and capped by the drillers, and then were transported to an onshore laboratory near the drill site.

The lithology of the samples and drill cuttings are presented in the appendix. The uppermost unit in all three boreholes is a silty sand/sandy silt (SM/ML) with shell fragments (upper yellow unit Figures 10.7, 10.8, and 10.9). Beneath this is a silty sand unit (gray) that thickens toward the north stern area. Borehole B1A is shoreward of the vessel and the silty clay there is interbedded with a coralline rubble and sand. Likewise, the silty sand near the stern is interbedded with silt and sandy silt that coarsens down core. What is most noteworthy regarding the cross-sections in Figures 10.7, 10.8, and 10.9, is the heterogeneity of the sediment beneath the vessel. A relatively stiff profile of silty sands and sandy silts is found near the bow section at B3, whereas, soft deformable fine-grained deposits thicken toward the stern (B2) with a corresponding thinning of stiffer silty sand and sandy silt deposits. Midship on the starboard, shoreward, side, a coraline rubble may provide some stiffening element to the sediment deposit that is not present at the stern, bow, or port side. A seaward thickening wedge of silty-sand is present in the bow (B3) area, whereas, a seaward thickening wedge of finer grained clay is found near the stern.

Figure 10.3. Gunnery deck and deck railings visible above the harbor water in 1942 (USS Arizona Memorial Photo Archive).

Figure 10.4. A photograph of USS *Arizona*'s damaged exposed deck (USS Arizona Memorial Photo Archive).

Figure 10.5. Salvage crews in 1942 were able to work on the deck above water and cut entry-ways into the vessel for recovery operations (USS Arizona Memorial Photo Archive).

Figure 10.6. A small anchored barge was used to advance the borehole. The deck and railings of USS *Arizona* are completely submerged in 2003, with the vessel tilting several degrees to the southeast (USGS Photo).
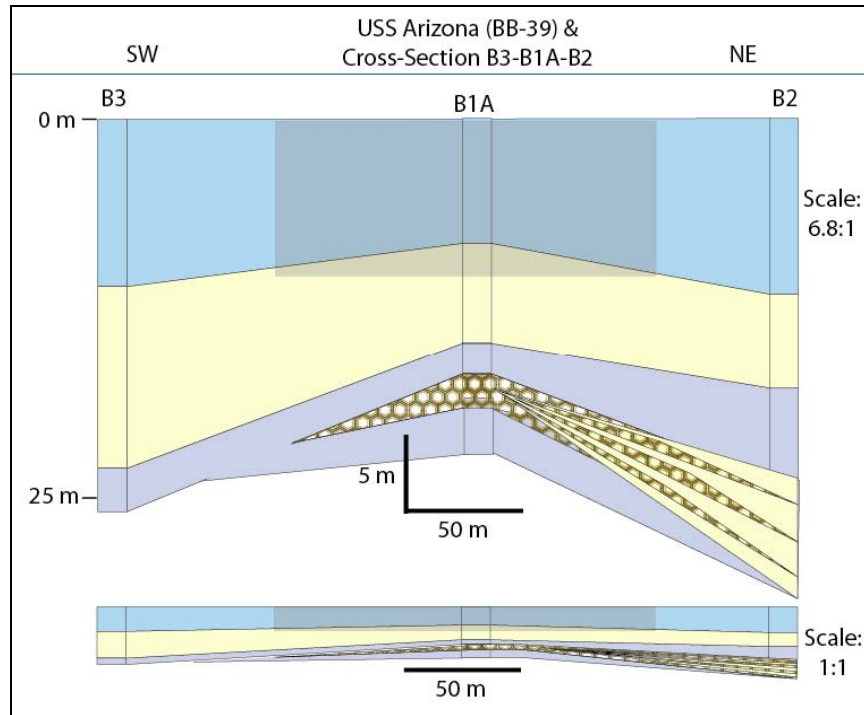
Figure 10.7. Cross-section from bow area (B3) to stern area (B2) through the shoreward midship boring (B1A). The upper blue unit is the water column. The seafloor is a silty sand and sandy silt underlain by a silty clay. The B1A clay unit is interbedded with a coralline rubble. B2 is a silty clay that transitions into a clayey silt with interbedded sandy silt. The gray shaded area is USS *Arizona*.
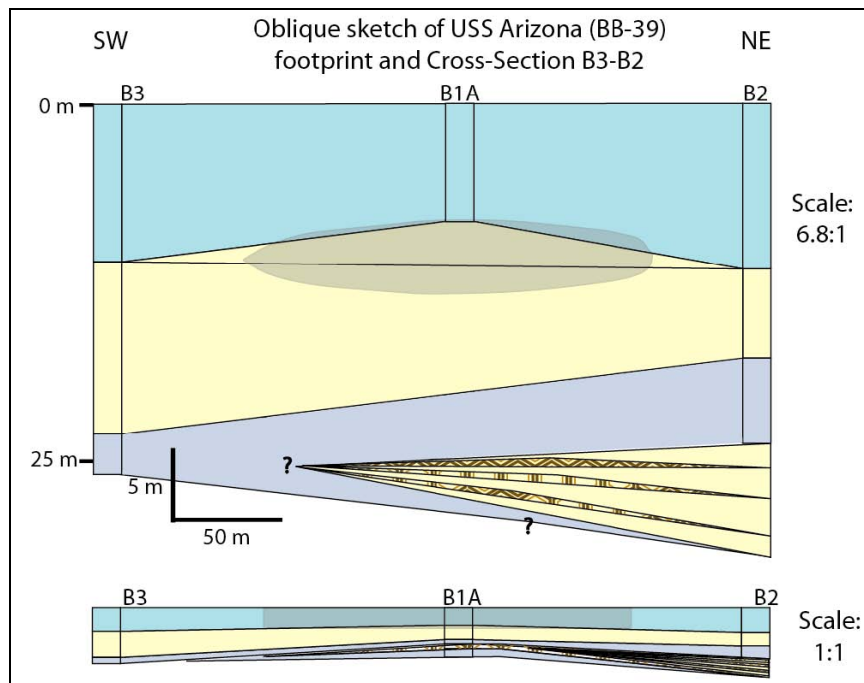
Figure 10.8. A proposed model of the lithology directly beneath *Arizona* between B3 and B2. The silty clay unit thickens toward the northeast (stern). Coraline rubble may be beneath the vessel midship, offshore B1A.
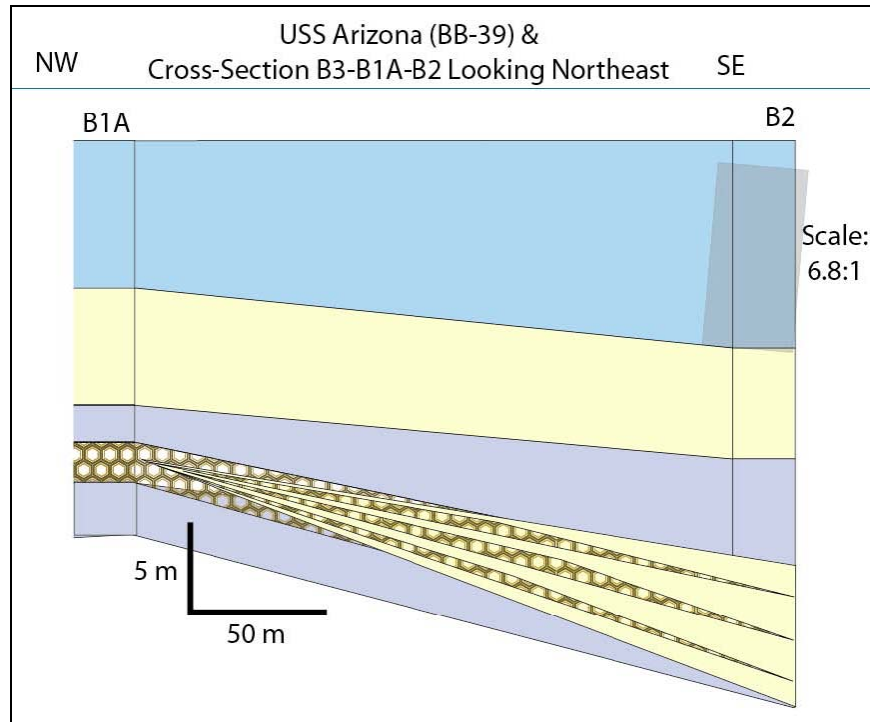
Figure 10.9. A proposed model of the downslope lithology between B1A and *Arizona* based on the B2 borehole to the northeast. The silty clay unit and the clay silt-to-sandy silt thickens toward the southeast (port side). Coralline rubble may be beneath the starboard side of the vessel midship, offshore B1A.

USGS MULTI-SENSOR CORE LOGGER

At the lab in Building 42, on Ford Island, samples in Shelby tubes were logged for their geotechnical properties on the USGS multi-sensor whole core sediment-logging device, built in Great Britain by Geoteck, Ltd. Sealed cylindrical sediment cores were placed horizontally upon a transport sled and moved by a computer-controlled stepper motor through a frame supporting three sensors (Figure 10.10). In a sequence, the logging device measures core diameter and attenuation of gamma rays from a ^{137}Cs source to compute soil wet bulk density. Measurements of density were typically taken at 1cm increments, often within the first hour after the cores are sampled. The transport sled is capable of carrying individual core sections up to 1.5 m in length. Because the core liner is steel, we are able to only characterize the bulk density of the sediment, but not the magnetic susceptibility of p-wave velocity.

The USGS developed an Apple HyperTalk™ driven software program called HYPERSCAN to automate the logger system and support a number of user and system tailored scanning options (Kayen and Phi, 1997). The program includes a suite of subroutines for system

USGS Core Sediment Logger, Bldg. 42,
Pearl Harbor

Figure 10.10. USGS core sediment logger set up in Navy Building 42 during the drilling operations. An enameled steel Shelby tube is being scanned (USGS Photo).

calibration and permits the sensors to be activated or disabled. For example, at Pearl Harbor the cores retained sediment within metal core liner (e.g. Shelby tube samples) that not allow for measurement of magnetic properties: in this case we disabled the magnetic susceptibility sensor to increase the efficiency of the system. Computer automation also allows the technician to maintain some physical distance from the Cesium (^{137}Cs) gamma-ray source. During automated scanning, an un-split sediment core is driven down a track system in user-prescribed increments and the Macintosh computer interrogates sensors. As data enter the computer, the bulk density, and p-wave velocity and magnetic susceptibility if they were logged, are calculated, logged into a matrix data file, and presented in real-time on a 3-plot graphics display window.

<u>Wet Bulk Density</u>

Bulk density is the ratio of the total soil weight, to the soil volume. The configuration of our device allows for a core to pass between a scintillation counter and a vessel emitting a

one-cm columnated beam of gamma rays from a radioisotope ^{137}Cs source. Sediment bulk

density (ρ_b) is calculated from the gamma ray attenuation characteristics of the cores according

to Lambert's law. For a user-defined time period, the number of gamma decays emitted from

the Cesium-vessel, passing through the core and received at the scintillation detector is counted.

To address the health and safety concerns of technicians and satisfy the requirements of our

radiation use permits and NRC license, we use lead shielding to reduce the amount of gamma

ray emission away from the scintillation counter sensor to nearly background levels. The

number of scintillation's transmitted from the source to the scintillation counter through air, is

referred to as the unattenuated gamma count, Io. For the case where a homogeneous material of

some thickness, d, lies between the Cesium source and sensor, the attenuated gamma ray count,

I, can be related to the unattenuated number of gamma decays, Io, the material thickness, d, the

soil bulk density, ρb, and the soil Compton scattering coefficient, μs, by Lambert's Law (CRC

1969):

$$I = Io \exp \{-\mu_s \rho_b d\} \qquad [1]$$

The bulk density of the soil can be determined as follows:

$$\rho_b = 1/\mu_s d \ln (Io/I) \qquad [2]$$

For recovered whole sediment cores encased in liners, we must account for the influence of the

core liner to get an accurate estimation of the soil density. The liner correction accounts for

liner attenuation of the gamma-ray beam through absorption and scattering, effects controlled

by 1) the liner Compton scattering coefficient, μl; 2) liner wall thickness, l; and 3) liner wall

density, ρ_l. For sediment contained within a core liner of outer diameter, D, and double-wall

thickness, 2l, equation [2] can be rewritten as:

$$I = Io \exp\{-\mu s \rho_b (D-2l)\} \cdot \exp\{-\mu_l \rho_l 2l\} \qquad [3]$$

Equation 3 relates the attenuated gamma-ray count to the partial scattering influences of the

liner and soil, and can be used to assess the density of material contained within a variety of liner-types, both plastic and metal. To determine the bulk density of soil, equation [3] must first undergo transformation to base-e logarithm.

$$\rho_b = \ln (Io/I) - \mu_l \rho_l 2l / 1 / \mu_s (D\text{-}21) \qquad\qquad [4]$$

CALIBRATIONS

Density measurements of soil contained within intact core-liner are calibrated to the known standards of water (ρ_w=1.00 g/cc) and aluminum (ρ_{al}=2.70 g/cc). These two standards serve as end-members that fully-bound the limits of soil density found at Pearl Harbor. The added advantage of using these materials is that their respective Compton scattering coefficients, μ_w and μ_{al}, are similar to those of soil pore water and soil alumina-silicate particles, although we determine these parameters empirically. To account for the influence of the liner, a water-aluminum standard is prepared by inserting a solid-cylinder of 6250 or 1100F aluminum into an unsplit section of core liner identical to the liner used for soil sampling. The length of milled aluminum fills one-half the total length of the "calibration standard"-core liner and distilled water fills the remaining portion. Caliper measurements of the liner diameter and wall thickness are made to determine the travel path-length through the liner and interior space.

During the density calibration, the numbers of scintillation's-per-second are logged for transmission of gamma rays through air to give a measure of Io. Similar measurements are made for the "calibration standard" to determine the scintillation count for water-filled liner, I_w, and aluminum-filled liner, I_{al}. We determine the attenuation ratios for water and aluminum (Io/I_w and Io/I_{al}) and solve for the remaining unknowns, $\mu l \rho_l$ and μs, by setting up two simultaneous equations and eliminating one of the variables. For each soil-core, we scan the whole-round sections using the same Compton scattering parameters that correct the calibration-standards water and aluminum to their known values of density.

Calibration standards are run repeatedly during testing programs. Typically, to calibrate the sediment-core profiles for density, measurements are made from our calibration-standard after every core is logged on our device. The empirical Compton scattering coefficient for soil that is determined by this method tends to be approximately 40% lower than the published value

for water, and at present the reason for this is unknown. The circular cross-section of soil cores, as compared with an idealized tabular cross-section may be the cause of the lower μs, and future experiments are planned to assess the influence of core liner geometry on the scattering of gamma-rays.

After system calibration is complete, soil cores are run through the logger system and calibration corrected densities and velocities are presented, along with magnetic susceptibility, on a real-time graphics display. Typical run-time for driving a 150 cm core through the sensor array is approximately 35 minutes.

SYSTEM QUALITY ASSURANCE AND QUALITY CONTROL

Several approaches are taken to assess the quality of our non-invasive measurements of bulk density and sound speed velocity through a core liner. After extensive use of our system at sea and in our shore-based laboratory, several hundred calibration log files containing 30 or more data points were separated into individual files for water-filled and aluminum-filled core liner. These material dependent sub-sets of the calibration files were then used to calculate the mean and standard deviation for the measured density and velocity and compared with the known values for water and aluminum presented in parenthesis (Table 10.1).

The mean value of the calculated and measured density of distilled water was within 0.4% of the known value and the mean value for aluminum was exactly the known value. It was found that the standard deviation for density measurements is on the order of 0.6-1.0% of the measured value.

Density Statistics	Distilled Water	Aluminum
Mean Density (g/cc) (Known ρb)	1.004 (1.00)	2.700 (2.70)
Density Std. Dev. (g/cc)	0.010	0.016

Table 10.1. Data quality for gamma-ray bulk density (Known values are shown in parentheses).

RESULTS FROM THE USGS MULTI-SENSOR CORE LOGGER

Whole round core samples were scanned using the logger device within 24 hours of their initial sampling. Sediment recovery varied widely depending upon lithology type. Almost no recovery occurred in the uppermost silty sand, sandy silt, gravel, and coralline rubble deposits of the three borings. Beneath the coarse upper unit are silty-clay and sandy-silt deposits that had recovery of 68-100% of the length of the sample tube. The wet bulk density profiles are intermittent sections through the sediment column with gaps of unknown density properties in-between, although the lithologies of these gaps are recorded. The tops of the tubes are only partly filled, such that the computed density falls off due to the large water filled void. This void is eliminated in our stress calculations, but presented here in Figure 10.11.

Consistent with the lithologies noted in the Hirata & Associates report (see Appendix), a higher density deposit, typical of coarse grained sediments is found toward the bow of the vessel (B3); a low density deposit, typical of finer grained sediment is found near the stern of the vessel (B2). At B1A, mid-ship and shoreward of the hull, a coarse higher density deposit fines downward through the sampled section. The density profile for B2 was used to compute the natural seafloor effective overburden stress above consolidation test samples.
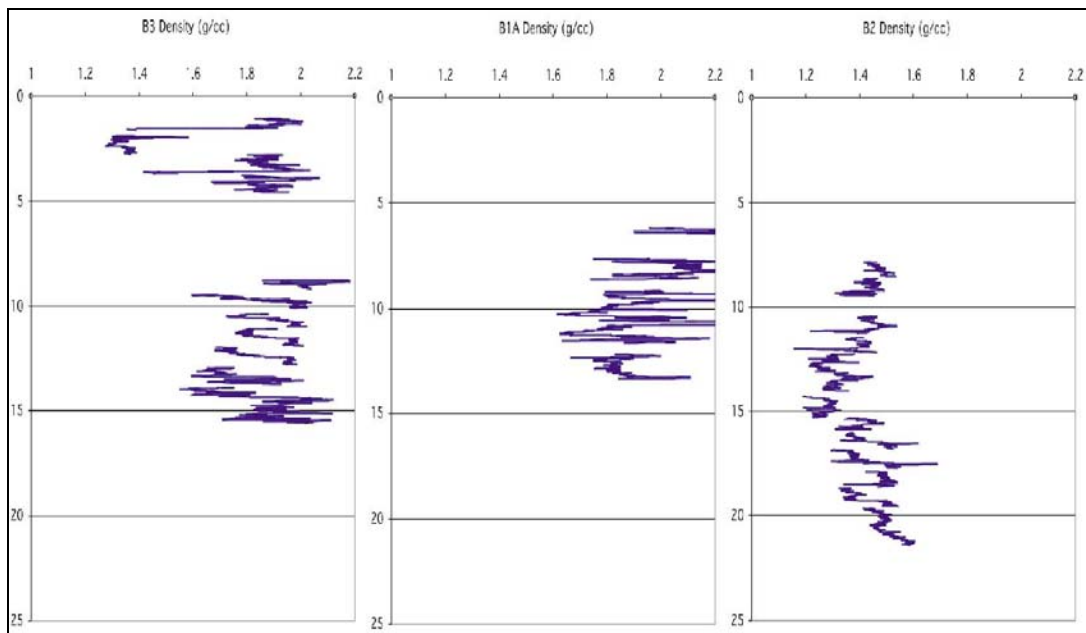

Figure 10.11. Wet bulk density of samples taken at borings B1A, B2, and B3.

CONSOLIDATION TESTING FOR STRESS HISTORY

A suite of 12 consolidation tests were performed on sediment samples from borehole B2, the thickest accumulation of fine grained sediment among the three boreholes (Table 10.2). Consolidation tests are performed to determine the settlement characteristics and the maximum past pressure felt by the sediment (σ'_{vm}). Twelve consolidation tests were performed within a triaxial cell using either a constant rate of strain-loading technique developed by Wissa and others (1971) or the traditional incremental loading method of Casagrande (1936). In preparation for this procedure, a thin wafer of sediment was confined within a cylindrical ring and placed at the base of a fluid filled cell. After the cell was filled with de-aired water the sediment was uniaxially loaded either at a constant rate of compressive strain or incrementally loaded with static weight. During this procedure pore water pressure, axial deformation, and axial load were continually monitored and automatically computer-logged at predetermined intervals.

From the consolidation data the void ratio (e) (volume of the voids/volume of the solids) was plotted versus the log of the vertical effective stress. With such a plot, a curve similar to that in Figure 10.10 is usually produced. The right side of the curve defines a straight line called the "virgin compression line." The slope of this line is the compression index (Cc). The compression index indicates the amount of void ratio change for a tenfold increase in vertical stress beyond σ'_{vm}. Extrapolating the virgin curve to higher void ratios and employing the

Core	Depth ft.	Interval cm	Icon #	σ'_{vm} (ksc)	C_c	e_o	σ'_{vo} (ksc)	OCR	σ'_e (ksc)	Quality	Sample lith type
B2	27.5-30	65.8-68.3	Icon 205			3.23	0.45466071			Unusable	soft clay , swirled disturbed mix
B2	32.5-35	86.3-88.8	Icon 202	0.64	0.97	2.5	0.530125574	1.207261132	0.109874426	Poor	soft, darkgreenish-blackish gray clay, homogeneous
B2	42.5-45	87.5-90	Icon 208			3.11	0.681055301			Poor/Unusable	soft, sticky, dark greenish gray clay
B2	45-47.5	88.3-85.8	Icon 206	0.52	2.3	4.69	0.718787732	0.723440282	-0.198787732	Poor	uniform, soft gray clay
B2	47.5-50	82.3-84.8	Icon 203	0.82		2.31	0.756520164	1.083910302	0.063479836	Good	gray silty clay
B2	47.5-50	87.3-89.8	Icon 204	0.86	2.5	4.34	0.756520164	1.136783976	0.103479836	Fair	soft, gray silty clay, homogeneous; wood fragment?
B2	52.5-55	06.3-00.0	Icon 207	0.93	1.89	3.18	0.031905020	1.117808577	0.098014972	Very Good	soft, greenish gray clay
B2	55-57.5	87.3-89.8	Icon 200	0.86	1.19	2.49	0.86971746	0.988826878	-0.00971746	Very Good	soft, uniform, olive gray clay; minor thin shell fragments
B2	57.5-60	86.2-88.8	Icon 199	0.9	1.2	1.49	0.907449891	0.9917903	-0.007449891	Fair	olive gray sticky clay
B2	65-67.5	86.3-88.8	Icon 201			2.44	1.020647187			Poor/Unusable	soft, dark gray, sticky clay; minor thin-walled shell fragments
B2	67.5-70	81.8-84.3	Icon 197	0.82	0.71	1.98	1.058379618	0.774769266	-0.238379618	Fair	grayish black sticky clay
B2	67.5-70	85-88	Icon 196	0.55	0.71	2.18	1.058379618	0.519662312	-0.508379618	Poor	soft, dark greenish gray, sticky clay
B3	40-42.5	84.6-87.3	Icon 198			1.43				Poor/Unusable	stiff, mottled, yellowish-greenish gray clay

Table 10.2. Consolidation test results from fine-grained samples. Listed are the borehole (core); sub-bottom depth (ft); depth in the Shelby tube (cm); test number; maximum past pressure; compression index; initial void ratio; estimated effective overburden pressure (ksc); OCR; excess effective stress; test quality; and sediment characteristics.

Casagrande (1936) graphical construction, the maximum past stress can be calculated. A measure of the consolidation state is the overconsolidation ratio, the ratio of the maximum past pressure felt by the sample (σ'_{vm}) by the *in situ* effective (buoyant) overburden stress (σ'_c). The individual test plots for each consolidation test are presented in the Appendix with calculations of initial void ratio and the coefficient of compression.

An OCR of 1.0 indicates normally consolidated sediment, meaning that the sediment is in equilibrium with the current thickness of overburden of sediment. For OCR of less than 1.0, the sediment has not yet fully consolidated to the *in situ* overburden stress, whereas for OCR greater than 1.0 indicates that the sediment has experienced pressures in excess of current overburden loads. Overconsolidation of near-surface sediment is caused by, among other factors, electro-chemical bonds, overburden erosion, cementation, and current reworking. Often, overconsolidation is a near surface phenomenon and is lost at depth. Another measure of consolidation state is the effective excess pressure, σ'_e, that is σ'_{vm} - σ'_{vo}. This parameter is useful for estimating the amount of stress equivalent of material removed above a sediment deposit.

The results of the consolidation test suite strongly indicate that the sediment surrounding USS *Arizona* is normally consolidated. Overall, the samples lack excess effective stress; that is, they are in equilibrium with the overburden sediment. Thus any application of new stress will drive the sediment into the virgin compression regime, initiating new settlements of the loaded sediment.

STATIC SEDIMENT STRESS EXERTED BY THE SINKING OF USS *ARIZONA*

USS *Arizona* was commissioned in 1916 at the Brooklyn Navy Yard, New York. The full weight displacement of the vessel, assumed here to be the vessel weight in December 1941, was approximately 37,600 tons. The total and buoyant density of steel is 7.85 and 6.82 g/cc, respectively, thus the submerged weight of the vessel beneath the waterline is approximately 33,000 tons (30.5M kg). The Length and beam, at the waterline, of the vessel are 185 m and 29.6 m, respectively, and we estimate the area of the flat bottom to be 4,300 m^2. Thus the effective stress of the vessel acting uniformly on the seafloor directly beneath the centerline of the vessel is approximately 30.5M kg/43M cm^2, or 0.70 kg/ cm^2. This stress level is equivalent to approximately 9 m of deposited sandy sediment with a bulk density of 1.8 g/cc.

SETTLEMENT ANALYSIS

A preliminary analysis of the vertical settlement of sediment beneath the vessel assumes that the hull is a rigid mat that is uniformly loading the ground beneath the centerline of the vessel. The initial void ratio (volume of the solid particles/volume of the void space) of the soil deposit can be estimated from the core sediment logger profiles assuming a grain specific gravity for the solid particles, and from the initial state and consolidation characteristics of the consolidation test samples. Table 10.3 lists the initial void ratio estimates for each of the Shelby Tube soil samples tested, and the individual test results are presented in the Appendix. Based on the observation of normal consolidation (OCR ~ 1.0) in all the test samples, the void ratio and full consolidation under an additional load of 0.70 kg/ cm^2 is computed as follows:

$$e = eo - C_c LOG \{P/P_o\} \qquad [5]$$

where P is the effective overburden stress of the overlying soil (P_o) plus the added stress of the vessel pressure on the seafloor (assumed to be 0.7 kg/ cm^2). The fine-grained portion of the sediment column, susceptible to the majority of the settlement was subdivided into individual layers represented by the Shelby tube sample taken within it. These layers have variable thicknesses $H_{inc.}$ depending on the sampling depths. We compute the individual layer settlement as:

$$\Delta H_{inc.} = H_{inc.} *(eo - e)/(eo + 1) \qquad [6]$$

And the total settlement ΔH beneath the vessel as the sum of the incremental settlements, or

$$\Delta H = \Sigma \Delta H_{inc.} \qquad [7]$$

The addition of the USS *Arizona* pressing on the seafloor exerts 0.7 kg/cm2 on top of the prior stress level of the sediment effective overburden (Table 10.3). We estimate that near the borehole area B2, these loads resulted in ~1.6 m (5 ft.) of settlement of the foundation sediment beneath the vessel. This slow process of consolidation followed the abrupt initial impact of the vessel on the seafloor. These settlements, unlike the initial loading of the seafloor on December 7 that likely resulted in some bearing failure of the near surface sediment, would

Core	Depth ft.	σ'_{vm} (ksc)	C_c	e_o	σ'_{vo} (ksc)	e	H_{inc} (m)	Δh (m)	$\Delta h/H$
B2	27.5-30			3.23	0.455	2.650	2.846	0.391	0.137
B2	32.5-35	0.64	0.97	2.5	0.530	2.145	0.762	0.077	0.101
B2	42.5-45			3.11	0.681	2.670	3.049	0.327	0.107
B2	45-47.5	0.52	2.3	4.69	0.719	4.011	0.762	0.091	0.119
B2	47.5-50	0.82		2.31	0.757	1.902	0.762	0.094	0.123
B2	47.5-50	0.86	2.5	4.34	0.757	3.629			
B2	52.5-55	0.93	1.89	3.18	0.832	2.679	1.524	0.183	0.120
B2	55-57.5	0.86	1.19	2.49	0.870	2.185	0.762	0.067	0.087
B2	57.5-60	0.9	1.2	1.49	0.907	1.192	0.762	0.091	0.120
B2	65-67.5			2.44	1.021	2.115	2.287	0.216	0.095
B2	67.5-70	0.82	0.71	1.98	1.058	1.823	0.762	0.040	0.053
B2	67.5-70	0.55	0.71	2.18	1.058	2.023			
					Total Settlement	TOTAL H (m)		1.576	

Table 10.3. Settlement analysis of sediment beneath the hull of USS *Arizona*. A load of 0.7 kg/ cm[2] was used in addition to the effective overburden pressure to represent the new application of loads of the USS Arizona and overburden sediment on the seafloor directly beneath the centerline of the vessel. At the edges of the hull, and away from the vessel, the load exerted by the hull diminishes as a function of depth and lateral distance.

need years or even decades to complete before equilibrium was reached between the new loads. Thus, portions of the vessel subaerially exposed in the 1942 salvage operations are now submerged beneath approximately1-2 m of water. The tilt of the vessel, seaward is likely due to the seaward thickening wedge of fine-grained sediment. In a future analysis we will estimate the amount of total predicted tilting that can be expected at the memorial site. The heterogeneity of the soil deposits beneath the vessel indicates that the stern overlies a large wedge of soft-fine-grained sediment capable of large settlements, whereas the bow is founded on stiffer deposits of sandy silt and silty sand, with less clay near the surface. It is likely that this sediment variability has resulted in the stern settling to a greater extent than the bow.

CONCLUSIONS

The study presented here, addresses the potential for normal settlement processes to affect the orientation and elevation of USS *Arizona*, with respect to the seafloor and the waterline. Three boreholes around the vessel indicate that the vessel rests upon highly variable sediment. The settlement potential of the vessel is greater toward the stern, and toward the port side (bay side). A coralline rubble layer observed at boring B1A midship on the shoreward side

may act to prevent settlement of the vessel there and may amplify tilting toward the bay. The presence of the stiffer rubble zone may also enhance differential settlement beneath the vessel that can result in hull stresses that deform the underbody of the vessel. In the area of maximum settlement potential, we compute a estimated settlement at full consolidation of approximately 1.6 m. Future measurement of the stiffness properties of the sediment, and monitoring of the settlement of the vessel is recommended. A 2-dimensional settlement analysis is needed to estimate the final degree of seaward tilting that is expected to occur.

REFERENCES

Casagrande, Arthur
     1936 The Determination of the Pre-Consolidation Load and Its Practical Significance. In *Soil Mechanics and Foundation Engineering* Vol. III, pp. 60-64. Cambridge, Ma.

Kayen, R. and Phi, T.N.
     1997 A Robotics and Data Acquisition Program for Manipulation of the U.S. Geological Survey's Ocean Sediment Core Logger. *SciTech Journal* 7 (5):24-29.

Kayen, R., Edwards, B. D., Lee, H. J.
     1999 Nondestructive Laboratory Measurement of Geotechnical and Geoacoustic Properties through Intact Core-liner *Nondestructive and Automated Testing for Soil and Rock Properties, ASTM Special Technical Publication-1350,* W. A. Marr and C.E. Fairhurst *eds., American Society for Testing and Materials*, p. 83-94.

Wissa, A. E., Christian, J. T., Davis, E. H., and Heiberg, Sigurd
     1971 Consolidation at Constant Rate of Strain. *Journal of the Soil Mechanics and Foundations Division, ASCE,* 97 (SM10):1393-1413.

CHAPTER 11

Conclusions and Recommendations

Matthew A. Russell and Larry E. Murphy

The interdisciplinary research approach to characterizing and understanding USS *Arizona* deterioration and integration into a predictive model reported here was designed to produce cumulative data whose synthesis will inform management actions regarding long-term stewardship of this National Historic Landmark vessel. Beyond informing management decisions about *Arizona*, we believe this research approach has produced results that contribute to the disciplines involved, and are directly applicable to the thousands of steel legacy vessels submerged worldwide. Although lack of complete funding resulted in gaps in our knowledge about critical aspects of *Arizona*'s deterioration, we have learned a great deal that will allow National Park Service (NPS) and U.S. Navy managers to make correct decisions about immediate needs within a stewardship framework. In addition, because the *Arizona* research is not complete and is ongoing, the work reported here is an important step toward refining questions that guide future research directed toward a full understanding of *Arizona*'s deterioration.

In this concluding chapter, we briefly reiterate the goals and objectives of the USS *Arizona* Preservation Project. We then summarize conclusions from each of the research domains that contributed to the overall research project, and synthesize the data to provide some answers to our basic research questions. Finally, we present specific recommendations for future

research, which, along with continuing the monitoring program, requires sufficient dedicated funding to ensure completion.

This chapter's conclusions represent what we have learned so far about USS *Arizona*'s deterioration. Because *Arizona* research is not complete, and data derived from the monitoring program have not been generated and incorporated, these conclusions will be refined and may change as data-gaps are filled and new information is added. Data presented here represents the most informed view of the ship based on observations, investigations and experimentation by experts in numerous fields, but it is necessarily incomplete because not all research domains could be completed.

GOALS AND OBJECTIVES

The USS *Arizona* Preservation Project's primary focus was to acquire requisite data for understanding and characterizing the complex corrosion and deterioration processes affecting *Arizona*'s hull, both internally and externally, and to model and predict the nature and rate of structural changes resulting from corrosion. In simple terms, our basic question, which was articulated by the first two superintendents, Gary Cummins and Bill Dickinson, has been "what is happening to *Arizona*'s hull, and how quickly is it happening?" Hull deterioration rates have direct implications for potential release of oil still contained within the ship. Understanding the complex hull corrosion processes, structural changes and oil release patterns studied during this research project offers the most effective method of mitigating the potential oil-release hazard and achieving the balance between site stewardship and environmental impact.

PRINCIPAL RESEARCH DOMAIN CONCLUSIONS

Each of the specific research domains addressed during this project either directly or indirectly relates to our principal goals and objectives. Here, we briefly discuss each research domain and highlight how they are related, beginning with broadest research domain and working through the contributing studies.

The finite element model (FEM) created by the National Institute of Standards and Technology (NIST) is the cumulative product incorporating field and experimental data that

most directly addresses questions regarding how quickly *Arizona* is deteriorating (Chapter 6). This model incorporates all the data gathered and synthesizes it into a computer-based mathematical projection depicting actual structural deterioration in calendar years, which are derived from corrosion rates. For now, funding has only allowed development of an 80-ft. section, frames 70–90, from the midships of the 608-ft. battleship.

To accurately predict deterioration rates of *Arizona*'s structural elements, we needed to know steel corrosion rates in all locations of *Arizona*'s hull. Determining these corrosion rates was the primary goal of a corrosion study coordinated by University of Nebraska-Lincoln and the NPS (along with contributions by many other organizations) (Chapter 5). The corrosion study included a metallurgical and metallographic analysis to characterize *Arizona*'s steel to allow a more accurate corrosion characterization. It included direct measurements of corrosion rate by sampling *Arizona*'s hull steel, and it also involved a detailed concretion study to determine a minimum-impact way to predict corrosion rates in locations where direct measurement could not be accomplished. In addition to accurately constructing the baseline FEM using original construction data, corrosion rates determined by this corrosion study were the most important elements in the FEM for accurately predicting structural deterioration sequence and rates.

An important element in determining the nature and rate of steel corrosion is characterization of the environment in which steel corrosion is taking place. Basic chemical properties of seawater and data about water movement are critical for accurate corrosion characterization. In addition, because seawater properties directly influence corrosion, correlating measured seawater properties with known corrosion rates on *Arizona*'s directly accessible exterior was an important goal. It allows us to infer corrosion rates inside the hull, where we cannot directly measure corrosion rates either through hull sample collection or concretion analysis, but where we can collect environmental data using an ROV-mounted water quality instrument. Long-term environmental monitoring coordinated by the U.S. Geological Survey (USGS) and the NPS was therefore a key project component (Chapter 4). Although these measurements are ongoing, interior measurements are limited to accessible spaces. However, the interior has very little to no dissolved oxygen present. These data will be incorporated into the next iteration of the FEM to refine interior corrosion rates.

Also contributing to the overall corrosion study is an analysis of microbially induced corrosion undertaken by Harvard University (Chapter 7). The presence and effect of microorganisms on corrosion rates is especially relevant in the anaerobic environment deep within *Arizona*'s hull. Combined with oil within bunker spaces, microbes may have created a unique corrosion environment. Because these areas are impractical to sample, laboratory experimentation will be necessary to determine microbial impact to corrosion in the interior and in the oil bunker spaces.

In addition to the corrosion study, an analysis of hull stability was also necessary for completing an accurate FEM. The FEM would be compromised if *Arizona* were sitting in an unstable geological matrix, or was continuing to shift or sink within the supporting sediments of the Pearl Harbor bottom. In addition, high-resolution GPS hull monitoring would not be valid. To address these concerns, the USGS conducted a detailed geotechnical analysis of sediments surrounding *Arizona* to ascertain their stability and state of compression and determine if *Arizona* were potentially experiencing external movement from sediment shifts (Chapter 10). At the same time, the NPS conducted on-going GPS and other monitoring of the hull to measure both external and internal hull movement (Chapter 9), for which sediment compression provides the basic control.

Finally, the Medical University of South Carolina's (MUSC) chemical characterization of oil being released from *Arizona*'s hull was important for a number of reasons (Chapter 8). First, data were used in a supporting role, indirectly allowing us to make limited inferences about the condition of oil bunkers deep within *Arizona*'s hull that also allows an important monitoring variable. Second, MUSC's oil analysis was a key research domain because it allowed us to trace the environmental impact of the continually seeping oil presently being released into Pearl Harbor from *Arizona*. On-going monitoring of oil release rates by the NPS contribute to this analysis and give us another line of evidence for assessing the overall condition of the battleship's hull (Chapter 9). Continuing periodic analysis of oil samples are important to track potential internal hull structure changes.

In the following sections, we summarize conclusions from each research domain and from supporting studies through the final product, to demonstrate how data from each research domain contributes to the next, building towards answers to our most basic questions.

ENVIRONMENTAL PARAMETERS

Principal Questions: What is the nature of the interior and exterior environment of *Arizona*? How is *Arizona*'s environment changing? How does it affect *Arizona*'s deterioration?

Exterior Environment

Continuous current and wave data, along with water-column properties, were collected on and near *Arizona* from November 2002 to April 2005. Oceanographic measurement indicate that tides are a mixed, semi-diurnal type with a minimum, mean and maximum tidal range of 0.4 m, 0.6 m and 0.9 m, respectively. Generally, waves are not an important factor in the vicinity of USS *Arizona*'s hull. Those observed were, while long period (~20 s), very small (order of cm's) and likely due to open-ocean long-period swell. Vessels passing close to the study site are likely responsible for the high-amplitude, low-period motions that were observed. Water flow along the 10-m isobath is dominated by semi-diurnal and diurnal tidal motions, which are modulated to some degree by what appears to be wind forcing during the mid- to late afternoon. Water flow at the surface is down-wind to the southwest. Water flow throughout most of the water column is primarily parallel to *Arizona*'s hull at 0.01-0.02 m/sec and net flow is to the northeast. Flow closer to the seafloor, however, is weaker and more variable in direction. Flow speeds are faster off the port side than the starboard side of *Arizona*'s, and thus the water replenishment times on the port side of the hull are shorter than off the starboard side.

Water column studies showed temperatures were generally slightly higher (mean = 26.03 °C) and less variable (standard deviation = 1.17 °C) along the 10-m isobath than along the 3-m isobath (mean = 24.55 °C, standard deviation = 2.08 °C). A thermocline was often present in the harbor's waters, with the shallower (3 m) and deeper (10 m) water temperatures often differing by more than 2 °C. Water temperatures along the 10-m isobath were generally cooler and less variable off the port side of the hull than off the starboard side, possibly due to faster replenishment times and greater mixing of the water column. Salinity ranged from 16.78 PSU and 42.56 PSU, with a mean ± one standard deviation of 34.33 ± 4.25 PSU. Salinity appears to positively correlate with water temperature and suggests that Pearl Harbor's waters are influenced by freshwater runoff or groundwater effluence in the winter months. pH ranged

between 7.60 and 9.10, with a mean ± one standard deviation of 8.04 ± 0.15 and dissolved oxygen 0% and 288.5%, with a mean ± one standard deviation of 69.5 ± 58.8%. Both pH and dissolved oxygen tended to correlate with the daily insolation cycle, increasing during the morning into the early afternoon followed by decreasing through the night to minimum levels just before sunrise. Oxygen-reduction potential ranged between 150.0 mV and 397.2 mV, with a mean ± one standard deviation of 289.2 ± 50.6 mV. Oxygen-reduction potential had an *inverse* with pH and the percentage of dissolved oxygen during the summer months and a *positive* relationship with pH and the percentage of dissolved oxygen during the winter months when temperature and salinity were more variable. During the vertical profiling, near-surface temperatures were on average roughly 1.03 °C warmer than the near-bed temperatures, near-surface temperatures were roughly 0.85 PSU less saline on average than the near-bed salinities and near-surface dissolved oxygen levels were on average roughly 43.9% higher than the near-bed dissolved oxygen levels.

Combined, these observations support the conclusion that on *Arizona*'s exterior, corrosion rates are higher in shallow water near the surface, and they decline in deeper water near the harbor bottom. In addition, this analysis supports the observation that corrosion rates are slightly higher on the port side of *Arizona*'s hull than the starboard side.

Interior Environment

On *Arizona*'s interior, in general, most parameters were very similar inside the ship as outside. Temperature, salinity, and pH were all within a normal range of variability. Dissolved oxygen and oxygen-reduction potential, on the other hand, varied significantly from baseline measurements outside the hull. The most significant observation is that dissolved oxygen decreased to near-zero within interior spaces that do not receive active seawater exchange. Most significantly, on the third deck, which has no direct access to exterior seawater except through a single vertical hatch, dissolved oxygen averaged only 4.1% saturated. With the exception of a small portion of the first platform accessible through barbette no. 3, there is no access to any interior spaces below the third deck. However, based on data from the third deck and within the torpedo blisters, which indicate that dissolved oxygen can reach 0.0% saturated in spaces that do not have seawater exchange, it is probable that *Arizona*'s interior spaces below the third deck

have extremely low levels of dissolved oxygen, and may even be at 0.0% saturated. Because all of *Arizona*'s original oil storage spaces are below the third deck, and the majority of *Arizona*'s remaining oil is likely still stored in those spaces, it is probable they are undergoing very low corrosion rates. These measurements are supported by dissolved oxygen measurements of interior water during removal of hull coupons. There was no detectable oxygen at all in the interior water.

MICROBIOLOGY

Principal Questions: What microbially induced corrosion (MIC) is taking place in *Arizona*'s interior and exterior areas, and what is the impact on structural deterioration? Can laboratory experimentation model microbially induced corrosion on the oil/bunker interface?

The purpose of microbiological research on *Arizona* was to investigate the role of microorganisms in steel hull corrosion. Specific goals included isolating and identifying microorganisms from the Pearl Harbor, especially within the concretion covering *Arizona*'s steel hull; determining the organisms within the community responsible for corrosion of steel; and investigating environmental parameters that may influence the rate of corrosion by microorganisms.

Harvard University researchers examined the potential role of microorganisms from Pearl Harbor in steel corrosion through laboratory experimentation. Preliminary indications suggest a trend toward pitting corrosion caused by microbes in the biofilm. The bacterial community in concretions on *Arizona*'s hull is dominated by organisms from three groups: Firmicutes, Flavobacteria, and Proteobacteria. Further investigations of concretion microorganisms are needed to determine if the results obtained here are applicable to concretions on other submerged heritage sites and to determine the effect of the microorganisms on corrosion of the underlying metal.

Ultimately, this research is a work in progress. Because key elements of this project remained unfunded during the USS *Arizona* Preservation Project, few conclusions can be made regarding the role of microorganisms in *Arizona*'s corrosion rate. Future work to be done on this project includes further study of the potential of microorganisms to cause corrosion of ASTM A-

36 steel, determining the effects of environmental factors such as temperature, nutrient levels and redox on MIC, and examining microbial corrosion rates on other types of steel that may be found in USS *Arizona*.

<div align="center">CORROSION ANALYSIS</div>

Principal Questions: What is the nature and rate of corrosion taking place on *Arizona*? How does concretion formation affect corrosion rate? Is there a difference in corrosion rate among the original construction steel, the refit materials, and structure affected by the blast and fires?

<u>Metallurgical and Metallographic Analysis</u>

Metallurgical and metallographic analysis indicates steel used to fabricate USS *Arizona* battleship during original construction, 1913–1915, and reconstruction, 1929–1931, were consistent with the best steel available during each time period. The structural steel used in original construction was of surprisingly good quality for a basic open hearth steel technology that was only about 25 years old at the time the first materials were ordered for delivery to the New York Navy Shipyard for *Arizona*'s construction. The somewhat lower quality of the early steel in terms of chemistry and microstructure had no measurable consequences on the damage that occurred on December 7, 1941 or on the results of the present investigation into the deterioration of the *Arizona*'s hull. Typical analysis and comparison with present-day ASTM A-36 steel show minor differences in chemistry between the USS *Arizona*-era steel and present-day ASTM A-36 steel, however they are not considered significant with regard to corrosion response.

Heavy banding in steels from both periods could adversely affect the corrosion resistance under anaerobic conditions that prevail during a corrosion cycle developed under hard concretion layers that began to form when the ship sank. Banding would have no effect on corrosion rate under aerobic conditions that may occur on local areas on the exterior hull.

Exterior Corrosion Analysis

Concretion Analysis

Results of concretion analysis confirm that concretion acts as a sink for iron corroded from the adjacent steel hull, accounting at one location for about 60% of the iron lost from the hull. In other words, as the steel corrodes, iron molecules migrate from the hull into the concretion covering the ship. Based on x-ray diffraction (XRD) data, iron appears primarily as iron carbonate with lesser amounts of magnetite. These observations are confirmed from *in situ* corrosion potential and pH measurements by superimposing the data on a calculated potential/pH Pourbaix diagram. The data correspond to fields stable with respect to iron carbonate and magnetite.

Concretion XRD reveals the compounds $FeCO_3$, $CaCO_3$ and Fe_3O_4. A mean iron content of 53% is calculated from environmental scanning electron microscopy (ESEM) data while x-ray fluorescence (XRF) reveals 43% on a different sample. Direct chemical analysis of the same sample used for XRD reveals comparable iron content. Superposition of E_{corr}/pH data on the water-iron-CO_2 system confirms the presence of siderite and magnetite from the steel hull through the concretion cross-section to sea water. Results indicate that concretion characteristics vary as a function of water depth. Studies continue to correlate these properties with corrosion rate.

Corrosion Rate

For assessing corrosion rate of *Arizona*'s hull, direct measurement of hull thickness and comparison to original thickness is the most accurate methodology, but obviously it is not minimum-impact nor is it impractical for quick and cost-effective assessment. An alternative methodology developed on USS *Arizona* by University of Nebraska-Lincoln researchers, Concretion Equivalent Corrosion Rate (CECR), is beginning to prove itself in this and other applications as a minimum-impact approach for assessing corrosion rate.

Sufficient data at exterior hull locations are now available to determine corrosion rates from the water surface to the harbor bottom, port and starboard. While hull coupon sampling

was only undertaken at frame 75, previous E_{corr} transect surveys indicate that these data are typical of corrosion rates anywhere along the hull in contact with sea water above the harbor bottom. Data suggest that the corrosion rate is slightly higher on the port side above about 20 ft. water depth—deeper than that, the rates converge to equivalent values. On the exterior hull, the corrosion rate follows an empirical equation derived from the best fit for combined data, port and starboard, which is valid to just above the harbor bottom and which can be used to predict corrosion rates across the hull:

$$i_{corr} = 2.956– 0.050 \text{ WD})$$

where

> i_{corr} is the corrosion rate in mils per year (mpy)
> WD is water depth in ft.

Corrosion rate decreases with water depth, as is consistent with a decreasing dissolved oxygen concentration to the harbor bottom. Oxygen concentration inside the torpedo blister decreases into the harbor bottom, suggesting the same behavior occurs beneath the harbor bottom. Based on metal coupon analysis at frame 75, the corrosion rate on the USS *Arizona*'s exterior hull is approximately 3.0 mpy near the surface and decreases by nearly one third to about 1.0 mpy just below the harbor bottom. By comparison, corrosion rates for unconcreted steel in open seawater at the surface are in the 4–8 mpy range. Lower than predicted corrosion rates are directly related to metal-concretion interaction, and subsequent decreased oxygen availability. At the harbor bottom and below, where most of the fuel oil is bunkered, steel-hull coupon samples show that the corrosion rate remains constant or increases somewhat, consistent with potential increased bacterial activity in this region. How far this region extends into the harbor bottom is unknown, although current evidence suggests that corrosion rates below the harbor bottom and in interior compartments of *Arizona* remain low when compared to exterior rates.

As a heuristic device, based on these data, time interval from August 2002 until the plate thickness is reduced to one–half its original thickness can be determined. One–half original thickness was arbitrarily taken as a thickness below which structural integrity is severely compromised, although the FEM provides a more precise value. At 5 ft. depth, port, 27% of 20

lb. plate remains whereas at 5 ft. starboard, 40% of 20 lb. plate remains; these plates have been subjected to corrosion from both sides. Both sides have exceeded the one-half thickness criteria, which are the highest corrosion rates recorded. This area and depth is subject to the heaviest water movement and highest dissolved oxygen; and because the samples were from plate that had corrosion occurring on both sides. At 19½ ft., port, 77% of 37½ lb. plate remains whereas at 15 ft., starboard, 90% of 37½ lb. plate remains. These data translate to time to one–half thickness of 130 years, port, and nearly twice that time, starboard. At 26 ft., port, 87% of 20 lb. plate remains whereas at 22 ft., starboard, 81% of 20 lb. plate remains. These data translate to time to one–half thickness of 160 years, port, and about 90 years, starboard. Below the harbor bottom at 34 ft., port, 90% of 25 lb. plate remains whereas at 32½ ft. starboard, 87% of 30 lb. plate remains. These data translate to time to one–half thickness of 220 years port, and 170 years starboard. These projections are based on exterior shell plate measurements and do not represent what is expected for interior spaces under anaerobic conditions. Further metallographic analysis, especially of the hull coupons, is necessary as well as E_{corr} measurements the hull deeper below the mud line to verify projection of these corrosion rates to the full buried hull.

Interior Corrosion Analysis

Based on a variety of data and analytic methods, a comprehensive understanding of corrosion processes occurring on the hull above the harbor bottom has been accomplished. With this information as background, corrosion analysis at and below the harbor bottom and in interior compartments can be inferred, however, research should continue to further refine calculated corrosion rates on inaccessible hull components. Based on environmental data collected in *Arizona*'s interior spaces, which indicate low to no detectable dissolved oxygen levels, information to date suggests corrosion levels will be at or below the 1.0 mpy rate we recorded just below the harbor bottom. In fact, if the lower spaces within the hull are entirely anaerobic, which is likely, the corrosion rate could be lower than any measured so far.

GEOLOGICAL ANALYSES

Principal Question: How stable are the sediments upon which *Arizona* rests?

The study presented here addresses the potential for normal settlement processes to affect the orientation and elevation of USS *Arizona*, with respect to the seafloor and the waterline. Three boreholes around the vessel indicate that the vessel rests upon highly variable sediment. The settlement potential of the vessel is greater toward the stern, and toward the port side (bay side). A coralline rubble layer observed at the boring midship on the shoreward side may act to prevent settlement of the vessel there and may amplify tilting toward the bay and be responsible for the slight, 2–3° port list. The presence of the stiffer rubble zone may also enhance differential settlement beneath the vessel that can result in hull stresses that potentially deform the underbody of the vessel. For maximum settlement potential, there is an estimated settlement at full consolidation of approximately 1.6 m. Future measurement of the stiffness properties of the sediment and monitoring of the settlement of the vessel is recommended. A two-dimensional settlement analysis is needed to estimate the final degree of seaward tilting that is expected to occur.

STRUCTURAL STABILITY DETERMINATION

Principal Questions: How stable is *Arizona*'s hull? How can we measure structural changes?

External Stability

GPS Monitoring

Horizontal and vertical differences recorded from by high-resolution GPS measurements from 2003–2006 have consistently been below the 5-cm circle of error, well below the 10-cm level we determined necessary to indicate significant movement. From these data we conclude that no measurable movement occurred during that 2½ year period.

Internal Stability

Internal structural monitoring of USS *Arizona* has been a qualitative process primarily using the VideoRay ROV to visually examine interior areas and note observable changes over time. Interior investigation took place from 2001–2005 in all accessible areas for measuring and monitoring interior environmental factors and corrosion parameters. During this process, overall internal structural condition were observed and noted, and no observable changes to internal spaces were noted during this period.

FINITE ELEMENT ANALYSIS

Principal Question: How can the cumulative results of *Arizona* research be used for modeling and predicting long-term changes in the hull, and how and when will those changes occur? Can a predictive model be developed that will allow incorporation of new data and information? How do we validate such a model?

Results of the USS *Arizona* FEA seem to indicate that, after nearly 67 years on the bottom of Pearl Harbor, the wreck is approximately one-fifth to one-fourth of the way to an eventual collapse due to corrosion. A surprising aspect of the results is that collapse is predicted to initiate in the side and bottom of the hull before any significant collapse events in the exposed regions of the upper decks. In addition, an important observation from this analysis is that, while the exposed decks above the harbor bottom become extensively deteriorated, the core cylinder of the wreck, consisting of the volume bounded by the third deck, the inner bottom and the side oil tanks, is still relatively intact even after 95% of steel thickness has corroded. This means that many of the oil containing spaces within the ship may retain integrity until the year 2250 or beyond. This may be a conservative estimation based on the corrosion-rate data incorporated into the model.

We believe this hull section selected for analysis, frame 70–90, to be representative of the rest of the ship, and its investigation and analysis provide a conservative estimate of corrosion rates for the initial FEM for two reasons. Project principals desired a conservative, faster, corrosion rate for the FEM, which should present more the worst case scenario rather than the

most optimistic projection. The analytical hull section's location adjacent to blast-damaged hull areas provides two factors that make the FEM conservative. The forward portion of the hull section was subjected to heat and blast damage during the explosion and sinking of the vessel, and it may be subject to somewhat increased corrosion rates. The second aspect, and more important, is that hull corrosion appears to be mostly oxygen driven. By projecting corrosion rates measured from the analytical hull section's exterior, which has been subjected to normally oxygenated sea water, to the interior, which we know to be nearly to fully anaerobic, we produce a conservative FEM.

The NIST FEM can be increased in accuracy as better data are collected and key variables are added and refined. A variety of refinements are recommended for the model, which are outlined below. To date, however, the model closely matches observations by researchers on site; we, of course, cannot project its accuracy into the future without inclusion of refined variables and verification through long-term monitoring data. During site mapping and other research activities in the 1980s, NPS personnel noted little upper deck damage in the area of *Arizona*'s galley beyond that attributable to initial damage from the Pearl Harbor attack and subsequent salvage activities. No oil release from upper deck breaches was observed. These observations mesh well with the model predicting that at 10% corrosion thickness loss (approximately 1980), the deck beams in the upper deck would jump significantly in stress, while the second, first and main decks remain in a near unstressed state. No collapsing is predicted, and none was observed during research from 1982–1986. In addition, the upper deck area was undercut by the explosions of the forward magazines; consequently, its support structure has been compromised. This is the only area where deck sagging and collapsed has been observed.

As the vessel reaches 20% corrosion thickness loss (estimated at 2020), the model predicts that upper deck areas begin to show sagging of the beams and deck plates as they continue to thin. This corresponds well with recent (2006) observations of limited upper deck collapse in the galley area, and increased release of secondary oil in the area as more breaches begin to open. To date, therefore, the model seems to be predicting actual behavior reasonably well. It will important to monitor this as we move into the future as one way to validate FEM accuracy.

OIL ANALYSES

Principal Questions: What is the nature of *Arizona*'s oil? How and at what rate does it degrade? What is its impact on the immediate environment of the ship? Is there a signature that distinguishes *Arizona* oil from other Pearl Harbor point sources? How do we measure oil leak volume?

The objectives of the oil study included characterizing oil leaking from USS *Arizona*, characterizing petroleum hydrocarbons in the sediments surrounding the ship and determining if oil leaking from the ship was degradable by microorganisms enriched from surrounding sediments. Oil characterized from *Arizona* suggests that oil leaking from different ship locations are exposed to different environments, based on the extent of *n*-alkane weathering for oil leaking from the stern starboard hatches compared to oil leaking near barbette no. 4. Biomarkers in oil leaking from the ship were also identified in sediments collected near and on atop the hull. Several biomarkers were of special interest because they are not found in Bunker C and were detected on the ship and in surrounding sediments, for example, butylated hydroxytoluene, which is a component of jet fuel. It is likely that oil leaking from *Arizona* is present in surrounding sediments, but it is also likely that hydrocarbons, including biomarkers, from other sources are present in the sediments as well. Aerobic enrichment cultures initiated from *Arizona* sediments were capable of degrading different components of Bunker C in 30–40 days. Certain components remained in oil extracted from enrichment cultures and did not decrease in concentration. These enrichments were capable of degrading certain biomarkers. Other biomarkers were also present in sediments, although in varying concentrations.

The oil studies have contributed to our fundamental understanding of the oil that is leaking from *Arizona*, and the potential of microorganisms indigenous to Pearl Harbor sediments in degrading this oil. In addition, the study was the first comprehensive hydrocarbon fingerprint of Pearl Harbor sediments adjacent to and surrounding the ship, and can be used as a baseline for future studies. A full environmental assessment of the area around *Arizona* and down current along the Ford Island shoreline, is needed to accurately determine the leaking oil's environmental impact.

Oil Release Monitoring

Measured release rates have gradually increased each year in direct proportion to the number of locations monitored: in 1998, 1.0 quart (0.95 liters) was measured from one location; in 2003, 2.1 quarts (2.0 liters) were measured from two locations; in 2004, 2.3 quarts (2.2 liters) were measured from two locations; in 2006, 9.5 quarts (9.0 liters) were measured from eight locations. June 2006 oil release measurements are the most comprehensive completed to date—increase in oil release over previous years is in part explained by more release locations being successfully measured than previously.

Although observed rates of oil coming to the surface has gradually increased over the past several years, there is no indication of increase in amount of oil released from the primary oil containment spaces in the ship's lower decks. The increase in oil volume observed is likely from redistribution of secondary oil contained in overhead spaces on the main and upper decks caused by gradual collapse of upper decks forward of the Memorial, which have the highest corrosion rates and were also affected by the 1941 explosion and subsequent salvage activities.

Primary oil containment spaces, located on *Arizona*'s lower decks, are well below the harbor bottom and probably have corrosion rates lower than any measured on the hull so far. Observed deformation of the upper deck in the galley area, whose support structure is weakened and with the highest corrosion rates, does not reflect the condition of primary oil containment spaces in the lower hull.

Undegraded oil release from the hatch on the starboard side of barbette no. 4 measured in June 2006 is lower than in previous years. These latest data suggest that oil release directly from primary oil containment spaces has decreased over the last several years, supporting the supposition that increased oil release is from secondary oil containment in upper and main deck overhead spaces forward of the Memorial.

Oil release rates vary considerably with differing wind, tide and harbor conditions. More oil is released during choppy harbor conditions and when tour boat and other ship's wakes pass over *Arizona*'s hull, which further supports the oil source as shallow overhead spaces rather than from primary oil containment spaces.

RECOMMENDATIONS

PROPOSED FUTURE STUDIES

There are a number of additional studies recommend as the USS *Arizona* Preservation Project continues that are planned to fill data gaps in the research presented in this report. Several of these studies are critical for developing a complete picture of *Arizona* deterioration.

<u>Finite Element Modeling</u>

There are several recommendations regarding the FEM that are necessary for increasing the accuracy of the results presented here. First, this model should be extended to the entire length of the ship. This would increase the calculation time needed dramatically, but key insights into the behavior of structural elements in the present study can be used to cut down the computation time. For example, once it is determined how a section of deck plating and supporting deck beam deform as the members thin, and it is found to be consistent across the model, this region can be replaced with a single element that has hybrid parameters calculated from the model. Thus, instead of performing calculations on thousands of connected elements, one could be used.

Second, a significant unknown in this study is the damage to the internal load-bearing structures in the lower decks. It is almost certain that the region forward of the main stacks suffered significant damage, but since submersibles and divers cannot reach these regions for direct observations, we must speculate and make best and worst case scenario assumptions for our analyses. These assumptions could be fine-tuned with input from experts in blast damage in the naval community, perhaps at the Naval Surface Warfare Center in Carderock, MD. Initial contacts with researchers at that facility indicated interest but inability to assist due to lack of funding. A comprehensive analysis of blast damage to the ship based on multiple lines of data, and modeled by a FEM similar to that for *Arizona*'s deterioration, would increase the accuracy of this and future models.

Third, *Arizona*'s remains are listing slightly to port, and this causes the self-load to be directed slightly off of vertical onto the load bearing structures. Elastic-plastic collapse of

columns and stanchions will be significantly affected by deviations from vertical, and the effect of the list will be for some structures to collapse sooner than predicted in this model. The effect of the list and how it is changing over time is a factor that should be added to refine the model, based on analysis by USGS.

Fourth, in the present study, the differences in corrosion rates from different regions of the ship were only modeled as differences between whole decks above and below the mud line. A further refinement to the model that would allow for more accurate spatial location of potential developing weak points would be to map detailed, measured differences in corrosion rate onto the structure. Collecting detailed corrosion rate data from multiple locations around the hull, and mapping variations, is recommended.

Finally, because Pearl Harbor is an active naval base, with ship traffic constantly entering and exiting, wakes from passing ships could potentially deliver a significant impact to the hull. The present model deals with slow, steady-state decay of the structure, attempting to predict the timeframe of collapse. It is more likely that a significant failure will be precipitated by a more sudden event such as a wave or a large storm. Using new modules developed to study the effect of landslide-induced waves within reservoirs upon dams, a study could be conducted looking at the magnitude of stress spikes in the wreck with the passing of ships or during large storms.

Microbiological Analysis

One of the most important studies that remains on hold due to lack of funding is an analysis of the role of microbially induced corrosion on *Arizona*'s deterioration, as well as the effect of microbes combined with Bunker C fuel oil within the battleship's fuel bunkers on corrosion rates of lower-deck, oil-containing spaces. Early results from this research are reported in Chapter 7, but the experiments have been on hold for several years. This research is critical because the FEM and analysis of long-term structural deterioration is based on measured corrosion rates from *Arizona*'s exterior, with interior rates estimated using data gathered to date, along with several reasonable assumptions. These assumptions do not factor in the role of microbes in corrosion, and therefore their effect is not calculated into the final FEM developed by NIST. Complete characterization of microbially induced corrosion both on *Arizona*'s exterior

and interior spaces is critical for validating experimental results of the FEM reported in this document.

Exterior Corrosion Analysis

While corrosion rate from hull coupon samples is determined to just below the harbor bottom, there is a continuing question about corrosion below it. Right at the harbor bottom, there appears to be some increase in corrosion due to accelerated bacterial activity there, while the corrosion rates a meter below the mud show the lowest corrosion rates found. What is not established yet is the extent of corrosion between this region and the hull bottom. The data are conflicting, but the concern is that this region is deficient in oxygen compared to the region above it in the water and could lead to a large scale oxygen cell causing accelerated corrosion in the lower part of hull. This can be addressed by implementing corrosion potential monitoring. A permanent high chloride reference electrode could be placed in tubing driven well below the harbor bottom toward the hull bottom to a depth of around 15 ft., and monitored remotely via the internet. A decrease in corrosion potential with depth, consistent with trends reported in sea water, would establish that there is no large scale oxygen cell activity and eliminates this as a variable of concern. Because the unit can access four locations, it would be possible to install at least one electrode at this location. The advantage of monitoring for a one year period is that disturbance of the mud in the vicinity of the hull may bias initial readings and extended time in place would assure that *in situ* readings were reliable.

The same instrumentation could be used to monitor over time the effect of season, wind, temperature and other environment variables on corrosion potential at selected hull sites above the harbor bottom. The data we have obtained are extensive above the harbor bottom but each field operation has occurred from June to December and no data has been obtained during the remaining part of the year. Part of the reason for varying corrosion potential data at the same site over several field operations may be related to seasonal effects. Due to dilution in the drill hole before probes are inserted, pH and corrosion potential readings may be biased and may have yielded data that may not represent true values. To determine if this is a problem and to determine how much of an error was created, it is proposed that pH and corrosion potential

probes be permanently embedded in the concretion with the tip of the probes at the interface, sealed with epoxy and monitored for a one year period.

A corrosion rate sensor (Barnacle cell) that sits on top of a sponge placed directly on the concretion, coupled to a linear polarization resistance (LPR) probe, could give instantaneous corrosion rates. Grounding above the water line on barbette no. 3 would assure adequate contact on the hull while calibration would be accomplished at frame 75, since the corrosion rate is already well-known there. The barnacle cell, once calibrated could then be moved to any site desired on the hull for corrosion rate measurement without having to remove the concretion. Such a device could also be used to correlate with concretion equivalent corrosion rate (CECR) data already obtained between frames 70–90. This would allow rapid and improved ability to collect the detailed corrosion rate data necessary to refine the FEM.

Interior Corrosion Analysis

While some information has been obtained on corrosion rate in interior spaces, the data are indirect and not conclusive. It is believed that more could be done with the barnacle cell (LPR) to determine whether or not some arrangement could be made to mount this cell on an ROV in such a way that corrosion rate readings could be taken directly from a bulkhead.

Cathodic Protection

Cathodic protection is a technique for protecting a structure from appreciable corrosion by incorporating a metal into the corrosion circuit that has a greater tendency to corrode than the structure. Alternately, the equivalent effect can be achieved by inducing a direct current into the structure using a rectification circuit design. The prevention or limitation of corrosion of the external fabric using cathodic protection would reduce fresh sea water entry into regions where corrosion could begin to develop on both sides of hull plate as has already noted from analysis of hull coupon samples. Once the outer fabric is penetrated, cathodic protection would be less effective as a protective measure because current cannot be as effectively "thrown" onto the interior side of outer fabric or onto interior load bearing structures. Cathodic protection could potentially be designed to protect the outer hull or torpedo blister into the mud to the keel. Based

on data from USS *Bowfin*, current demand would be about 3 ma/ft^2 or roughly ⅓ the demand for bare steel.

It is recommended to continue to develop background information regarding the advantages and limitations of cathodic protection as a timely means of arresting what appears to be a gradual top/down deterioration as fresh sea water enters the structure at lower depths. It should be noted that continuous monitoring of rectifier system effectiveness could be automated, and simple to interpret as in the case of the USS *Bowfin*.

OVERALL CONCLUSIONS

USS *Arizona*'s complete structural deterioration, and eventual release of oil within its hull, is by all indications **NOT** imminent. This study has allowed us to quantify, and therefore better understand, the complex corrosion and degradation processes taking place on *Arizona*'s hull. Data combined from many different research studies have been brought together to give us the most complete picture to date on *Arizona*'s status. These are the key points from the study:

- The FEM, which incorporates a detailed analysis of corrosion nature and rate, indicates that the hull is deteriorating slowly. Since sinking in 1941, the battleship has only progressed one-fifth to one-quarter to the way towards total loss of steel due to seawater corrosion. The model predicts that oil-containing spaces on *Arizona*'s lower decks may remain intact for 200+ years from the present. As predicted, *Arizona*'s upper deck areas, closest to the water surface and with the highest corrosion rates on site, are experiencing increased deterioration. It is important to remember, however, that these areas are not integral to *Arizona*'s structural integrity, and do not include primary oil-containing spaces. All oil-containing spaces are deep below the present harbor bottom, within the structural core of the ship that is presently experiencing the lowest corrosion rates on site, and which are predicted to have not yet suffered significant corrosion.

- Environmental impact of the oil currently being released from *Arizona*'s hull is low. Although the amount of oil released daily from the vessel may have increased slightly over the years, this is likely due to increased release of secondary oil trapped in higher

deck overheads because of increased deterioration of the upper deck. This is likely not indicative of an increase in oil release from primary oil containing spaces.

MANAGEMENT RECOMMENDATIONS

1)   At this time there is no scientific justification to alter current management policies of *in situ* preservation. There are critical variables that need to be refined for inclusion into the FEM.

2)   For the present, status quo should be maintained regarding any intervention in *Arizona*'s hull.

3)   Continued research on both *Arizona* and any environmental impact should be supported and stable, sustainable funding should be developed.

4)   Institute the monitoring program consistent with monitoring variables discussed in this report and make it part of the park's core operations. This requires maintenance and expansion of the park dive team. Unauthorized diving should be eliminated. Submerged remote sensing intrusion devices should be investigated and deployed.

5)   Oil containment and diversion alternatives should be investigated. Remote sensing oil quantity detection devices should be explored.

6)   Public education regarding the status of *Arizona*'s deterioration and the NPS's site stewardship should be expanded. Consideration should be given to continuing development of the USS *Arizona* GIS Project and supporting its access on the Internet along with development of video clips and podcasts directed toward answering the most frequently asked questions.

REFERENCES

Aeckersberg, F., F. A. Rainey, and F. Widdel
    1998 Growth, Natural Relationships, Cellular Fatty Acids and Metabolic Adaption of
      Sulfate-Reducing Bacteria that Utilize Long Chain Alkanes Under Anoxic Conditions.
      Archives Microbiology. 170: 361-369.

Alberdi, M., and L. Lopes
    2000 Biomarker 18α(H)-oleanane: Ageochemical Tool to Assess Venezuelan Petroleum
      Systems. *Journal of South American Earth Sciences* 13:751-759.

Altschul S.F., T.L. Madden, A.A. Schäffer, J. Zhang, Z. Zhang, W. Miller, and
      D.J. Lipman
    1997 Gapped BLAST and PSI-BLAST: a New Generation of Protein Database Search
      Programs, *Nucleic Acids Research* 25:3389-3402.

Anwar, H., J.L. Strap, and J.W. Costerton
    1992 Establishment of Aging Biofilms: Possible Mechanism of Bacterial Resistance to
      Antimicrobial Therapy. *Antimicrobial Agents and Chemotherapy* 36:1347-1351.

Anderson, R. T., and D. R. Lovely
    2000 Hexadecane Decay by Methanogenesis. *Nature* 404:722.

American Society for Metals
    1975 *Metals Handbook, Failure Analysis and Prevention*. 8th ed 10.

Ashwood, T. L., and C. R. Olsen
    1988 Pearl Harbor Bombing Attack: A Contamination Legacy Revealed in the
      Sedimentary Record. *Marine Pollution Bulletin* 19:68-71.

Atlas, R. M.
    1981 Microbial Degradation of Petroleum Hydrocarbons: An Environmental Perspective.
      Microbiological Reviews 45:180-209.

    1984 *Petroleum Microbiology*. 1st ed. Macmillan, New York.

Baars, B. J.
    2002 The Wreckage of the Oil Tanker *Erika* : Human Health Risk Assessment of Beach
      Cleaning, Sunbathing and Swimming. *Toxicology Letters* 128:55-68.

Barron, M. G., T. Podrabsky, S. Ogle, and R. W. Ricker
    1999 Are Aromatic Hydrocarbons the Primary Determinant of Petroleum Toxicity to
      Aquatic Organisms? *Aquatic Toxicology* 46:253-268.

Bartholomew, C.A. Capt.
    1990 *Mud, Muscle, and Miracles: Marine Salvage in the United States Navy*. Department of the Navy, Washington, D.C.

Beam, H. W., and J. J. Perry
    1974 Microbial Degradation and Assimilation of *n*-Alkyl-Substituted Cycloparaffins. *Journal of Bacteriology* 118:394-399.

Beckles, D. M., C. H. Ward, and J. B. Hughes
    1998 Effect of Mixtures of Polycyclic Aromatic Hydrocarbons and Sediments on Flouranthene Biodegradation Patterns. *Environmental Toxicology and Chemistry* 17:1246-1251.

Bernard L., H. Schäfer, F. Joux, C. Courties, G. Muyzer, and P. Lebaron
    2000 Genetic Diversity of Total, Active and Culturable Marine Bacteria in Coastal Sea Water, *Aquatic Microbial Ecology* 23:1-11.

Bixian, M., F. Jiamo, Z. Gan, L. Zheng, M. Yushun, S. Guoying, and W. Xingmin
    2001 Polycyclic Aromatic Hydrocarbons in Sediments from Pearl River and Estuary, China: Sapatial and Temporal Distribution and Sources. *Applied Geochemistry* 16:1429-1445.

Blumer, M. and J. Sass
    1972 Oil Pollution: Persistence and Degradation of Spilled Fuel Oil. *Science* 176:1120-1122.

Boll, M., G. Fuchs, and J. Heider
    2002 Anaerobic Oxidation of Aromatic Compounds and Hydrocarbons. *Current Opinion in Chemical Biology* 6:604-611.

Bost, F. D., R. Frontera-Suau, T. J. McDonald, K. E. Peters, and P. J. Morris
    2001 Aerobic Biodegradation of Hopanes and Norhopanes in Venezuelan Crude Oils. *Organic Geochemistry* 32:105-114.

Bram J.B., H.M. Page, and J.E. Dugan
    2005 Spatial and Temporal Variability in Early Successional Patterns of an Invertebrate Assemblage at an offshore oil Platform, *Journal of Experimental Marine Biology and Ecology* 317:223-237.

Candries M.
    12 December 2000 Paint Systems for the Marine Industry, *Notes to Complement the External Seminar on Antifoulings*, Department of Marine Technology, University of Newcastle-upon-Tyne, http://www.geocities.com/maxim_candries

Casagrande, Arthur
    1936 The Determination of the Pre-Consolidation Load and Its Practical Significance. In *Soil Mechanics and Foundation Engineering* Vol. III, pp. 60-64. Cambridge, Ma.

Cerniglia, C. E.
    1992 Biodegradation of Polycyclic Aromatic Hydrocarbons. *Biodegradation* 3:351-368.

Chang, Y. J., J. R. Stephen, A. P. Richter, A. D. Venosa, J. Bruggemann, S. J Macnaughton, G. A. Kowlachuk, J. R. Haines, E. Kline, and D. C. White
    2000 Phylogenetic Analysis of Aerobic Freshwater and Marine Enrichment Cultures Efficient in Hydrocarbon Degradation: Effect of Profiling Method. *Journal of Microbial Methods* 40:19-31.

Chosson, P., C. Lanau, J. Connan, and D. Dessort
    1991 Biodegradation of Refractory Hydrogen Biomarkers from Petroleum Under Laboratory Conditions. *Nature* 351(6328):640-642.

Christensen, B.E. and W.G Characklis
    1990 Physical and Chemical Properties of Biofilms, In *Biofilms*, edited by W.G. Characklis and K.C. Marshall, John Wiley and Sons Inc., New York.

Commander Battle Force, US Pacific Fleet
    January 29, 1942 Memorandum for File: Damages Sustained by the Ships of the Battle Force, Pacific Fleet as a result of the Japanese Air Raid on December 7, 1941. Wallin Papers, Box 2, 50 Salvage Reports, Naval History Center, Washington, D.C.

Commander Base Force to Commander in Chief, Pacific Fleet
    December 28, 1941. Damaged Ships – Preliminary Estimates of Problems of Salvage. 7pp. Wallin Papers, Box 1, 50 Salvage Reports, Naval History Center, Washington, D.C.

Cook, E.
    1937 *Open Hearth Steel Making*. ASM International, Cleveland.

Costerton, J.W., Z. Lewandowski, D.E. Caldwell, D.R. Korber, and H.M. Lappin-Scott.
    1995. Microbial Biofilms. *Annual Review of Microbiology* 49:711-745.

Cummins, G. and B. Dickinson
    1989 The Management Experience. In *Submerged Cultural Resources Study: USS Arizona Memorial and Pearl Harbor National Historic Landmark*, edited by D. J. Lenihan, pp. 157-168. Submerged Resources Center Professional Papers No. 9. National Park Service, Santa Fe.

Davison, H.D.
    1941 Statement of Ensign H. D. Davison, US Navy, USS *Arizona*. Wallin Papers, Box 2, 50 Salvage Reports, Naval History Center, Washington, D.C.

DeAngelis, R.

   2002 X-Ray Diffraction and Environ mental Scanning Electron Microscope Investigation of Concretion from the USS Arizona. Manuscript on File, National Park Service, Santa Fe.

Dean-Ross, D., J. Moody, and C. E.Cerniglia

   2002 Utilization of Mixtures of Polycyclic Aromatic Hydrocarbons by Bacteria Isolated from Contaminated Sediment. *FEMS Microbiology Ecology* 41:1-7.

de Beer, D., P. Stoodley, F. Roe, and Z. Lewandowski

   1994. Effects of Biofilm Structures on Oxygen Distribution and Mass Transport. *Biotechnology and Bioengineering* 43:1131-1138.

Delgado, J. P.

   1989 Memorials, Myths and Symbols. In *Submerged Cultural Resources Study: USS Arizona Memorial and Pearl Harbor National Historic Landmark*, edited by D. J. Lenihan, pp. 169-183. Submerged Resources Center Professional Papers No. 9. National Park Service, Santa Fe.

   1992 Recovering the Past of USS Arizona: Symbolism, Myth, and Reality. *Historical Archaeology* 26(4):69-80.

Elshahed, M. S., L. M. Gieg, M. J. Mcinerney, and J. M. Suflita

   2001. Signature Metabolites Attesting to the *in situ* Attenuation of Alkylbenzenes in Anaerobic Environments. *Environmental Science and Technology* 35:682-689.

Environmental Protection Agency [EPA].

   1984 *List of the Sixteen PAHs with Highest Carcinogenic Effect*. IEA Coal Research, London.

Felkins, K., J. Leighly, H.P and A. Jankovic

   1998 The Royal Mail Ship Titanic: Did a Metallurgical Failure Cause a Night to Remember? *Journal of Metals* 50(1):12-18.

Ferris, M. J., G. Muyzer, and D. M. Ward

   1996 Denaturing Gradient Gel Electrophoresis Profiles of 16S rRNA-Defined Populations Inhabiting a Hot Spring Microbial Mat Community. *Applied and Environmental Microbiology* 62:340-346.

Flannigan, G. S. Ensign

   1941 Statement of G.S. Flannigan, Ensign, D-V (a), USS *Arizona*. Wallin Papers, Box 2, 50 Salvage Reports, Naval History Center, Washington, D.C.

Floodgate, G. D.

   1984. The Fate of Petrolum in Marine Ecosystems. In *Petroleum Microbiology* (R. M. Atlas, Ed.), pp. 61-98. McMillan Publishing Co., New York, NY.

Fontana, M. G.
  1986 *Corrosion Engineering*. 3rd ed. McGraw-Hill, New York.

Ford, T.E. and R. Mitchell
  1991. The Ecology of Microbial Corrosion. In *Advances in Microbial Ecology,* Vol.
  11, edited by K.C. Marshall, Plenum Press, New York

Fries, E. and W. Puttman
  2002 Analysis of the Antioxidant Butylated Hydroxytoluene (BHT) in Water by Means
  of Solid Phase Extraction Combined with GC-MS. *Water Research* 36:2319-2327.

Frontera-Suau, R., F. D. Bost, T. J. McDonald, and P. J. Morris
  2002 Aerobic Biodegradation of Hopanes and Other Biomarkers by Crude Oil-Degrading
  Enrichment Cultures. *Environmental Science and Technology* 36:4585-4592.

Fuqua, S.G. CDR
  December 15, 1941. USS *Arizona* BB-39, Pearl Harbor Attack: Report of Salvage
  Operations Following Preliminary Dives to Inspect Hull Damage and to Determine what
  Sections of the Vessel Could be Entered. Memo From Commanding Officer, USS
  Arizona to Commander Battleships, Battle Force. Wallin Papers, Box 2, 50 Salvage
  Reports, Naval History Center, Washington, D.C.

  1941 Statement, USN of the attack on the USS Arizona, 7 December 1941. Wallin
  Papers, Box 2, 50 Salvage Reports, Naval History Center, Washington, D.C.

Furlong, W.R.
  March 15, 1942 Salvage operations on USS *Arizona*, USS *Oklahoma*, and USS *Utah* –
  Decision as to Extent of. Wallin Papers, Box 1,50 Salvage Reports, Naval History
  Center, Washington, D.C.

  July 24, 1942 Memo from Commandant, Navy Yard, Pearl Harbor to the Vice Chief of
  Naval Operations. On file, USS *Arizona* Memorial Archives, Honolulu.

Garrett, R. M., I. J. Pickering, C. E. Haith, and R. C. Prince
  1998 Photooxidation of Crude Oils. *Environmental Science and Technology* 32:3719-
  3723.

Geiselman, E.H.
  December 17 1941 From Commanding Officer, USS Arizona to Commander
  Battleships, Battle Force. Material Damages Sustained in Attack on December 7, 1941. 3
  pp. Wallin Papers, Box 2, 50 Salvage Reports, Naval History Center, Washington, D.C.

Giovannoni S.J., T.B. Britschgi, C.L. Moyer, and K.G. Field
  1990 Genetic Diversity in Sargasso Sea Bacterioplankton, *Nature* 345:60-63

Gould, R. A.
   2000 *Archaeology and the Social History of Ships*. Cambridge University Press, Cambridge.

Gregory, D.
   1999 Monitoring the Effect of Sacrificial Anodes on the Large Iron Artifacts on the Duart Point Wreck, 1997. *International Journal of Nautical Archaeology* 28(2):164-173.

   1995 Experiments into the Deterioration Characteristics of Materials on the Duart Point Wreck Site: An Interim Report. *The International Journal of Nautical Archaeology* 24:61-65.

Gu, J.-D., T.E. Ford, and R. Mitchell
   2000 Microbial Corrosion of Metals. In *Uhlig's Corrosion Handbook, Second Edition,* edited by R. Winston Revie, John Wiley and Sons Inc., NY.

Haines, J. R., and M. Alexander
   1974 Microbial Degradation of High Molecular Weight Alkanes. *Applied Microbiology* 28:1084-1085.

Haynes, H.E. Lt. CDR
   November 14, 1943 Memo from Diving Supervisor to Salvage Superintendent re; Diving Operations in Connection with the Salvage of the USS *Arizona*. On file, USS *Arizona* Memorial Archives, Honolulu.

Henderson, S.
   1989 Biofouling and Corrosion Study. In *Submerged Cultural Resources Study: USS Arizona Memorial and Pearl Harbor National Historic Landmark*, edited by D. J. Lenihan, pp. 117-156. Submerged Resources Center Professional Papers No. 9. National Park Service, Santa Fe.

Hir, M. L., and C. Hily
   2002 First Observations in a High Rocky-Shore Community After the *Erika* Oil Spill (December 1999, Brittany France). *Marine Pollution Bulletin* 44:1243-1252.

Ho, K., Patton, J. S., Latimer., R. J. Pruell, M., Pelletier, R. McKinney, and S. Jayaraman 1999 The Chemistry and Toxicity of Sediment Affected by Oil from the *North Cape* Spilled into Rhode Island Sound. *Marine Pollution Bulletin* 38:314-323.

Homann, A. J. Cmdr.
   January 28, 1942 (a) Material Damage Sustained in Attack on December 7. 1941. Memo from USS *Arizona* Commanding Officer to the Chief, Bureau of Ships. Wallin Papers, Box 2, 50 Salvage Reports, Naval History Center, Washington, D.C.

1942 (b) Information on Damage Control, ref. Pacific Fleet Conf. Lrt. No2Cl-42 of January 6, 1942. Memo from USS Arizona Commanding Officer to Chief, Naval Operations. Wallin Papers, Box 2, 50 Salvage Reports, Naval History Center, Washington, D.C.

Hughes, J. B.
1999. Cytological-Cytogentic Analyses of Winter Flounder Embryos Collected from the Benthos at the Barge *North Cape* Oil Spill. *Marine Pollution Bulletin* 38:30-35.

Hughes J.B., J.J. Hellman, T.H. Ricketts, and J.M. Bohannan
2001 Counting the Uncountable: Statistical Approaches to Estimating Microbial Diversity, Applied Environmental Microbiology 67:4399-4406.

Hunt, J. M.
1995 *Petroleum Geochemistry and Geology*. 2nd ed. W.H. Freeman and Company, New York.

Husler, J. and C. Dodson
2003 *X-Ray Fluorescence Analysis of Concretion*. Unpublished Manuscript on File at National Park Service, Santa Fe.

Inui, H., K. Itoh, M. Matsuo, and J. Miyamoto
1979 Studies on Degradation of 2,6-di-*tert*-butyl-4-methylphenol (BHT) in the Environment. Part-II: Biodegradability of BHT with Activated Sludge. *Chemosphere* 6:383-91.

Irwin, R. J., M. VanMouwerik, L. Stevens, M. D. Seese, and W. Basham
1997 National Park Service, Water Resources Division Environmental Contaminants Encyclopedia, Fuel Oil No. 6 Entry.

Jackson CR, KG Harrison, and S.L. Dugas
2005 Enumeration and Characterization of Culturable Arsenate Resistant Bacteria in a Large Estuary, *Systematic Applied Microbiology* 28:727-734.

Jannasch H.W., and C.O. Wirsen
1981 Morphological Survey of Microbial Mats Near Deep Sea Thermal Vents, Applied Environmental Microbiology 41:528-538.

Jeffery, B.
2004 World War II Underwater Cultural Heritage Sites in Truk Lagoon: Considering a Case for World Heritage Listing. *International Journal of Nautical Archaeology* 33(1):106-121.

Johnson, D. L., J. D. Makinson, R. DeAngelis, B. M. Wilson and W. N. Weins
>   2003   *Metallurgical and Corrosion Study of Battleship USS Arizona, USS Arizona Memorial, Pearl Harbor*. Unpublished Manuscript on File at National Park Service, Santa Fe.

Johnson, D.L., W.N. Weins, J.D. Makison, and D.A. Martinez
>   1999 Metallographic Studies of the USS *Arizona*. Proceedings of the International Metallographic Society.

Johnson, D. L., W. N. Weins and J. D. Makinson
>   2000   Metallographic Studies of the U.S.S. Arizona. In *Microstructural Science Vol. 27: Understanding Processing, Structure, Property, and Behavior Correlations*, edited by W. N. Weins, pp. 85-91. ASM International, New York.

Johnson, D. L., B. M. Wilson, J. D. Carr, M. A. Russell, L. E. Murphy and D. L. Conlin
>   2006a Corrosion of Steel Shipwrecks in the Marine Environment: USS Arizona - Part 1. *Materials Performance* 45(10):40-44.

>   2006b Corrosion of Steel Shipwrecks in the Marine Environment: USS Arizona - Part 2. *Materials Performance* 45(11):54-57.

Jones, D. A.
>   1996   *Principles and Prevention of Corrosion*. 2nd ed. Prentice Hall, New York.

Juhasz, A. L. and R. Naidu
>   2000 Bioremediation of High Molecular Weight Polycyclic Aromatic Hydrocarbons: A Review of the Microbial Degradation of benzo[*a*]pyrene. *International Biodeterioration and Biodegradation* 45:57-88.

Jungclaus, G. A., V. Lopez-Avila and R. A. Hites
>   1978 Organic Compounds in Industrial Waste Water: A Case Study of Their Environmental Impact. *Environmental Science and Technology* 12:88-96.

Kanaly, R. A. and S. Harayama
>   2000 Biodegradation of High-Molecular-Weight Polycyclic Aromatic Hydrocarbons by Bacteria. *Journal of Bacteriology* 182:2059-2067.

Kayen, R. and Phi, T.N.
>   1997 A Robotics and Data Acquisition Program for Manipulation of the U.S. Geological Survey's Ocean Sediment Core Logger. *SciTech Journal* 7 (5):24-29.

Kayen, R., Edwards, B. D., Lee, H. J.
>   1999 Nondestructive Laboratory Measurement of Geotechnical and Geoacoustic Properties through Intact Core-liner *Nondestructive and Automated Testing for Soil and Rock Properties, ASTM Special Technical Publication-1350,* W. A. Marr and C.E. Fairhurst *eds*., *American Society for Testing and Materials*, p. 83-94.

Kelly, M.
1996 Enshrining History: The Visitor Experience at Pearl Harbor's USS Arizona Memorial. *Museum Anthropology* 20(3):45-57.

Kerr, R. A.
2001 Life--Potential, Slow, or Long Dead. *Science* 294(5548):1820-1821.

Korb, L. J.
1987 *Metals Handbook: Volume 13, Corrosion*. 9th ed. American Society for Metals.

Kvenvolden, K. A., F.D. Hostettler, J. B. Rapp, and P. R. Carlson
1993 Hydrocarbons in Oil Residues on beaches of Islands of Prince William Sound, Alaska. *Marine Pollution Bulletin* 26:24-29.

Kvenvolden, K. A., F. D. Hostettler, P. R. Carlson, J. B. Rapp, C. N. Threlkeld. and A. Warden
1995 Ubiquitous Tar Balls with a California-Source Signature on the Shorelines of Prince William Sound, Alaska. *Environmental Science and Technology* 29:2684-2694.

Kvenvolden, K .A., F. D. Hostettler, R. W. Rosenbauer, T. D. Lorensen, W. T. Castle and S. Sugarman
2002 Hydrocarbons in Recent Sediment of the Monterey Bay National Marine Sanctuary. *Marine Geology* 181:101-113.

Lane D.J.
1991 16S/23S rRNA Sequencing, In *Nucleic Acid Techniques in Bacterial Systematics*, edited by E. Stackebrandt, and M. Goodfellow, pp. 115-175, John Wiley and Sons, New York

Lenihan, D. J.
1989a Introduction. In *Submerged Cultural Resources Study: USS Arizona Memorial and Pearl Harbor National Historic Landmark*, edited by D. J. Lenihan, pp. 1-12. Submerged Resources Center Professional Papers No. 9. National Park Service, Santa Fe.

1989b *Submerged Cultural Resources Study: USS Arizona Memorial and Pearl Harbor National Historic Landmark*. Submerged Resources Center Professional Papers No. 9. National Park Service, Santa Fe.

1990 *USS Arizona Memorial and Pearl Harbor National Historic Landmark*. 2 ed. Vol. No. 23. Submerged cultural resources study. Santa Fe, NM: Southwest Cultural Resources Center Professional Papers

Lenihan, D. J. and L. E. Murphy
1989 Archeological Record. In *Submerged Cultural Resources Study: USS Arizona Memorial and Pearl Harbor National Historic Landmark*, edited by D. J. Lenihan. Submerged Resources Center Professional Reports No. 9. National Park Service, Santa Fe.

Linley E.A.S., R.C. Newell, and M.I. Lucas
1983 Quantitative Relationships Between Phytoplankton, Bacteria, and Heterotrophic Microflagellates in Shelf Waters, *Marine Ecology Progress Series* 12:77-89.

Linenthal, E. T.
1991 *Sacred Ground: Americans and Their Battlefields*. University of Illinois Press, Chicago.

Little, B. J., R. I. Ray and R. K. Pope
2000 Relationship Between Corrosion and the Biological Sulfur Cycle: A Review. *Corrosion* 56(4):433-443.

Lott, A.S. General Editor
1978 *USS* Arizona *Ship's Data: A Photographic History*. Fleet Reserve Association, Honolulu.

Luckenbach Trustee Council
2006 *S.S. Jacob Luckenbach and Associated Mystery Oil Spills Final Damage Assessment and Restoration Plan/Environmental Assessment.* Prepared by California Department of Fish and Game, National Oceanic and Atmospheric Administration, United States Fish and Wildlife Service, National Park Service.

Lunel, T., A. Crosbie, L. Davies, and R. P. J. Swannell
2000 The Potential for Dispersing Bunker C (IFO-380) Fuel Oils: Initial Results. Prepared by: National Environmental Technology Centre, Culham, Abingdon Oxfordshire, United Kingdom. 12 pp.

MacLeod, I. D
1982 The Electrochemistry and Conservation of Iron in Sea Water. *International Journal of Nautical Archaeology and Underwater Exploration* 2(4):267-275.

1987 Conservation of Corroded Iron Artifacts – New Methods for On-Site Preservation and Cryogenic Deconcreting. *International Journal of Nautical Archaeology and Underwater Exploration* 16(1):49-56.

1989 Electrochemistry and Conservation of Iron in Sea Water. *Chemistry in Australia* 56(7):227-229.

1995 *In Situ* Corrosion Studies on the Duart Point Wreck, 1994. *International Journal of Nautical Archaeology* 24(1):53-59.

2002 In Situ Corrosion Measurements and Management of Shipwreck Sites. In *International Handbook of Underwater Archeology*, edited by C. V. Ruppe and J. F. Barstad, pp. 697-714. Kluwer Academic/Plenum Publishers., New York.

Mackenzie, A. S.
  1984 Applications of Biological Markers in Petroleum Geochemistry. In *Advances in Petroleum Geochemistry* (J. Brooks, and D. Weite, Eds.), Vol. 1, pp. 115-213. Academic Press, London.

Madsen, D.
  2003 *Resurrection: Salvaging the Battle Fleet at Pearl Harbor.* Naval Institute Press, Annapolis.

Maki J.S., D. Rittschof, A.R. Schmidt, A.G. Snyder, and R. Mitchell
  1989 Factors Controlling Attachment of Bryozoan Larvae: A Comparison of Bacterial Films and Unfilmed Surfaces, *Biology Bulletin* 177:295-302.

Makinson J.D., D.L. Johnson, M.A. Russell, D.L. Conlin, and L.E. Murphy
  2002 *In situ* Corrosion Studies on the Battleship USS *Arizona*, *Materials Performance* 41:56-60.

Marshall K.C., R. Stout, and R. Mitchell
  1971 Mechanism of the Initial Events in the Sorption of Marine Bacteria to Surfaces. *Journal of General Microbiology* 68:337-348.

McDonald, T. J. and M. C. Kennicutt
  1992 Fractionation of Crude Oils by HPLC and Quantitative Determination of Aliphatic and Aromatice Biological Markers by GC-MS with Selected Ion Monitoring. *LC-GC* 10:935-938.

McEldowney, S. and M. Fletcher
  1987 Adhesion of Bacteria from Mixed Cell Suspensions to Solid Surfaces. *Archives of Microbiology* 148:57-62.

McNamara C.J., T.D. Perry, K. Bearce, G. Hernandez-Duque, and R. Mitchell
  2006 Epilithic and Endolithic Bacterial Communities in Limestone from a Mayan Archaeological Site, *Microbial Ecology* 51:51-64.

Makinson, J. D., D. L. Johnson, M. A. Russell, D. L. Conlin and L. E. Murphy
  2002 *In situ* Corrosion Studies on the Battleship USS Arizona. *Materials Performance* 41(10):56-60.

Mardikian, P.
  2004 Conservation and Management Strategies Applied to Post-Recovery Analysis of the American Civil War Submarine H. L. Hunley (1864). *International Journal of Nautical Archaeology* 33(1):137-148.

McCarthy, M.
    1988 S.S. Xantho: The Pre-Disturbance, Assessment, Excavation and Management of an Iron Steam Shipwreck off the Coast of Western Australia. *International Journal of Nautical Archaeology and Underwater Exploration* 17(4):339-347.

    2000 *Iron and Steamship Archaeology: Success and Failure on the S.S. Xantho.* The Plenum Series in Underwater Archaeology, New York.

McClung, M. L. Lt.
    n.d. Survey of Damage on U.S.S. *Arizona*. Reference; Verbal Orders to Conduct a Survey of the Hull of U. S. S. *Arizona*. Correspondence from the Assistant Salvage Engineer to The Salvage Engineer. Wallin Papers, Box 2, 50 Salvage Reports, Naval History Center, Washington, D.C.

Miller J. D.
    1941 Bombing of USS *Arizona*, Report of Ensign Jim D. Miller. Wallin Papers, Box 2, 50 Salvage Reports, Naval History Center, Washington, D.C.

Mills H.J., C. Hodges, K. Wilson, I.R. MacDonald, and P.A. Sobecky
    2003 Microbial Diversity in Sediments Associated with Surface-Breaching Gas Hydrate Mounds in the Gulf of Mexico, *FEMS Microbiology and Ecology* 46:39-52.

Mills, M. A., T. J. McDonald, J. S. Bonner, M. A. Simon, and R. L. Autenrieth
    1999 Method for Quantifying the Fate of Petroleum in the Environment. *Chemosphere* 39:2563-2582.

Michael, J. and M. O. Hayes
    1999 Weathering Patterns of Oil Residues Eight Years After the *Exxon Valdez* Oil Spill. *Marine Pollution Bulletin* 38:855-863.

Mikami, N., H. Gomi, and J. Miyamoto
    1979 Studies on Degradation of 2,6-di-*tert*-butyl-4-methylphenol (BHT) in the Environment. Part-I: Degradation of ^{14}C-BHT in soil. *Chemosphere* 5:305-310.

Minas, W. and W. Gunkel
    1995 Oil Pollution in the North Sea- A Microbiological Point of View. *Helgolander Meeresunters* 49:14-158.

Moldowan, J. M., J. Dahl, M. A. Mcaffrey, W. J. Smith and J. C. Fetzer
    1995 Application of Biological Marker Technology to Bioremediation of Refinery By-products. *Energy and Fuels* 9:155-162.

Moss J.A., A. Nocker, J.E. Lepo, and R.A. Snyder
    2006 Stability and Change in Estuarine Biofilm Bacterial Community Diversity, *Applied Environmental Microbiology* 72:5679-5688.

Mulkins-Phillips, G. J., and J. E. Stewart
    1974 Effect of Environmental Parameters on Bacterial Degradation of Bunker C Oil, Crude Oils, and Hydrocarbons. *Applied Microbiology* 28:915-922.

Munoz, D., M. Guiliano, P. Doumenq, F. Jacquot, P. Scherrer, and G. Mille
    1997 Long Term Evolution of Petroleum Biomarkers in Mangrove Soil (Guadeloupe). *Marine Pollution Bulletin* 34:868-874.

Murphy, L.E. and T.G. Smith
    1995 Submerged in the Past: Mapping the Beguiling Waters of Florida's Biscayne and Dry Tortugas National Parks. *Geoinfo Systems* 5(10):26-33.

    1996 Global Positioning System (GPS). In Encyclopedia of Underwater Archaeology, edited by James P. Delgado, pp. 171 -172. British Museum Press, London.

National Climate Data Center, National Oceanographic and Atmospheric Administration
    2005 NCDC Hourly Surface Climate Data for Hawaii, Online Dataset, http://www.ncdc.noaa.gov/oa/climate/climatedata.html#hourly

National Oceanic and Atmospheric Administration [NOAA]
    1994 NOAA/ Hazardous Materials Response and Assessment Division Fact sheet: No. 6 fuel oil (Bunker C) spills.

National Research Council [NRC]
    2003. Oil in the sea III: Inputs, Fates, and Effects.

Navy Department, Bureau of Construction and Repair
    1913 *Detail Specifications for Building Battleship No. 39 for the United States Navy*. Government Printing Office, Washington D.C. On file, USS *Arizona* Memorial Archives, Honolulu.

Neilson, A. J.
    1994 *Organic Chemicals in the Aquatic Environment: Distribution, Persistence, and Toxicity*. CRC Press, Boca Raton, FL.

New-York-Navy-Yard
    1913 Correspondence. National Archives and Records Administration, North East Region, New York.

Nishigima, F. N., R. R. Weber, and M. C. Bicego
    2001 Aliphatic and Aromatic Hydrocarbons in Sediments of Santos and Cananeia, SP, Brazil. *Marine Pollution Bulletin* 42:1064-1072.

Norman, R. S., R. Frontera-Suau, and P. J. Morris
    2002 Variability in *Psuedomonas aeruginosa* lipopolysaccharide Expression During Crude Oil Degradation. *Applied and Environmental Microbiology* 10:5096-5103.

North, N. A.
1976 Formation of Coral Concretions on Marine Iron. *International Journal of Nautical Archaeology and Underwater Exploration* 5(3):253-258.

North, N. A. and I. D. MacLeod
1987 Corrosion of Metals. In *Conservation of Marine Archaeological Objects*, edited by C. Pearson, pp. 68-98. Butterworth & Co., London.

North N.A.
1976 Formation of Coral Concretions on Marine Iron, *International Journal of Nautical Archaeology and Underwater Exploration* 5:253-258.

Paine R.W.
October 7, 1943 Memo from Commandant Navy Yard , Pearl Harbor to Chief, Bureau of Ships. Subject: U.S.S. *Arizona* (BB-39) War Damage Report. On file, USS *Arizona* Memorial Archives, Honolulu.

Parker W.W.
1941 Statement of William W. Parker, SEA1c, USN. Wallin Papers, Box 2, 50 Salvage Reports, Naval History Center, Washington, D.C.

Pearl Harbor Natural Resource Trustees.
1999 Restoration Plan and Environmental Assessment for the May 14, 1996 Chevron Pipeline Oil Spill into Waiau Stream and Pearl Harbor, Oahu, Hawaii. Prepared by: U.S. Department of Defense, U.S. Department of the Interior, National Oceanic and Atmospheric Administration, and State of Hawaii. 122 pp.

Perry IV T.D., V. Klepac-Ceraj, X.V. Zhang, C.J. McNamara, M.F. Polz, S.T Martin., N. Berke, and R. Mitchell
2005 Binding of Harvested Bacterial Exopolymers to the Surface of Calcite, *Environmental Science and Technology* 39:8770-8775.

Perry, J. J.
1977 Microbial Metabolism of Cyclic Hydrocarbons and Related Compounds. *CRC Critical Reviews in Microbiology* 5:387-412.

1984 Microbial metabolism of cyclic alkanes. *In* "Petroleum Microbiology" (R. M. Atlas, Ed.), pp. 61-98. McMillan Publishing Co., New York, NY.

Peters, K. E., and J. M. Moldowan
1993 *The Biomarker Guide: Interpreting Molecular Fossils in Petroleum.* Prentice-Hall Inc., Englewood Cliffs, NJ.

Pirnik, M. P.
1977 Microbial Oxidation of Methyl Branched Alkanes. *Critical Reviews in Microbiology* 5:413-422.

Pollard, J. T., M. Whittaker, and G. C. Risden
  1999 The Fate of Heavy Oil Wastes in Soil Microcosms I: A Performance Assessment of Biotransformation Indices. *The Science of the Total Environment* 226:1-22.

Porter K.G., and Y.S. Feig
  1980 The Use of DAPI for Identifying and Counting Aquatic Microflora, *Limnology and Oceanography* 25:943-948.

Postgate, J. R.
  1979 *The Sulphate-Reducing Bacteria*. Cambridge University Press, Cambridge, Great Britain.

Pourbaix, M.
  1974 *Atlas of Electrical Chemical Equilibria in Aqueous Solutions*. National Association of Corrosion Engineers, Houston.

Prabagaran S.R., R. Manorama, D. Delille, and S. Shivaji
  2007 Predominance of Roseobacter, Sulfitobacter, Glaciecola, and Psychrobacter in Seawater Collected off Ushuaia, Argentina, Sub-Antarctica, *FEMS Microbiology and Ecology* 59:342-355.

Prince, R. C., D. L. Elmendorf, J. R. Lute, C. S. Hsu, C. E. Halth, J. D. Senius, G. J. Dechert, G. S. Douglas, and E. L. Butler
  1994 $17\alpha(H),21\beta(H)$-Hopane as a Conserved Internal Marker for Estimating the Biodegradation of Crude Oil. *Environmental Science and Technology* 28:142-145.

Prince, R. C., R. T. Stibrany, J. Hardestine, G. S. Douglas, and E. H. Owens
  2002 Aqueous Vapor Extraction: A Previously Unrecognized Weathering Process Affecting Oil Spills in Vigorously Aerated Water. *Environmental Science and Technology* 36:2822-2825.

Rabus, R., H. Wilkes, A. Behrends, A. Armstroff, T. Fischer, A. J. Pierik, and F. Widdel 2001 Anaerobic Initial Reaction of *n*-alkanes in a Denitrifying Bacterium: Evidence for (1-methylpentyl) Succinate as Initial Product and for Involvement of an Organic Radical in *n*-hexane Metabolism. *Journal of Bacteriology* 183:1707-1715.

Raymer, Commander E. C.
  1996 *Descent into Darkness Pearl Harbor, 1941: A Navy Diver's Memoir*. Presidio Press, Novato.

Reed, W. E.
  1977 Molecular Compositions of Weathered Petroleum and Comparison with its Possible Source. *Geochimica et Cosmochimica Acta* 41:237-247.

Richmond, S. A., J. E. Lindstrom, and J. F. Braddock
2001 Effects of Chitin on Microbial Emulsification, Mineralization Potential, and Toxicity of Bunker C Fuel Oil. *Marine Pollution Bulletin* 42:773-779.

Rittman, B.E., M. Pettis, H.W. Reeves, and D.A. Stahl
1999 How Biofilm Clusters Affect Substrate Flux and Ecological Selection. *Water Science and Technology* 39:99-105.

Rodgers, B. A., W. M. Coble and H. K. Van Tilburg
1998 The Lost Flying Boat of Kaneohe Bay: Archaeology of the First US Casualties of Pearl Harbor. *Historical Archaeology* 32(4):8-18.

Russell, M. A., D. L. Conlin, L. E. Murphy, D. L. Johnson, B. M. Wilson and J. D. Carr
2006 A Minimum-Impact Method for Measuring Corrosion Rate of Steel-Hulled Shipwrecks in Seawater. *International Journal of Nautical Archaeology* 35(2):310-318.

Russell, M. A. and L. E. Murphy
1997 Minimum Impact Archaeology. In *Encyclopaedia of Underwater and Maritime Archaeology*, edited by J. P. Delgado, pp. 278-279. British Museum Press, London

2003 *"Long-Term Management Strategies for the USS Arizona: A Submerged Cultural Resource in Pearl Harbor, Hawaii." Legacy Resources Management Fund Project No. 02-170: 2002 Annual Report*. Submerged Resources Center Technical Report No. 14. National Park Service, Santa Fe.

2004 *"Long-Term Management Strategies for the USS Arizona: A Submerged Cultural Resource in Pearl Harbor, Hawaii." Legacy Resources Management Fund Project No. 03-170: 2003 Annual Report*. Submerged Resources Center Technical Report No. 15. National Park Service, Santa Fe.

Russell, M. A., L. E. Murphy, D. L. Johnson, T. J. Foecke, P. J. Morris and R. Mitchell
2004 Science for Stewardship: Multidisciplinary Research on USS Arizona. *Marine Technology Society Journal* 38(3):54-63.

Salanitro, J. P., P. B Dorn, M. H. Huesemann, K. O. Moore, I. A. Rhodes, L. M. R. Jackson, T. E. Vipond, M. M. Western, and H. L. Wisniewski
1997 Crude Oil Hydrocarbon Bioremediation and Soil Ecotoxicity Assessment. *Environmental Science and Technology* 31:1769-1776.

Salvage Diary, Pearl Harbor
1943 1 March – 1942 through 15 November, 1943. Industrial Department War Diary Collection, Naval Historical Center, Washington D.C.

Schaeffer, T. L., S. G. Cantwell, J. L. Brown, D. S. Watt, and R. R. Fall
1979 Microbial Growth on Hydrocarbons: Terminal Branching Inhibits Biodegradation. *Applied and Environmental Microbiology* 38:742-746.

Samanta, S. K., O. V. Singh, and R. K. Jain
2002 Polycyclic Aromatic Hydrocarbons: Environmental Pollution and Bioremediation. *Trends in Biotechnology* 20:243-248.

Saveur, A.
1935 *The Metallography and Heat Treatment of Iron and Steel*. McGraw-Hill, New York.

Schumacher, M. (editor)
1979 *Sea Water Corrosion Handbook*. Noyes Data Corporation, Park Ridge, NJ.

Shikuma N.J., and M.G. Hadfield
2005 Temporal Variation of an Initial Marine Biofilm Community and its Effects on Larval Settlement and Metamorphosis of the Tubeworm *Hydroides elegans*, *Biofilms* 2:231-238.

Sierfert W. K. and J. K. Moldowan
1979 The Effect of Biodegradation on Steranes and Terpanes in Crude Oil. *Geochimica et Cosmochimica Acta* 43:111-126.

Simberloff D.
1978 Use of Rarefaction and Related Methods in Ecology, In *Biological Data in Water Pollution Assessment: Quantitative and Statistical Analysis*, edited by K.L. Dickson, J. Cairns Jr., and R.J. Livingston, ASTM STP 652, American Society for Testing and Materials.

Shope S.M., L.E. Murphy and T. G. Smith
1995 Found at Sea: Charting Florida's Sunken Treasures *GPS World* 6(5):22-34.

So, C. M., and L. Y.Young
1999 Isolation and Characterization of a Sulfate-Reducing Bacterium that Anaerobically Degrades Alkanes. *Applied and Environmental Microbiology* 65:2969-2976.

Spormann, A. M., and F. Widdel
2000 Metabolism of Alkylbenzenes, Alkanes, and Other Hydrocarbons in Anaerobic Bacteria. *Biodegradation* 11:85-105.

Stillwell, Paul
1991 *Battleship* Arizona: *An Illustrated History*. Naval Institute Press, Annapolis.

Stirling, L. A., R. J. Watkinson, and I. J. Higgins
1977 Microbial Metabolism of Alicyclic Hydrocarbons: Isolation and Properties of a Cyclohexane Degrading Bacterium. *Journal of General Microbiology* 99:119-125.

Storlazzi, C. D., M. A. Russell, M. D. Owens, M. E. Field and L. E. Murphy
    2004 *Dynamics of the Physical Environment at the USS Arizona Memorial: 2002-2004*.
    U.S. Geological Survey Open-File Report 2004-1353,
    http://pubs.usgs.gov/of/2004/1353/.

Storlazzi, C. D., M. A. Russell, M. K. Presto and J. E. Burbank
    2005 *Flow Patterns and Current Structure at the USS Arizona Memorial: April, 2005*.
    U.S. Geological Survey Open-File Report 2005-1334,
    http://pubs.usgs.gov/sir/2005/1334/.

Strand, J. A., V. I. Cullinan, E. A. Crecelium, T. J. Fortman, R. J. Citterman, and M. L.
    Fleischmann
    1992 Fate of Bunker C Fuel Oil in Washington Coastal Habitats Following the December
    1988 *NESTUCCA* Oil Spill. *Northwest Science* 66:1-14.

Summary of Damage Reported to the Planning Section
    December 7, 1941 Wallin Papers, Naval Historical Center, Washington, D.C. Wallin
    Papers, Box 1,50 Salvage Reports, Naval History Center, Washington, D.C.

Swofford D.L.
    2003 *PAUP*. Phylogenetic Analysis Using Parsimony (*and Other Methods),* Ver. 4,
    Sinauer Associates, Sunderland, Massachusetts.

Thompson F.L., T. Iida, and J. Swings
    2004 Biodiversity of Vibrios, *Microbiology And Molecular Biology Reviews* 68:403-431.

Thompson J.D., T.J. Gibson, F. Plewniak, F. Jeanmougin, and D.G. Higgins
    1997 The ClustalX Windows Interface: Flexible Strategies for Multiple Sequence
    Alignment Aided by Quality Analysis Tools, *Nucleic Acids Research* 24:4876-4882.

Trudgill, P. W.
    1978 Microbial Degradation of Alicyclic Hydrocarbons. *In Developments in
    Biodegradation of Hydrocarbons* (J. R. Watkinson, Ed.), pp. 47-84. Marcel Dekker, Inc.,
    New York.

Uhlig, H. H. and R. W. Revie
    1985 *Corrosion and Corrosion Control*. 3rd ed. John Wiley & Sons, New York.

U.S. Navy
    1998 Fact Sheet No. 2: Pearl Harbor Sediment Remedial Investigation/Feasibility Study.

    2003 Overview of Survey/Salvage Operation: USS Mississinewa,
    www.supsalv.org/00c2_posseA0_59.asp?destPage=00c2.

United States Pacific Fleet Battle Force
    n.d. USS *California*, Flagship, Memorandum No.7. Wallin Papers, Box 1, 50 Salvage
    Reports, Naval History Center, Washington, D.C.

van Loosdrecht, M.C.M., J. Lyklema, W. Norde, and A.J.B. Zehnder
     1990 Influence of Interfaces on Microbial Activity. *Microbiological Reviews* 54:75-87.

Vandermeulen, J. H., and J. G. Singh
     1994 *Arrow* Oil Spill, 1970-90: Persistence of 20-yr Weathered Bunker C Fuel Oil.
     Canadian Journal of Fisheries Aquatic Science 51:845-855.

Vesilind, P. J.
     2001 Oil and Honor at Pearl Harbor. *National Geographic Magazine* 199(6):84-99.

Volkman, J. K., D.G. Holdsworth, G. P. Neill and H. J. Bavor, Jr.
     1992 Identitfication of Natural, Anthropogenic and Petroleum Hydrocarbons in Aquatic
     Sediments. *The Science of the Total Environment* 112:203-219.

von Graevenitz A., J Bowman., C. Del Notaro, and M. Ritzler
     2000 Human infection with *Halomonas venusta* Following Fish Bite, *Journal of Clinical
     Microbiology* 38:3123-3124.

Walker, J. D., L. Petrakis, and R. R. Colwell
     1976 Comparison of the Biodegradability of Crude and Fuel Oils. *Canadian Journal of
     Microbiology* 22:598-602.

Wallin, H.N. Cmdr.
     December 7, 1941 Memorandum Covering Apparent Damage to Vessels in Pearl As of
     1345 This Date. US Pacific Fleet, USS Pennsylvania, flagship. Wallin Papers, Box 1, 50
     Salvage Reports, Naval History Center, Washington, D.C.

     January 25, 1942 Progress of Salvage Work in Pearl Harbor. Wallin Papers, Box 1, 50
     Salvage Reports, Naval History Center, Washington, D.C.

     February 8, 1942 Present Situation with Respect to Salvage of Vessels in Pearl Harbor.
     3pp. Wallin Papers, Box 1,50 Salvage Reports, Naval History Center, Washington, D.C.

     1946 Rejuvenation of Pearl Harbor. Typescript sent to Admiral Nimitz and Navy
     Director of Public Information. Wallin Papers, Box 1,50 Salvage Reports, Naval History
     Center, Washington, D.C.

     1968 *Pearl Harbor: Why, How, Fleet Salvage and Final Appraisal.* Naval History
     Division, Washington, D.C.

Wang, Z., M. Fingas, S. Blenkinsopp, G. Sergy, M. Landriault, L. Sigouin, J. Foght, K. Semple,
     and D. W. S. Westlake
     1998a Comparison of Oil Compositional Changes Due to Biodegradation and Physical
     Weathering in Different Oils. *Journal of Chromatography* 809:89-107.

Wang, Z., M. Fingas, S. Blenkinsopp, G. Sergy, M. Landriault, L. Sigouin, and P. Lambert

   1998b. Study of the 25-year-old *Nipisi* Oil Spill: Persistence of Oil Residues and Comparisons Between Surface and Subsurface Sediments. *Environmental Science and Technology* 32:2222-2232.

Wang, Z., M. Fingas, E. H. Owens, L. Sigouin, and C. E. Brown
   2001 Long-Term Fate and Persistence of Spilled *Metula* Oil in a Marine Salt Marsh Environment: Degradation of Petroleum Biomarkers. *Journal of Chromatography* 926:275-290.

Wang, Z., M. Fingas, and S. P. Page
   1999 Oil Spill Identification. *Journal of Chromatography A*. 843:369-411.

Wang, Z., M. Fingas, and G. Sergy
   1994 Study of 22-Year Old *Arrow* Oil Samples Using Biomarker Compounds by GC/MS. *Environmental Science and Technology* 28:1733-1746.

Wang, Z., M. Fingas, and G. Sergy
   1995 Chemical Characterization of Crude Oil Residues from an Arctic Beach by GC/MS and GC/FID. *Environmental Science and Technology* 29:2622-2631.

Wang, Z., M. Fingas, and L. Sigouin
   2001 Characterization and Identification of a "Mystery" Oil Spill from Quebec (1999). *Journal of Chromatography A* 909:155-169.

Weeks O.B.
   1981 The Genus Flavobacterium, *In The Prokaryotes: a Handbook on Habitats, Isolation, and Identification of Bacteria*, edited by M.P. Starr, H. Stolp, H.G. Trüper, A. Balows, pp. 1365-1370, H.G. Schlegel, Springer-Verlag, New York.

Wheeler, A. J.
   2002 Environmental Controls on Shipwreck Preservation: the Irish Context. *Journal of Archaeological Science* 29:1149-1159.

Whittaker, M., and J. T. Pollard
   1997 A Performance Assessment of Source Correlation and Weathering Indices for Petroleum Hydrocarbons in the Environment. *Environmental Toxicology and Chemistry* 16:1149-1158.

Whitfield, C.
   1988 Bacterial Extracellular Polysaccharides. *Canadian Journal of Microbiology* 34:415-420.

Widdel, F., and R. Rabus
    2001 Anaerobic Biodegradation of Saturated and Aromatic Hydrocarbons. *Current Opinion in Biotechnology* 12:259-276.

Wilson, B. M., D. L. Johnson, H. Van Tilburg, M. A. Russell, L. E. Murphy, J. D. Carr, R. J. DeAngelis and D. L. Conlin
    2007 Corrosion Studies on the USS Arizona with Application to a Japanese Midget Submarine. *Journal of Metals* 59(10):14-18.

Wissa, A. E., Christian, J. T., Davis, E. H., and Heiberg, Sigurd
    1971 Consolidation at Constant Rate of Strain. *Journal of the Soil Mechanics and Foundations Division, ASCE,* 97 (SM10):1393-1413.

Witt, G.
    1995 Polycyclic Aromatic Hydrocarbons in Water and Sediment of the Baltic Sea. *Marine Pollution Bulletin* 31:237-248.

Yiming, X., W. N. Weins and A. Dhir
    1992 A Metallographic Investigation of Banding Diffusion of Phosphorous in Steels. In *Microstructural Science* 20. ASM International, New York.

Zakaria, M. P., T. Okuda, and H. Takada
    2001 Polycyclic Aromatic Hydrocarbons (PAHs) and Hopanes in Stranded Tar-balls on the Coasts of Peninsular Malaysia: Applications of Biomarkers for Identifying Sources of Oil Pollution. *Marine Pollution Bulletin* 42:1327-1366.

Zvyaginstev A.Y.
    1990 Fouling and Corrosion Damage to Supporting Pillars of Oil Platforms in the South China Sea, *Soviet Journal of Marine Biology* 15:392-397.

Zvyaginstav A.Y., and V.V. Ivin
    1995 Study of Biofouling of the Submerged Structural Surfaces of Offshore Oil and Gas Production Platforms, *Marine Technology Society Journal* 29:59-62.

APPENDIX A

SonTek Triton Information

Instrument:	SonTek Triton; s/n: R57
Transmitting Frequency:	10 Mhz
Depth of Transducer:	10 m
Blanking Distance:	0.18 m
Height of Sampling Volume:	0.80 m
Operating Mode:	High-resolution, broad bandwidth
Beam Angle:	15 deg
Sound Speed Calculation:	Set salinity, updating temperature via sensor

Current Sampling

Sampling Frequency:	1 Hz
Time Ping:	00:00:00.30
Pings per Ensemble:	60
Time Between Ensembles:	00:10:00.00

Waves Sampling

Sampling Frequency:	2 Hz
Time per Ping:	00:00:00.30
Pings per Ensemble:	1024
Time Between Ensembles:	02:00:00.00
Total Files:	7
Data Processing:	The data were averaged over 1 hour (6 ensembles) and all of the data where the beam correlation dropped below 70% were removed for visualization and analysis.

APPENDIX B

YSI 6600 Sonde Information

Instruments: YSI 6600 Sonde; s/n: 02g0147
Initial Height of Measurement above Bed: 0.25 m
Sampling Frequency: 2 Hz
Samples per Ensemble: 60
Time Between Ensemble: 00:10:00.00
Total Files: 5
Data Processing: The data were averaged over 1 hour (6 ensembles) and all of the data where the beam correlation dropped below 70% were removed for visualization and analysis.

APPENDIX C

Geotechnical Soil Testing

DRILLING SERVICES FOR NATIONAL PARK SERVICE USS ARIZONA PROJECT

for

ENGINEERING SOLUTIONS, INC.

ERNEST K. HIRATA & ASSOCIATES, INC.
W.O. 03-3832
December 17, 2003

ERNEST K.
HIRATA & ASSOCIATES, INC.

99-1433 Koaha Place
Aiea, Hawaii 96701
Ph: 808-486-0787 Fax: 808-486-0870
Email: eha@hawaii.rr.com

December 17, 2003
W.O. 03-3832

Mr. Richard Frey
Engineering Solutions, Inc.
98-1268 Kaahumanu Street, Suite C-7
Pearl City, Hawaii 96782

Dear Mr. Frey:

Re: **Drilling Services for National Park Service**
USS Arizona Project

This letter summarizes the work performed for the project. Drilling services were conducted in general conformance with the scope of work presented in our proposal dated September 16, 2003. Our work scope for this study included the following:

- Coordinate entry and obtain approval from Naval authorities for the proposed borings.

- Mobilize men and equipment to construct a floating barge and mount drilling equipment.

- Drill and sample 3 exploratory borings at selected locations to depths ranging from 15.2 to 21.3 meters, measured from harbor bottom. Four borings were originally proposed, but one was eliminated by the National Park Service during the time of our fieldwork. The general location of the project site is shown on the enclosed Location Map, Plate 1.1. The approximate boring locations are shown on the USS Arizona Core Location Plan, Plate 1.2, prepared by the National Park Service.

- Provide a field engineer to log all borings and handle soil samples. The boring logs are presented on Plates 3.1 through 3.7. The Boring Log Legend is presented on Plate 2.1, and the Unified Soil Classification System is presented on Plate 2.2.

- Demobilize men and equipment from the project site.

- Preparation of this letter and the attached boring logs.

Drilling Services

Three borings were drilled to depths ranging from 15.2 to 21.3 meters below the harbor bottom. The borings were drilled using portable drilling equipment mounted on a temporary barge. In general, 100 mm O.D. steel casing was driven down to selected sampling depths and cleaned out with a rock-bit. Samples were recovered using thin-walled shelby tubes driven with a 63.5 kg hammer dropped from a height of approximately 760 mm inches. Continuous sampling was performed from the harbor bottom down to the

501

maximum depths drilled in all borings. Some Shelby tubes were damaged by the granular material present in the soil layers. Therefore, Shelby tubes were placed in 1.5 meter long by 75 mm O.D. schedule 40 steel pipe during sampling to protect the thin-walled tubes. The steel pipe was used from harbor bottom down to the maximum depth drilled in boring B1A and to a depth of about 7.6 meters in boring B2. The blow counts presented on the boring logs are those required to drive the Shelby tube or 75 mm steel pipe sleeved Shelby tubes 300 mm, unless noted otherwise. Zero blow counts are indicated in areas where the weight of the extension rods were enough to drive the sampler through the soil. Therefore, no hammer energy was required.

During drilling operations, the soils were continuously logged by our field engineer and classified by visual examination in accordance with the Unified Soil Classification System. The boring logs indicate the depths at which the soils or their characteristics change, although the change could actually be gradual. Only the ends of the Shelby tubes were visible to our field engineer. Therefore, if the change occurred within the 0.76 meter sample tube, the depth was interpreted based on field observations. Classifications and sampling intervals are shown on the boring logs.

We appreciate this opportunity to be of service. Should you have any questions concerning this letter, please feel free to call on us.

Respectfully submitted,

ERNEST K. HIRATA & ASSOCIATES, INC.

Ernest K. Hirata, President

EKH:EHS:ph

Attachments:
Location Map   Plate 1.1
USS Arizona Geological Core Locations   Plate 1.2
Boring Log Legend   Plate 2.1
Unified Soil Classification System   Plate 2.2
Boring Logs   Plates 3.1 through 3.7

PROJECT SITE

PEARL HARBOR
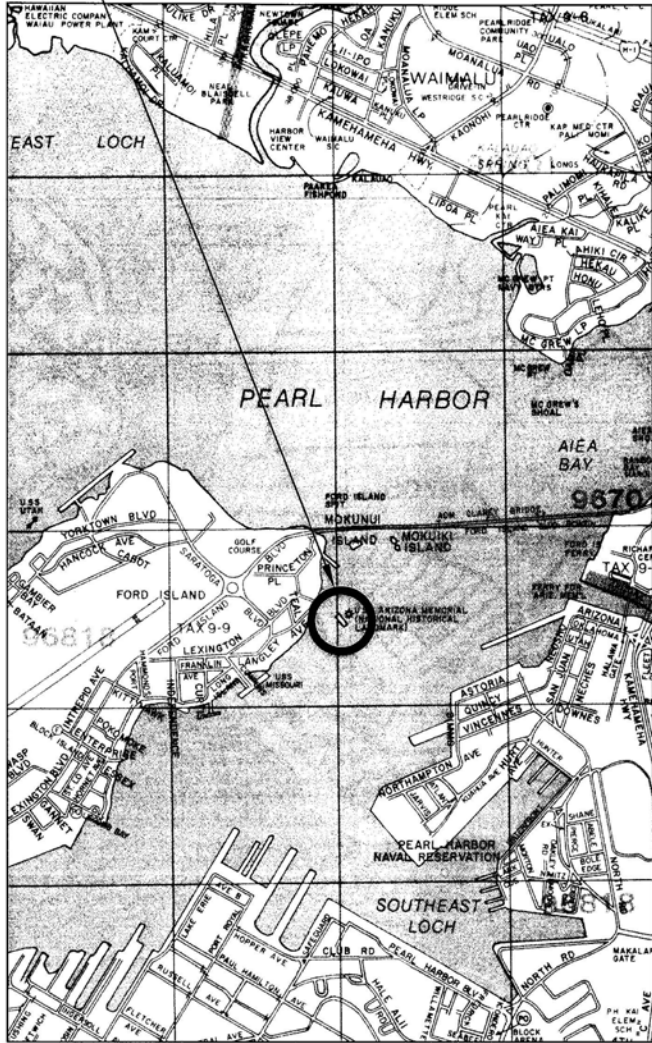
Reference: Bryan's Sectional Maps, 2003 Edition
(Copyright J.R. Clere, used with permission)

Scale: 1:24,000

W.O. 03-3832	USS Arizona Project – Drilling Services
Ernest K. Hirata & Associates, Inc.	LOCATION MAP
	Plate 1.1

USS Arizona Geological Core Locations
November 2003

Core Location B2
E608943, N2362957

Core Location B1A
E608813, N2362945

Core Location B3
E608749, N2362811
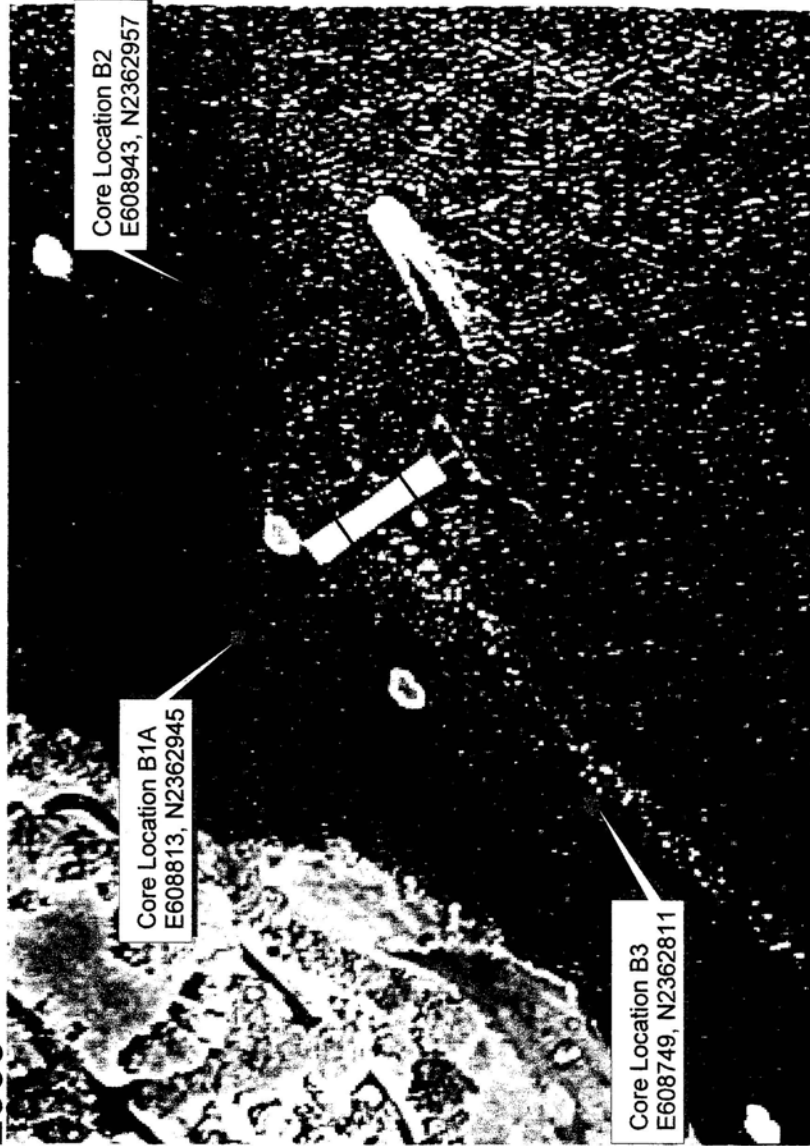
All Coordinates UTM Zone 4, NAD83

20   0   20   40   Meters

N

504

MAJOR DIVISIONS			GROUP SYMBOLS		TYPICAL NAMES
COARSE GRAINED SOILS (More than 50% of the material is LARGER than No. 200 sieve size.)	GRAVELS (More than 50% of coarse fraction is LARGER than the No. 4 sieve size.)	CLEAN GRAVELS (Little or no fines.)		GW	Well graded gravels, gravel-sand mixtures, little or no fines.
				GP	Poorly graded gravels or gravel-sand mixtures, little or no fines.
		GRAVELS WITH FINES (Appreciable amt. of fines.)		GM	Silty gravels, gravel-sand-silt mixtures.
				GC	Clayey gravels, gravel-sand-clay mixtures.
	SANDS (More than 50% of coarse fraction is SMALLER than the No. 4 sieve size.)	CLEAN SANDS (Little or no fines.)		SW	Well graded sands, gravelly sands, little or no fines.
				SP	Poorly graded sands or gravelly sands, little or no fines.
		SANDS WITH FINES (Appreciable amt. of fines.)		SM	Silty sands, sand-silt mixtures.
				SC	Clayey sands, sand-clay mixtures.
FINE GRAINED SOILS (More than 50% of the material is SMALLER than No. 200 sieve size.)	SILTS AND CLAYS (Liquid limit LESS than 50.)			ML	Inorganic silts and very fine sands, rock flour, silty or clayey fine sands or clayey silts with slight plasticity.
				CL	Inorganic clays of low to medium plasticity, gravelly clays, sandy clays, silty clays, lean clays.
				OL	Organic silts and organic silty clays of low plasticity.
	SILTS AND CLAYS (Liquid limit GREATER than 50.)			MH	Inorganic silts, micaceous or diatomaceous fine sandy or silty soils, elastic silts.
				CH	Inorganic clays of high plasticity, fat clays.
				OH	Organic clays of medium to high plasticity, organic silts.
HIGHLY ORGANIC SOILS				PT	Peat and other highly organic soils.

	FRESH TO MODERATELY WEATHERED BASALT
	VOLCANIC TUFF / HIGHLY TO COMPLETELY WEATHERED BASALT
	CORAL

LAB/FIELD TEST ABBREVIATIONS

TV = Torvane   LL = Liquid Limit
DS = Direct Shear   PI = Plasticity Index
CT = Consolidation   UC = Unconfined
Test   Compression Test

SAMPLE DEFINITION		
2" O.D. Standard Split Spoon Sampler	Shelby Tube	RQD Rock Quality Designation
3" O.D. Split Tube Sampler	NX / 4" Coring	Water Level

W.O. 03-3832	USS Arizona Project - Drilling Services
Ernest K. Hirata & Associates, Inc.	**BORING LOG LEGEND** Plate 2.1

PLASTICITY CHART

Liquid Limit

Plasticity Index

CH

A-Line

CL

MH & OH

ML-CL

ML & OL
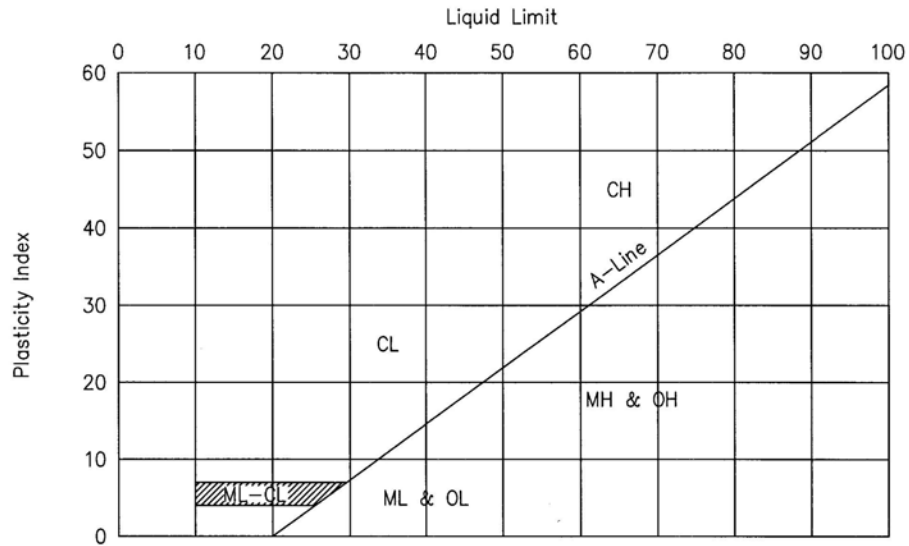
GRADATION CHART

COMPONENT DEFINITIONS BY GRADATION	
COMPONENT	SIZE RANGE
Boulders	Above 12 in.
Cobbles	3 in. to 12 in.
Gravel	3 in. to No. 4 (4.76 mm)
Coarse gravel	3 in. to 3/4 in.
Fine gravel	3/4 in. to No. 4 (4.76 mm)
Sand	No. 4 (4.76 mm) to No. 200 (0.074 mm)
Coarse sand	No. 4 (4.76 mm) to No. 10 (2.0 mm)
Medium sand	No. 10 (2.0 mm) to No. 40 (0.42 mm)
Fine sand	No. 40 (0.42 mm) to No. 200 (0.074 mm)
Silt and clay	Smaller than No. 200 (0.074 mm)

W.O. 03-3832	USS Arizona Project – Drilling Services
Ernest K. Hirata & Associates, Inc.	UNIFIED SOIL CLASSIFICATION SYSTEM Plate 2.2

ERNEST K. HIRATA & ASSOCIATES, INC.
Geotechnical Engineering

BORING LOG

W.O. 03-3832

BORING NO. B1A	DRIVING WT. 63.5 kg	START DATE 11/13/03
SURFACE ELEV. N/A	DROP 760 mm	END DATE 11/14/03

DEPTH 0	GRAPH	SAMPLE	BLOWS PER 0.3 m	SAMPLE NO.	RECOVERY (%)	DESCRIPTION
			7			Silty SAND/Sandy SILT (SM/ML) – Gray to brownish gray, soft to firm, with shell fragments.
			5			
1			5	1	0	
			7			
			16			Increase in sand content from 1.2 to 2 meters.
			22			
2			18			
			4	2	5	
			0			
3			0			Increase in sand content from 3 to 3.5 meters.
			52			
			23			
			6	3	0	
4			2			
			0			
			32			
5			51			
			8	4	0	
			4			
6			4			
			59			Grade with coralline gravel from 6 meters.
			47			
7			33	5	30	Silty CLAY (CL–CH) – Grayish brown, medium stiff to stiff, with coralline gravel and sand.
			44			
			42			
8			26			
			35			
			37	6	40	
			51			
9			68			CORAL RUBBLESTONE – Tan, medium dense to dense.
			44			
			23			
10			31	7	100	Plate 3.1

507

ERNEST K. HIRATA & ASSOCIATES, INC.

Geotechnical Engineering

BORING LOG

W.O. 03-3832

BORING NO. B1A (Continued)   DRIVING WT. 63.5 kg   START DATE 11/13/03
SURFACE ELEV. N/A   DROP 760 mm   END DATE 11/14/03

DEPTH	GRAPH	SAMPLE	BLOWS PER 0.3 m	SAMPLE NO.	RECOVERY (%)	DESCRIPTION
0						
			44			
			55			
			101			
11			29			
			38	8	77	Silty CLAY (CL–CH) – Grayish brown, medium stiff to stiff, with coralline gravel and sand.
			59			
12			76			
			20			
			41			
13			83	9	68	
			86			
			104			
			14			
14			26			
			54	10	83	
			76			
15			124			
						End boring at 15.2 meters.
16						Depth to mudline measured at 8.5 meters below water at 11:24 am on 11/13/03.
17						
18						
19						
20						Plate 3.2

508

ERNEST K. HIRATA & ASSOCIATES, INC.
Geotechnical Engineering

BORING LOG

W.O. __03-3832__

BORING NO.	B2	DRIVING WT.	63.5 kg	START DATE	11/18/03
SURFACE ELEV.	N/A	DROP	760 mm	END DATE	11/20/03

DEPTH 0	GRAPH	SAMPLE	BLOWS PER 0.3 m	SAMPLE NO.	RECOVERY (%)	DESCRIPTION
0			0			Silty SAND/Sandy SILT (SM/ML) — Gray to brownish gray, soft to firm, with shell fragments.
			0			
			0	1	0	
1			0			
			0			
			0			
			0			
2			0			
			0	2	5	
			0			
3			0			
			0			
			0			
			0	3	0	
4			0			
			0			
			0			
5			4			Grade with coralline gravel from 6 meters.
			6	4	0	
			7			
			2			
6			6			
			35			Silty CLAY (CL–CH) — Grayish brown, medium stiff to stiff, with coralline gravel and sand.
7			47	5	0	
			95			
			118			
			58			
8			121	6	100	
			87/150mm			
			35			
			65	7	90	
9			44/150mm			
			41			
			97	8	90	
10			73/150mm			Plate 3.3
			39			

509

ERNEST K. HIRATA & ASSOCIATES, INC.
Geotechnical Engineering

BORING LOG

W.O. 03-3832

BORING NO.	B2 (Continued)	DRIVING WT.	63.5 kg	START DATE	11/18/03
SURFACE ELEV.	N/A	DROP	760 mm	END DATE	11/20/03

DEPTH	GRAPH	SAMPLE	BLOWS PER 0.3 m	SAMPLE NO.	RECOVERY (%)	DESCRIPTION
0						
			47	9	100	
			31/150mm			
			20			
11			32	10	80	
			26/150mm			
			22			
12			43	11	93	
			29/150mm			
			102			
			160	12	100	Silty SAND/Sandy SILT (SM/ML) — Tan, loose to dense, with coralline gravel and sand, and shell fragments.
13			96/150mm			
			46			
			70	13	100	
			16/150mm			
			81			
14			110	14	93	
			14/150mm			
			39			
15			126	15	60	
			84/150mm			
			44			
			17	16	70	
16			16/150mm			
			11			
			17	17	100	
			15/150mm			
			14			
17			18	18	63	
			9/150mm			
			20			
18			43	19	77	
			29/150mm			
			11			
			17	20	67	
19			15/150mm			
			27			
			11	21	93	
			9/150mm			
20			0			Plate 3.4

ERNEST K. HIRATA & ASSOCIATES, INC.
Geotechnical Engineering

BORING LOG

W.O. 03-3832

| BORING NO. | B2 (Continued) | DRIVING WT. | 63.5 kg | START DATE | 11/18/03 |
| SURFACE ELEV. | N/A | DROP | 760 mm | END DATE | 11/20/03 |

DEPTH	GRAPH	SAMPLE	BLOWS PER 0.3 m	SAMPLE NO.	RECOVERY (%)	DESCRIPTION
0			0 0/150mm	22	10	
21			0 0/150mm	23	80	
22						End boring at 21.3 meters.
23						Depth to mudline measured at 11.9 meters below water at 8:38 am on 11/18/03.
24						
25						
26						
27						
28						
29						
30						Plate 3.5

511

ERNEST K. HIRATA & ASSOCIATES, INC.
Geotechnical Engineering

BORING LOG

W.O. 03-3832

BORING NO.	B3	DRIVING WT.	63.5 kg	START DATE	11/15/03
SURFACE ELEV.	N/A	DROP	760 mm	END DATE	11/15/03

DEPTH 0	GRAPH	SAMPLE	BLOWS PER 0.3 m	SAMPLE NO.	RECOVERY (%)	DESCRIPTION
0			0 / 0 / 0/150mm	1	0	Silty SAND/Sandy SILT (SM/ML) — Gray to brownish gray, soft to firm, with shell fragments.
1			0 / 0 / 0/150mm	2	0	
2			0 / 0 / 0/150mm	3	0	
3			0 / 0 / 0/150mm	4	0	
			0 / 0 / 0/150mm	5	0	
4			0 / 0 / 0/150mm	6	0	
5			0 / 0 / 0/150mm	7	0	
6			0 / 0 / 0/150mm	8	100	
			0 / 0 / 0/150mm	9	0	
7			0 / 2 / 0/150mm	10	0	
8			0 / 1 / 0/150mm	11	0	
9			0 / 4 / 2/150mm	12	77	
10			2 / 4 / 2/150mm / 4	13	0	

Plate 3.6

512

ERNEST K. HIRATA & ASSOCIATES, INC.
Geotechnical Engineering

BORING LOG

W.O. 03-3832

BORING NO. B3 (Continued)   DRIVING WT. 63.5 kg   START DATE 11/15/03
SURFACE ELEV. N/A   DROP 760 mm   END DATE 11/15/03

DEPTH	GRAPH	SAMPLE	BLOWS PER 0.3 m	SAMPLE NO.	RECOVERY (%)	DESCRIPTION
0						
			4 0/150mm	14	0	
11			0 4 2/150mm	15	100	
			0 0 0/150mm	16	0	
12			0 0 0/150mm	17	100	Silty CLAY (CL–CH) — Grayish brown, soft to firm.
13			0 0 0/150mm	18	100	
14			0 0 0/150mm	19	100	
15			0 0 0/150mm	20	100	
16						End boring at 15.2 meters. Depth to mudline measured at 11.3 meters below water at 11:25 am on 11/15/03.
17						
18						
19						
20						Plate 3.7

513